PhD Program in Physiology

Redox signaling in acute pancreatitis: roles of PGC-1α and sulfiredoxin

PhD Thesis

SERGIO RIUS PÉREZ

PhD Thesis supervised by

Prof. Dr. JUAN SASTRE BELLOCH

Dr. SALVADOR PÉREZ GARRIDO

Department of Physiology, Faculty of Pharmacy

February 2020

Prof. Dr. JUAN SASTRE BELLOCH, Catedrático del Departamento de Fisiología de la Universitat de València.

Dr. SALVADOR PÉREZ GARRIDO, Profesor Ayudante Doctor del Departamento de Fisiología de la Universitat de València.

CERTIFICAN:

Que la presente memoria, titulada "Redox signaling in acute pancreatitis: roles of PGC-1α and sulfiredoxin", corresponde al trabajo realizado bajo su dirección por D. **SERGIO RIUS PÉREZ**, para su presentación como Tesis Doctoral en el Programa de Doctorado en Fisiología de la Universitat de València.

Y para que conste a los efectos oportunos, firmamos la presente certificación en Valencia, a 21 de febrero de 2020

Fdo.: JUAN SASTRE BELLOCH	Fdo.: SALVADOR PÉREZ GARRIDO
Director	Director

Acknowledgments

En primer lugar, me gustaría agradecer a mis directores Prof. Juan Sastre Belloch y Prof. Salvador Pérez Garrido, todo vuestro esfuerzo y dedicación para que esta Tesis se haya desarrollado. Resulta difícil imaginar unos directores mejores.

A mis compañeros de grupo de investigación Pablo Martí e Isabela Finamor su ayuda y su constante apoyo. Hacemos un gran equipo.

A todos aquellos que han colaborado en el desarrollo de esta Tesis Doctoral. Al Prof. Luis Torres, al Prof. Gerardo López y al Prof. Luis Franco del Departamento de Bioquímica y Biología Molecular. A la Dra. María Monsalve del Instituto de Investigaciones Biomédicas Alberto Sols. A la Dra. Isabel Torres del Instituto de Investigación Sanitaria La Fe. También al Dr. Michel TOLEDANO y a todo su equipo con quien pasé unos meses increíbles. A la Dra. Ángela Martínez Valverde y a todos los miembros de su laboratorio con quienes realicé una estancia que recuerdo con especial cariño.

A todos mis compañeros y compañeras del Departamento de Fisiología, que me han enseñado y me han prestado ayuda siempre que lo que he necesitado. Con vuestro buen humor hacéis que el Departamento sea un lugar inmejorable donde realizar un doctorado.

A mis padres que sin vuestro cariño y apoyo esta Tesis nunca hubiese sido posible. Os quiero. A mi abuela que, aunque no lo recordará, podrá ver finalizado este trabajo. A mis otros abuelos, se que estaríais orgullosos.

A Guillermo Lisarde por su ayuda en el diseño de la portada y por su amistad.

A todos mis amig@s que siempre me habéis animado y apoyado.

A mis padres.

Table of Contents

Table of Figures XIII

List of Tables XIX

List of Abbreviations XXI

ABSTRACT XXXI

I. INTRODUCTION 1

1 Acute pancreatitis 3

- 1.1 Exocrine pancreas 3
- 1.2 Definition and classification of acute pancreatitis 6
- 1.3 Etiology 10
- 1.4 Epidemiology 11
- 1.5 Pathogenesis 13
  - 1.5.1 Intracellular activation of zymogens 13
  - 1.5.2 Secretion of zymogens 15
  - 1.5.3 Inflammatory response and cell death 16
    - 1.5.3.1 Inflammatory signaling pathways 17
    - 1.5.3.2 Cytokines 24
    - 1.5.3.3 Cell death pathways 29

2 Oxidative stress and redox signaling 40

2.1 Concept of oxidative stress 40

2.2 Reactive oxygen species: types and endogenous sources 40

2.3 GSH: role in antioxidant defense and redox signaling 43

2.3.1 Structure and function of GSH 43

2.3.2 GSH synthesis and the trans-sulfuration pathway 44

2.3.3 Regulation of the trans-sulfuration pathway................. 46

2.4 Peroxiredoxins: role in oxidative stress and redox signaling..... 47

2.4.1 Peroxiredoxins classification and catalytic mechanisms.. 47

2.4.2 Hyperoxidation of peroxiredoxins: role of sulfiredoxin . 51

2.4.3 Functions of peroxiredoxins and its hyperoxidized forms.. 53

2.5 Reactive nitrogen species, nitrosative stress and redox signaling 54

2.5.1 •NO chemistry and reactive nitrogen species generation 55

2.5.2 Peroxynitrite and protein nitration 56

2.5.3 Peroxynitrite, mitochondrial function and cell death.... 60

2.5.4 Peroxynitrite and peroxiredoxins 61

2.6 Oxidative and nitrosative stress in acute pancreatitis 63

3 PGC-1α... 66

3.1 PGC-1α family members 66
3.2 Regulation of PGC-1α expression and activity........................... 67
3.3 Physiological functions of PGC-1α.. 68
3.3.1 PGC-1α and mitochondrial biogenesis 68
3.3.2 PGC-1α and metabolic regulation 69
3.3.3 PGC-1α and ROS detoxification................................... 69

II. OBJECTIVES 71

III. MATERIAL AND METHODS 75
1 Experimental model of acute pancreatitis 77
1.1 Induction of acute pancreatitis in mice 78
2 Experimental design 78
2.1 Design of the time-course experiments 78
2.2 Design of the study with SAM-treated mice............................... 79
2.3 Design of the study with SRX KO mice....................................... 80
2.4 Design of the study with obese mice 81
2.5 Design of the study with PGC-1α KO mice................................. 81
3 Experimental techniques 83
3.1 Mass spectrometry by UHPLC-MS/MS....................................... 83

3.2 Protein quantification by MRM 85
3.3 Western blotting 86
  3.3.1 Sample preparation 87
  3.3.2 Electrophoresis and protein transfer 87
  3.3.3 Immunoblotting 88
3.4 Immunoprecipitation 91
3.5 Nuclei isolation 92
3.6 Mitochondrial isolation 92
3.7 RT-qPCR analysis for gene expression 93
  3.7.1 RNA extraction 93
  3.7.2 Reverse transcription and cDNA amplification 94
3.8 Chromatin immunoprecipitation assay (ChIP) 96
3.9 Hydrogen peroxide levels 98
3.10 α-Amylase activity in plasma 98
3.11 Plasma cfDNA levels 99
3.12 Plasma nucleosomes levels 99
3.13 Plasma IL-6 levels 100
3.14 Histological analysis 101
3.15 Myeloperoxidase activity 101
3.16 Statistical analysis 102

IV. RESULTS 103

1 Regulation of the trans-sulfuration pathway in acute pancreatitis 105

1.1 Changes in trans-sulfuration metabolites levels during acute pancreatitis 105

1.2 Levels of proteins involved in the trans-sulfuration pathway during acute pancreatitis 106

1.3 Acute pancreatitis triggered tyrosine nitration of cystathionine-β-synthase in pancreas 108

1.4 Administration of S-adenosylhomocysteine triggered homocysteine accumulation in acute pancreatitis 109

1.5 S-adenosylhomocysteine administration aggravated the inflammatory response in acute pancreatitis 112

1.6 S-adenosylhomocysteine administration enhanced *Nos2* gene expression and cystathionine-β-synthase nitration in acute pancreatitis 114

2 Modulation of nitrosative stress and cell death by sulfiredoxin in acute pancreatitis 116

2.1 Acute pancreatitis upregulated mRNA and protein levels of sulfiredoxin 116

2.2 Acute pancreatitis triggered transient hyperoxidation of peroxiredoxins 116

2.3 Acute pancreatitis induced translocation of sulfiredoxin into mitochondria 119

2.4 Sulfiredoxin deficiency enhanced pancreatic inflammation and necrosis in acute pancreatitis 120

2.5 SRX deficiency increased hyperoxidation of peroxiredoxins in acute pancreatitis 124

2.6 SRX deficiency enhanced mitochondrial protein nitration in acute pancreatitis 125

2.7 SRX deficiency induced necroptosis and p53 mitochondrial translocation in acute pancreatitis 126

2.8 Mito-TEMPO reduced inflammation and necroptosis in SRX-deficient mice with acute pancreatitis 127

2.9 Mito-TEMPO did not recover PGC-1α downregulation in SRX-deficient mice with acute pancreatitis 131

3 Regulation of the inflammatory response by PGC-1α in acute pancreatitis 133

3.1 PGC-1α levels are markedly reduced in pancreas from obese mice at basal conditions and in acute pancreatitis 133

3.2 PGC-1α deficiency enhanced pancreatic inflammation in acute pancreatitis 133

3.3 PGC1α deficiency induced apoptosis but not necroptosis in acute pancreatitis 135

3.4 PGC-1α acetylation and downregulation of its target genes in acute pancreatitis 137

3.5 PGC-1α deficiency enhanced NF-κB activation and *Il-6* upregulation in acute pancreatitis 138

3.6 PGC1α formed a complex with p-p-65 subunit of NF-κB in pancreas 140

3.7 PGC-1α deficiency enhanced IL-6 plasma levels inducing pulmonary infiltrate and damage in acute pancreatitis 140

3.8 gp-130 antagonist LMT-28 abrogated pulmonary damage induced by PGC-1 deficiency in acute pancreatitis 142

V. DISCUSSION 145

1 Nitrosative stress blockades the trans-sulfuration pathway in acute pancreatitis due to nitration of cystathionine β-synthase . 147

2 Sulfiredoxin protects from mitochondrial nitrosative stress and necroptosis in acute pancreatitis 152

3 PGC1α restrains IL-6 expression via inhibition of NF-kB in acute pancreatitis 158

VI. CONCLUSIONS 165

Bibliography 169

Resumen 235

Table of Figures

Figure 1. Pancreas. 4

Figure 2. Multifaceted paradigm of the pathogenesis of acute pancreatitis. 17

Figure 3. The NF-κB family members 19

Figure 4. NF-κB signaling pathways 20

Figure 5. MAPKs pathways. 24

Figure 6. Apoptosis signaling pathways. 31

Figure 7. Necroptosis pathway 38

Figure 8. Sources of reactive oxygen species (ROS). 42

Figure 9. Methionine metabolism and trans-sulfuration pathway 45

Figure 10. Reaction mechanisms of peroxiredoxins 49

Figure 11. Thioredoxin-Peroxiredoxin system and role of sulfiredoxin 52

Figure 12. Nitric oxide (•NO) chemistry and peroxynitrite ($ONOO^-$) fates in the biological context 56

Figure 13. Tyrosine nitration 59

Figure 14. Structure of PGC-1 family coactivators 67

Figure 15. Experimental design of time-course experiment 79

Figure 16. Levels of trans-sulfuration metabolites, GSH and MTA in pancreas during cerulein-induced acute pancreatitis 106

Figure 17. Protein levels of enzymes involved in trans-sulfuration pathway in pancreas with acute pancreatitis.. 107

Figure 18. Levels of protein nitration and CBS nitration in pancreas with acute pancreatitis. 108

Figure 19. Thiol oxidation of CBS in pancreas with acute pancreatitis 109

Figure 20. Gene expression of *Nos* genes and protein levels of NOS2 in pancreas with acute pancreatitis. 110

Figure 21. Levels of trans-sulfuration metabolites, GSH and MTA in pancreas from mice with acute pancreatitis treated with SAM 111

Figure 22. Gene expression of *Tnf-α* and *Il-6*, and levels of H3K4me3 in the promoter of these genes in pancreas from mice with acute pancreatitis treated with SAM 112

Figure 23. Histological analysis of pancreas from mice with acute pancreatitis treated with SAM.. 113

Figure 24. Gene expression of *Nos2* and levels of H3K4me3 in the promoter of *Nos2* in pancreas from mice with acute pancreatitis treated with SAM.. 114

Figure 25. Levels of CBS nitration in pancreas with acute pancreatitis treated with SAM... 115

Figure 26. Gene expression and epigenetic markers in the promoter of *Srxn1*, and protein levels of SRX in pancreas during acute pancreatitis.. 117

Figure 27. Protein levels of PRX1, PRX2 and PRX3 in pancreas during acute pancreatitis 118

Figure 28. Protein levels of sulfinic and sulfonic forms of PRX1, PRX2 and PRX3 and levels of H_2O_2 in pancreas during acute pancreatitis.. 119

Figure 29. Mitochondrial translocation of SRX in pancreas during acute pancreatitis.. 120

Figure 30. Histological analysis of pancreas and serum amylase activity in SRX KO mice with acute pancreatitis................. 121

Figure 31. Gene expression of *Tnf-α*, *Il-6* and *Il-1β* together with MAPKs and NF-κB activation in pancreas from SRX KO mice with acute pancreatitis 122

Figure 32. Plasma levels of cell free DNA and nucleosomes in SRX KO mice with acute pancreatitis 123

Figure 33. Protein levels of sulfinic and sulfonic forms of PRX1, PRX2 and PRX3 in the pancreas from SRX KO mice with acute pancreatitis.. 124

Figure 34. Mitochondrial protein nitration and NOS2 protein levels in the pancreas from SRX KO mice with acute pancreatiti 125

Figure 35. p-MLKL, cleaved caspase-3, and p53 levels in the pancreas from SRX KO mice with acute pancreatitis........................ 127

Figure 36. Histological analysis of pancreas from SRX KO mice with acute pancreatitis treated with mito-TEMPO...................... 128

Figure 37. Plasma levels of cell free DNA and nucleosomes in the pancreas from SRX KO mice with acute pancreatitis treated with mito-TEMPO 129

Figure 38. p-MLKL levels, mitochondrial protein nitration, gene expression of *Tp53* and mitochondrial levels of p53 in the pancreas from SRX KO mice with acute pancreatitis treated with mito-TEMPO.. 130

Figure 39. Gene expression of *Ppargc1a* and *Prx3* in the pancreas from SRX KO mice with acute pancreatitis and with mito-TEMPO treatment.. 131

Figure 40. Gene expression and protein levels of PGC-1α in lean and obese mice at basal conditions and in acute pancreatitis. 134

Figure 41. Histological analysis of pancreas, and plasma amylase activity of PGC-1α KO with acute pancreatitis 135

Figure 42. Gene expression of *Srxn1* and western blots of cleaved caspase-3 and p-MLKL in pancreas from PGC-1α KO mice with acute pancreatitis 136

Figure 43. Gene expression of peroxiredoxin 3, superoxide dismutase 2 and catalase in the pancreas from PGC-1α KO mice with acute pancreatitis and acetylated protein levels of PGC-1α in mice with acute pancreatitis 137

Figure 44. Gene expression of *Tnf-α*, *Il-6* and *Il-1β* and p65 recruitment to their promoters in the pancreas from PGC-1α KO mice with acute pancreatitis. 139

Figure 45. Complex formation between PGC-1α and p-65 in pancreas with acute pancreatitis. 140

Figure 46. Plasma IL-6 levels and pulmonary myeloperoxidase activity and damage in PGC-1α KO mice with acute pancreatitis 141

Figure 47. Histological analysis of pancreas from PGC-1α KO mice with acute pancreatitis treated with LMT-28 143

Figure 48. Plasma IL-6 levels and pulmonary damage of PGC-1α KO mice with acute pancreatitis treated with LMT-28 144

Figure 49. Acute pancreatitis induces nitration of cystathionine β-synthase (CBS) and blockade of the trans-sulfuration pathway 150

Figure 50. Proposed mechanism for the protective role of sulfiredoxin in acute pancreatitis. 157

Figure 51. PGC-1α acts as a selective repressor of NF-κB towards *Il-6* in pancreas with acute pancreatitis 163

List of Tables

Table 1. Pancreatic digestive proenzymes and enzymes 5

Table 2. Mammalian peroxiredoxins 50

Table 3. Reactivity of mammalians peroxiredoxins with H_2O_2 and $ONOO^-$ 62

Table 4. Experimental design of the study with SAM-treated mice with acute pancreatitis 80

Table 5. Experimental design of the study with SRX KO mice with acute pancreatitis 81

Table 6. Experimental design of the study with PGC-1α KO mice with acute pancreatitis 82

Table 7. Transitions for trans-sulfuration metabolites determined by UHPLC–MS/MS 84

Table 8. Primary antibodies used for western blotting 89

Table 9. Secondary antibodies used for western blotting 91

Table 10. Primary antibodies used for immunoprecipitation assays.... 92

Table 11. Oligonucleotides used for RT-qPCR 95

Table 12. TaqMan® probe used for RT-qPCR 96

Table 13. Antibodies used for ChIP assay 97

Table 14. Oligonucleotide used for ChIP assay 98

List of Abbreviations

3-NT, 3-nitrotyrosine

5,10-MTHF, 5,10-methylenetetrahydrofolate

5-MTHF, 5-methyltetrahydrofolate

AD, activation domain

AhpC, alkyl hydroperoxide reductase C

AKT, protein kinase B

AMPK, AMP-activated protein kinase

AnkR, ankyrin repeats

ANT, adenine nucleotide translocator

AP-1, activator protein-1

APAF1, apoptotic protease-activating factor 1

ASC, apoptosis-associated speck-like protein containing a caspase recruitment domain

ATP, adenosine triphosphate

BAD, BCL-2 associated agonist of cell death

BAF-R, B-cell-activating-factor receptor

BAK, BCL-2 homologous antagonist/killer

BAX, BCL-2-associated X protein

BCL-3, B-cell lymphoma 3-encoded protein

BH3, BCL-2 homology 3 proteins

BID, BH3 interacting-domain death agonist

BLC-2, B-cell lymphoma 2 protein

CAT, catalase

CBP ,CREB binding protein

CBS, cystathionine β synthase

CCK, cholecystokinin

cfDNA cell free DNA

c-FLIP, c-FLICE-like inhibitory protein

CHAC1, glutathione specific γ-glutamyl cyclotransferase

cIAP, cellular inhibitor of apoptosis protein () 1,

CK2, casein kinase 2

CLC, cardiotrophin-like cytokine

CLK2, Dual specificity kinase

CNTF, ciliary neurotrophic factor

C_P, peroxidatic cysteine

C_R, resolving cysteine

CREB, AMP responsive element binding protein

CSE, cystathionase

CT-1, cardiotrophin 1

CXCL1, chemokine C-X-C motif ligand 1

CYLD, cylindromatosis lysine 63 deubiquitinase

CYPD, mPTP regulator cyclophilin D

DAMPs, damage-associated molecular pattern molecules

dcSAM, decarboxylated SAM

DRP1, dynamin-1-like protein

DUOX, dual oxidase

EDRF, endothelial-derived vascular relaxation factor

ER, endoplasmic reticulum

ERK, extracellular signal-regulated kinase,

FADD, FAS-associated death domain

FOXO forkhead box O

GCL, glutamate cysteine ligase

GGT, γ-glutamyl transpeptidase

gp130, glycoprotein 130 kDa

GPXs, glutathione peroxidases

GR, glutathione reductase

GRP, gastrin-releasing peptide

GS, GSH synthase

GSH, Reduced glutathione

GSK3β, glycogen synthase kinase 3

GSNO, S-nitrosoglutathione

GSNOR S-nitrosoglutathione reductase

GSSG, oxidized glutathione

HAUSP, herpesvirus-associated ubiquitin-specific protease

HCysNO, S-nitrosohomocysteine

HIPK2, homeodomain-interacting protein kinase 2

HMGB1, high-mobility group box 1

HSP90, heat shock protein 90

HtRA2, HtrA serine peptidase 2

IAPs, inhibitor of apoptosis proteins

Icam1, intercellular adhesion molecule 1

IKK, inhibitor of kappa B kinase

IL-10, interleukin-10

IL-1R1, IL-1 receptor type I

IL-1Ra, IL-1 receptor antagonist

IL-1RAP, IL-1R accessory protein

IL-1β, interleukin-1β

IL-6, interleukin-6

IL-6R, IL-6 receptor

IRAK4, IL-1R- associated kinase 4

IκB, inhibitor of kappa B

JAKs, Janus kinases

JNK, c-Jun N-terminal kinase

L-CysNO, S-nitrosocysteine

LIF, leukemia inhibitory factor

LTβR, lymphotoxin-β receptor

MAPKK, MAPK kinase

MAPKKK, MAPK kinase kinase

MAPKs, mitogen-activated protein kinases

MAT, methionine adenosyltransferase

MDM2, murine doble minute 2

MK2, MAPK-activated protein kinase 2

MLKL, pseudokinase mixed-lineage kinase domain–like

MPO, myeloperoxidase

mPTP, mitochondrial permeability transition pore

MS, methionine synthetase

MTA, methylthyoadenosine

mtDNA, mitochondrial DNA

MTHFR, methylenetetrahydrofolate reductase

mYD88, myeloid differentiation primary response protein 88

NADH nicotinamide adenine dinucleotide

NADPH, nicotinamide adenine dinucleotide phosphate nDNA, nuclear DNA

NDUFB8, NADH:ubiquinone oxidoreductase subunit B8

NEMO, NF-kB essential modifier

NFAT, nuclear factor associated with activated T cells

NF-κB, nuclear factor kappa-B

NIK, NF-κB-inducing kinase

NLR, nucleotide-binding domain and leucine-rich repeat containing receptor

NLS, nuclear localization sequence

NOS, nitric oxide synthase

NOXA, phorbol-12-myristate-13-acetate-induced protein 1

NOXs, NAD(P)H oxidases

NR, nuclear receptor

NRF, nuclear respiratory factor

NRF-2, nuclear factor erythroid 2–related factor 2

OSM, oncostatin M

PAMPs, pathogen-associated molecular pattern molecules

PAP1, pancreatitis-associated protein 1

PARP-1, poly (ADP-ribose) polymerases

PGAM5, mitochondrial serine/threonine protein phosphatase

PGC-1α, peroxisome proliferator-activated receptor-γ coactivator 1α

PIN1, peptidyl-prolyl cis-trans isomerase NIMA-interacting 1

PLP, pyridoxal-5′-phosphate

PPARs, peroxisome proliferator-activated receptors

PRC, PGC related coactivator

PRRs, pattern recognition receptors

PRXs, peroxiredoxins

PUMA, p53 upregulated modulator of apoptosis

RHD, REL homology región

RIPK, receptor-interacting protein kinase

RNS, reactive nitrogen species

ROS, reactive oxygen species

RRM, RNA recognition motif

RS, short serine/arginine-rich stretches

RSK1, ribosomal s6 kinase-1

SAH, S-adenosylhomocysteine

SAHH, S-adenosylhomocysteine hydrolase

SAM, S-adenosylmethionine

SCF^{Cdc4}, Skp1/Cullin/F-box-cell division control 4

SIRT1, silent information regulator 1

SMAC/DIABLO, caspase/diablo homolog

SOD, superoxide dismutase

SPI2a, serine protease inhibitor 2A

SPINK1, serine protease inhibitor Kazal type 1

SRC-1, steroid receptor coactivator 1

SRX, sulfiredoxin

STAT, Janus kinase-signal transducer and activator of transcription

TAB, TAK1 binding protein

TACE, TNFα-converting enzyme

TAD, transactivation domain

TAK1, transforming growth factor-β-activated kinase 1 (),

TFAM, mitochondrial transcription factor A

TIR, Toll/IL-1 receptor

TLR, Toll-like receptor

TNFR, TNF-α receptor

TNF-α, tumor necrosis factor-α

TOM, outer membrane complex

TRADD, TNFR1-associated death domain protein

TRAF, TNFR-associated factor

TRAIL-R, Tnf-α-related apoptosis-inducing ligand receptor

TRX, thioredoxin

TRXR, thioredoxin reductase

VIP, vasoactive intestinal polypeptide

XIAP, X-linked IAP

XOD, xanthine oxidase

πGST, π isoform of glutathione S-transferase

ABSTRACT

Acute pancreatitis is an inflammatory process of the pancreatic gland that may lead to local and systemic complications. The general aim of this PhD Thesis was to find out new mechanisms involved in redox regulation of the antioxidant defense and inflammatory cascade in acute pancreatitis, and also to assess their impact in its pathophysiology. Firstly, we studied the redox regulation of the trans-sulfuration pathway in pancreas with acute pancreatitis. For this purpose, acute pancreatitis was induced by cerulein in mice, and a group of animals received S-adenosylmethionine treatment. Acute pancreatitis blocked the trans-sulfuration pathway through nitration of cystathionine β-synthase promoting homocysteine accumulation upon S-adenosylmethionine treatment. Secondly, sulfiredoxin knock-out mice were used to assess the role of sulfiredoxin in the regulation of the inflammatory cascade and cell death in acute pancreatitis. Sulfiredoxin up-regulation and its translocation into the mitochondria prevented mitochondrial nitrosative stress and necroptosis during acute pancreatitis. Finally, we assessed the contribution of PGC-1α to the regulation of the antioxidant defense and inflammatory response in this disease. Acute pancreatitis was induced by cerulein in lean and obese mice; subsequently, PGC-1α knock-out mice with cerulein-induced acute pancreatitis were used. PGC-1α protein levels were markedly decreased in pancreas from obese mice with pancreatitis. PGC-1α formed an inhibitory complex with NF-κB and selectively repressed NF-κB towards *Il-6* in pancreas with acute pancreatitis. Hence, in acute pancreatitis PGC-1α knock-out mice exhibited very high plasma and pancreatic levels of IL-6 levels, which are considered a marker of severity in this disease. PGC-1α was inactivated by acetylation during acute pancreatitis in wild type mice and hence, its antioxidant targets genes were downregulated. In summary, we provide here new mechanisms related to cytosolic and mitochondrial nitrosative stress, sulfiredoxin and PGC-1α critically involved in the regulation of the inflammatory cascade and cell death in acute pancreatitis, which can decisively contribute to a better understanding of the pathophysiology of this disease and the associated redox molecular mechanisms.

I. INTRODUCTION

1 Acute pancreatitis

1.1 Exocrine pancreas

The pancreas is a retroperitoneal organ located deep in the abdomen, behind the stomach, that measures 12-15 cm in length and weighs about 80 g in human adults [1, 2]. The pancreas, thicker at its medial end and thinner towards the lateral end, is divided anatomically into four main regions: head, neck, body, and tail (Figure 1) [3]. The head of the pancreas lies in the C-shape of the duodenum from where the neck, the body, and the tail run through the retroperitoneum to the hilum of the spleen [2]. The pancreatic duct (also known as Wirsung duct) runs from left to right of the pancreas and joins the common bile duct at the head of the pancreas. Through the hepatopancreatic ampulla (also known as the ampulla of Vater), the pancreatic duct opens into the descending part of the duodenum at the major duodenal papilla [4]. An accessory pancreatic duct (also known as Santorini duct) drains the upper part of the anterior portion of the pancreatic head communicating with the main pancreatic duct near the neck of the pancreas [2]. The accessory duct opens at the minor duodenal papilla situated around 2 cm proximal to the major duodenal papilla [5].

The pancreas is both an exocrine and an endocrine gland. The exocrine component constitutes around 95% of the pancreatic mass and it is composed of groups of acini and its draining ducts [6]. The groups of acini form lobules that are surrounded and separated from other lobules by connective tissue [2]. Individual acini contain clusters of pyramidal acinar cells that synthesize, store, and secrete a range of digestive enzymes including trypsinogen, chymotrypsinogen, pro-carboxypeptidase, and pro-elastase, among others [1].

Centro-acinar cells are present at the junction between acinar and ductal cells. Ductal cells line the progressively larger ducts (intercalated ducts, intralobular ducts, interlobular ducts, and main pancreatic ducts) where acinar cells release its secretion (Figure 1) [7].

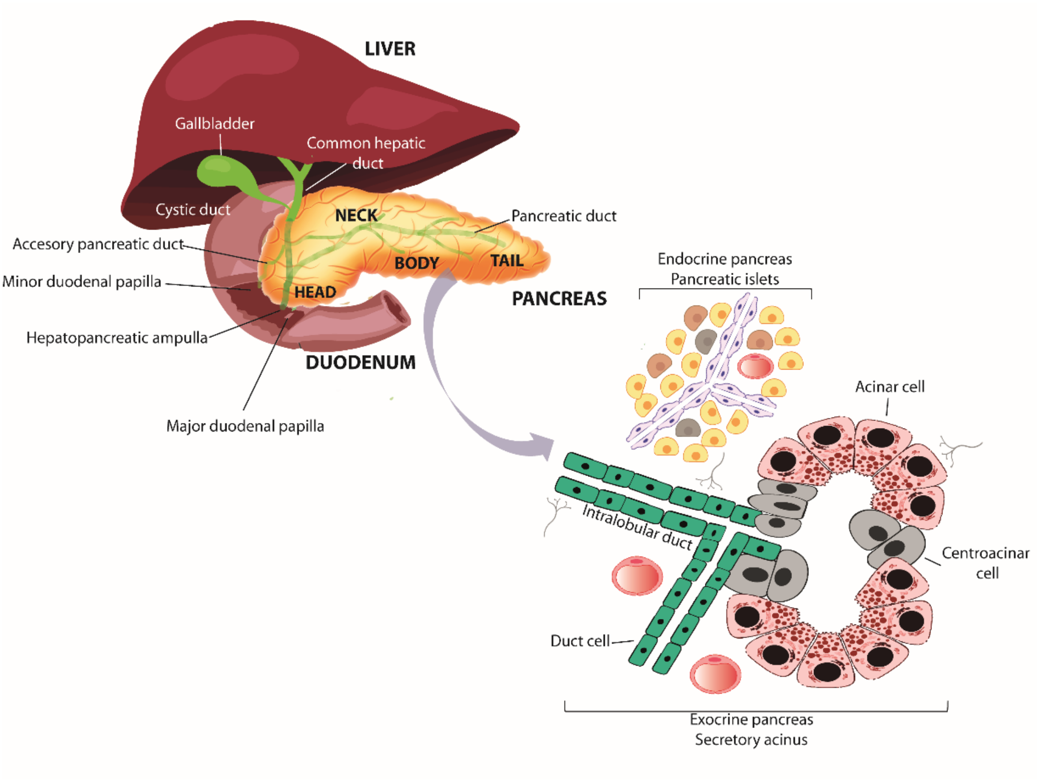
LIVER
Gallbladder
Common hepatic duct
Cystic duct
NECK
Pancreatic duct
Accesory pancreatic duct
Minor duodenal papilla
BODY
TAIL
HEAD
PANCREAS
Hepatopancreatic ampulla
DUODENUM
Major duodenal papilla
Endocrine pancreas
Pancreatic islets
Acinar cell
Intralobular duct
Centroacinar cell
Duct cell
Exocrine pancreas
Secretory acinus

Figure 1. Pancreas. Anatomic regions and relations of the pancreas. Schematic view of the pancreas microstructure.

In order to prevent the autodigestion of the pancreatic gland, most of the digestive enzymes are synthesized as inactive precursor forms known as zymogens [8, 9]. Zymogens are activated only when they reach the surface of duodenum where a brush-border glycoprotein peptidase, enterokinase, activates trypsinogen by a proteolytic cleavage. Then, the active form of trypsinogen, trypsin, catalyzes the activation of the other inactive proenzymes [1]. The main pancreatic proenzymes, their counterpart activated enzymes as well as their physiological functions are summarized in Table 1.

Table 1. Pancreatic digestive proenzymes and enzymes [1]

Enzyme	Proenzyme	Physiological function
Trypsin	Trypsinogen	Activation of other proenzymes Digestion of proteins
Chymotrypsin	Chymotrypsinogen	Digestion of proteins
Carboxypeptidase	Pro-carboxypeptidase	Digestion of proteins
Elastase	Pro-elastase	Digestion of proteins
α- amylase	-	Digestion of starch and glycogen
Lipase	-	Triglyceride hydrolysis
Phospholipase	Pro-phospholipase	Phospholipid hydrolysis
Cholesterol esterase	-	Cholesterol esters hydrolysis
DNAase	-	DNA hydrolysis to free nucleotides
RNAase	-	RNA hydrolysis to free nucleotides

The secretion of digestive enzymes occurs through exocytosis [10]. The acinar cell is a polarized secretory cell with two different apical and basolateral plasma membrane domains [1]. In order to ensure a rapid release of the digestive enzymes during meal, inactive digestive enzymes are stored in zymogen granules at the apical surface of the acinar cell, near the secretion site [10]. In response to several secretagogue agents including cholecystokinin (CCK), secretin, gastrin-releasing peptide (GRP), acetylcholine, and vasoactive intestinal polypeptide (VIP), the content of zymogen granules is secreted to the ductal system [1]. Vagal stimulation and the entry of fatty acids, bile salts and polypeptides into the duodenum trigger the release of acetylcholine and CCK by duodenal cells, which in turn stimulate acinar cells to secrete the digestive enzymes [11, 12]. On the other hand, acidification and the presence of fatty acids and bile salts into of the duodenum cause production of secretin and VIP by duodenal cells [13-15]. Secretin and VIP contribute to stimulate the secretion of acinar cells, but also trigger the release of bicarbonate and water by duct cells [7].

1.2 Definition and classification of acute pancreatitis

Regarding the inflammatory processes that affect the exocrine pancreas, acute pancreatitis is one of the most relevant. Most episodes of acute pancreatitis are mild and self-limiting, however, sometimes appear as a severe disease that leads to local and systemic complications [16].

The first description of acute pancreatitis was in 1652 by the Dutch anatomist Nicholas Tulp [17]. Nevertheless, the first systematic analysis of acute pancreatitis was not published until 1882 by Reginald Fitz [18]. He contributed decisively to the current concept of acute pancreatitis reviewing the clinical symptoms of 53 cases of acute pancreatitis, addressing several of its etiologies and greatly facilitating subsequent pancreatic research at the turn of the 20th century. In his publication, Fitz proposed a descriptive classification of pancreatitis into acute, hemorrhagic, and suppurative pancreatitis based on clinical and pathological features of this disease [18]. Later, other authors such as Joske, Howard and Dreiling and Blumenthal and Probstein proposed other classifications based on the etiology of the disease [19]. Unfortunately, these classifications were not widely applicable to clinical practice, so additional efforts were necessary to establish a clinical-based classification system [17, 18]. The principal problem to devise a useful clinical-based classification system was the variability in the presentation and in the clinical course of acute pancreatitis. The Atlanta Symposium in 1992 achieved a global consensus to define a universal clinical classification system in acute pancreatitis [20]. According to the 1992 Atlanta Symposium, acute pancreatitis was defined as an acute inflammatory process of the pancreas with variable involvement of other regional tissues or remote organ system associated with raised pancreatic enzyme levels in blood and/or urine [20, 21].

The 1992 Atlanta Classification distinguished mild acute pancreatitis from the severe form of the disease [20]. Mild acute pancreatitis was associated with minimal organ dysfunction lacking the features of severe acute pancreatitis. Severe acute pancreatitis was associated with organ failure and/or local complications such as necrosis, abscess or pseudocyst [20, 21]. Nevertheless, some of the definitions reached at the Atlanta symposium proved confusing and it was necessary to introduce several new terms [22]. In addition, a better understanding of the pathophysiology of this disease and an improvement in diagnostic imaging techniques made it necessary to revise the Atlanta Classification [21-23]. Therefore, in order to establish a more accurate definition and classification system for acute pancreatitis, the Atlanta Classification was revised in 2012. New modern concepts of the disease were incorporated to the updated revision of the Atlanta Classification to address areas of confusion, to improve clinical assessment of severity, to enable standardized reporting of data, to assist the objective evaluation of new treatments, and to facilitate communication among physicians and institutions [22].

According to the 2012 revised version of the Atlanta Classification, the definition of acute pancreatitis requires two of the following three features: (1)

abdominal pain consistent with acute pancreatitis (acute onset of a persistent, severe, epigastric pain often radiating to the back); (2) serum lipase activity (or amylase activity) at least three times greater than the upper limit of normal; and (3) characteristic findings of acute pancreatitis on contrast-enhanced computed tomography (CECT) and less commonly magnetic resonance imaging (MRI) or transabdominal ultrasonography [22].

The 2012 revised Atlanta classification distinguished two types of acute pancreatitis based on morphological criteria:

(1) **Interstitial edematous pancreatitis** characterized by a diffuse, occasionally localized, enlargement of the pancreatic tissue due to interstitial edema without recognizable tissue necrosis. It is accompanied by inflammation of the pancreatic fat and sometimes peripancreatic fluid. The clinical symptoms usually resolve within the first week [22, 24].

(2) **Necrotizing pancreatitis** with pancreatic parenchymal necrosis and/or peripancreatic necrosis. The necrotizing area commonly involves both the pancreas and the peripancreatic tissues. It may have a variable evolution: it may remain solid or liquefy, remain sterile or become infected, persist or disappear over time. Infected necrosis, rare during the first week, is associated with increased morbidity and mortality [22]. When organ failure and infected pancreatic necrosis are both present the relative risk of mortality is dramatically increased, and the disease is extremely severe [25].

The 2012 revised Atlanta classification also included a standard classification of the severity of acute pancreatitis. This classification defines three degrees of severity (mild, moderately severe, and severe) based on the presence or absence of organic failure and its duration as well as on the presence or absence of local or systemic complications [22]. In order to characterize the organ failure associated with acute pancreatitis, during the last decades several scoring systems were developed including the Ranson criteria [26, 27], Glasgow score [28], Acute Physiology and Chronic Health Evaluation (APACHE) II system [29, 30], Marshall Score [31] and Sequential Organ Failure Assesment (SOFA) score [32]. Nevertheless, the 2012 revised Atlanta classification recommended the use of a modified Marshall scoring system to classify accurately the severity of acute pancreatitis. According to the revised Atlanta classification, organ failure is defined as a score of 2 or more for one of the following three organ systems: respiratory, cardiovascular and renal [22].

Furthermore, the revised Atlanta classification established the presence or absence of local or systemic complications as another important criterion in the classification of severity of acute pancreatitis [22]. Systemic complications include any exacerbations of pre-existing comorbidities that precipitate along with acute pancreatitis, while local complications include acute peripancreatic fluid collection, pancreatic pseudocyst, acute necrotic collection and walled-off necrosis. Other local complications are gastric outlet dysfunction, splenic and portal vein thrombosis, and colonic necrosis [22, 33].

Thus, according to the definitions described above, the revised Atlanta criteria classify the severity of acute pancreatitis as follows [22]:

(1) **Mild acute pancreatitis** is characterized by absence of organ failure and absence of local or systemic complications.

(2) **Moderately severe acute pancreatitis** is defined by the presence of transient organ failure (less than 48 hours) and/or local complications, such as peripancreatic collection, resulting in prolonged abdominal pain,

leukocytosis and fever, and/or exacerbations of comorbidities such as coronary artery disease, chronic liver disease or chronic lung disease triggered by acute pancreatitis.

(3) **Severe acute pancreatitis** characterized by persistent single or multiple organ failure (> 48 hours). Patients with persistent organ failure usually develop local and systemic complications.

1.3 Etiology

Despite Claude Bernard associated the reflux of bile as a triggering cause of acute pancreatitis in 1856 [34], the etiology of the disease was still a matter of intense speculation during the late 19th and early 20th century. In 1901, Eugene Opie proposed the migration of gallstones into the common bile duct as the main cause of acute pancreatitis, which would lead to a reflux of bile into the pancreatic duct. He reached this conclusion after observing in two autopsies of young patients the presence of a gallstone occluding the orifice of the pancreatic duct [35]. To substantiate his hypothesis, which he named “the common channel hypothesis”, he performed various animal experiments infusing bile into the pancreatic duct, which resulted in the induction of acute hemorrhagic pancreatitis [16, 17]. Nevertheless, since then, many other causes of acute pancreatitis have been discovered, increasing substantially our knowledge about the etiology of this disease.

Nowadays, the two main causes of acute pancreatitis are gallstones (including small gallstones and microlithiasis) and alcohol abuse, accounting for more than 80% of cases [36, 37]. Although the first cause of acute pancreatitis are gallstones, alcohol consumption increases the risk of acute pancreatitis in a dose-dependent manner and it is especially high in heavy drinkers [38-40].

The risk factors for acute pancreatitis include certain metabolic conditions, medications, duct obstruction, trauma, and vascular disorders (ischemia) [36, 37]. Hypertriglyceridemia is the most important metabolic factor associated with acute pancreatitis [41]. In fact, even moderate serum levels of triglycerides increased the risk of acute pancreatitis [42]. It is noteworthy that obesity increases the risk of local and systemic complications in acute pancreatitis [43, 44]. Indeed, a body mass index >30 and a higher percentage of body fat are associated with higher risk of severe acute pancreatitis [45]. In addition, obese rats with acute pancreatitis showed increased systemic complications and higher mortality rates than control animals [46, 47].

Other metabolic risk factors associated with acute pancreatitis are hypercalcemia, renal failure and acidosis [41]. Regarding medications, several drugs have been associated with the developing of acute pancreatitis such as azathioprine, thiazides and estrogens [36, 48]. Pancreatic duct obstruction induced by a pancreatic tumor or some anatomic abnormalities of the pancreas, such as annular pancreas and ductal stricture, can subsequently trigger acute pancreatitis [36, 41]. Nevertheless, in around 20% of cases, the cause of acute pancreatitis cannot be determined, and they are classified as idiopathic acute pancreatitis [36].

1.4 Epidemiology

According to a recent update on the burden of gastrointestinal disorders, acute pancreatitis is the third most common gastrointestinal cause of hospital admissions [49]. Acute pancreatitis caused approximately 279.145 hospitalizations in the United States and the hospitalizations costs reached $2.6 billion annually [49].

The annual incidence of acute pancreatitis in the United States ranges from 13 to 45/10.000 persons [41]. In Europe, the incidence largely varies from 4,6 to 100 cases per 100.000 inhabitants, having the eastern and northern countries the highest rates [50]. In Spain, retrospective study using the Spanish National Hospital Database revealed that the incidence is 72/100.000 inhabitants-year [51].

The epidemiological variations of acute pancreatitis related to age and gender depend on its etiology. In children, the main causes of acute pancreatitis are trauma, systemic diseases, infections, and drugs [16]. Regarding the gender, although equal proportions of men and women developed acute pancreatitis, alcohol-related acute pancreatitis was more common in men [40]. In contrast, it is more likely related to gallstones, surgery, autoimmune diseases or idiopathic causes in women [41]. Nevertheless, this trend may vary attending, for example, to differences in alcohol consumption between geographical locations [38]. On the other hand, the risk of acute pancreatitis was 2-3 folder higher among Blacks than in Whites; however, the reasons for this racial disparity remains unclear [52].

The mortality rate of acute pancreatitis varies from 1% to 5% and it is closely related to its severity [41]. In 80% of patients, acute pancreatitis is mild and usually resolves within days, but in up to 20% appears in its severe form causing substantial morbidity and mortality [16]. In fact, the presence of infected necrotizing pancreatitis as well as organ failure increased the mortality rate up to 30% [25]. Although hospitalizations due to acute pancreatitis exhibited an increase during the last decade, several studies have reported a significant reduction in the mortality rate and length of hospital stay associated with acute pancreatitis [53-55]. Nowadays, the mild cases of acute pancreatitis and the related complications are becoming easier to detect, and the intensive care management is better. Nevertheless, the disease-related morbidity and the hospitalization costs of acute pancreatitis are still significant [38, 55].

1.5 Pathogenesis

In 1896, Hans Chiari proposed the autodigestion of the pancreatic gland as the central mechanism responsible for acute pancreatitis [56]. The detection of activated pancreatic enzymes within the pancreas in clinical and experimental forms of acute pancreatitis was the basis to support that the intracellular activation of trypsinogen could lead to pancreatic autodigestion [57]. This led to the hypothesis that the acinar injury underlying this autodigestive process would trigger the inflammatory response during acute pancreatitis [58]. Nevertheless, it was not until the middle of the 20th century when the development of new animal models allowed to improve our knowledge about the molecular mechanisms involved in the initiation of acute pancreatitis [17, 58].

Nowadays, it is considered that there are three characteristic responses in acinar cells in the early phases of acute pancreatitis: (1) intracellular activation of proteases, (2) changes in the secretory phenotype and (3) activation of the inflammatory response and cell death. Frequently, these responses are interrelated and act synergistically during the initiation and progression of acute pancreatitis [8].

1.5.1 Intracellular activation of zymogens

Strong experimental evidences support that the early activation of trypsinogen has a central role in the pathogenesis of acute pancreatitis. The activation of trypsinogen was detected early in the course of acute pancreatitis [57] and Whitcomb *et al.* reported that hereditary pancreatitis is caused by a mutation in the cationic trypsinogen gene [59]. In addition, overexpression of serine protease inhibitor Kazal type 1 (SPINK1), which forms an inhibitory stable complex with trypsin, ameliorated the severity of experimental acute pancreatitis [9, 16, 60].

The molecular mechanism responsible for the early activation of trypsinogen during acute pancreatitis remains unclear. Diverse morphologic studies have shown that trypsinogen activation occurs by lysosomal hydrolases in small vesicles and in larger vacuoles identified as lysosomes and/or endosomes [61-63]. Steer *et al.* proposed that lysosomal hydrolases such as cathepsins and digestive zymogens co-localize with lysosomes in acute pancreatitis, leading to trypsinogen activation by cathepsin B and subsequent autodigestive injury [58]. Although cathepsin inhibitors and genetic deletion of cathepsin B ameliorated the severity of experimental acute pancreatitis [64, 65], newer specific inhibitors of cathepsin have shown that trypsin activity is not critically involved in intrapancreatic trypsinogen activation during acute pancreatitis [66]. In addition, subcellular redistribution of cathepsin B did not induce trypsinogen activation nor acute pancreatitis [67]. Thus, other authors have proposed alternative mechanisms to explain the activation of intracellular zymogens in acute pancreatitis [8]. Some of these alternative mechanisms are commented below.

As optimal intracellular Ca^{2+} concentrations ($[Ca^{2+}]_i$) are required to activate proteases [68] and this process is highly dependent on the spatial and temporal distribution of Ca^{2+} [69, 70], a disruption in this factor have been associated with the early intracellular activation of zymogens in acute pancreatitis [71, 72]. Furthermore, zymogen activation requires a low pH compartment [73]. A large number of acidic vacuoles were detected in pancreas with acute pancreatitis [74] and chloroquine, an agent that rise intracellular pH, reduced zymogen activation and ameliorated the severity of acute pancreatitis

[75]. In addition, inhibition of vacuolar ATPase, which acidifies many intracellular compartments, diminished cerulein-induced trypsinogen activation [76].

On the other hand, zymogen activation have been also associated with the autophagic process [77]. Although autophagosome formation is stimulated in acute pancreatitis [78], lysosomal dysfunction leads to autophagic impairment [79]. In basal conditions, the autophagic process mediates the physiological degradation of digestive enzymes in autolysosomes, where zymogens colocalize with cathepsins [80]. However, during acute pancreatitis the defective lysosomal proteolytic activity leads to inefficient autophagic degradation of zymogens and intra-acinar activation of trypsin [77]. The roles of cathepsin B and cathepsin L in this process is opposite: whereas cathepsin B converts trypsinogen to trypsin, cathepsin L degrades both [81]. According to this hypothesis, lysosomal dysfunction in acute pancreatitis results in imbalance between these two cathepsins. Consequently, the activity of cathepsin L was lower than cathepsin B, which lead to the accumulation of trypsin in the autophagic vacuoles [78]. Nevertheless, the precise role of autophagy in the pathogenesis of acute pancreatitis remains to be elucidated [77].

In general, the pathological activation of zymogens decisively contributes to the pathogenesis of acute pancreatitis, but the exact mechanism that regulates it remains unclear.

1.5.2 Secretion of zymogens

Together with the early activation of zymogens in pancreatic tissue, a recognized feature of acute pancreatitis is a dramatic decrease in secretion of digestive enzymes from acinar cells. Thus, the retention of activated enzymes could be a mechanism underlying cell damage caused by early activated zymogens in acute pancreatitis [8].

During acute pancreatitis, the reduction in pancreatic secretion has been attributed to three pathologic factors: (1) decreased apical secretion from the acinar cell; (2) disruption of the paracellular barrier in the pancreatic duct; and (3) redirection of secretion from the apical pole to the basolateral regions of the acinar cell [73]. These three factors together lead to the intracellular retention of activated zymogens and their release to the pancreatic interstitial space [8]. Nevertheless, the molecular mechanisms that explain these pathological responses are not fully understood.

1.5.3 Inflammatory response and cell death

For many years, the paradigm of the pathogenesis of acute pancreatitis was the intracellular activation of trypsin. Nevertheless, different works have shown that early zymogen activation is not the only factor associated with the initiation of acute pancreatitis [82-84]. Thus, another important early event associated with acute pancreatitis is the expression of inflammatory mediators and the subsequent inflammatory response in acinar cells [58]. In 2011, Dawra *et al.* used a novel genetic mouse model with a deletion in the most prominent form of trypsinogen, trypsinogen-7 in which total trypsinogen content was reduced by 60% [84]. After cerulein-induced acute pancreatitis these mice lacked pathologic activation of trypsinogen that led to reduce acinar cell necrosis. Nevertheless, these mice showed similar degrees of local and systemic inflammation than wild type mice [84]. Accordingly, other works have shown that intracellular trypsinogen activation is directly associated with pancreatic acinar cell death, but not with the inflammatory response [65, 85-87].

Therefore, trypsinogen activation is only one face of the multifaceted response associated with acute pancreatitis. In this new “multifaceted paradigm” (Figure 2), the inflammatory response plays a central role in the initiation and progression of acute pancreatitis [58, 88]. During acute pancreatitis, the inflammatory response can promote further acinar cell injury, including necrosis, creating a feed-forward process that induces more inflammation [88].

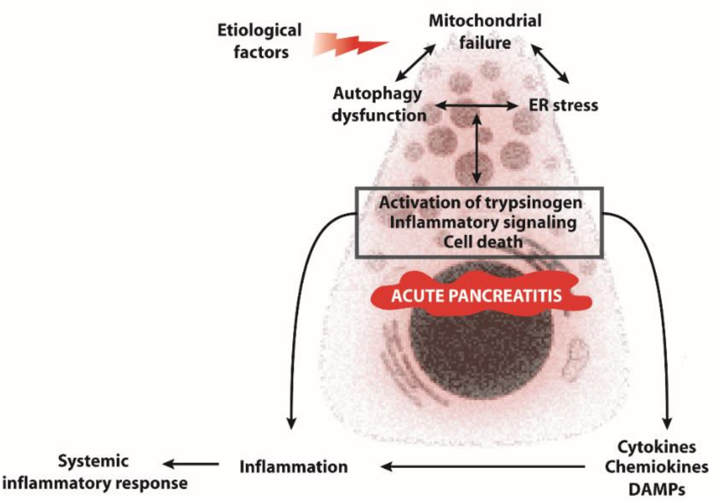
Etiological factors
Mitochondrial failure
Autophagy dysfunction
ER stress
Activation of trypsinogen
Inflammatory signaling
Cell death
ACUTE PANCREATITIS
Systemic inflammatory response
Inflammation
Cytokines
Chemiokines
DAMPs

Figure 2. Multifaceted paradigm of the pathogenesis of acute pancreatitis. When acinar cells are injured, several pathologic mechanisms are simultaneously activated promoting early trypsinogen activation, inflammation, and cell death. The inflammatory response increases acinar injury and promote systemic inflammation.

1.5.3.1 Inflammatory signaling pathways

The inflammatory response comprises the coordinated activation of different signaling pathways in cells by primary inflammatory stimuli. The most important inflammatory signaling pathways in acute pancreatitis include nuclear factor kappa-B (NF-κB) and mitogen-activated protein kinases (MAPKs), although the activator protein-1 (AP-1), Janus kinase (JAK)-signal transducer and activator of transcription (STAT) pathways and the inflammasome also play an important role [89, 90].

(1) Nuclear factor kappa B (NF-κB)

In 1986 Ranjan Sen and David Baltimore found a protein binding on a specific conserved DNA sequence in the mouse κ light-chain gene intronic enhancer in the nuclei of activated B lymphocytes. They named this protein nuclear factor binding near the κ light-chain gene in B cells or nuclear factor kappa B (NF-κB) [91]. Nowadays, NF-κB has been found in the enhancers or promoter regions of hundreds of genes, including those related to the inflammatory response as well as other cellular functions [92]. In these genes, NF-κB binds to a nearly palindromic DNA sequence with a consensus of 5’-GGGRNWYYCC-3’ (N, any base; R, purine; W, adenine or thymine; Y, pyrimidine), named kB region [93].

In mammals, the NF-κB family includes five related transcription factors subdivided into two classes: one class comprises p65/RELA, RELB, and c-REL, and the other class includes p50 (and its precursor p105) together with p52 (and its precursor p100) [94, 95]. p65/RELA, RELB, and c-REL are synthesized as mature proteins and contain a C-terminal transactivation domain (TAD). The TAD region confers to p65/RELA, RELB and c-REL the ability to promote the initiation of gene transcription. However, in the case of p105 and p100, these proteins lack TAD but contain a C-terminal region with ankyrin repeats (AnkR), which is post-translationally cleaved to form p50 and p52, respectively (Figure 3) [93, 96].

The five protein members of the NF-κB family interact with each other to form homodimers or heterodimers through an amino-terminal REL homology region (RHD) [94, 95]. RHD is a conserved 300 amino acid long region followed by a nuclear localization sequence (NLS) shared among these five proteins. RHD is required for DNA binding, interaction with inhibitor of kappa B (IκB) proteins, nuclear translocation as well as dimerization [97]. The two most common heterodimeric combinations are p50-p65 and p52-RELB, although up to 15 different compositions are possible including p50-p50 and p52-p52 homodimers or p52-p65 and p-50-RELB heterodimers [93, 95].

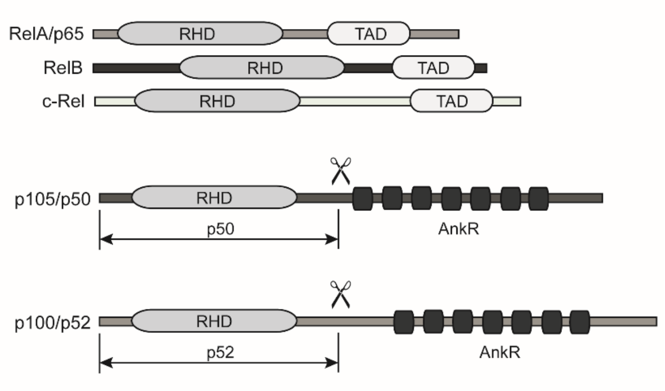

Figure 3. The NF-κB family members. Schematic view of the proteins comprising the NF-κB family. AnkR, ankyrin repeats; NLS, nuclear localization sequence; RHD, REL homology region; TAD, transactivation domain.

NF-κB activation can occur through the canonical or non-canonical pathways (Figure 4). As a response to a variety of signals, including inflammatory cytokines, pathogen-associated molecules, and antigen receptors, NF-κB can be activated through the canonical pathway. The canonical pathway involves the inhibitor of kappa B kinase (IKK) complex formed by the regulatory subunit NF-kB essential modifier (NEMO, also called IKKγ/FIP-3/IKKAP), and two kinase subunits, IKKα and IKKβ [93, 97]. IKKβ phosphorylates IκB, an inhibitory protein that binds NF-kB dimers composed of p65, c-REL and p50 -mainly p65-p50 heterodimers- retaining them in the cytoplasm. The IκB protein family includes three typical IκB proteins, IκBα, IκBβ, and IκBε; and two atypical IκB proteins, B-cell lymphoma 3-encoded protein (BCL-3) and IκBζ with functions different from maintaining NF-κB dimers sequestered in the cytoplasm [98]. The phosphorylation of IκB by IKKβ promotes its degradation by proteasome 26S and the release of NF-κB dimers for nuclear translocation [93, 97, 99].

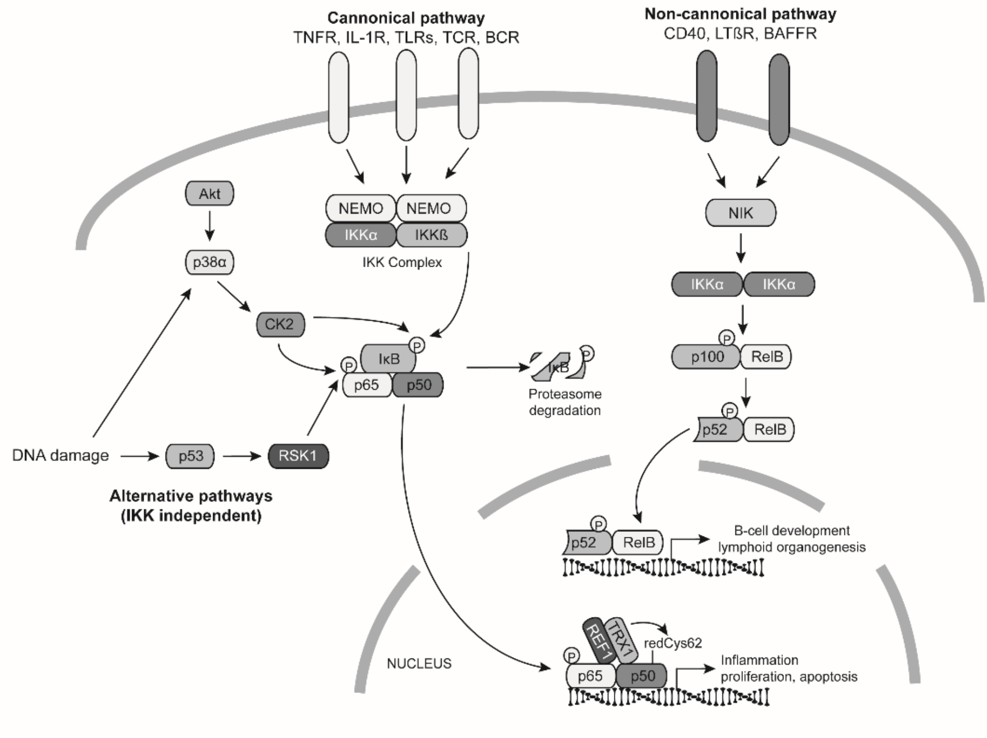
Cannonical pathway
TNFR, IL-1R, TLRs, TCR, BCR
Non-cannonical pathway
CD40, LTßR, BAFFR
Akt
p38α
NEMO
NEMO
IKKα
IKKß
IKK Complex
NIK
IKKα
IKKα
CK2
P
IκB
p65
p50
IκB
Proteasome degradation
p100
RelB
p52
RelB
DNA damage
p53
RSK1
Alternative pathways (IKK independent)
p52
RelB
B-cell development lymphoid organogenesis
REF1
TRX1
redCys62
NUCLEUS
p65
p50
Inflammation proliferation, apoptosis

Figure 4. NF-κB signaling pathways. Representation of the different NF-κB activation pathways: canonical, non-canonical, and alternative pathway. AKT, Protein kinase B; BAFF-R, B-cell-activating-factor receptor; BCR, B cell receptor; CK2, casein kinase 2; IκB, inhibitor of kappa B; IKK, inhibitor of kappa B kinase; IL1-R, interleukin-1 receptor; LTβR, lymphotoxin-b receptor; NEMO, NF-κB essential modifier; NIK, NF-κB-inducing kinase; REF-1, redox-factor 1; RSK1,ribosomal s6 kinase-1; TCR, T-cell receptor; TLRs, Toll-like receptors; TNFR, Tnf-α receptor 1; TRX1, thioredoxin-1.

NF-κB activation can also occur through the non-canonical pathway, an IκB-independent pathway triggered by at least three members of the TNF receptor superfamily: CD40, lymphotoxin-β receptor (LTβR), and B-cell-activating-factor receptor (BAF-R) (Figure 4) [95]. Activation of the non-canonical NF-κB pathway causes sequential activation of NF-κB-inducing kinase (NIK) and IKKα

[100]. Subsequent phosphorylation of p100 by IKKα leads to its polyubiquitinylation and processing to generate p52-containing complexes, primarily p52-RELB. p52-RELB dimers induce the expression of essential genes for B-cell development and lymphoid organogenesis [93, 95, 101].

Apart from the canonical and non-canonical pathways, NF-κB activation can also be triggered through alternative IKK-independent mechanisms [102] (Figure 4). UV induced NF-κB activation through the p38-casein kinase 2 (CK2) axis that phosphorylated IκBα and subsequently induced p65-p50 translocation into the nucleus [103]. In addition, DNA-damage agents such as doxorubicin induced nuclear translocation of p65 by a p53 and ribosomal s6 kinase-1 (RSK1)-dependent pathway, as p65 phosphorylation by RSK1 decreased its affinity for IκBα triggering its translocation into the nucleus [104].

NF-κB can induce or repress the expression of hundreds of genes. Hence, a fundamental feature of NF-κB is the high selective ability to regulate only a subset of target genes after its activation [105]. The different homodimeric and heterodimeric forms of NF-κB family members contribute to this selective response but, in recent years, other selective protein–protein interactions with other transcription factors, coregulatory proteins, and chromatin proteins have emerged as potential contributors to the transcriptional specificity of NF-κB [93, 106]. This is an additional level of complexity in the rich NF-κB signaling network not yet fully explored.

In cerulein model of acute pancreatitis, NF-kB activation occurs in a biphasic manner. Transient degradation of IκBα underlies the first phase of NF-kB activation. The second phase is initiated after IκBα returned to the basal levels and it is sustained by IκBβ degradation [107]. Several factors have been identified as activators of NF-kB during acute pancreatitis including CCK, proinflammatory cytokines, and reactive oxygen species (ROS) [108]. In addition, damage-associated molecular pattern molecules (DAMPs) released from dead, dying or injured pancreatic acinar cells, such as nuclear DNA (nDNA), mitochondrial DNA (mtDNA), histones, extracellular nucleosomes, high-mobility group box 1 (HMGB1), and adenosine triphosphate (ATP) can activate NF-kB during acute pancreatitis [109]. In cerulein induced-acute pancreatitis in mice, nDNA, mtDNA and ATP released from injured acinar cells bound to Toll-like receptor (TLR)-9 in pancreatic macrophages inducing subsequent nuclear translocation of NF-kB [110]. Furthermore, HMGB1-induced pancreatic injury in mice with acute pancreatitis was mediated through the TLR4-NF-kB signaling pathway [111].

The impact of NF-κB activation on the inflammatory response during acute pancreatitis has been widely studied [108]. Inhibition of NF-κB pathway ameliorated the inflammatory response in acute pancreatitis [108, 112, 113] whereas overexpression of p65 or IKKβ increased the severity of acute pancreatitis [114-116]. It is noteworthy that although the lack of IKKα triggered spontaneous pancreatitis in mice, the underling mechanism is independent of NF-κB activation. The loss of IKKα in acinar cells diminished autophagic protein degradation and led to the accumulation of p62 aggregates and endoplasmic reticulum (ER) stress [117]. Strikingly, genetic ablation of p65 in pancreatic exocrine cells induced severe injury in acinar cells in mice with cerulein-induced acute pancreatitis [118]. Indeed, mice with pancreas-specific deletion of IκBα exhibited a constitutive activation of p65 and, in these mice, acute pancreatitis was attenuated. However, pancreas-specific deletion of both IκBα and p65 increased its severity [119]. p65 regulates the expression of a protective cluster of NF-κB-regulated genes against acute pancreatitis, including pancreatitis-associated protein 1 (PAP1), a protein that protects acinar cells from death, as well as serine protease inhibitor 2A *(*SPI2a) [118, 119].

In general, these data suggest a complex pleiotropic role of NF-κB regulating both pro- and anti-inflammatory pathways in acute pancreatitis. Therefore, given the complexity of the IKK/IκB/NF-κB system, further studies are required to clarify the tight regulation of NF-κB during acute pancreatitis [113].

(2) Mitogen-activated protein kinases (MAPKs)

MAPKs are a family of serine/threonine protein kinases that drive cellular responses to a variety of stimuli. Each MAPK signaling cascade comprises at least three components: a MAPK, a MAPK kinase (MAPKK), and a MAPK kinase kinase (MAPKKK). MAPKKKs phosphorylate and activate MAPKKs and subsequently MAPKKs phosphorylate and activate MAPKs [120]. Once activated, MAPKs phosphorylate target substrates on serine or threonine residues. In mammals, four different MAPKs have been identified: extracellular signal-regulated kinase 1 and 2 (ERK1/2), c-Jun N-terminal kinase (JNK), p38, and ERK5 [89, 121]. The components of each MAPK family are summarized in Figure 5.

ERK1/2, JNK and p38 are activated early in the course of acute pancreatitis and are highly involved in the development of the inflammatory response [122, 123]. During acute pancreatitis, activation of MAPKs regulates the activation of NF-kB as well as the synthesis of other pro-inflammatory mediators [123, 124]. Pharmacological inhibition of MAPKs reduced the synthesis of cytokines and ameliorated the severity of acute pancreatitis [123, 125, 126]. In addition, MAPK-activated protein kinase (MK)-2-knockout-mice exhibited less cytokine production and pancreatic damage after cerulein-induced acute pancreatitis [127].

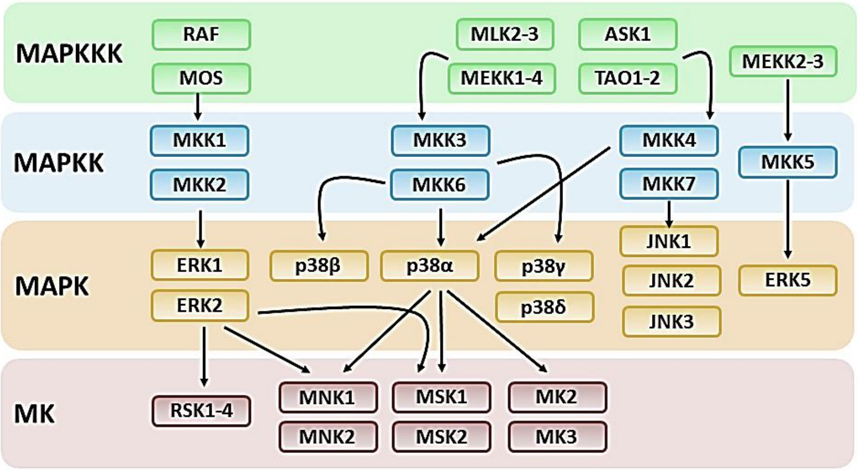
MAPKKK
RAF
MOS
MLK2-3
MEKK1-4
ASK1
TAO1-2
MEKK2-3
MAPKK
MKK1
MKK2
MKK3
MKK6
MKK4
MKK7
MKK5
MAPK
ERK1
ERK2
p38β
p38α
p38γ
p38δ
JNK1
JNK2
JNK3
ERK5
MK
RSK1-4
MNK1
MNK2
MSK1
MSK2
MK2
MK3

Figure 5. MAPKs pathways. Overview of mitogen-activated protein kinases (MAPKs) family and pathways [89, 121]. ASK1, apoptosis signal-regulating kinase 1; ERK1/2, extracellular signal-regulated kinase 1 and 2; JNK, c-Jun N-terminal kinase; MAPKK, MAPK kinase; MAPKKK, MAPK kinase kinase; MK, mitogen-activated protein kinase-activated protein kinase; MLK, mixed lineage kinase; MNK, mitogen-activated protein kinase interacting protein kinase; MOS, Moloney murine sarcoma virus serine/threonine kinase; MSK, mitogen and stress activated protein kinase; RAF, rapidly accelerated fibrosarcoma kinase; RSK, ribosomal s6 kinase; TAO, thousand-and-one amino acid protein kinase.

1.5.3.2 Cytokines

An early key event associated with the inflammatory response during acute pancreatitis is the expression of proinflammatory mediators by acinar cells and resident macrophages in pancreas [128]. These proinflammatory mediators include cytokines and chemokines. Cytokines are a family of low-molecular weight proteins (<40 kDa) secreted by different types of cells in response to an inflammatory stimulus [129]. The most relevant proinflammatory cytokines involved in acute pancreatitis are (1) tumor necrosis factor-α (TNF-α), (2) interleukin-6 (IL-6) and (3) interleukin-1 (IL-1β) [130]. Chemokines are a family of small molecules involved in leukocyte activation and trafficking into the inflamed areas. During acute pancreatitis, both cytokines and chemokines act locally and amplify the inflammatory cascade inducing the infiltration of inflammatory cells including neutrophils, monocytes, and lymphocytes to the pancreatic tissue [128, 131]. The inflammatory process is balanced by the release of anti-inflammatory cytokines such as interleukin-10 (IL-10) [128, 131].

(1) Tumor necrosis factor-α (TNF-α)

TNF-α was discovered in 1975 as an endotoxin-inducible molecule with cytotoxic activity [132]. It is a member of the cytokine family that plays an essential role in many cellular responses including inflammation, cell differentiation, proliferation, apoptosis, necrosis, and survival [133]. TNF-α is a transmembrane 26 kDa protein (pro-Tnf-α), which is cleaved by the TNFα-converting enzyme (TACE), to release the 17 kDa active soluble form of TNF-α [134]. TNF-α is produced by inflammatory cells, such as monocytes and macrophages, but it can also be expressed by other cell types including acinar cells [133, 135]. Gukovskaya *et al.* showed that not only inflammatory cells can produce TNF-α in pancreas. Acinar cells can also produce, release, and respond to TNF-α during acute pancreatitis [136]. In fact, in experimental models of acute pancreatitis the primary sources of TNF-α are pancreatic acinar cells, and later TNF-α is produced by immune infiltrating cells [137, 138]. The expression of *Tnf-α* is transcriptionally controlled by NF-κB, AP-1, and nuclear factor associated with activated T cells (NFAT) [131]. Blockade of NF-κB activation prevented the expression of TNF-α and attenuated the severity of cerulein-induced acute pancreatitis in rats [139].

Intracellular TNF-α signaling is initiated by interaction of this cytokine with two different surface receptors, 55 kDa TNF-α receptor 1 (TNFR-1) and 75 kDa TNF-α receptor 2 (TNFR-2). TNFR1 is ubiquitously expressed, whereas TNFR2 is mainly expressed on lymphocytes and endothelial cells [133]. The extracellular domains of TNFR-1 and TNFR-2 are homologous, but the intracellular domains are distinct, so either receptor can mediate different downstream responses. TNFR1 contains a death domain absent in TNFR2. This domain recruits other signaling proteins including TNFR1-associated death domain protein (TRADD). TNFR1 interaction with TRADD promotes the recruitment of TNFR-associated factor (TRAF)-2 or TRAF-5 and receptor-interacting protein kinase (RIPK)-1, triggering the inflammatory response through the activation of NF-κB or MAPKs [133, 140].

Inhibition of TNF-α signaling seems to be an effective strategy to decrease the inflammatory response in experimental models of acute pancreatitis. Thus, recombinant soluble TNFR-1 as well as polyclonal anti-TNF antibody significantly reduced the inflammatory response and tissue damage in experimental acute pancreatitis [141, 142]. In addition, genetic deletion of TNFR1 as well as etanercept administration, a novel anti-TNF-alpha agent, ameliorated the course of experimental acute pancreatitis in a similar degree [143]. Our group showed that pentoxifylline decreased TNF-α levels and reduced pancreatic inflammation and edema in cerulein-induced acute pancreatitis in rats [144]. In addition, pentoxifylline markedly reduced the expression of intercellular adhesion molecule 1 (*Icam1*) and nitric oxide synthase 2 (*Nos2*) in AR42J cells [145].

(2) Interleukin-6 (IL-6)

First discovered in 1986 by Hirano *et al.* [146] IL-6 belongs to the IL-6 family cytokines, a group of cytokines which includes IL-6, IL-11, ciliary neurotrophic factor (CNTF), leukemia inhibitory factor (LIF), oncostatin M (OSM), cardiotrophin 1 (CT-1), cardiotrophin-like cytokine (CLC), and IL-27 [147]. These cytokines are grouped in one family because they use the common signaling receptor subunit glycoprotein 130 kDa (gp130) [148]. gp130 is a protein expressed in all cell types and thus, the expression of a second binding receptor

(IL-6R in the case of IL-6) may determine whether a specific cell type responds or not to a specific IL-6 family cytokine [147].

Hence, IL-6 signaling pathway requires both IL-6R and gp130. IL-6 binds to the IL-6R and this complex recruits and promotes gp130 dimerization, which triggers intracellular signaling [147]. Once activated gp130 recruits Janus kinases (JAKs), which phosphorylate specific tyrosine residues in the cytoplasmic domain of gp130, providing binding sites for STATs through their conserved SH2 domains [147, 149]. In the case of gp130, the major signal transducers through this receptor are JAK1 and STAT3 [147]. Binding of STAT3 to phosphorylated gp130 receptors causes STAT3 phosphorylation and its dimerization [149]. Then, STAT3 dimers translocate into the nucleus, where they enhance the transcription of a large variety of genes related to the inflammatory response, proliferation, cell survival, and cell migration [150-152].

In the early 1990s, it was discovered that IL-6R can be cleaved from the cell surface by an unknown protease at that time [153, 154]. Interestingly, soluble IL-6R (sIL-6R) in presence of IL-6 stimulated cells that not express IL-6R [155]. This process was called IL-6 trans-signaling [156]. IL-6 trans-signaling has received great attention in recent years because it provides new insights into the complexity of IL-6-dependet signaling pathways. Some cells that do not express IL-6R and thus were considered unresponsive to IL-6, now are recognized as susceptible to IL-6 stimulation through IL-6 trans-signaling [147]. Importantly, accumulative evidences show that proinflammatory activities of IL-6 depend mainly on the trans-signaling pathway via sIL-6R, whereas the anti-inflammatory action of IL-6 is mediated through classical IL-6 signaling [147].

During experimental acute pancreatitis, *Il-6* is up-regulated in acinar cells and serum levels of IL-6 dramatically increase [157-160]. Interestingly, serum levels of IL-6 correlated with the severity of acute pancreatitis and thus, it is considered a reliable severity marker [161, 162]. Accordingly, inhibition of IL-6 signaling ameliorated acute pancreatitis and its associated lung injury [127, 163, 164]. Remarkably, the systemic effects of secreted IL-6 in pancreatitis seem to be mediated by trans-signaling after complexation with sIL-6R which triggered persistent and strong STAT3 phosphorylation in the pancreas and high circulating levels of neutrophil attractant chemokine C-X-C motif ligand 1 (CXCL1) that correlated with acute lung injury [165]. In fact, the IL-6 trans-signaling/STAT3/CXCL1 pathway, but not classical IL-6 signaling, seems to mediate IL-6-dependent acute lung injury in acute pancreatitis [165].

(3) Interleukin-1β (IL-1β)

The IL-1 family comprises 11 members: IL-1α, IL-1β, IL-1 receptor antagonist (IL-1Ra), IL-18, IL-33 and IL-1F5–IL-1F10 [166]. IL-1 signaling is initiated through a family of IL-1 receptors that includes 10 members [167]. These receptors contain extracellular immunoglobulin domains and a Toll/IL-1 receptor (TIR) domain in the cytoplasmic portion [166]. When the cytokine binds to the receptor (IL-1 receptor type I (IL-1R1) in the case of IL-1) a second receptor subunit is recruited. This second receptor is the IL-1R accessory protein (IL-1RAP) for IL-1 [166]. As result of receptor heterodimerization, TIR domains recruits myeloid differentiation primary response protein 88 (mYD88), IL-1R- associated kinase 4 (IRAK4), TRAF-6 or other signaling intermediates. These bindings trigger the activation of NF-κB and MAPKs signaling pathways [166].

Human IL-1β was first purified in 1977 [168] and it is mainly produced by monocytes and macrophages [166]. IL-1β is synthesized as an inactive precursor (pro- IL-1β) and accumulates in the cytosol until it is processed when cells are exposed to pathogen-associated molecular pattern molecules (PAMPs) or DAMPs stimulation [167, 169]. PAMPs and DAMPs activate cytosolic pattern recognition receptors (PRRs), often the nucleotide-binding domain and leucine-rich repeat containing receptor (NLR) family -among which is NLRP3-, to form large multiprotein complexes called inflammasomes [169]. Inflammasomes are composed of PRR, pro-caspase-1, and an adaptor protein called apoptosis-associated speck-like protein containing a caspase recruitment domain (ASC), which interact through homology binding domains [170]. After inflammasome activation, pro-IL-1β is cleaved by caspase-1 to a mature form that is secreted [169].

Il-1β expression in pancreas was rapidly up-regulated in acute pancreatitis in mice [171]. In fact, caspase-1, ASC, and NLPR3 were required for development of the inflammatory response in acute pancreatitis, and hence genetic deletion of *Tlr9* reduced pancreatic edema, inflammation, and pro-IL-1β expression in pancreas with pancreatitis [172]. In addition, inhibition of caspase-1 reduced the death rate associated with severe acute pancreatitis in rats [173].

1.5.3.3 Cell death pathways

During acute pancreatitis, cell death occurs in pancreatic acinar cells via two main mechanisms: apoptosis and necrosis [174]. Current evidence suggests that activation of a specific program of cell death decisively contributes the severity of acute pancreatitis. The induction of pancreatic acinar cell apoptosis protected mice against cerulein-induced pancreatitis [175] and accordingly, suppression of the apoptotic cascade in pancreatic acinar cells led to necrotizing pancreatitis [176]. In addition, mild acute pancreatitis was associated with presence of apoptotic acinar cells, whereas severe acute pancreatitis involved extensive acinar cell necrosis and abrogated apoptosis [177]. Therefore, at present it is accepted that the severity of experimental pancreatitis directly correlates with the extent of necrosis [176], whereas apoptosis is considered a favorable response by opposing to the necrotic cell fate [178]. However, the precise mechanisms that regulate the switch between apoptosis and necrosis cell death during acute pancreatitis remain to be elucidated.

(1) Apoptosis

Apoptosis is a genetically regulated and programmed form of cell death characterized by cell shrinkage, chromatin condensation, DNA cleavage and flipping of phosphatidylserine from the inner to the outer side of the membrane [179]. In contrast to necrosis, apoptosis does not cause inflammation because the structural integrity of the plasma membrane is preserved and thus, the intracellular components are not released [174, 176].

Apoptosis may occur through two distinct pathways: the extrinsic and intrinsic pathways (Figure 6). The extrinsic pathway is initiated by activation of death receptors such as TNFR1, Tnf-α-related apoptosis-inducing ligand receptor (TRAIL-R) or FAS, which trigger activation of the initiator caspase-8 (or caspase-10) [178, 180]. Caspases are a family of cysteine–aspartic proteases constitutively expressed as proenzymes that undergo activation by proteolytic cleavage [181]. Activation of the initiator caspases (caspase 2, 8, 9 and 10) leads to activation of effector caspases (caspase 3, 6 and 7) [182]. Effector caspases cleave a large number of proteins located in the cell membrane, nucleus, and cytoplasm, causing the morphological features of apoptotic cells [179, 182]. Apoptosis is regulated by c-FLICE-like inhibitory protein (c-FLIP), which inhibits activator caspases [183], and by the inhibitor of apoptosis proteins (IAPs), which inhibits both activator and effector caspases [184]. The most important mammalian IAPs is the X-linked IAP (XIAP), which binds and inactivates caspases 3, 7 and 9 [185, 186].

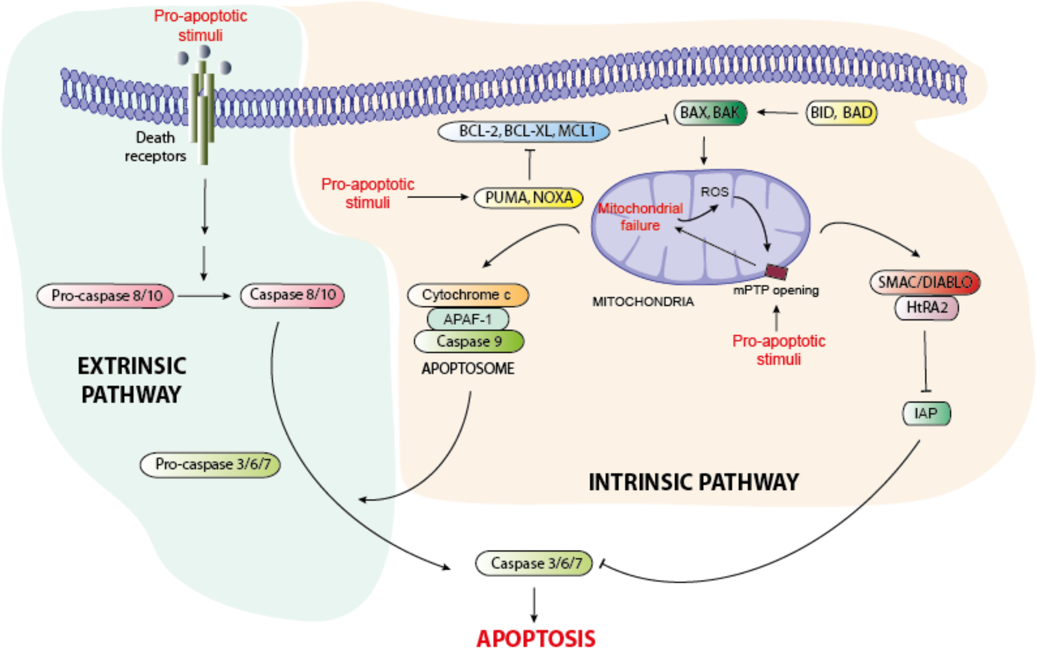
Pro-apoptotic stimuli
Death receptors
Pro-caspase 8/10
Caspase 8/10
EXTRINSIC PATHWAY
Pro-caspase 3/6/7
BCL-2, BCL-XL, MCL1
BAX, BAK
BID, BAD
Pro-apoptotic stimuli
PUMA, NOXA
Mitochondrial failure
ROS
mPTP opening
MITOCHONDRIA
Pro-apoptotic stimuli
Cytochrome c
APAF-1
Caspase 9
APOPTOSOME
SMAC/DIABLO
HtRA2
IAP
INTRINSIC PATHWAY
Caspase 3/6/7
APOPTOSIS

Figure 6. Apoptosis signaling pathways. Overview of the extrinsic and intrinsic apoptosis pathways. The extrinsic pathway is initiated by the activation of death receptors. The intrinsic pathway involves the permeabilization of the mitochondrial membrane and the release of pro-apoptotic factors. APAF-1, protease-activating factor 1; BAD, BCL-2 associated agonist of cell death; BAK, Bcl-2 homologous antagonist/killer; BAX, BCL-2-associated X protein; BCL-2, B-cell lymphoma 2; BCL-XL, B-cell lymphoma-extra large; BID, BH3 interacting-domain death agonist; HtRA2; HtrA serine peptidase 2; IAP, inhibitor of apoptosis proteins; MCL1, induced myeloid leukemia cell differentiation protein; NOXA, phorbol-12-myristate-13-acetate-induced protein 1; PUMA p53 upregulated modulator of apoptosis; SMAC/DIABLO, second mitochondria-derived activator of caspase/diablo homolog.

On the other hand, the intrinsic pathway involves permeabilization of the mitochondrial outer membrane, which leads to release of pro-apoptotic factors including second mitochondria-derived activator of caspase/diablo homolog (SMAC/DIABLO), HtrA serine peptidase 2 (HtRA2), and cytochrome c [178]. In the cytoplasm, the released mitochondrial proteins trigger caspase activation directly (cytochrome c) or indirectly (Smac/DIABLO and HtRA2) [187]. Mitochondrial-released cytochrome c binds to the scaffold protein apoptotic protease-activating factor 1 (APAF1) to form the apoptosome, a molecular platform that activates initiator and effector caspases [188, 189]. SMAC/DIABLO and HtRA2 bind and neutralize caspase-inhibitory proteins such as XIAP [190-192]. It is noteworthy that in the cytoplasm, the proapoptotic activity of mitochondrial proteins is regulated by the joint action of pro- (BAX, BAK, and BOK) and antiapoptotic (BCL-2, BCL-XL, BCL-w, MCL-1, and A1) B-cell lymphoma 2 (BLC-2) protein family members [187, 193]. In addition, another relevant family of apoptotic regulators is BCL-2 homology 3 (BH3)-only proteins, which include BH3 interacting-domain death agonist (BID), BCL-2 associated agonist of cell death (BAD), phorbol-12-myristate-13-acetate-induced protein 1 (NOXA), p53 upregulated modulator of apoptosis (PUMA), among others [193, 194]. These proteins can activate proapoptotic BCL-2 family members or inactivate its antiapoptotic members [194].

Mitochondria have a decisive role in apoptosis [195]. Opening of the mitochondrial permeability transition pore (mPTP) in response to pro-inflammatory stimuli or elevated levels of Ca^{2+} in the mitochondrial matrix is crucial to trigger the release of cytochrome c and the subsequent initiation of apoptosis [196, 197]. In addition, ROS can modify key proteins of apoptotic pathways leading to collapse of the mitochondrial membrane potential ($\Delta\psi_m$), mPTP opening, mitochondrial translocation of BCL-2-associated X protein (BAX) and BAD, and cytochrome c release [198, 199].

On the other hand, p53 is a key factor in the regulation of apoptosis. p53 exhibits a very short half-life and it is expressed in low levels in cells [200]. In response to stress, DNA damage or chronic mitogenic stimulation, p53 is transiently stabilized and activated [201, 202]. p53 induces mainly apoptosis by direct transcriptional activation of pro-apoptotic BH3-only proteins PUMA and NOXA [200]. In addition, translocation of p53 into the mitochondria also regulates apoptosis induction. In the mitochondria, p53 physically interacts with antiapoptotic BCL-2 protein family members and proapoptotic BCL-2 homologous antagonist/killer (BAK) causing BAK oligomerization, mitochondrial pore formation, permeabilization of the outer membrane, and release of cytochrome c and other pro-apoptotic factors [203-206]. Multiple mechanisms for p53 mitochondrial translocation have been proposed, which involve different p53 post-translational modifications including murine doble minute (MDM2)-2 -mediated monoubiquitination and p53 phosphorylation at Ser46 [204]. In unstressed cells the cytoplasmic pool of p53 is inactivated and degraded via MDM2-mediated polyubiquitination [207]. Upon stress conditions, homeodomain-interacting protein kinase 2 (HIPK2) induces p53 phosphorylation at Ser46 and the subsequent recruitment of peptidyl-prolyl cis-trans isomerase NIMA-interacting 1 (PIN1) causing a phospho-dependent cis/trans isomerization of p53 [208-210]. As a result, p53 reduces its affinity for Mdm2, resulting in a switch from polyubiquitination to monoubiquitination that masks the p53 nuclear localization sites promoting mitochondrial translocation of p53 [211]. In the mitochondria, p53 is rapidly deubiquitinated by herpesvirus-associated ubiquitin-specific protease (HAUSP), which in turn favors p53 interaction with the MDM4/BCL-2/ BCL-XL complex [212].

Activation of apoptosis during acute pancreatitis and its protective role are related with the inflammatory response. However, pro-inflammatory cytokines exhibited a dual role regulating cell death in acute pancreatitis. NF-κB dependent activation of TNF-α enhanced the percentage of apoptotic cell death in pancreas with acute pancreatitis [159, 213]. In contrast, apoptosis activation via NF-κB/TNF-α axis in acinar cells is concomitant with augmented levels of the TNF-α -induced antiapoptotic PAP1 [214]. It is noteworthy that NF-κB regulates the expression of a large number of antiapoptotic genes, including *c-IAPs, c-Flip, Xiap and Pap1* [118, 215]. Strikingly, overexpression of *Pap1* reduced the extent of necrosis and inflammation found in the pancreas of mice with selective deletion of p65 without affecting the number of apoptotic cells [118]. However, when *Pap1* expression was abolished, both apoptosis and necrosis increased in pancreas with pancreatitis [216]. On the other hand, deletion of *Xiap* attenuated the severity of acute pancreatitis by increasing apoptosis and decreasing necrosis as well as the activation of NF-κB [217]. In addition, blockade of IL-6 enhanced acinar cell apoptosis, diminished necrosis, and attenuated acute pancreatitis [163].

Taken together, these results suggest the existence of a complex interplay, not yet fully understood, between apoptosis and necrosis in acute pancreatitis [178]. NF-κB-dependent anti-apoptotic gene expression has been demonstrated to be crucial to regulate the balance between these two types of cell death in acute pancreatitis [217, 218]. Nevertheless, the contribution of other mechanisms, including those related with mitochondrial dysfunction, are discussed below.

(2) Necrosis and necroptosis

Necrosis is characterized by severe cellular changes including mitochondrial swelling, disruption of actin cytoskeleton, cell swelling, membrane blebbing, and leakage of intracellular content [174, 178]. In contrast to apoptosis, which is an ATP-dependent process, the most relevant pathophysiological feature of necrosis is ATP depletion [219]. Severe depletion of ATP triggers ATP-dependent failure of ion pumps, leading to an influx of Na^+ and water that results in swelling and collapse of the cell [220]. In addition, ATP depletion activates nonselective Ca^{2+} channels, resulting in massive cytosolic Ca^{2+} accumulation [178]. Increased levels of Ca^{2+} activate endonucleases and proteases which degrade DNA as well as structural and signaling proteins, respectively [178, 220].

Mitochondrial membrane permeabilization and mPTP opening is a common event of both necrosis and apoptosis [219]. In necrosis, opening of mPTP causes loss of $\Delta\Psi_m$ and ATP depletion [221, 222]. Increased levels of cytosolic [Ca^{2+}] and ROS stimulate mPTP opening [223-225]. In response to oxidative stress, p53 translocates into the mitochondria and triggers PTP opening by physical interaction with the mPTP regulator cyclophilin D (CYPD) causing necrosis [203].

Interestingly, the pattern of acinar cell death in acute pancreatitis seems to be regulated at the mitochondrial level. Indeed, acute pancreatitis induced Ca^{2+}-dependent loss of $\Delta\Psi_m$ causing mPTP opening, ATP depletion, and necrosis [226-230]. Conversely, other authors reported that mitochondrial depolarization in acute pancreatitis triggered cytochrome c release and apoptosis [231-233]. It has been proposed that oscillatory rises of cytosolic Ca^{2+} in acinar cells in response to moderate stress, cause transient mitochondrial depolarization, which induces apoptosis [174]. However, sustained pathological elevations of cytosolic [Ca^{2+}], as occur in severe acute pancreatitis [234], may lead to persistent mPTP opening and irreversible inhibition of mitochondrial function, causing dramatic ATP depletion and necrosis [174]. Therefore, mitochondrial ATP production is crucial in the regulation of cell death fate and accordingly, necrosis induction by mPTP opening was prevented by maintaining intracellular ATP in CCK-stimulated isolated pancreatic acinar cells [235, 236].

Booth *et al.* reported that increased levels of mitochondrial ROS induced by bile acids promoted apoptosis but protected against necrosis in pancreatic acinar cells [236], whereas inhibition of mitochondrial ROS generation shifted the balance from apoptosis toward necrosis, and large sustained increased levels of [Ca^{2+}] in the mitochondria caused necrosis [236]. However, it is important to note that the effect of ROS on cell death fate seems to be dependent on their ROS levels. Thus, low H_2O_2 concentrations (1-10 μM) promoted acinar cell apoptosis, whereas higher levels (0.5-1 mM) elicited rapid necrosis through a CYPD-independent mechanism [237]. Interestingly, although lower H_2O_2 doses decreased O_2 consumption, they did not cause ATP depletion. In contrast, higher levels of H_2O_2 abrogated ATP turnover and caused bioenergetic collapse in acinar cells [237].

For decades, necrosis has been considered an uncontrolled form of cell death. However, in recent years it has been reported that necrosis cell death can be triggered through complex signal transduction pathways and execution mechanisms [238, 239]. This regulated form of necrosis, different from nonregulated necrosis that occurs by physical or chemical injuries, was named necroptosis [240]. Necroptosis is defined as a genetically controlled cell death process, morphologically characterized by cytoplasmic granulation and cellular swelling that eventually results in leakage of intracellular components [241]. Thus, necroptosis is considered an inflammatory type of death because the released intracellular material can act as DAMPs, which in turns promote inflammatory responses in distal tissues [242]. Consequently, it has been proposed that necroptosis plays a decisive role in inflammatory diseases, including acute pancreatitis [243-246].

The necroptosis pathway is regulated by RIPK1 and RIPK3 and its downstream substrate pseudokinase mixed-lineage kinase domain–like (MLKL) [243]. Typically, necroptosis is regulated by Tnf-α when caspase-8 is inhibited [247, 248]. Tnf-α-dependent TNFR1 stimulation recruits TRADD, which binds to RIPK1, cellular inhibitor of apoptosis protein (cIAP) 1, cIAP2, TRAF2 and TRAF5. Then, RIPK1 is polyubiquitinated by cIAP1 and cIAP2, promoting the recruitment of transforming growth factor-β-activated kinase (TAK1), TAK1 binding protein (TAB)-2 or TAB3, and the IKK complex which in turns activates NF-κB [241].

Subsequently, cylindromatosis lysine 63 deubiquitinase (CYLD) removes polyubiquitins from RIPK1 triggering RIPK1 dissociation and allowing its interaction with FAS-associated death domain (FADD), pro-caspase 8 and FLIPs [241, 249, 250]. Activated caspase 8 cleaves and inactivates RIPK1 and RIPK3 preventing necroptosis activation [251, 252]. However, when caspase 8 is inhibited, RIP1K and RIP3K form the necrosome signaling complex to trigger necroptosis [253]. Within the necrosome, RIP1K and RIP3K phosphorylate each other, further stabilizing the complex [244]. Phosphorylated RIPK3 then phosphorylates MLKL triggering the formation of oligomers that translocate and destabilize the plasma membrane (Figure 7) [243, 254-256].

Although TNF-α-dependent signaling is considered the prototypical pathway for necroptosis activation, novel mechanisms are emerging some of them involving mitochondrial dysfunction (Figure 7) [257]. Inhibition of mitochondrial ROS attenuated necroptosis activation, but this effect was not found blocking cytoplasmic ROS generation [258, 259]. Recently, it has been reported that mitochondrial ROS activate RIP1K autophosphorylation via oxidation of three specific cysteines in RIPK1, promoting RIPK3 recruitment into the necrosome [260]. Furthermore, overproduction of ROS caused by ER stress and RIPK up-regulation induced mPTP opening and necroptosis [261]. In addition, upon necroptosis activation, recruitment of the mitochondrial serine/threonine protein phosphatase (PGAM5) induced mitochondrial fission factor dynamin-1-like protein (DRP1) activation, causing mitochondrial fragmentation [262]. Accordingly, necrostatin-1, an inhibitor of RIPK1, decreased DRP1 levels [263], and DRP1 blockade with metformin also rescued from necroptosis [264]. Nevertheless, some evidences have questioned the key role of mitochondria in necroptosis and it has been proposed that mitochondria could not be absolutely required for this process, at least in some cell types [257]. In fact, mitochondria-deficient cells were resistant to apoptosis, but efficiently died by necroptosis induced by TNF-α [265]. Furthermore, PGAM5 and DRP1 deletion did not prevent TNF-α-induced necroptosis [266-268]. Remarkably, Linkermann *et al.* showed that the ablation of *Ripk3* or *CypD* protected mice from necroptosis but the double knockout exhibited a higher protection, suggesting that these two independent pathways could regulate necroptosis *in vivo* [269]. Further studies are required to clarify the role of mitochondria in necroptosis execution.

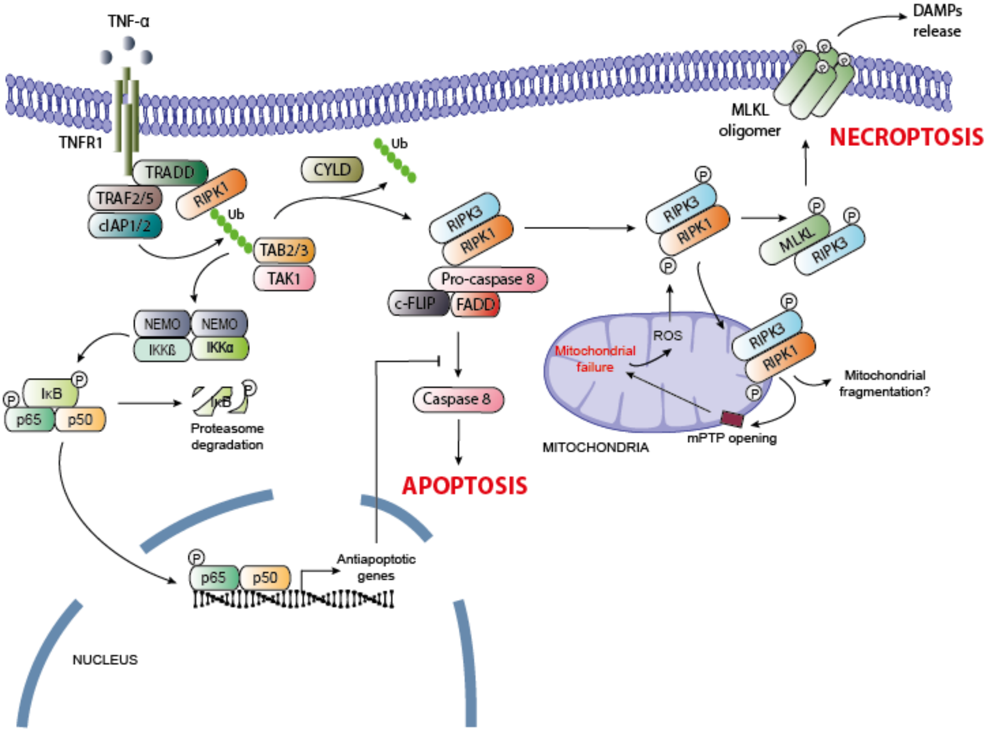
TNF-α
TNFR1
TRADD
TRAF2/5
cIAP1/2
RIPK1
Ub
CYLD
Ub
TAB2/3
TAK1
NEMO
NEMO
IKKβ
IKKα
P
IκB
P
p65
p50
IκB
P
Proteasome degradation
RIPK3
RIPK1
Pro-caspase 8
c-FLIP
FADD
Caspase 8
APOPTOSIS
P
p65
p50
Antiapoptotic genes
NUCLEUS
DAMPs release
MLKL oligomer
NECROPTOSIS
P
RIPK3
RIPK1
P
P
MLKL
P
RIPK3
ROS
Mitochondrial failure
P
RIPK3
RIPK1
P
Mitochondrial fragmentation?
mPTP opening
MITOCHONDRIA

Figure 7. Necroptosis pathway. Overview of the necroptosis pathway which leads to the formation of the necrosome signaling complex with RIP1K and RIP3K when apoptosis is inhibited. Phosphorylated RIP1K and RIP3K phosphorylates MLKL triggering the formation of oligomers that translocate and destabilize the plasma membrane allowing DAMPs release. cFLIP, c-FLICE-like inhibitory protein; cIAP, cellular inhibitor of apoptosis protein; CYLD, cylindromatosis lysine 63 deubiquitinase; DAMPs; damage-associated molecular patterns; FADD, FAS-associated death domain; IKK, inhibitor of kappa B kinase; MLKL, pseudokinase mixed-lineage kinase domain–like; NEMO, NF-kB essential modifier; RIPK, receptor-interacting protein kinase; TAB, TAK1 binding protein; TAK1, transforming growth factor-β-activated kinase 1; TNFR1, Tnf-α receptor 1; TRADD, TNFR1-associated death domain protein.

Regarding acute pancreatitis, so far, several studies have addressed the role of necroptosis in the pathophysiology of this disease. Pancreatic damage as well as serum amylase activity were reduced in RIPK3-knockout-mice with acute pancreatitis [253]. In addition, genetic *Mlkl* deficiency protected mice from cerulein-induced acute pancreatitis [270]. In contrast, strikingly inhibition of RIPK1 with necrostatin-1 increased the severity of cerulein-induced acute pancreatitis, suggesting that despite RIPK3 and RIPK1 are closely related proteins, the inhibition of both of them exhibits different dual effect in the regulation of necroptosis [271]. Hence, therapeutic inhibition of necroptosis in acute pancreatitis should be performed at the level of RIPK3 or further downstream [245]. Recently, Ma *et al.* showed that deletion of *miR-21* prevented necroptosis and reduced the severity of acute pancreatitis in two experimental models [272]. *miR-21* deletion up-regulated activated caspase 8 and reduced the RIPK3 levels in acute pancreatitis; however, elevated caspase 8 activity in *mir-21*-knockout-mice was insufficient to induce massive apoptosis [272]. In contrast, enhanced apoptosis and caspase 3 and 9 activation by *Xiap* deletion caused RIPK1 degradation, which in turn ameliorated necrosis in pancreatic tissue [217, 218].

2 Oxidative stress and redox signaling

2.1 Concept of oxidative stress

The concept of oxidative stress was first introduced in 1985 by Helmut Sies and it was defined as “a disturbance in the prooxidant-antioxidant balance in favor of the former” [273]. However, during the last decades, redox reactions have emerged as fundamental processes in normal cell physiology being this redox regulation collectively denoted as redox signaling [274]. Consequently, the original definition of oxidative stress has been updated in order to include the essential role of redox signaling in living cells [275, 276]. Thus, at present, oxidative stress is defined as “an imbalance between oxidants and antioxidants in favor of the oxidants, leading to a disruption of redox signaling and control and/or molecular damage” [276]. Nowadays, it is considered that low levels of oxidants are required to regulate physiological functions (oxidative eustress), while excessive oxidant levels cause oxidative damage in cells (oxidative distress) [273, 277, 278].

2.2 Reactive oxygen species: types and endogenous sources

Free radicals are defined as atoms, molecules, or molecular fragments containing one or more unpaired electrons in atomic or molecular orbitals [279]. The unpaired electron confers to the free radical a high reactivity degree with other molecules including proteins, lipids, or nucleic acids [279-281]. The oxidation of biomolecules can cause numerous detrimental effects in cells such as protein inactivation, oxidative membrane damage, mitochondrial depolarization, and DNA fragmentation. In general, the injuries produced by free radicals in cells are collectively named oxidative damage [282].

ROS are the most important class of oxidants in cells [279]. The addition of one electron to the triplet-state molecular oxygen ($^3O_2$) forms the superoxide anion radical ($O_2^{\bullet-}$) (Figure 8) [279, 280]. $O_2^{\bullet-}$ is mainly produced in mitochondria when the electrons leak prematurely from electron carriers associated with the electron transport chain to oxygen [283, 284]. Although the relative contribution of different mitochondrial complexes to total $O_2^{\bullet-}$ generation depends on tissue, complex I and III are principal sources of $O_2^{\bullet-}$ [285, 286]. On the other hand, $O_2^{\bullet-}$ is also produced enzymatically by xanthine oxidase (XOD) and by NAD(P)H oxidases (NOXs) [287]. XOD catalyzes the oxidation of hypoxanthine to xanthine, and xanthine to uric acid forming $O_2^{\bullet-}$ or H_2O_2 [286, 287]. NOXs are a family of multi-subunit enzymes that includes five NOX isoforms (NOX1, NOX2, NOX3, NOX4, and NOX5) and two related enzymes (dual oxidase (DUOX)1 and DUOX2). NOX isoforms catalyze $O_2^{\bullet-}$ production by the reduction of O_2 using nicotinamide adenine dinucleotide phosphate (NADPH) or nicotinamide adenine dinucleotide (NADH) as the electron donor [286, 288, 289]. NOX2 is the prototypical isoform found in phagocytic cells such as macrophages and neutrophils. In these cells, the production of $O_2^{\bullet-}$ occurs during the respiratory burst and it is necessary for bacterial destruction [287, 290]. The nonphagocytic NOXs generate 1–10% of the superoxide levels produced in neutrophils, but play an essential role in redox signaling [279]. Furthermore, cytochrome P-450, cyclooxygenase, and lipoxygenase can also produce $O_2^{\bullet-}$ [291].

$O_2^{\bullet-}$ is rapidly reduced in cells spontaneously or enzymatically by superoxide dismutase (SOD) into the nonradical species H_2O_2 (Figure 8) [280]. In mammals there are three isoforms of SOD: SOD1 (CuZnSOD) mainly located in the cytosol, SOD2 (MnSOD) located in the mitochondrial matrix, and SOD3 (ecSOD) present in the extracellular matrix. In the active site of the enzyme, a redox active transition metal (Cu^{2+} or Mn^{3+}) is alternately reduced and reoxidized to dismutate $O_2^{\bullet-}$ to H_2O_2 [292].

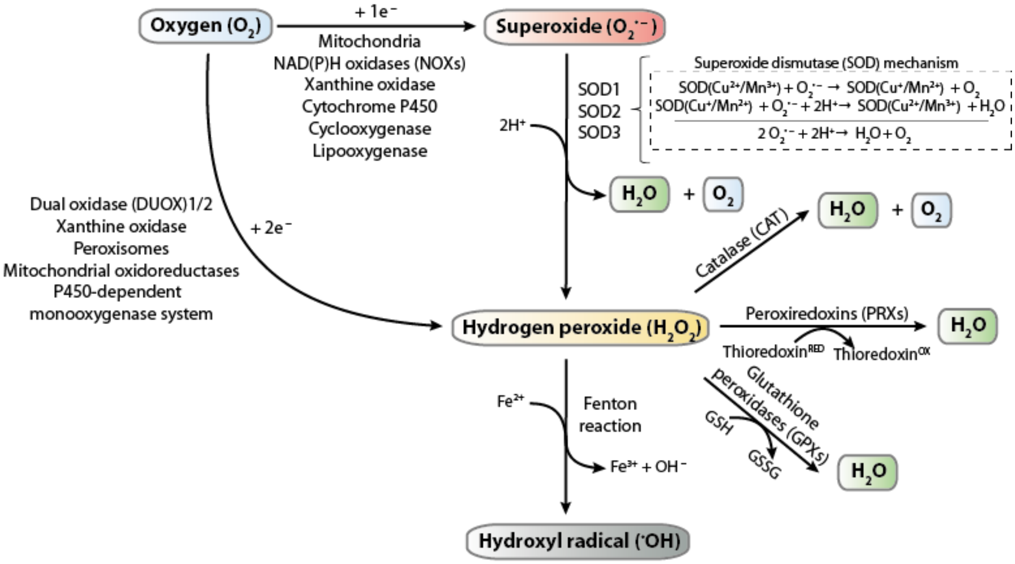
Oxygen (O_2)
+ 1e⁻
Mitochondria
NAD(P)H oxidases (NOXs)
Xanthine oxidase
Cytochrome P450
Cyclooxygenase
Lipooxygenase
Superoxide ($O_2^{\bullet -}$)
SOD1
SOD2
SOD3
2H⁺
Superoxide dismutase (SOD) mechanism
$SOD(Cu^{2+}/Mn^{3+}) + O_2^{\bullet -} \rightarrow SOD(Cu^{+}/Mn^{2+}) + O_2$
$SOD(Cu^{+}/Mn^{2+}) + O_2^{\bullet -} + 2H^{+} \rightarrow SOD(Cu^{2+}/Mn^{3+}) + H_2O$
$2O_2^{\bullet -} + 2H^{+} \rightarrow H_2O + O_2$
H_2O + O_2
Catalase (CAT)
H_2O + O_2
Dual oxidase (DUOX)1/2
Xanthine oxidase
Peroxisomes
Mitochondrial oxidoreductases
P450-dependent
monooxygenase system
+ 2e⁻
Hydrogen peroxide (H_2O_2)
Peroxiredoxins (PRXs)
H_2O
Thioredoxin^{RED}
Thioredoxin^{OX}
Glutathione peroxidases (GPXs)
GSH
GSSG
H_2O
Fe²⁺
Fenton reaction
Fe³⁺ + OH⁻
Hydroxyl radical ($^{\bullet}OH$)

Figure 8. Sources of reactive oxygen species (ROS). Overview of generation and reactions of ROS.

H_2O_2 is also generated by DUOX1 and DUOX2 [293]. Furthermore, peroxisomes and the microsomal cytochrome P450-dependent monooxygenase system located in the endoplasmic reticulum, also produce H_2O_2 in cells [286]. Additionally, several mitochondrial oxidoreductases might contribute to H_2O_2 generation including monoamine oxidases [294], dihydroorotate dehydrogenase [295], α-glycerophosphate dehydrogenase [296], and α-ketoglutarate dehydrogenase complex [297].

In presence of reduced transition metals (e.g., ferrous or cuprous ions), H_2O_2 can be converted into the highly reactive hydroxyl radical ($^{\bullet}OH$) through the Fenton reaction (Figure 8) [280]. Indeed, $^{\bullet}OH$ is considered the most biologically reactive free radical in cells [298]. Catalase (CAT), peroxiredoxins (PRXs), and glutathione peroxidases (GPXs) catalyze the conversion of H_2O_2 into H_2O (Figure 8) [292].

2.3 GSH: role in antioxidant defense and redox signaling

2.3.1 Structure and function of GSH

Reduced glutathione (GSH) is the most important non-protein thiol that acts as a key intracellular antioxidant against oxidative and nitrosative stress [299]. GSH is the tripeptide γ-L-glutamyl-L-cysteinyl-glycine. The free thiol group confers to GSH the ability to intervene in redox reactions. In addition, glutamate and cysteine are linked in GSH through the γ-carboxyl group of glutamate rather than the conventional α-carboxyl group [300]. Consequently, GSH is resistant to intracellular degradation by proteases and only one membrane-bound enzyme, named γ-glutamyl transpeptidase (GGT), can degrade GSH [300, 301]. However, in recent years, a member of the γ-glutamyl cyclotransferase family, glutathione specific γ-glutamyl cyclotransferase (CHAC1), has been also implicated in GSH degradation [302].

GSH exists in cells in equilibrium with oxidized glutathione (GSSG), which is formed by a disulfide bond between two molecules of GSH [300]. Under physiological conditions, the concentration of GSH (in the range of 1-10 mM) is around 10 to 100-fold higher than that of GSSG [299, 303]. GSSG is produced in cells by GPx or through the reaction of GSH with electrophilic compounds such as free radicals, and it is efficiently reduced back to GSH by glutathione reductase (GR) [299]. Hence, GSH contributes to free radical scavenging and the GSSG/GSH ratio is considered a reliable marker of oxidative stress because it reflects the balance between antioxidant status and oxidant reactions in cells [275, 304]. In addition, as a key thiol antioxidant, GSH regulates the thiol redox status of proteins and thus, it has a relevant role in redox signaling [303]. Furthermore, GSH has a direct role in redox signaling through two mainly mechanisms: regulating protein S-glutathionylation [305], and interacting with nitric oxide (•NO) to regulate S-nitrosylation [299], as we further develop in the following sections.

2.3.2 GSH synthesis and the trans-sulfuration pathway

The synthesis of GSH depends on two ATP-requiring enzymatic steps, the first one catalysed by glutamate cysteine ligase (GCL) and the second one by GSH synthase (GS) [300]:

1. L-glutamate + L-cysteine + ATP → γ-glutamyl-L-cysteine + ADP + Pi

2. γ-glutamyl-L-cysteine + L-glycine + ATP → GSH + ADP + Pi

Methionine is an essential sulfur amino acid that is not only involved in protein biosynthesis, but it also acts as a metabolic precursor for critical metabolic pathways [306, 307]. Using S-adenosylmethionine (SAM), S-adenosylhomocysteine (SAH), homocysteine and cystathionine as intermediaries through the trans-sulfuration pathway (Figure 9), methionine acts as the primary source of cysteine, a limiting factor for the synthesis of GSH [306]. Methionine is the first precursor for synthesis of SAM, the major biological methyl donor in cells, in a reaction catalysed by methionine adenosyltransferase (MAT). SAM donates its methyl group to a large variety of acceptors molecules including nucleic acids, proteins, and lipids [300]. SAH, the product of all trans-methylation reactions, is reversibly converted into homocysteine by SAH hydrolase (SAHH). Homocysteine is condensed with serine to generate cystathionine in a reaction catalysed by cystathionine β synthase (CBS), and then cystathionine is cleaved by cystathionase (CSE) to form cysteine for GSH synthesis [300]. Hence, methionine metabolism through the trans-sulfuration pathway decisively contributes to the maintenance of redox homeostasis in cells [308].

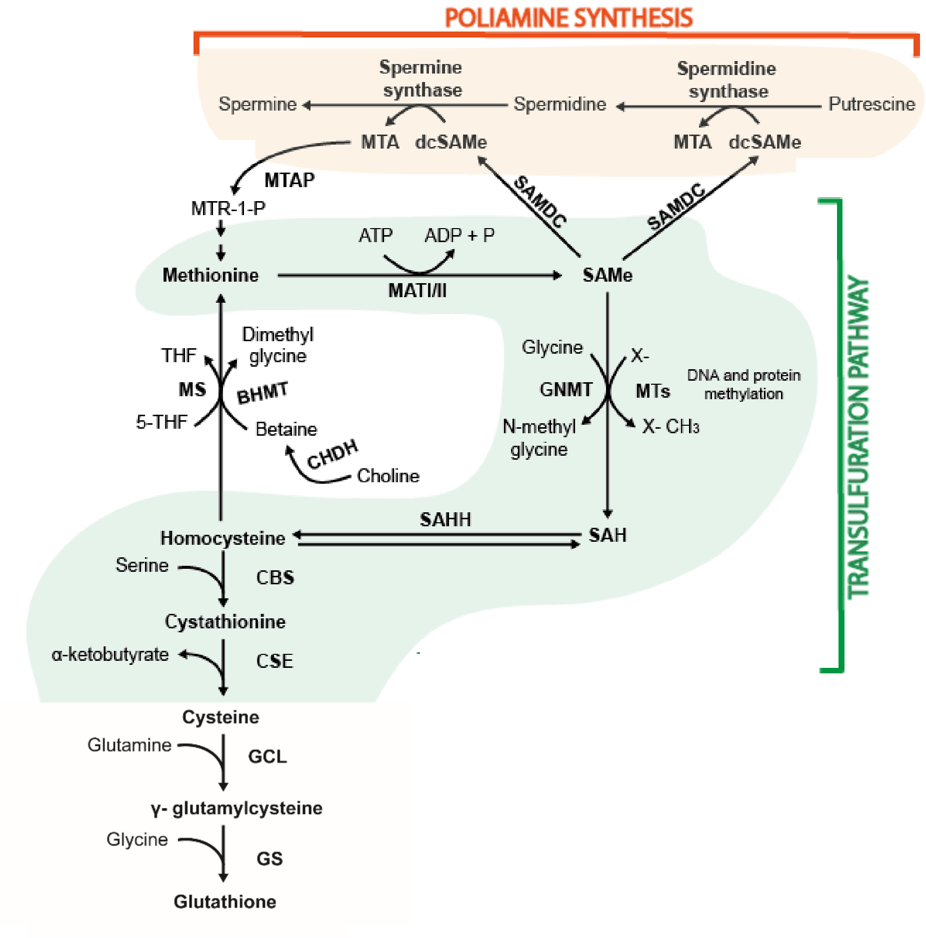
POLIAMINE SYNTHESIS
Spermine synthase
Spermidine synthase
Spermine
Spermidine
Putrescine
MTA
dcSAMe
MTA
dcSAMe
MTAP
MTR-1-P
SAMDC
SAMDC
ATP
ADP + P
Methionine
MATI/II
SAMe
TRANSULFURATION PATHWAY
THF
Dimethyl glycine
MS
BHMT
5-THF
Betaine
CHDH
Choline
Glycine
X-
GNMT
MTs
DNA and protein methylation
N-methyl glycine
X- CH3
SAHH
Homocysteine
SAH
Serine
CBS
Cystathionine
α-ketobutyrate
CSE
Cysteine
Glutamine
GCL
γ- glutamylcysteine
Glycine
GS
Glutathione

Figure 9. Methionine metabolism and trans-sulfuration pathway. MAT, methionine adenosyltransferase; SAM, S-adenosylmethionine; GNMT, glycine N-methyltransferase; MTs, methyl transferases; SAH, S-adenosylhomocysteine; SAHH, S-adenosylhomocysteine-hydrolase; CBS, cystathionine β synthase; CSE, cystathionase; GCL, glutamate cysteine ligase; GS, gluta thione synthase; CHDH, choline dehydrogenase; BHMT, betaine--homocysteine S-methyltransferase; MS, methionine synthase; THF, tetrahydrofolate; SAMDC, S-adenosylmethionine decarboxylase; dcSAM, decarboxylated SAM; MTA, methylthioadenosine; MTAP, methylthioadenosine phosphorylase; MTR-1-P, methylthioribose-1-phosphate.

Homocysteine may be remethylated via methionine synthetase (MS) into methionine to allow methionine recycling in cells (Figure 9) [309, 310]. This reaction requires 5-methyltetrahydrofolate (5-MTHF), which is derived from 5,10-methylenetetrahydrofolate (5,10-MTHF) by a reaction catalysed by methylenetetrahydrofolate reductase (MTHFR) [300]. Alternatively, SAM can be converted into decarboxylated SAM (dcSAM) to provide an aminopropyl group for the synthesis of polyamines [311].

Hence, homocysteine is a point branch that can be irreversibly metabolized through the trans-sulfuration pathway or remethylated to methionine [302]. Thus, increased level of homocysteine is considered a sign of dysregulation of the trans-sulfuration pathway and it has been detected in plasma of patients with a variety of gastrointestinal disorders including inflammatory bowel disease [312], Chron's disease [313], colorectal cancer [314] as well as acute pancreatitis [315].

2.3.3 Regulation of the trans-sulfuration pathway

CBS and CSE are key enzymes that regulate the flux through the trans-sulfuration pathway. CBS and CSE are regulated both at transcriptional and post-transcriptional levels [316].

CBS is a cytosolic homotetrametic enzyme composed of 63 kDa subunits. Each subunit consists of three domains: a highly conserved pyridoxal-5′-phosphate (PLP)-binding catalytic core; a SAM-binding C-terminal regulatory domain; and N-terminal heme binding domain [317, 318]. PLP acts as a cofactor in the catalytic mechanism mediated by CBS [319, 320]. SAM allosterically activates and stabilizes CBS [321]. In fact, SAM depletion derived from methionine restriction destabilized and decreased CBS levels [322]. In contrast, CBS activity is inhibited by CO [323, 324] and $^{\bullet}$NO [325, 326].

The role of heme in CBS structure is not clear although it seems to be associated with the redox regulation of CBS [327]. Indeed, CBS is a redox sensitive enzyme. The redox status of the heme cofactor might act as a redox modulator of CBS activity because the ferrous form of CBS exhibits lower activity than the ferric form of CBS [327]. In addition, the central domain contains a $^{272}CXX^{C275}$ motif that can form an intramolecular disulphide bond, and the reduced state of this disulphide bond further increases CBS activity ~2-3-fold [328]. Furthermore, it has been recently reported that CBS is a target of nitrosative stress and tyrosine nitration at Tyr^{163}, Tyr^{223}, Tyr^{381} and Tyr^{518} reduces its catalytic activity [329].

On the other hand, the regulation of CSE activity, the only enzyme that can directly generate cysteine *de novo* in mammals, has also a direct impact on the metabolic flux through the trans-sulfuration pathway [316]. CGL is a homotetramer enzyme composed of 45 kDa subunits, which binds to the PLP cofactor [330]. CSE is a highly inducible protein, through a large variety of transcription factors under various stressful conditions such as starvation, oxidative stress, ER stress, Golgi stress, mitochondrial stress and inflammation [316].

2.4 Peroxiredoxins: role in oxidative stress and redox signaling

2.4.1 Peroxiredoxins classification and catalytic mechanisms

First discovered in 1988 in yeast [331], PRXs are a family of cysteine-dependent peroxidase enzymes ubiquitously expressed in prokaryotes and eukaryotes, which reduce H_2O_2, alkyl hydroperoxides, and peroxynitrite ($ONOO^-$) into water [332, 333]. All PRXs contain a conserved cysteine residue in the NH_2-terminal region named peroxidatic cysteine (C_P) within a universally conserved PxxxTxxC motif (with T in some PRXs replaced by S), which is the oxidation site by ROS and reactive nitrogen species (RNS) [333-335].

PRXs are subdivided into three subfamilies: typical 2-cysteine (2-Cys) PRXs, atypical 2-Cys PRXs, and 1-Cys PRXs [336]. This classification system is based on the catalytic mechanism used by each of them, which depends on the presence and location of a second conserved cysteine residue, named resolving cysteine (C_R) [337]. 2-Cys PRXs (typical and atypical) contain a C_R residue in the COOH-terminal region of the protein, whereas it is not present in the 1-Cys PRXs subfamily [338]. In all three types of PRXs, in the first step of the catalytic mechanism (peroxidatic step) the sulhydryl group of the C_P residue attacks the peroxide substrate, forming an unstable cysteine sulfenic acid (C_P-SOH) and releasing water (Figure 10) [339]. This catalytic step requires the previous deprotonation of C_P-SH [333]. Normally, in biological systems at neutral pH, the sulhydryl groups are in their protonated forms (R-SH) because typically the pK_a for cysteine residues is ~8.5 [340]. However, the pK_a for the PRXs C_P residue is around 5.1-6.3 and thus, over 83% of the C_P residue are present in the thiolate form ($R\text{-}S^-$) at physiological pH [341, 342]. This low pK_a is because the protein microenvironment that surrounds the active site of PRXs is positively charged, lowering the cysteine residue pK_a and stabilizing the anionic thiolate form [336]. This is one of the most important reasons that explains the high reactivity of PRXs towards hydroperoxides [343].

The next step of the PRXs' catalytic mechanism (resolving step) distinguishes the three types of PRXs (Figure 10) [337]. In 2-Cys PRXs, the unstable intermediate C_P-SOH immediately reacts with the sulfhydryl group of the C_R residue located in the carboxyl terminus of another subunit forming a dimer [339]. This intermolecular disulfide bond is subsequently reduced in the third step of the catalytic mechanism (recycle step) by thioredoxin (TRX) in a reaction coupled with thioredoxin reductase (TRXR) and NADPH [333, 338]. In the non-typical 2-Cys PRXs, both C_P and C_R are located in the same polypeptide and thus, in the resolving step, C_P-SOH forms an intramolecular disulfide bond that is also reduced by TRX [344]. In 1-Cys PRXs, the C_P-SOH is resolved by a heterodimeric disulfide bond with a cysteine thiol located in the π isoform of glutathione S-transferase (πGST) [345, 346]. This heterodimeric dimer formed between the 1-Cys PRXs and πGST is then reduced using two GSH molecules [347].

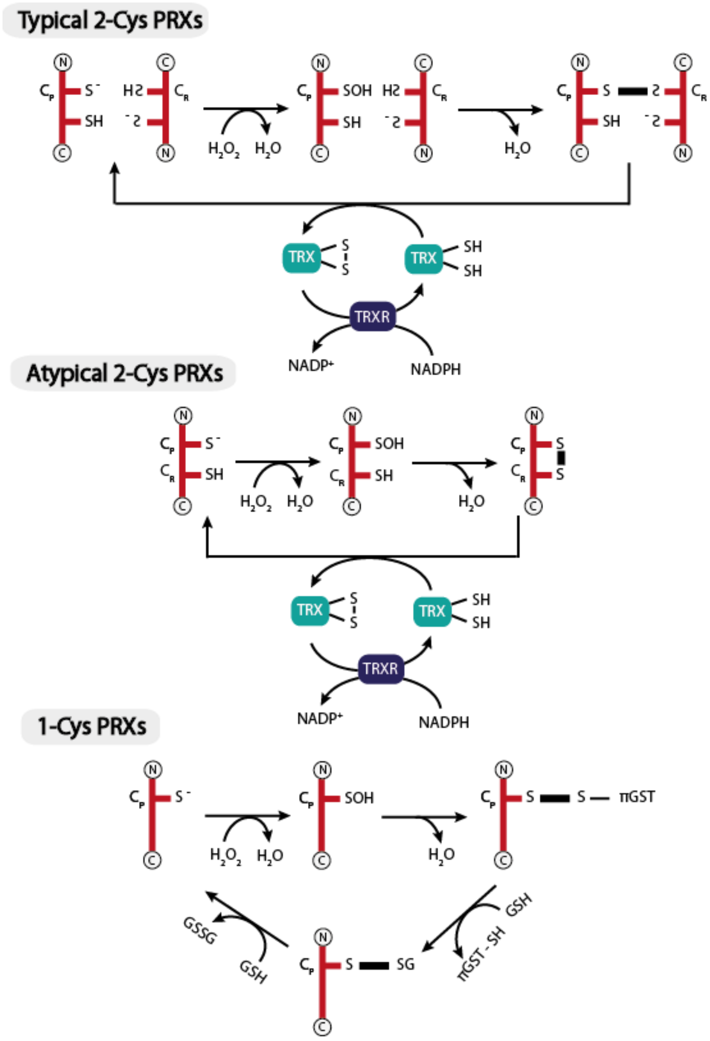
Typical 2-Cys PRXs
N
C
C_P
S^-
SH
SH
S^-
C_R
H_2O_2
H_2O
SOH
S
TRX
TRXR
NADP+
NADPH
Atypical 2-Cys PRXs
1-Cys PRXs
πGST
GSSG
GSH
SG
πGST-SH

Figure 10. Reaction mechanisms of peroxiredoxins. Catalytic mechanism of typical 2-Cys, atypical 2-Cys, and 1-Cys peroxiredoxins. C_P, peroxidatic cysteine; C_R, resolving cysteine; GSH, reduced glutathione; GSSG, oxidized glutathione; GST, glutathione S-transferase; PRX, peroxiredoxin; TRX, thioredoxin; TRXR, thioredoxin reductase.

Mammalian cells express six PRXs isoforms: four 2-Cys PRXs isoforms (PRX1, PRX2, PRX3 and PRX4), one atypical 2-Cys PRX isoform (PRX5), and one 1-Cys PRX isoform (PRX6) (Table 2) [333]. Mammalian 2-Cys PRXs are located either in the cytosol and nucleus (PRX1 and PRX2), in the mitochondria (PRX3) and in the endoplasmic reticulum (PRX4) [343, 348, 349]. PRX5 is located in the peroxisomes, mitochondria, and cytosol whereas PRX6 is exclusively cytosolic [350, 351].

Table 2. Mammalian peroxiredoxins [333]

	Subcellular location	Classification based on C_R	Subfamily
PRX1	Cytosol and nucleus	Typical 2-Cys	Prx1
PRX2	Cytosol and nucleus	Typical 2-Cys	Prx1
PRX3	Mitochondria	Typical 2-Cys	Prx1
PRX4	Endoplasmic reticulum	Typical 2-Cys	Prx1
PRX5	Peroxisomes, mitochondria, and cytosol	Atypical 2-Cys	Prx5
PRX6	Cytosol	1-Cys	Prx6

In 2011, Nelson *et al.* performed a bioinformatic analysis of 29 crystal structures and >3500 sequences of PRXs from the 2008 GenBank database, and proposed an alternative classification system for PRXs (Table 2) [352]. This is a global evolutionary classification system that subdivides PRXs enzymes into six subfamilies: Prx1, Prx5, Prx6, Tpx, PrxQ, and AhpE [353]. Prx1 comprises those traditionally referred as typical 2-Cys PRXs, including mammalian PRX1, PRX2, PRX3 and PRX4; mammalian PRX5 and PRX6 are included in the Prx5 and

Prx6 subgroup, respectively; PrxQ members are not present in animals and those members of the Tpx and AhpE subfamilies are exclusively found in bacteria [333, 343].

2.4.2 Hyperoxidation of peroxiredoxins: role of sulfiredoxin

Occasionally, during catalysis of 2-Cys PRXs, C_P–SOH is further oxidized to the sulfinic (C_P–SO_2H) or sulfonic form (C_P–SO_3H) [340, 354]. This hyperoxidation occurs when the formation of the disulfide bond between C_P–SOH and C_R–SH is slow enough to allow a faster reaction of C_P–SOH with peroxide [333]. It is noteworthy that the sensitivity for hyperoxidation significantly varies among mammalian PRXs. Thus, mitochondrial PRX3 is greatly more resistant to hyperoxidation than PRX1 and PRX2 [334, 339]. Recently, Bolduc *et al.* determined that PRX1 was 10-fold more resistant than PRX2 to hyperoxidation and PRX3 was 25-fold more resistant than PRX2 [332].

As a result of hyperoxidation, the peroxidase activity of PRXs decreases leading to inactivation of these enzymes [340]. However, in contrast with the sulfonic state of PRXs, which is an irreversible modification [336], the sulfinic state of PRXs is reversed by sulfiredoxin (SRX) [338], an enzyme first discovered by Sun *et al.* in 1994 [335] and later identified as the responsible for the reduction of C_P–SO_2H in yeast by Toledano *et al* [337].

SRX defines a conserved family of proteins with only one conserved cysteine residue widely present in eukaryotes [333, 342]. SRX catalyzes the reduction of C_P–SO_2H to C_P–SOH in a reaction that requires the conserved cysteine of SRX, ATP hydrolysis, Mg^{2+}, and a thiol as an electron donor (generally GSH or TRX) (Figure 11) [338, 344]. In response to oxidative stress, SRX is markedly upregulated in order to prevent PRXs inactivation [345, 355]. *Srxn1* gene expression is transcriptionally regulated by AP-1 and nuclear factor erythroid 2–related factor 2 (NRF-2), although the responsive elements for these two transcriptional factors are embedded in the same sequence at the promoter of SRX [356-358]. Hence, transcriptional regulation of *Srxn1* exerted by AP-1 and NRF-2 is mutually exclusive [342].

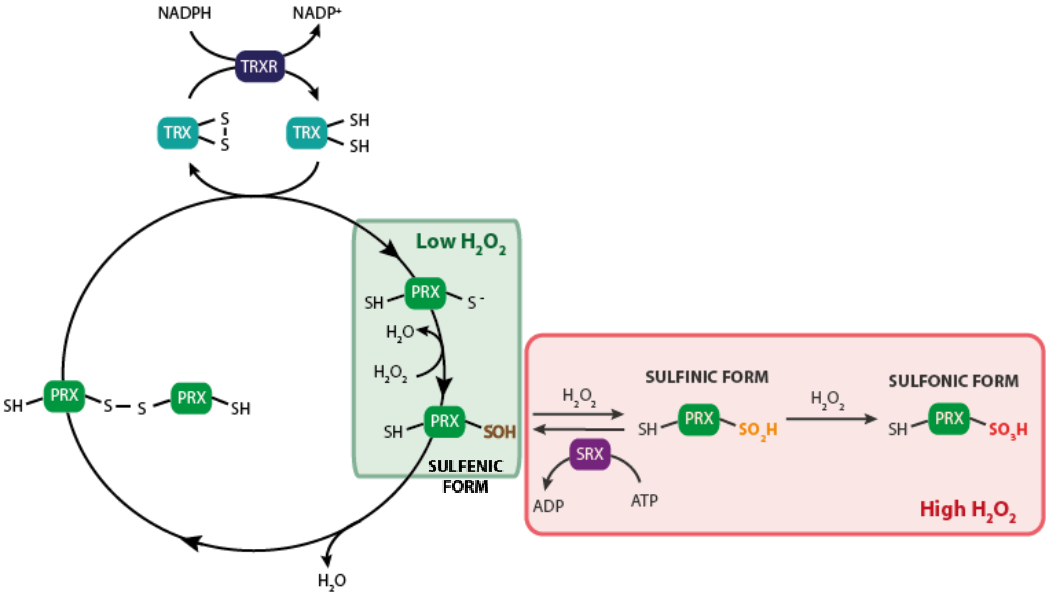
NADPH
NADP+
TRXR
TRX
S
S
TRX
SH
SH
Low H2O2
SH
PRX
S-
H2O
H2O2
SH
PRX
SOH
SULFENIC FORM
SH
PRX
S
S
PRX
SH
H2O
H2O2
SULFINIC FORM
SH
PRX
SO2H
SRX
ADP
ATP
H2O2
SULFONIC FORM
SH
PRX
SO3H
High H2O2

Figure 11. Thioredoxin-Peroxiredoxin system and role of sulfiredoxin. H_2O_2 oxidizes the peroxydatic cysteine of peroxiredoxins (PRXs) to sulfenic acid (SOH), which reacts to the resolving cysteine forming a dimer. The thioredoxin (TRX)/thioredoxin reductase system (TRXR) recovers reduced PRXs. When H_2O_2 exceeds normal levels, the peroxydatic cysteine of PRXs is hyperoxidized to sulfinic acid, which is reverted by sulfiredoxin (SRX) to the sulfenic form. The further oxidized sulfonic form (SO_3H) of peroxydatic Cys of PRXs is irreversible.

Importantly, although SRX is a cytosolic protein [344], it can translocate into the mitochondria under oxidative conditions to maintain a proper balance between mitochondrial H_2O_2 production and elimination [359]. In addition, in adrenal gland, mitochondrial translocation of SRX is coupled with the circadian oscillation of corticosterone synthesis [360]. H_2O_2 released from mitochondria triggers the formation of a disulfide-linked complex between the active cysteine of SRX and the cysteine of heat shock protein 90 (HSP90), which is imported into mitochondria through the outer membrane complex (TOM) [361]. In mitochondria, SRX is degraded by the protease LON, which restores the basal levels of SRX within this organelle [346, 361].

2.4.3 Functions of peroxiredoxins and its hyperoxidized forms

PRXs seems to be essential proteins in biology taking into account their ubiquity and abundance [343]. One of the most important functions of PRXs derives from their peroxidase activity, acting as important contributors to the antioxidant defense in cells [349]. On the other hand, during last years, it has been highlighted the essential role of PRXs modulating H_2O_2 levels in redox signaling processes [362]. The reversible hyperoxidation and resultant inactivation of PRXs provide a switch mechanism to allow oxidants to reach higher levels in order to oxidized key molecules in redox signaling pathways (floodgate model) [363-365]. Alternatively, PRXs together with associated signaling proteins can form redox relays complexes where oxidized PRXs transfer the oxidized equivalents to key proteins, such as protein phosphatases or transcription factors, promoting the activation of particular signaling cascades [362, 366-368].

It is noteworthy that, although hyperoxidation of PRXs inactivates their peroxidase activity, new physiological functions have been attributed to hyperoxidized PRXs. Thus, hyperoxidation of 2-Cys PRXs promotes the formation of spherical aggregates with very high molecular mass (>2,000 kDa) [344, 350]. These aggregates act as chaperones preventing the unfolding and precipitation of substrate proteins [348, 351]. Therefore, SRX seems to act regulating a complex balance, not fully understood, between peroxidase activity, hyperoxidation, and chaperone function of PRXs [338].

2.5 Reactive nitrogen species, nitrosative stress and redox signaling

In the mid-1980s, the chemical identity of the endothelial-derived vascular relaxation factor (EDRF) described by Furchgott [369] was revealed to be •NO by Moncada and coworkers [370] and by Ignarro *et al.* [371]. •NO contains one unpaired electron and thus, is as a free radical [279].

•NO is generated in cells by specific NOSs which metabolize arginine to citrulline producing •NO [279, 372]. In mammal, NOSs are present in three isoforms: neuronal NOS (NOS1/nNOS), inducible NOS (NOS2/iNOS), and endothelial NOS (NOS3/eNOS) [372]. NOS1 is predominantly expressed in neurons and in skeletal muscle, NOS2 is mostly expressed in macrophages and cells of macrophage/monocyte lineage and NOS3 is mainly expressed in endothelial cells [373]. However, other cells types express these three isoforms and it is usual that tissues express more than one isoform [372].

•NO can regulate cellular functions in adjacent cells because it is a small hydrophobic molecule that exhibits a high ability to diffuse through cell membranes [373, 374]. However, the diffusion of •NO across tissues is limited because •NO is rapidly converted to nitrate (NO_2^-) into red blood cells by reaction with oxyhemoglobin [373, 375]. Consequently, the biological half-life of •NO and its diffusion distances are around the order of 1–10 s and 50–1,000 μm, respectively [375]. Therefore, •NO mainly exerts local and paracrine actions within a tissue [373, 375], acting as a fundamental intercellular messenger in the regulation of a large variety of physiological processes including blood pressure regulation, thrombosis, smooth muscle relaxation, and neural activity [279, 372, 373].

2.5.1 $^{\bullet}$NO chemistry and reactive nitrogen species generation

Depending on the microenvironment, $^{\bullet}$NO can be converted to various RNS such as nitrogen dioxide ($^{\bullet}NO_2$), nitrosonium cation (NO^+), nitroxyl anion (NO^-) or peroxynitrite ($ONOO^-$) (Figure 12) [280]. Upon reaction with $O_2^{\bullet -}$, $^{\bullet}$NO forms $ONOO^-$ [279, 376]. Alternatively, $ONOO^-$ may react with $^{\bullet}$NO to produce $^{\bullet}NO_2$ and NO_2^-. As NO, $^{\bullet}NO_2$ is a free radical, and can be also produced by the reaction between $^{\bullet}$NO and O_2 although this reaction is very slow. $^{\bullet}NO_2$ may undergo a further radical reaction with $^{\bullet}$NO to form dinitrogen trioxide (N_2O_3). In the presence of a nucleophile, like a thiolate (Cys-S^-), N_2O_3 can transfer its nitrosonium group (NO^+) and generate a nitrosothiol (−SNOs) in a process named S-nitrosylation. Alternatively, nitrosothiols can also derive from NO if the thiol is previously oxidized by $O_2^{\bullet -}$, $^{\bullet}$OH, $^{\bullet}NO_2$, or $ONOO^-$ to a thiyl radical (Cys-$S^{\bullet}$) [377].

The overproduction of RNS can lead to the oxidation of biomolecules triggering cytotoxic effects in cells [279]. This is called nitrosative stress and occurs in cells when the generation of RNS overwhelms the antioxidant systems and causes oxidative damage [378]. On the other hand, $^{\bullet}$NO can act a signal molecule through the reaction with sulfhydryl groups on low-molecular weight compounds to form S-nitrosoglutathione (GSNO), S-nitrosocysteine (L-CysNO), and S-nitrosohomocysteine (HCysNO); or on high molecular proteins to form S-nitrosylated proteins [379]. Interestingly, S-nitrosylation levels in cells are controlled by the balance between S-nitrosylation and denitrosylation. TRX)/TRXR and GSNO/GSNO reductase (GSNOR) systems are the two major denitrosylase systems in cells [379, 380]. Strikingly, nitrosyl groups can also be transferred from one thiol to another through trans-nitrosylation reactions [381]. Therefore, the nitrosyl group could be further transferred to another protein in a distant site through trans-nitrosylation reactions in order to propagate NO signaling [382].

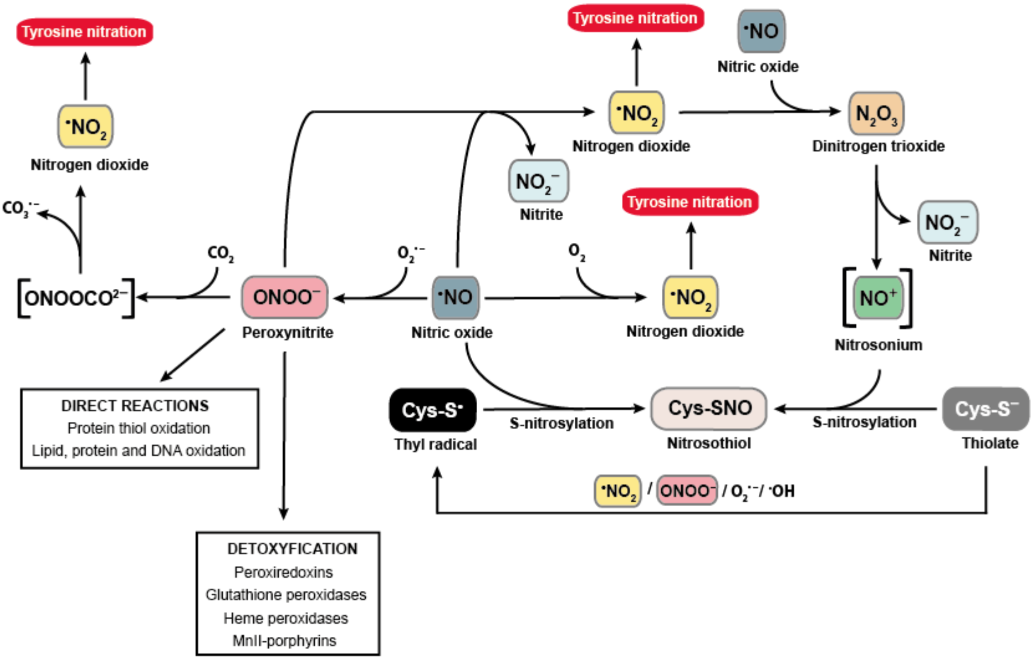
Tyrosine nitration
•NO2
Nitrogen dioxide
CO3•−
[ONOOCO2−]
CO2
ONOO−
Peroxynitrite
DIRECT REACTIONS
Protein thiol oxidation
Lipid, protein and DNA oxidation
DETOXYFICATION
Peroxiredoxins
Glutathione peroxidases
Heme peroxidases
MnII-porphyrins
O2•−
•NO
Nitric oxide
NO2−
Nitrite
Tyrosine nitration
•NO2
Nitrogen dioxide
•NO
Nitric oxide
N2O3
Dinitrogen trioxide
Tyrosine nitration
O2
•NO2
Nitrogen dioxide
NO2−
Nitrite
NO+
Nitrosonium
Cys-S•
Thyl radical
S-nitrosylation
Cys-SNO
Nitrosothiol
S-nitrosylation
Cys-S−
Thiolate
•NO2 / ONOO− / O2•−/ •OH

Figure 12. Nitric oxide ($^{\bullet}NO$) chemistry and peroxynitrite ($ONOO^-$) fates in the biological context. Overview of the most relevant chemical reactions of $^{\bullet}NO$ and $ONOO^-$ in the biological context.

2.5.2 Peroxynitrite and protein nitration

Peroxynitrite ($ONOO^-/ONOOH$, $pK_a = 6.8$) is a powerful and short-lived (half life *ca.* 10 ms) oxidant formed *in vivo* through $^{\bullet}NO$ reaction with $O_2^{\bullet -}$ [279, 376]. $ONOO^-$ was first proposed as a biologically relevant cytotoxic intermediate in 1900 by Beckman *et al.* [383]. These authors demonstrated that $ONOO^-$ decomposition generates a strong oxidant with a reactivity similar to that of $^{\bullet}OH$ [383]. Posterior studies by Radi *et al.* [384, 385] established the preferential fates of $ONOO^-$ in biological systems and reported the direct reactivity of $ONOO^-$ with biomolecules, showing for the first time that $ONOO^-$ acts as a cytotoxic effector in biological systems [386].

The initial studies by Beckman *et al*. proposed that SOD may protect cells by preventing the formation of $ONOO^-$ [383]. In fact, one of the most intriguing questions about $ONOO^-$ generation *in vivo* was the presence of SODs, because SOD activity should largely limit the reaction of $O_2^{\bullet-}$ with $^{\bullet}NO$. SODs are typically present in significant amounts (4–40 μM SOD1 and 1–30 μM SOD2 in the cytosol and mitochondria, respectively). Hence, it was difficult to conceive the competition for $O_2^{\bullet-}$ by $^{\bullet}NO$, which is present at submicromolar concentrations under physiological conditions [375, 386]. However, the rate constant for the reaction of $O_2^{\bullet-}$ with $^{\bullet}NO$ to form $ONOO^-$ ($4–16 \times 10^9$ M^{-1} s^{-1}) is around one order of magnitude higher than that of SOD-catalyzed $O_2^{\bullet-}$ dismutation ($1–2 \times 10^9$ M^{-1} s^{-1}) [375, 386]. In addition, due to the favored diffusion of $^{\bullet}NO$ across cellular membranes and its longer half-life in comparison to $O_2^{\bullet-}$, $ONOO^-$ is formed in the proximity of $O_2^{\bullet-}$ generation sites [386]. Therefore, when both $O_2^{\bullet-}$ and $^{\bullet}NO$ are synthesized closely from each other, they faster combine spontaneously to form $ONOO^-$ [373]. Upon sustained overactivation of the constitutive NOS (eNOS or nNOS) or induction of iNOS, $^{\bullet}NO$ approaches or exceeds micromolar levels and consequently competes more efficiently with SOD favoring $ONOO^-$ generation [375].

Beckman *et al.* proposed that the homolysis of peroxynitrous acid to yield $^{\bullet}OH$ and $^{\bullet}NO_2$ was the principal mechanism responsible for the cytotoxic effect of $ONOO^-$ [383]. However, this homolytic reaction is too slow (1.13 s^{-1} at pH 7.4 and 37 °C) to compete with the direct targets of $ONOO^-$ such as CO_2, thiol and selenol peroxidases, metalloproteins, and others including methionine, tryptophan, uric acid, and ascorbate [386]. The reaction of $ONOO^-$ with CO_2 is quantitatively one of the most importants for $ONOO^-$ consumption *in vivo* [386]. The fast reaction of $ONOO^-$ with CO_2 leads to a transient adduct ($ONOOCO^{-2}$), which is decomposed in carbonate radical ($CO_3^{\bullet-}$) and $^{\bullet}NO_2$ [375]. In living cells, $CO_3^{\bullet-}$ and $^{\bullet}NO_2$ trigger oxidative damage to biomolecules including protein nitration and oxidation as well as DNA nitration and oxidation [375, 376]. Additionally, $ONOO^-$ can diffuse through membranes and react with lipids and proteins via its secondary radicals within biological membranes [376].

Tyrosine nitration represents the most specific and illustrative oxidative modification induced by $ONOO^-$ in biological systems [386]. Although during the first half of the 20th century it was studied the effect of nitrating agents on protein activity [386], it was not until the early 1990's when nitration of tyrosine residues in proteins was considered a biologically relevant oxidative post-translational modification [387-389]. At present, tyrosine nitration is recognized the most relevant footprint of $ONOO^-$ and it is commonly used as a marker of nitrosative stress in cells and tissues [373, 386].

Tyrosine nitration is defined as the replacement of hydrogen by a nitro group ($-NO_2$) in the 3-position of the phenolic ring of free or protein-bound tyrosine, being 3-nitrotyrosine (3-NT) the product of this reaction (Figure 13) [376]. Protein tyrosine nitration is a free radical-mediated reaction, which involves the intermediate formation of $Tyr^\bullet$ radical from tyrosine [376]. $ONOO^-$ does not react directly with tyrosine, which is oxidized and nitrated by $ONOO^-$-derived secondary radicals [390]. In biological systems, $Tyr^\bullet$ radical formation can be generated by $^\bullet NO_2$, $CO_3^{\bullet -}$ and $^\bullet OH$ radicals as well as by the lipid-derived radicals peroxyl ($LOO^\bullet$) and alkoxyl ($LO^\bullet$) [376]. In addition, the same radicals that lead to tyrosine nitration can also produce other secondary products that are usually found during $ONOO^-$-mediated protein nitration, including 3,3′-dityrosine (the tyrosine dimerized form); 3,4-dihydroxyphenylalanine, also known as 3-hydroxytyrosine (as a result of $^\bullet OH$ addition to tyrosine); and tyrosine hydroperoxide (as a result of the reaction of tyrosine with $O_2^{\bullet -}$ radical) (Figure 13) [376, 390].

Protein tyrosine nitration is considered a low yield and highly selective process as usually in whole tissue/cells only 1–5 over 10,000 tyrosine residues become nitrated [376, 390]. Nitration of a particular tyrosine residue depends on several physicochemical factors including protein structure, the nitration mechanism, and the environment where the tyrosine residue is located [376, 386].

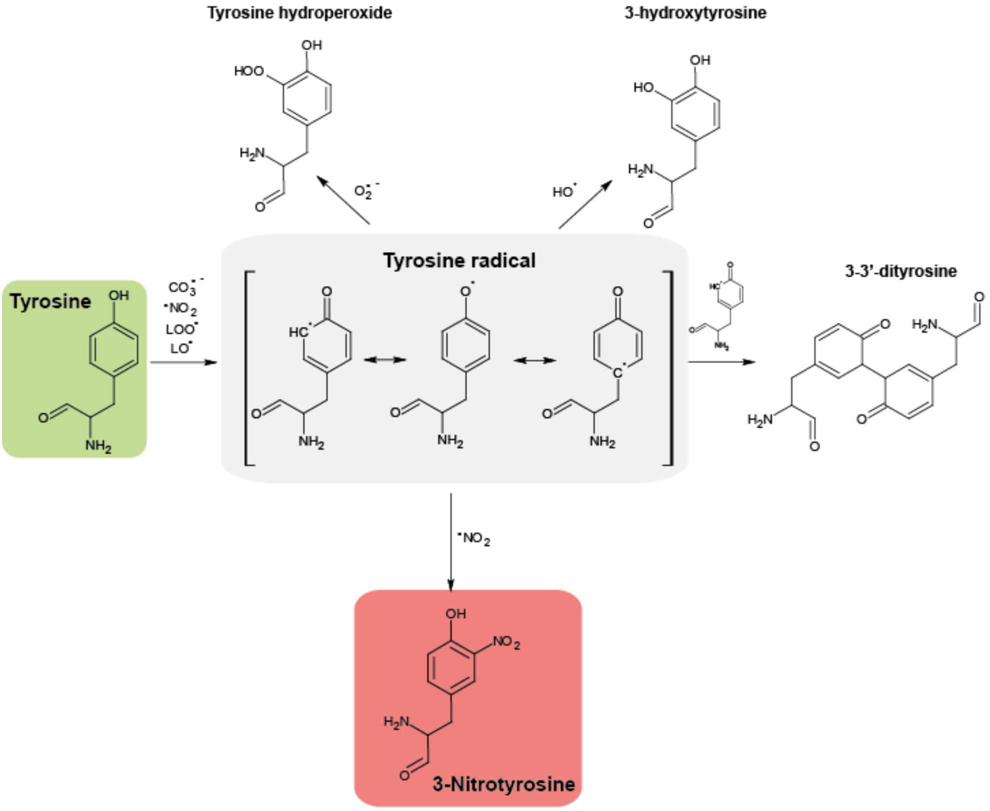
Tyrosine hydroperoxide
3-hydroxytyrosine
Tyrosine
Tyrosine radical
3-3'-dityrosine
3-Nitrotyrosine
CO3•-
•NO2
LOO•
LO•
O2•-
HO•
•NO2

Figure 13. Tyrosine nitration. Overview of tyrosine oxidation pathways that lead to the formation of 3-nitrotyrosine, 3-3'-dityrosine, 3-hydroxytyrosine and tyrosine hydroperoxide.

As a result of protein nitration, protein structure and function may result dramatically affected. Thus, tyrosine nitration can promote generation of new antigenic epitopes, changes in the catalytic activity of enzymes, alteration in cytoskeletal organization, and impairment in cell signal transduction [373]. Therefore, tyrosine nitration is one of the most relevant mechanisms that explain the cytotoxic effect of $ONOO^-$. In fact, tyrosine nitration is strongly associated with numerous pathologies, especially with inflammation and neurodegenerative diseases [391, 392].

It is noteworthy that $ONOO^-$ can also alter protein structure and function by reacting with cysteine residue, as described by Radi *et al*. in 1991 [384]. Thiol (particularly with the anion form, RS^-) oxidation by $ONOO^-$ results in the formation of an intermediate sulfenic acid, which then may react with another thiol to form a disulfide bridge [376]. Furthermore, thiols may also be oxidized by secondary radicals derived from $ONOO^-$ generating thiyl radicals which in turn can also react with $^{\bullet}NO$ to form nitrosothiols [373].

2.5.3 Peroxynitrite, mitochondrial function and cell death

Mitochondria are considered the principal source of $ONOO^-$ and are the primary locus for the cytotoxic effects of nitrosative stress [393, 394]. Extra and intra-mitochondrially formed $ONOO^-$ can diffuse into the mitochondria leading to nitration of critical mitochondrial components. In fact, $ONOO^-$-dependent protein modifications have a dramatic impact on mitochondrial physiology and are widely associated with cell death signalling pathways [393-395].

A large variety of proteins located in all mitochondrial compartments can become readily oxidized by $ONOO^-$. Mn-SOD [396, 397], electron chain components [398-403], aconitase [404], ATPase [399, 403, 405], adenine nucleotide translocator (ANT) [405, 406] and creatine kinase [407] are some of the direct targets of $ONOO^-$ in mitochondria. These protein modifications collapse the mitochondrial energy metabolism and thus, initiate a selfpropagated cascade of events into the mitochondria that alters calcium homeostasis and causes mPTP opening, leading to cell death [225, 393].

$ONOO^-$ can induce either cellular apoptosis and necrosis depending on its production rates, exposure time and antioxidants levels [408]. Low concentrations of $ONOO^-$ produce apoptotic cell death, whereas higher concentrations of $ONOO^-$ trigger necrotic cell death due to acute and severe energetic collapse [408, 409]. Nitration of mitochondrial components promotes caspase 3 activation and the release of proapoptotic factors, such as AIF and cytochrome c [409-412]. In addition, $ONOO^-$ also oxidizes and damages DNA activating the nick sensor enzyme poly (ADP-ribose) polymerases (PARP-1), which consumes NAD^+ and consequently ATP, thus promoting necrosis [413, 414]. Hence, given the dual action of $ONOO^-$, it can serve as switch between the two modes of cell death [411].

Interestingly, Davis *et al.* reported that nitration of the mitochondrial complex I subunit NADH:ubiquinone oxidoreductase subunit B8 (NDUFB8) caused necroptosis through the activation of RIPK1 and RIPK3, which was prevented by MnSOD overexpression [259]. The authors concluded that mitochondrial ROS were required for $^{\bullet}NO$ -induced necroptosis in response to elevated levels of $^{\bullet}NO$ as it would occur during inflammation [259]. In fact, the release of intracellular content by necroptotic cells to the extracellular environment can trigger additional inflammatory responses, which can further promote $ONOO^-$ generation [408].

2.5.4 Peroxynitrite and peroxiredoxins

Different enzymes such as PRXs, GPx, some heme peroxidases, and Mn^{II}-porphyrins contribute to $ONOO^-$ detoxification in cells [415]. In 2000, Bryk *et al.* provided the first evidence that PRXs catalyze the reduction of $ONOO^-$ to $^{\bullet}NO_2$

[416]. They found that alkyl hydroperoxide reductase C (AhpC), a typical 2-Cys PRX present in bacteria, detoxifies $ONOO^-$ to $^{\bullet}NO_2$ fast enough (1×10^6 M^{-1} s^{-1} at pH 6.8, 25 °C) to avoid the oxidation of DNA [416]. Since then, it has been reported that several PRXs in mammals react with $ONOO^-$, including members of the 1-Cys, atypical and typical 2-Cys classes of PRXs [415]. PRX2 [417], PRX5 [418, 419], PRX6 [420] and more recently PRX3 [421] were found to react with $ONOO^-$ with different kinetic constants (Table 3).

Table 3. Reactivity of mammalians peroxiredoxins with H_2O_2 and $ONOO^-$

PROTEIN	k' $_{H2O2}$ ($M^{-1}s^{-1}$)	k' $_{ONOOH}$ ($M^{-1}s^{-1}$)	References
PRX2	1.3×10^7 - 1×10^8	1.4×10^7	[417, 422, 423]
PRX3	2×10^7	$1x\ 10^7$	[421, 424]
PRX5	3×10^5	1.2×10^8 / 7×10^7	[418, 419, 425]
PRX6	3.4×10^7	3.7×10^5	[420]

PRXs act as $ONOO^-$ oxido-reductases by the two-electron reduction of $ONOO^-$ to $^{\bullet}NO_2$ [375]:

$$ONOOH + RS^- \rightarrow RSOH + NO_2^-$$

This reaction occurs through the fast-reactive thiols (C_P) in PRXs, to form sulfenic acid [386]. It is noteworthy that the thiol group in PRXs is transformed in sulfenic acid as through the reaction of PRXs with H_2O_2 [333, 338]. Therefore, the reaction of PRXs C_p with $ONOO^-$ provide an additional mechanism for redox signaling in the same way that occurs with H_2O_2 [386]. In fact, in kinetic terms, PRXs show different degrees of preference between $ONOO^-$ and H_2O_2 [425]. While PRX2 and PRX6 tend to react faster with H_2O_2 than with $ONOO^-$, PRX5 reacts faster with $ONOO^-$ (Table 3). In the case of PRX3, the kinetic constants of the reaction with $ONOO^-$ and H_2O_2 are in the same range (Table 3). Taken together, these data show the selectivity of different protein thiols to react with $ONOO^-$ or H_2O_2, and suggest the existence of "peroxynitrite sensors" and "peroxynitrite relay systems" in signaling processes [375].

2.6 Oxidative and nitrosative stress in acute pancreatitis

Oxidative stress is presently considered a key factor implicated in the development of pancreatic injury during acute pancreatitis [304]. Clinical and experimental studies have reported increased levels of several oxidative markers in plasma and pancreatic tissue, which correlated with the severity of acute pancreatitis [426-431].

The principal sources of ROS during acute pancreatitis are NOXs and XOD [304]. Necro-hemorragic acute pancreatitis induced by intraductal taurocholate infusion increased the levels of XOD-derived ROS [432, 433]. However, pancreatic activity of XOD and levels of XOD-derived ROS were not elevated in cerulein-induced acute pancreatitis [433, 434]. These findings show that the generation of ROS by XOD depends on the etiology and severity of acute pancreatitis [282]. In cerulein-induced acute pancreatitis it is considered that NOXs are the main source of ROS, whereas XOD seems to play a major role in necrotizing acute pancreatitis induced by bile salts [304]. NOX activation induced NF-κB activation as well as IL-6 up-regulation and apoptosis of acinar cells stimulated *in vitro* with cerulein [435, 436]. In pancreatic tissue, NOX activity as well as the mRNA and protein levels of NOX subunits p67phox, p47phox, and p22phox increased in pancreas during cerulein-induced acute pancreatitis [437]. Accordingly, mice deficient in the NOX subunit p47phox exhibited diminished intrapancreatic trypsin activation in the pancreas during cerulein-induced acute pancreatitis [438]. In addition, decreased levels of NADPH induced by dunnione, a substrate of NAD(P)H:quinone oxidoreductase 1, diminished pancreatic NOX activity and ameliorated pancreatic inflammation and injury [437].

Together with the increased generation of ROS during acute pancreatitis, down-regulation of the antioxidant system decisively contributes to the dysregulation of the redox balance in pancreatic tissue in pancreatitis. In the pancreas, GSH concentration is among the highest in the body and this tissue exhibits active trans-sulfuration pathway and GSH synthesis [282]. An early feature in the development of acute pancreatitis is pancreatic GSH depletion which, when maintained in a long term, contributes to the severity of the disease [439-441]. Accordingly, pre-treatment with glutathione monoethyl ester exhibited beneficial effects in acute pancreatitis by increasing pancreatic GSH levels [442], whereas inhibition of GSH synthesis with L-buthionine-(S,R)-sulfoximine increased pancreatic necrosis and reduced survival in rats with acute pancreatitis [443]. Interestingly, in experimental models of acute pancreatitis, GSH depletion is not accompanied by increased levels of GSSG but instead it is associated with protein cysteinylation and γ-glutamylcysteinylation, which was considered a subtype of oxidative stress called disulfide stress [444]. GCL expression was upregulated in mild cerulein-induced acute pancreatitis, but this up-regulation failed in the severe form of acute pancreatitis induced by taurocholate in rats [440]. Furthermore, SAM levels decreased in pancreas during acute pancreatitis in rats [445]. Nevertheless, the precise mechanism involved in the dysregulation of the trans-sulfuration pathway in acute pancreatitis remains to be explored.

Pancreatic GSH depletion is accompanied with diminished GPx activity as well as lower activities of other antioxidant enzymes such as SOD1, SOD2 and

CAT [446-448]. Moreover, the loss of multiple antioxidant enzymes impaired ROS scavenging and exacerbated pancreatic damage during acute pancreatitis [282]. Accordingly, overexpression of antioxidant enzymes SOD1 and TRX ameliorated pancreatic injury in cerulein-induced acute pancreatitis [449, 450].

On the other hand, nitrosative stress is also involved in the pathophysiology of acute pancreatitis [304]. Although limited normal amount of $^{\bullet}$NO production exhibited beneficial effects in acute pancreatitis, up-regulation of *Nos2* expression, as generally occurs in acute inflammation, triggered nitrosative stress in pancreas with acute pancreatitis [451, 452]. Accordingly, pancreatic levels of 3-NT increased in mice with cerulein-induced acute pancreatitis [453-455]. The different isoforms of NOS exhibited different impacts and profiles of activation in acute pancreatitis [282]. While NOS3-derived NO reduced the severity of the initial phase of acute pancreatitis [456], NOS2-deficient mice exhibited resistance to cerulein-induced acute pancreatitis [453]. Hence, contradictory data has been reported about the different NOS isoforms contribution to the pathophysiology of acute pancreatitis and thus, the clinical relevance of NOS inhibition remains to be clarified [457].

3 PGC-1α

First discovered in 1998 for its role in adaptive thermogenesis [458], peroxisome proliferator-activated receptor-γ coactivator (PGC)-1α is a member of a family of transcription coactivators presently considered a master regulator of mitochondrial biogenesis and function [459]. During the last years, PGC-1α has been associated with some inflammatory diseases by exerting a crucial role regulating oxidative stress and metabolic function in inflamed tissues [460-463].

3.1 PGC-1α family members

The PGC1 family consists of three members -PGC1α, PGC1β and PGC related coactivator (PRC)-, which interact with a broad range of transcription factors involved in a wide variety of biological functions [464]. As a result of these interactions, the transcriptional activities of these factors and the biological responses associated with them ends up modulated by PGC-1 [464, 465].

The PGC1 family members exhibit a high degree of amino acid sequence homology, specially within the amino- and carboxy-terminal regions [465] (Figure 14). The amino-terminal region of all PGC-1 co-activators contain a highly conserved activation domain (AD) required for the recruitment of histone acyltransferase proteins steroid receptor coactivator 1 (SRC-1) and CREB binding protein (CBP)/p300, which in turn favor the access of the transcriptional complex to the DNA [466]. In addition, the N-terminal domain also contains several leucine-rich LXXLL motifs (nuclear receptor (NR) boxes) which are crucial for the interaction between PGC1 and their transcriptional partners [458, 467]. On the other hand, the carboxy-terminal region contains a well-conserved RNA recognition motif (RRM), which is involved in both RNA and single-stranded DNA binding [465, 468]. Additionally, the short serine/arginine-rich stretches (RS) domains are present in PGC-1α and PRC, but not in PGC-1β [469, 470]. Interestingly, the RS and RRM motifs are typically found in proteins involved in RNA splicing, suggesting that PGC-1 co-activators interact with the splicing machinery [459, 465, 471].

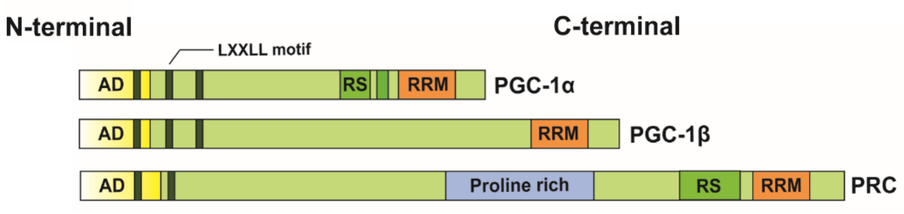

Figure 14. Structure of PGC-1 family coactivators. Schematic view of proteins comprising the PGC-1α family. AD, activation domain; RS, short serine/arginine-rich stretches; RRM, RNA recognition motif.

3.2 Regulation of PGC-1α expression and activity

PGC-1α expression is regulated at transcriptional and post-translational levels [472]. The transcriptional regulation of the gene encoding PGC-1α, *Ppargc1a*, is mainly orchestrated by AMP responsive element binding protein (CREB) activation in different tissues [468]. The *Ppargc1a* gene exhibits a well-conserved binding site for CREB, which drives *Ppargc1a* expression after CREB activation [473]. On the other hand, forkhead box O (FOXO) transcription factors also contribute to the transcriptional regulation of *Ppargc1a* in different cell types [474, 475]. In addition, epigenetic modifications in the promoter of *Ppargc1a* gene are emerging as novel mechanisms to regulate *Ppargc1a* expression [476-478].

Several post-translational modifications including phosphorylation, acetylation, and ubiquitination regulate PGC-1α activity [472]. These post-translational modifications positively or negatively modulate the stability of PGC-1α and affect its ability to recruit other transcriptional co-activators [465]. p38

MAPK, AMP-activated protein kinase (AMPK), protein kinase B (AKT), and glycogen synthase kinase 3 (GSK3β) are the best characterized kinases that regulate PGC-1α by phosphorylation. p38 MAPK phosphorylates PGC1α at Thr262, Ser265 and Thr298 [479, 480]. These modifications promote PGC-1α stabilization [480] and enhance its transcriptional activity [481]. AMPK binds to and activates PGC-1α by direct phosphorylation on Thr117 and Ser538. In contrast, the kinase activity of AKT and GSK3β is associated with inhibition of PGC-1α [482-485]. AKT inhibits PGC-1α activity by direct phosphorylation at serine-570 [482] or inducing CLK2, which in turn phosphorylates and reduces PGC-1α activity [486]. GSK3β phosphorylates and inhibit PGC-1α by promoting its proteasomal degradation [484]. Proteasomal degradation of PGC-1α can also be regulated by ubiquitination through Skp1/Cullin/F-box-cell division control 4 (SCF^{Cdc4}) [487]. On the other hand, PGC-1α activity is regulated by acetylation through a key mechanism that acts as a sensor of the energy status in cells. The acetyl transferase GCN5 catalyses the acetylation and promotes the inhibition of PGC-1α activity when the energy is abundant in cells [488, 489]. However, when the energy status is lower, PGC-1α is deacetylated and its activity on transcription restored by silent information regulator 1 (SIRT1) [490, 491].

3.3 Physiological functions of PGC-1α

3.3.1 PGC-1α and mitochondrial biogenesis

PGC-1α regulates the expression of key mitochondrial and nuclear genes involved in mitochondrial biogenesis [492]. PGC-1α activates nuclear respiratory factors (NRF1 and 2), peroxisome proliferator-activated receptors (PPARs), and mitochondrial transcription factor A (TFAM) [493, 494]. NRF-1 and NRF-2 trigger the transcription of different mitochondrial enzymes and interact with TFAM, a key factor involved in mtDNA transcription and replication [495].

3.3.2 PGC-1α and metabolic regulation

PGC-1α is involved in the regulation of pathways critical for cellular energy metabolism including gluconeogenesis and fatty acid β-oxidation [496, 497]. In response to different energy stressors, PGC-1α induces transcriptional networks that control oxidative phosphorylation in tissues with high energetic demands such as liver, cardiac and skeletal muscle, kidney, brown adipose tissue, brain, and retina [468].

3.3.3 PGC-1α and ROS detoxification

PGC1α regulates mitochondrial antioxidant defense in cells. PGC-1α increases the levels of *Sod2*, *Cat*, *Prx3, Prx5*, *Ucp-2*, *Trxr2*, and *Trx2* and consequently, protects cells from mitochondrial dysfunction [498, 499]. Indeed, the upregulation of antioxidant defense by PGC1α has been found essential to prevent cell death associated with mitochondrial failure [498]. In fact, PGC1α is upregulated when cells are exposed to oxidative stress and it is required to prevent oxidative damage [500-505].

It is noteworthy that the antioxidant function of PGC1α is paired with its role enhancing mitochondrial electron transport and mitochondrial mass in cells with high energy demands. Therefore, regulation of the mitochondrial antioxidant defense through PGC1α is considered an adaptive mechanism to ensure an adequate response to metabolic requirements avoiding the potential harmful and cytotoxic effects of ROS accumulation [500].

II. OBJECTIVES

The general aim of this PhD Thesis is to find out new mechanisms involved in redox regulation of the antioxidant defence and inflammatory cascade in acute pancreatitis, and also to assess their impact in its pathophysiology.

The specific objectives are:

1. To elucidate the redox regulation of the trans-sulfuration pathway in pancreas with acute pancreatitis and its contribution to glutathione depletion

2. To assess the role of sulfiredoxin in the regulation of the inflammatory cascade and cell death in acute pancreatitis

3. To evaluate the contribution of PGC-1α to the regulation of the antioxidant defence and inflammatory response in acute pancreatitis

III. MATERIAL AND METHODS

1 Experimental model of acute pancreatitis

In this work, cerulein-induced acute pancreatitis in mice was used as experimental model of acute pancreatitis. This model, based on the secretagogue properties of cerulein (an analogue of cholecystokinin originally isolated from the skin of the Australian frog *Litorea caerulea* [506]), was firstly introduced by Lampel and Kern in 1977 in rats [507]. Since then, this experimental model has been updated and widely utilized to study the early intracellular events associated with acute pancreatitis, including protease activation, cell signalling cascades and cell death pathways [508].

In contrast with other experimental models which require surgical intervention, cerulein-induced acute pancreatitis is a highly reproducible non-invasive model of acute pancreatitis [509]. Initially, induction of acute pancreatitis with cerulein required the insertion of an intravenous tail vein or jugular vein catheter in rodents [507]. However, this protocol was updated to use intraperitoneal injections [510]. In the present, the most widely used protocol for the induction of acute pancreatitis in mice consists of seven hourly intraperitoneal injections of 50 µg/kg body weight of synthetic cerulein. As a result of this protocol, mice develop pancreatic interstitial edema, inflammatory infiltrate, acinar necrosis and manifest systemic complications, particularly pulmonary injury [508, 511, 512]. However, both pancreatic and lung injury are fully reversible within hours to few days and in fact, a negligible mortality is associated with this experimental model [511, 513].

1.1 Induction of acute pancreatitis in mice

Cerulein-induced acute pancreatitis was produced in male C57BL/6 12-week-old mice (Jackson Laboratory, Barcelona, Spain). Mice received seven intraperitoneal injections of cerulein (Sigma-Aldrich, St. Louis, MO, USA) (50 µg/kg body weight) at 1 h intervals. Physiological saline (0.9% NaCl) was administered to the control group. Animals were sacrificed 1 h after the first, third, fifth and seventh injections of cerulein depend on the experimental study. For the sacrifice, mice were euthanized under anesthesia with isoflurane 3–5%, subsequently were exsanguinated, the blood collected, and the pancreas and lungs immediately removed and used as described below. The sacrifice was confirmed by cervical dislocation.

All animals were housed under standard environmental conditions, with food and water ad libitum. Experiments were conducted in compliance with the legislation on protection of animals used for scientific purposes in Spain (RD 53/2013) and the EU (Directive 2010/63/EU). Protocols were approved by the Ethics Committee of Animal Experimentation and Welfare of the University of Valencia (Valencia, Spain).

2 Experimental design

2.1 Design of the time-course experiments

In time-course study, animals were sacrificed 1 h after the first, third, fifth and seventh injections of cerulein. Mice that did not receive any injection of cerulein were used as controls. The number of animals per group was six (Figure 15).

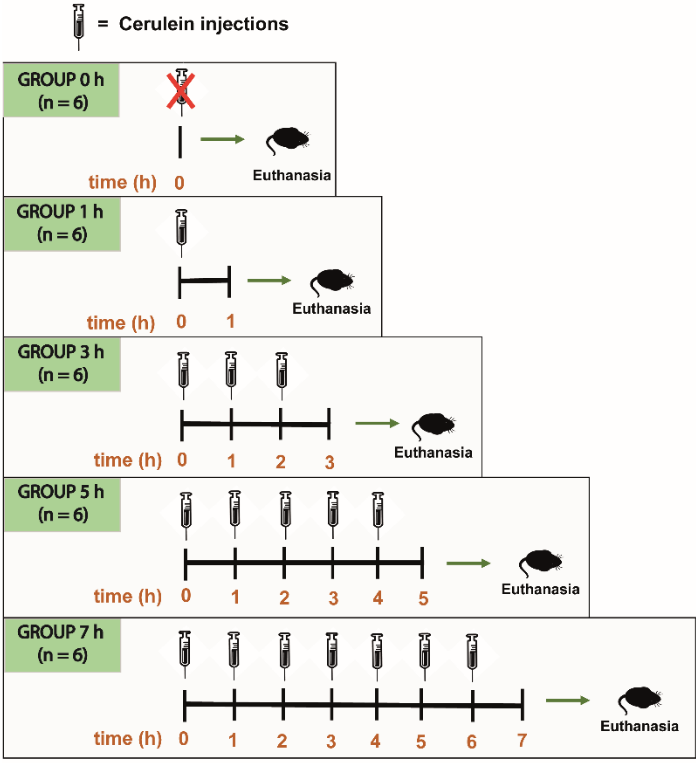
= Cerulein injections
GROUP 0 h
(n = 6)
time (h)
0
Euthanasia
GROUP 1 h
(n = 6)
time (h)
0
1
Euthanasia
GROUP 3 h
(n = 6)
time (h)
0
1
2
3
Euthanasia
GROUP 5 h
(n = 6)
time (h)
0
1
2
3
4
5
Euthanasia
GROUP 7 h
(n = 6)
time (h)
0
1
2
3
4
5
6
7
Euthanasia

Figure 15. Experimental design of time-course experiment. Mice were sacrificed 1 h after the first (group 1 h), third (group 3 h), fifth (group 5 h) and seventh (group 7 h) injection of cerulein. Control group (group 0 h) did not receive any injection of cerulein.

2.2 Design of the study with SAM-treated mice

SAM (Sigma-Aldrich, St. Louis, MO, USA) was administered intraperitoneally (15 mg/kg body weight) 10 min before the first and fourth cerulein injection. Physiological saline (0.9% NaCl) was administered to the control group of animals. In addition, one group of control animals received only SAM injections. The experimental design of this experiment is summarized in Table 4.

Table 4. Experimental design of the study with SAM-treated mice with acute pancreatitis

EXPERIMETAL GROUP	**Description**
Control (n = 6)	Mice with seven injections of 0.9% NaCl and sacrificed 1 h after the last injection
SAM (n = 6)	Mice with SAM-treatment without pancreatitis
Cer (n = 6)	Mice with pancreatitis induced by seven injections of cerulein and sacrificed 1 h after the last injection
Cer + SAM (n = 6)	Mice with pancreatitis induced by seven injections of cerulein and SAM-treatment, sacrificed 1 h after the last injection

.

2.3 Design of the study with SRX KO mice

Acute pancreatitis was induced in C57BL/6 mice with a null deletion of the SRX1-encoding *Srxn1* gene (SRX KO mice). SRX KO mice were provided by Dr. Michel Toledano (Institute for Integrative Biology of the Cell (I2BC), CEA-Saclay, CNRS, Université Paris-Saclay, DBJC/SBIGEM, Oxidative Stress & Cancer, Gif-sur-Yvette, France). The generation and phenotype of SRX KO mice were described previously [514].

In one group of animals, the specific scavenger of mitochondrial $O_2^{\bullet-}$ mitoTEMPO (Sigma-Aldrich, St. Louis, MO, USA) was administered intraperitoneally (25 mg/kg body weight) 10 min before the first and fourth cerulein injection. The experimental design of this study is summarized in Table 5.

Table 5. Experimental design of the study with SRX KO mice with acute pancreatitis

MICE GENOTYPE	EXPERIMETAL GROUP	Description
Wild-type	Sham (n = 6)	Mice with seven injections of 0.9% NaCl and sacrificed 1 h after the last injection
	Cerulein (n = 6)	Mice with pancreatitis induced by seven injections of cerulein and sacrificed 1 h after the last injection
SRX KO	Sham (n = 7)	Mice with seven injections of 0.9% NaCl and sacrificed 1 h after the last injection
	Cerulein (n = 11)	Mice with pancreatitis induced by seven injections of cerulein and sacrificed 1 h after the last injection
	Cerulein + mitoTEMPO (n = 4)	Mice with pancreatitis induced by seven injections of cerulein and mitoTEMPO-treatment, sacrificed 1 h after the last injection

2.4 Design of the study with obese mice

Male C57BL/6 J mice purchased from Jackson Laboratory (Bar Harbor, ME, USA) were used, fed either standard chow (lean: 23.4±1.0 g; n=10) or a high-fat diet with 60% calories from fat (obese: 29.4±1.2 g; n=10) for 12 weeks. The control diet and the high-fat diet will be obtained from Envigo® (TD88137).

2.5 Design of the study with PGC-1α KO mice

Acute pancreatitis was induced in C57BL/6 PGC-1α-deficient mice (PGC-1α KO mice). PGC-1α KO mice were originally provided by Dr Bruce Spiegelman (Dana-Farber Cancer Institute, Harvard Medical School, Boston, MA, USA) and, following embryo transfer, a colony was established at the Institute of Biomedical Research 'Alberto Sols' (Madrid, Spain) animal facility by Dr Maria Monsalve who provide us the animals for this work. The generation and phenotype of PGC-1α KO mice were described previously [515].

In one group of animals, the IL-6 antagonist LMT-28 (Sigma-Aldrich, St. Louis, MO, USA) was administered (1 mg/kg body weight) by oral gavage 1 h before the first and fourth cerulein injection, as described previously [516]. LMT-28 was dissolved in 0.5% carboxymethyl cellulose (Sigma-Aldrich, St. Louis, MO, USA). Carboxymethyl cellulose (0.5%) was administered as vehicle. The experimental design of this study is summarized in Table 6.

Table 6. Experimental design of the study with PGC-1α KO mice with acute pancreatitis

MICE GENOTYPE	EXPERIMETAL GROUP	Description
Wild-type	Sham (n = 6)	Mice with seven injections of 0.9% NaCl and sacrificed 1 h after the last injection
	Cerulein (n = 6)	Mice with pancreatitis induced by seven injections of cerulein and sacrificed 1 h after the last injection
	Cerulein + LMT-28 (n = 4)	Mice with pancreatitis induced by seven injections of cerulein and LMT-28-treatment, sacrificed 1 h after the last injection
PGC-1α KO	Sham (n = 6)	Mice with seven injections of 0.9% NaCl and sacrificed 1 h after the last injection
	Cerulein (n = 6)	Mice with pancreatitis induced by seven injections of cerulein and sacrificed 1 h after the last injection
	Cerulein + LMT-28 (n = 4)	Mice with pancreatitis induced by seven injections of cerulein and LMT-28-treatment, sacrificed 1 h after the last injection

3 Experimental techniques

3.1 Mass spectrometry by UHPLC-MS/MS

The UHPLC-MS/MS analysis of glutathione, homocysteine, cysteine, cystathionine, methionine, SAM, SAH and MTA was carried out at the Central Service for Experimental Research Support (SCSIE) of the University of Valencia. The chromatographic system used consisted of a Waters Acquity UHPLC-XevoTQsystem (Milford, MA, USA).

In the analysis of glutathione, homocysteine, cysteine, cystathionine, methionine and serine levels, pancreatic tissues were homogenized in phosphate buffered saline (PBS) and N-ethylmaleimide (NEM) (Sigma-Aldrich, St. Louis, MO, USA) 10 mM (pH 7.0), with a ratio of tissue and buffer of 1:4. To determine SAM, SAH and MTA levels, pancreatic samples were homogenized in 0.1% v/v HCOOH, adding 1 ml per 100 mg of tissue.

Perchloric acid solution was added to all samples to obtain a final concentration of 4%. Thereafter, samples were centrifuged at 11.000 rpm for 15 min at 4ºC. The pellets were re-suspended in NaOH 1N using an equivalent volume to that of supernatant and then, protein was determined by bicinchoninic acid (BCA) assay using Pierce™ BCA Protein Assay Kit (Thermo Fisher Scientific, Rockford, IL, USA). Briefly, 3 µL of protein extract was added to 260 µL of reagent containing BCA in a 96-well plate. The mixture was incubated 30 min at 37 ºC and then, the absorbance was measured at 562 nm in a plate reader Multiskan® Spectrum (Thermo Fisher Scientific, Rockford, IL, USA).

95 µL supernatants and 5 µL of internal standard (IS) solution (10 mmol L-1) were added and injected in the chromatographic system (UPLC-MS/MS).

The chromatographic system used consisted of a Waters Acquity UPLC-XevoTQsystem (Milford, MA, USA). The conditions employed were positive electrospray ionization (ESI+), capillary voltage 3.50 kV, cone 20.00 V, extractor 5.00 V, source temperature 120 ºC, desolvation temperature 300 ºC, nitrogen cone and desolvation gas flows were 25 and 690 L/h, respectively. Separation conditions were selected to achieve appropriate chromatographic retention and resolution by using a kinetex UPLC C8 column (100 x 2.1mm x 100 Å, 1.7 µm) from Phenomenex (Torrance, CA, USA).

Table 7. Transitions for trans-sulfuration metabolites determined by UHPLC–MS/MS

Analyte	m/z parent ion	Cone (v)	m/z daughter ion Quantification	Confirmation	Collision energy (eV)
GSH	433.2	30	304.3	201.2	15
Homocysteine	269.1	35	136.1	90	11
Cysteine	247.1	25	158.1	184.2	20
Cystathionine	223.2	20	88.1	134.1	15
Met	150.2	20	104.2	133.2	15
SAM	400.1	15	250.5	298.9	15
SAH	385.1	15	136.1	250.1	15
MTA	299.0	25	136.1	162.9	25

A binary gradient was used in which mobile phase A was H_2O (0.1% v/v HCOOH): Mobile phase B was acetonitrile (CH_3CN). The flow was 350 µL/min, the column temperature was 30 °C and the injection volume was 5 µL. The gradient started with 0% phase A, from 2.5 to 4.4 min, increased to 65%. The conditions were maintained for 1.6 min to return to the initial conditions for 3.9 min, and then the system was rebalanced.

Mass spectrometric detection was carried out by multiple reaction monitoring (MRM) employing the acquisition parameters summarized in Table 7. Two MRM transitions per analyte were acquired for quantification and confirmation.

3.2 Protein quantification by MRM

Proteomic quantification by MRM was carried out at the Proteomic Unit (Centro Nacional de Biotecnología, CSIC, Madrid, Spain).

Mechanical disruption of pancreatic tissue was performed using a Potter-Elvehjem homogenizer, in the presence of 7M urea, 2M thiourea, 4% CHAPS, 40 mM DTT and protease inhibitor cocktail (Roche Diagnostics, Basel, Switzerland). Individual sample homogenates were centrifuged for 5 min at 10,000 g and cleared supernatants stored at -80ºC until further processing. Total protein was determined using Pierce™ BCA Protein Assay Kit (Thermo Fisher Scientific, Rockford, IL, USA). After protein precipitation, 10 ug /sample was digested using a 1:25 trypsin:sample ratio, according to a method previously described [517]. After digestion, samples were desalted using ZipTip (Merck, Darmstadt, Germany) according to manufacturer instruction.

Digested samples were diluted with 0.2% TFA in water and subjected to MRM analysis using a 1D Plus nanoLC Ultra system (Eksigent, Dublin, CA, USA) interfaced to a Sciex 5500 QTRAP triple quadrupole mass spectrometer (Sciex, Framingham, MA, USA) equipped with a nano-ESI source and controlled by Analyst v.1.5.2. software (ABSciex, Alcobendas, Madrid, Spain) according to Mora MI et al. [518]. Samples were loaded online on a C18 PepMap 300 µm I.D.

X 5 mm trapping column (5 µm, 100 Å) (Thermo Fisher Scientific, Rockford, IL, USA) and separated using a BioSphere C18 75 µm i.d. × 150 mm capillary column (3 µm, 120 Å, Nanoseparations). Gradient elution was performed according the following scheme: isocratic conditions of 98% A (water containing 0.1% formic acid): 2% B (100 % ACN with 0.1% formic acid) for two minutes, a linear increase to 40% B in 45 min, a linear increase to 95% B in one minute, isocratic conditions of 95% B for five minutes and return to initial conditions in five minutes. Injection volume was 5 µL. The liquid chromatographic system was coupled via a nanospray source to the mass spectrometer.

Experimental settings for MRM analysis were taken initially from [518] and adapted with minor modifications with the help of Skyline v.3.6 software [519]. In summary, a list of transitions (usually 3-4 per peptide, with a preference toward higher-mass y series ions) as well as collision energy values were determined automatically for the candidate peptides. Experiments were performed at a scan time (dwell time) of 25 ms for 100–1250 m/z mass range. The MS analysis was conducted in the positive ion mode with the ion spray voltage set at 2800 V. Drying gas temperature was set to 150 °C at a flow rate of 20 L/min. Peak areas and signal-to-noise (S/N) values for each transition were determined using Skyline v.3.6.

3.3 Western blotting

Western blotting was used to detect the presence and to quantify relative levels of specific proteins in extracts of pancreatic tissue. In order to evaluate the thiol oxidized states of proteins, western blotting was performed under non-reducing conditions to preserve the oxidized thiol groups in proteins extracts.

3.3.1 Sample preparation

Pancreatic tissues were frozen at −80 ºC until homogenization in extraction buffer (100 mg/ml) on ice. The protein extraction buffer contained 20mM Tris–HCl (pH 7.5), 1 mM EDTA, 150mM NaCl, 0.1% SDS, 1% Igepal CA-630, 30mM sodium pyrophosphate, 50mM sodium fluoride, 50 µM sodium orthovanadate (all from Sigma-Aldrich, St. Louis, MO, USA) and a protease inhibitor cocktail (Sigma-Aldrich, St. Louis, MO, USA) at a concentration of 4 µl/mL. For western blotting under non-reducing conditions, 50 mM NEM (Sigma-Aldrich, St. Louis, MO, USA) was added to the extraction buffer.

After homogenization, the extract was centrifuged at 15.000 g during 15 min, the pellet was discarded, and protein concentration was determined by bicinchoninic acid (BCA) assay in the supernatant using Pierce™ BCA Protein Assay Kit (Thermo Fisher Scientific, Rockford, IL, USA).

3.3.2 Electrophoresis and protein transfer

Equal amounts of protein (20-40 µg) were added to sample buffer with a ratio of sample and buffer of 3:1 and then, the mixture was boiled 5 min at 95ºC. For electrophoresis under reducing conditions, the following loading buffer was used: 62.5 mM Tris–HCl, pH 6.8, 10% glycerol, 0.005% bromophenol blue, 1% SDS, and 50 mM DTT (all from Sigma-Aldrich, St. Louis, MO, USA). When electrophoresis was performed under non-reducing conditions, the loading buffer had the same composition but without DTT.

Proteins were separated in SDS-PAGE gel (gel percentage was selected depends on the size of the protein of interest) under constant voltage (120-150 V). Then, proteins were transferred onto nitrocellulose membrane using Trans-Blot® Turbo™ Transfer System (Bio-Rad Laboratories, Hercules, CA, USA), 20 min, 120 V. Protein transfer was confirmed by staining nitrocellulose membrane with Ponceau S stain (Thermo Fisher Scientific, Rockford, IL, USA) for 30 s. Then, Ponceau S stain was washed three times with TBS-T (20 mM Tris, 137 mM NaCl, 0,05% Tween-20, pH 7.6) (all from Sigma-Aldrich, St. Louis, MO, USA) and the membrane was blocked in 5% BSA (Sigma-Aldrich, St. Louis, MO, USA) diluted in TBS-T at room temperature for 1 h.

3.3.3 Immunoblotting

After the blocking step, the membrane was incubated overnight at 4 ºC with the suitable primary antibody to detect the protein of interest. Table 8 summarized the primary antibodies used in this work.

After incubation with the primary antibody, the membrane was washed three times with TBS-T and then, incubated with secondary antibody conjugated with horseradish peroxidase (HRP) 1 h at room temperature. The secondary antibodies were used according to the species of primary antibody host and are summarized in Table 9.

After that, the membrane was washed again three times with TBS-T and it was incubated with Pierce™ ECL Western Blotting Substrate (Thermo Fisher Scientific, Rockford, IL, USA) 5 min at room temperature. Chemiluminescence was detected with a charge-coupled device camera Biorad ChemiDoc™ XRS+ Molecular Imager (Bio-Rad Laboratories, Hercules, CA, USA) and LAS-3000 (Fujifilm, Minato-ku, Tokyo, Japan).

Table 8. Primary antibodies used for western blotting

Antigen	Reference	Source	Dilution
AcLys	Cell Signalling Technology (#9441)	Rabbit	1:1000 in 5% BSA/TBS-T*
β-tubulin	Abcam (ab6046)	Rabbit	1:1000 in 5% BSA/TBS-T*
CBS	Cell Signalling Technology (#14782)	Rabbit	1:1000 in 5% BSA/TBS-T*
Cleaved caspase-3	Cell Signalling Technology (#9661)	Rabbit	1:1000 in 5% BSA/TBS-T*
ERK1/2	Cell Signalling Technology (#9102)	Rabbit	1:1000 in 5% BSA/TBS-T*
H3	Abcam (ab1791)	Rabbit	1:1000 in 5% BSA/TBS-T*
IgG	Santa Cruz (sc-2025)	Mouse	1:1000 in 5% BSA/TBS-T*
JNK	Cell Signalling Technology (#9252)	Rabbit	1:1000 in 5% BSA/TBS-T*
3-Nitrotyrosine	Cell Signalling Technology (#9691)	Rabbit	1:1000 in 5% BSA/TBS-T*
NOS2	Abcam (ab15323)	Rabbit	1:1000 in 5% BSA/TBS-T*
p38α	Cell Signalling Technology (#9212)	Rabbit	1:1000 in 5% BSA/TBS-T*
p53	Cell Signalling Technology (#2524)	Mouse	1:1000 in 5% BSA/TBS-T*
p65	Cell Signalling Technology (#8242)	Rabbit	1:1000 in 5% BSA/TBS-T*
p-ERK1/2	Cell Signalling Technology (#9101)	Rabbit	1:1000 in 5% BSA/TBS-T*

PGC-1α	Santa Cruz (sc-518 025)	Rabbit	1:500 in 5% BSA/TBS-T*
p-JNK	Cell Signalling Technology (#9251)	Rabbit	1:1000 in 5% BSA/TBS-T*
p-MEK1/2	Cell Signalling Technology (#9121)	Rabbit	1:1000 in 5% BSA/TBS-T*
p-MKK3/6	Cell Signalling Technology (#9231)	Rabbit	1:1000 in 5% BSA/TBS-T*
p-MKK4	Cell Signalling Technology (#9156)	Rabbit	1:1000 in 5% BSA/TBS-T*
p-MLKL	Cell Signalling Technology (#91689)	Rabbit	1:1000 in 5% BSA/TBS-T*
p-p38α	Cell Signalling Technology (#9211)	Rabbit	1:1000 in 5% BSA/TBS-T*
p-p65	Cell Signalling Technology (#3033)	Rabbit	1:1000 in 5% BSA/TBS-T*
PRX1	Cell Signalling Technology (#8499)	Rabbit	1:1000 in 5% BSA/TBS-T*
PRX2	Abcam (ab109367)	Rabbit	1:1000 in 5% BSA/TBS-T*
PRX3	Abcam (ab73349)	Rabbit	1:1000 in 5% BSA/TBS-T*
PRX-SO$_{2/3}$	Abcam (ab16830)	Rabbit	1:1000 in 5% BSA/TBS-T*
SRX	Provided by Dr. Michel Toledano (I2BC, CEA-CNRS, Gif-sur-Yvette, France)	Rabbit	1:1000 in 5% BSA/TBS-T*
TOM20	Santa Cruz (sc-11415)	Rabbit	1:1000 in 5% BSA/TBS-T*

*BSA was purchased from Sigma-Aldrich (St. Louis, MO, USA). TBS-T was prepared with 20 mM Tris, 137 mM NaCl, 0,05% Tween-20, pH 7.6, all from Sigma-Aldrich (St. Louis, MO, USA).

Table 9. Secondary antibodies used for western blotting

Antigen	Reference	Source	Dilution
Anti-mouse	Cell Signalling Technology (#7076)	Horse	1:10000 in 5% BSA/TBS-T*
Anti-rabbit	Cell Signalling Technology (#7074)	Goat	1:10000 in 5% BSA/TBS-T*

*BSA was purchased from Sigma-Aldrich (St. Louis, MO, USA). TBS-T was prepared with 20 mM Tris, 137 mM NaCl, 0,05% Tween-20, pH 7.6, all from Sigma-Aldrich (St. Louis, MO, USA).

3.4 Immunoprecipitation

Pancreatic tissues were homogenised in extraction buffer (100 mg/ml) and protein concentration was determined using Pierce™ BCA Protein Assay Kit (Thermo Fisher Scientific, Rockford, IL, USA). For immunoprecipitation assay, 1 mg of protein (4 µg/µL) plus the appropriate primary antibody was incubated with gently rocking 2 h at 4 °C. The primary antibodies used for immunoprecipitation assays are summarized in Table 10.

After the incubation with the primary antibody, 50 µL of Pierce™ Protein A/G Agarose (Thermo Fisher Scientific, Rockford, IL, USA) was added and the samples were rocked overnight at 4 °C. After that, the beads were collected by centrifugation (1 min at 2000 rpm), washed three times with 1 mL of cold PBS and, finally resuspended in loading buffer (62.5 mM Tris–HCl, pH 6.8, 10% glycerol, 0.005% bromophenol blue, 1% SDS, and 50 mM DTT) (all from Sigma-Aldrich, St. Louis, MO, USA), boiled at 95°C and loaded on SDS-PAGE gel for western blotting.

Table 10. Primary antibodies used for immunoprecipitation assays

Antigen	Reference	Dilution
CBS	Cell Signalling Technology (#14782)	1:50
PGC-1α	Santa Cruz (sc-518 025)	1:25

3.5 Nuclei isolation

Pancreatic tissues were gently homogenised in NIM buffer (100 mg/ml) on ice. The NIM buffer contained 10mM Tris–HCl (pH 7.4), 0.25M Sacarose, 25mM KCl, 5mM $MgCl_2$ (all from Sigma-Aldrich, St. Louis, MO, USA). The lysate was filtered through a 50 μm pore filter and centrifuged 10 min, 800 g at 4 °C. The pellet was washed with NIM buffer (10 min, 800 g at 4 °C) and dissolved in extraction buffer (20mM Tris–HCl pH 7.5, 1 mM EDTA, 150mM NaCl, 0.1% SDS, 1% Igepal CA-630, 30mM sodium pyrophosphate, 50mM sodium fluoride, 50 μM sodium orthovanadate, and 4 μl/mL of protease inhibitor cocktail) (all from Sigma-Aldrich, St. Louis, MO, USA). Before western blotting analyse, protein concentration was determined using Pierce™ BCA Protein Assay Kit (Thermo Fisher Scientific, Rockford, IL, USA).

3.6 Mitochondrial isolation

Mitochondrial isolation was performed using Mitochondria Isolation Kit for Tissue (Thermo Fisher Scientific, Rockford, IL, USA). Briefly, a piece of around 80 mg of pancreas was gently homogenised in 800μL of 4 μg/μL BSA dissolved in a reagent provided by the kit. Afterwards, 800 μL of Mitochondria Isolation Reagent (provided by the kit) was added and the mixture was centrifuged at 700 g for 10 min at 4 °C. The pellet was discarded, and the supernatant centrifuged again at 3,000 g for 15 min at 4 °C. The supernatant was removed, and the mitochondrial pellet washed (12,000 g for 5 min at 4 °C) with 500 µL of the appropriate buffer provided by the kit. The mitochondria were lysate with 2% CHAPS (Thermo Fisher Scientific, Rockford, IL, USA) in Tris buffered saline (25mM Tris pH 7.2, 0.15M NaCl). After centrifuging the extract at 12,000 g for 5 min at 4 °C, protein concentration was determined at the supernatant using Pierce™ BCA Protein Assay Kit (Thermo Fisher Scientific, Rockford, IL, USA).

3.7 RT-qPCR analysis for gene expression

3.7.1 RNA extraction

A piece of around 30 mg of pancreas was excised, immediately immersed in RNA-later solution (Ambion, Thermo Fisher Scientific, Rockford, IL, USA) to stabilize the RNA, homogenized in 500 µl of TRIzol™ Reagent (Thermo Fisher Scientific, Rockford, IL, USA). The extract was centrifuged 10 min, 10,000 g, at 4 ºC, the pellet was discarded and 100 µl of chloroform was added to the supernatant. After a 15 min centrifugation at 12,000g at 4 ºC, three phases were obtained, a lower organic red (protein), a white interface (DNA) and an upper aqueous phase with RNA. The aqueous phase was collected, mixed with 250 µl of isopropanol, incubated 10 min at room temperature and then, centrifugated 10,000g for 10 min at 4 ºC to precipitate RNA. The supernatant was removed, and the pellet was dissolved in 500 µl of cold 75% ethanol. After a centrifugation at 7,500 g for 5 min at 4 ºC, the pellet was dissolved in 25 µl of Nuclease-Free Water (Ambion, Thermo Fisher Scientific, Rockford, IL, USA). The concentration and the purity of RNA were determined using NanoDrop™ Lite Spectrophotometer (Thermo Fisher Scientific, Rockford, IL, USA). To assess the quality of the RNA, isolated RNA (2 mg/lane) was size-fractionated by electrophoresis in a 1% agarose/formalin gel, and stained with GelRed® Nucleic Acid Gel Stain (Biotium, Landing Parkway Fremont, CA, USA).

3.7.2 Reverse transcription and cDNA amplification

The cDNA used as template for amplification in the PCR assay was obtained by the reverse transcription reaction using PrimeScript RT Enzyme with Oligo dT and random hexamers as primers (all from Takara, Kusatsu, Shiga, Japan), starting with equal amounts of RNA (50 ng/μL). The reverse transcription was performed using C1000™ Thermal Cycler (Bio-Rad Laboratories, Hercules, CA, USA) with the following protocol: 37 °C 15 min (reverse transcription) and 85 °C 5 s (inactivation of reverse transcriptase with heat treatment).

For some of the genes studied, specific oligonucleotides were designed and then, synthesized by Sigma-Aldrich, St. Louis, MO, USA (Table 11). The efficiency of each pair of primers (1.9 - 2.1) was checked using a standard curve of cDNA concentration. The RNA level was analysed by dsDNA binding dye SyberGreen PCR Master mix (Takara, Kusatsu, Shiga, Japan) in an iQTM5 Multicolor Real-Time PCR Detection System (Biorad Laboratories, Hercules, CA, USA). The amplification conditions were 10 min at 95 °C and 40 cycles of 15 s at 95 °C, 30 s at 60-64 °C (according to the optimal temperature of oligonucleotide hybridization) and 30 s of elongation at 72 °C.

For other genes, commercial TaqMan® probes (Applied Biosystems, Carlsbad, USA) were used (Table 12). The amplification was carried out with TaqMan Master Mix2X (Takara, Kusatsu, Shiga, Japan) under the same conditions, being the hybridization temperature 60 °C in all cases.

Table 11. Oligonucleotides used for RT-qPCR

Target gene	Direct/reverse oligonucleotide
Cat	5´- GGAGCAGGTGCTTTTGGATA - 3´ 5´- GAGGGTCACGAACTGTGTCA - 3´
Ppargc1a	5´- TTAAAGTTCATGGGGCAAGC - 3´ 5´- TAGGAATGGCTGAAGGGATG -3´
Prx3	5´- CAAGAAAGAATGGTGGTTTGG -3´ 5´- TGCTTGACGACACCATTAGG -3´
Sod2	5´- GGCCAAGGGAGATGTTACAA -3´ 5´- GAACCTTGGACTCCCACAGA - 3´
Srxn1	5´- AGAGCCTGGTGGACACGAT -3´ 5´- AGGTCTGAAAGGGTGGACCT - 3´
Tp53	5´- AGGGAGCGCAAAGAGAGC -3´ 5´- CCTGCTGTCTCCAGACTCCT - 3´
Tbp	5´- CAGCCTTCCACCTTATGCTC - 3´ 5´- CCGTAAGGCATCATTGGACT -3´

Each reaction was run in triplicate, and the melting curves were constructed using Dissociation Curves Software (Bio-Rad Laboratories, Hercules, CA, USA) to ensure that only a single product was amplified. The threshold cycle (CT) was determined and the relative gene expression was expressed as follows: fold change= $2^{-\Delta(\Delta CT)}$, where ΔCT = CT target – CT housekeeping, and Δ(ΔCT) = ΔCT treated - ΔCT control. *Tbp* was used as housekeeping gene to normalize the transcription analysis.

Table 12. TaqMan® probe used for RT-qPCR

Target gene	TaqMan® probe
Il-1β	Mm00434228_m1
Il-6	Mm00446190_m1
Tnf	Mm00443258_m1
Tbp	*Mm01277042*_m1

3.8 Chromatin immunoprecipitation assay (ChIP)

Chromatin immunoprecipitation assay was carried out using EZ-Magna ChIP HiSens Chromatin Immunoprecipitation Kit (Millipore, Burlington, MA, USA). Briefly, a piece of around 100 mg of pancreas was cut into small pieces, washed (800 x g at 4 °C for 5 min) with 10 mL ice cold PBS and immediately immersed in 37% formaldehyde for 10 min to crosslink the chromatin. After stopping the reaction by adding glycine to a final concentration of 0.125 M, the nuclei were isolated following the manufacturer's instructions.

For chromatin fragmentation, cross-linked isolated chromatin was subjected to 7 cycles of 5 min sonication (30 s on, 30 s off) in a Bioruptor Plus instrument (Diagenode, Seraing, Belgium). The sonicated chromatin was centrifuged at 10,000 *g* for 10 min and the supernatant containing soluble chromatin fragments was aliquoted and stored at −80 °C until use for chromatin immunoprecipitation. One of these aliquots was saved as *Input* fraction. Other aliquot was size-fractionated by electrophoresis in a 1% agarose gel, and stained with GelRed® Nucleic Acid Gel Stain (Biotium, Landing Parkway Fremont, CA, USA) to check that the average size of chromatin fragments obtained after the fragmentation protocol was 500 ± 200 bp.

For chromatin immunoprecipitation, A/G Magnetic Beads provided by the kit were used. Briefly, 10 µL of resuspended beads and 2 µg of the appropriate antibody (Table 13) were mixed up to a final volume of 200 µL of the buffer provided by the kit. Then, the mixture was rocked for 2 h at 4 °C. After that, magnetic beads were collected using a magnetic separator, mixed with an aliquot equivalent to 50 µg DNA and rocked at 4 °C overnight. The immunocomplex, containing chromatin fragments/protein target/magnetic beads, was recovered using a magnetic separator, washed three times, and eluted from the magnetic beads using the appropriate buffers provided by the kit. An aliquot of the crosslinked chromatin was treated as above but using IgG antibody (IgG sample). All samples (ChIP samples, IgG sample and input) were incubated with proteinase K (Millipore, Burlington, MA, USA) at 65 °C for 2 hours and then at 95 °C for 15 min with shaking. The DNA from all these samples was used for quantitative PCR analysis using the primer sequences designed against the promoter region of the target genes showed in Table 14.

Table 13. Antibodies used for ChIP assay

Antigen	Reference
p65	Millipore (17-10060)
H3K4me3	Abcam (ab8580)
H3K27me3	Abcam (ab195477)
H3K9Ac	Abcam (ab4441)
H3K9me3	Abcam (ab8898)

Table 14. Oligonucleotides used for ChIP assay

Target gene	Direct/reverse oligonucleotide
Srxn1	5´- TCCTGACGCTGAGCCTAGAT - 3´ 5´- ATTTCAGAGCGACCCTGCTA- 3´
Il-1β	5´- CACACTTCTGGGTGTGCATC - 3´ 5´- AGTGTGTCATCGTGGTGGAA - 3´
Il-6	5´- GCGTGCCTGCGTTTAAATA -3´ 5´- AGGAAGGGGAAAGTGTGCTT -3´
Tnf-α	5´- CTCCCAGAGACATGGTGGAT -3´ 5´- CACCCTCCCACTCCTAAACA - 3´

3.9 Hydrogen peroxide levels

The Amplex Red Hydrogen Peroxide/Peroxidase kit (Thermo Fisher Scientific, Rockford, IL, USA) was used to measure the levels of hydrogen peroxide in pancreas. For this purpose, pancreas were homogenised in PBS and hydrogen peroxide levels were measured by fluorimetry according to the manufacturer's instructions. The fluorescence signal was detected with excitation at 544 nm and emission at 590 nm. Each tested sample was done in duplicate.

3.10 α-Amylase activity in plasma

Immediately after the sacrifice of mice, the collected blood was centrifuged 15 min at 1800 g to obtain plasma. For measure amylase activity in plasma, α-amylase kit (Spinreact, St. Coloma, Girona, Spain) was used. Briefly, 1 mL of assay reagent (MES 100 mmol/L pH 6.0, 2, 2-chloro-4-nitrophenyl-α-D-maltotrioside ($CNPG_3$) 25 mmol/L, calcium acetate 6 mmol/L, potassium thiocyanate 900 mmol/L, NaCl 350 mmol/L, sodium azide 0, 95 g/L) was added to 20 μL of plasma in a 1 cm light path cuvettes.

α-Amylase hydrolyzes the $CNPG_3$ to release 2-chloro-4-nitrophenol (CNP) and form 2-chloro-4-nitrophenyl- -D-maltoside ($CNPG_2$), maltotriose and glucose according to the following reaction:

$$10\ CNPG_3 \rightarrow 9\ CNP + 1\ CNPG_2 + \text{maltotriose} + \text{glucose}$$

The rate of 2-chloro-4-nitrophenolformation, which is proportional to the catalytic concentration of α-amylase present in the sample, was measured photometrically at 405 nm, for 3 minutes at 1 min intervals.

3.11 Plasma cfDNA levels

For measurement of plasma cell-free DNA, 50 μl of plasma were added to a 96-well plate followed by addition of 50 μl of Sytox Green (1 μM in PBS) (Thermo Fisher Scientific, Rockford, IL, USA). Plates were read immediately at 485/528 nm excitation/emission wavelengths.

3.12 Plasma nucleosomes levels

Plasma nucleosomes were measured using the Cell Death Detection ELISA Plus kit (Sigma-Aldrich, St. Louis, MO, USA) according to manufacturer's instructions. Briefly, 20 μl of plasma was placed into a streptavidin-coated microplate and mixed with 80 μl of immunoreagent containing anti-histone-biotin monoclonal antibody and anti-DNA-POD monoclonal antibody. The mixture was incubated under gently shaking for 2 h at 25 °C to allow the binding of the histone-component and the DNA-component of the nucleosomes to the corresponding antibodies and simultaneously, to allow the capture of the immunocomplexes to the streptavidin-coated microplate. Then, the unbound components were removed by washing three times with 250 µl of incubation buffer provided by the kit. Subsequently, 100 µl of ABTS Substrate Solution (provided by the kit) was added to each well and the microplate was incubated 20 min. After that, the reaction was stopped with 100 µl of ABTS Stop Solution (provided by the kit) and the amount of nucleosomes in plasma was determined spectrophotometrically reading the plate at 405 nm in a plate reader Multiskan® Spectrum (Thermo Fisher Scientific, Rockford, IL, USA).

3.13 Plasma IL-6 levels

For measure IL-6 levels in plasma, a mouse IL-6 Quantikine enzyme-linked immunosorbent assay (ELISA) kit (M6000B, R&D Systems, Minneapolis, MN, USA) was used following the manufacture's protocol.

Briefly, 50 µL of Assay Diluent RD1-14 (provided by the kit) and 50 µL of sample was added to the wells of a microplate coated with a monoclonal antibody specific for mouse IL-6. The microplate was incubated for 2 h at room temperature and then, the wells were washed five times with 400 µL of Wash Buffer (provided by the kit). Subsequently, 100 µL of Mouse IL-6 Conjugate (provided by the kit) was added to each well and the microplate was incubated 2 h at room temperature. After that, 100 µL of Substrate Solution (provided by the kit) was added to each well and the microplate was incubated protected from light for 30 min at room temperature. The reaction was stopped adding 100 µL of Stop Solution (provided by the kit) to each well. After 30 min of incubation, the levels of IL-6 were determined measuring at 450 nm in a plate reader Multiskan® Spectrum (Thermo Fisher Scientific, Rockford, IL, USA) and using a standard curve. To correct optical imperfections in the microplate, readings at 540 nm were subtracted from the readings at 450 nm.

3.14 Histological analysis

Pieces of pancreas and lung were rapidly removed, fixed in 4% paraformaldehyde (Sigma-Aldrich, St. Louis, MO, USA) for 24 h and embedded in paraffin (Sigma-Aldrich, St. Louis, MO, USA). 4 µm sections were prepared using an automatic microtome and then mounted on glass slides. Afterward, the tissue sections were deparaffinized by xylene, rehydrated by different graded ethanol dilution (100%, 90%, and 70%) and then stained with hematoxylin and eosin (Sigma-Aldrich, St. Louis, MO, USA). These procedures were carried out at the Central Service for Experimental Research Support (SCSIE) of the University of Valencia.

Pancreatic sections were assessed at 20× objective magnification over 10 separate fields for severity of pancreatitis by scoring edema, inflammatory infiltrate and necrosis according to the score of Van Laethem *et al.* [520].

3.15 Myeloperoxidase activity

Myeloperoxidase activity was measured in lung tissue. Lungs were frozen at −80 °C until homogenization in 50 mM KH2PO4 (Sigma-Aldrich, St. Louis, MO, USA) at pH 6.0. The homogenates were then centrifuged at 20,000 g for 20 min. The supernatant were stored to determine protein concentration later using Pierce™ BCA Protein Assay Kit (Thermo Fisher Scientific, Rockford, IL, USA). The pellets were resuspended in 50 mM KH2PO4 (pH 6.0) supplemented with 0.5% hexadecyl-trimethylammonium bromide (Sigma-Aldrich, St. Louis, MO, USA) and then sonicated for 30 s using Branson Ultrasonics™ Sonifier™ SFX150 Cell Disruptor (Fisher Scientific, Thermo Fisher Scientific, Rockford, IL, USA), snap-frozen in dry ice and thawed on three consecutive occasions and finally, sonicated again for 30 s. After that, samples were incubated at 60 ° C for 2 h and then centrifugated at 15,000 g for 15 min. Supernatants were collected for myeloperoxidase assay. Enzyme activity was assessed photometrically at 620 nm. The assay mixture consisted of 20 μL supernatant, 10 μL tetramethylbenzidine (final concentration 1.6 mM) dissolved in DMSO, and 140 μL H2O2 (final concentration 3.0 mM) diluted in 80 mM phosphate buffer, pH 5.4. An enzyme unit is defined as the amount of enzyme that produces an increase of 1 absorbance unit per minute.

3.16 Statistical analysis

Results are expressed as mean ± standard deviation (SD). Statistical analysis was performed in two steps. One-way analysis of variance (ANOVA) was performed first. When the overall comparison of groups was significant, differences between individual groups were investigated using the Bonferroni test.

IV. RESULTS

1 Regulation of the trans-sulfuration pathway in acute pancreatitis

1.1 Changes in trans-sulfuration metabolites levels during acute pancreatitis

Firstly, we measured the levels of the trans-sulfuration metabolites in pancreas of mice during cerulein-induced acute pancreatitis at 1, 3, 5 and 7 h by mass spectrometry in order to assess the function of the trans-sulfuration pathway in pancreatic tissue during the time course of acute pancreatitis.

Early after the first cerulein injection (1 h), pancreatic levels of methionine were depleted by 50%, and this depletion was aggravated (by 80%) at 3 h of the first cerulein injection maintaining these low levels thereafter (Figure 16A). Pancreatic S-adenosylmethionine (SAM) levels remained unchanged during the first hour, but exhibited a marked decrease (50%) at the third hour and thereafter (Figure 16B). Both pancreatic S-adenosylhomocysteine (SAH) and homocysteine levels remained unchanged during the course of acute pancreatitis (Figure 16C, D). In contrast, levels of cystathionine and cysteine markedly diminished at 1 h after pancreatitis induction and thereafter (Figure 16E, F).

GSH levels were also measured to assess the profile of GSH depletion and they began to be markedly depleted at 3 h (Figure 16G).

Pancreatic methylthioadenosine (MTA) levels, a metabolite of SAM catabolism, increased significantly at 1 h after the first cerulein injection, but progressively diminished after this time point reaching at 7 h a lower level than the basal conditions (Figure 16H).

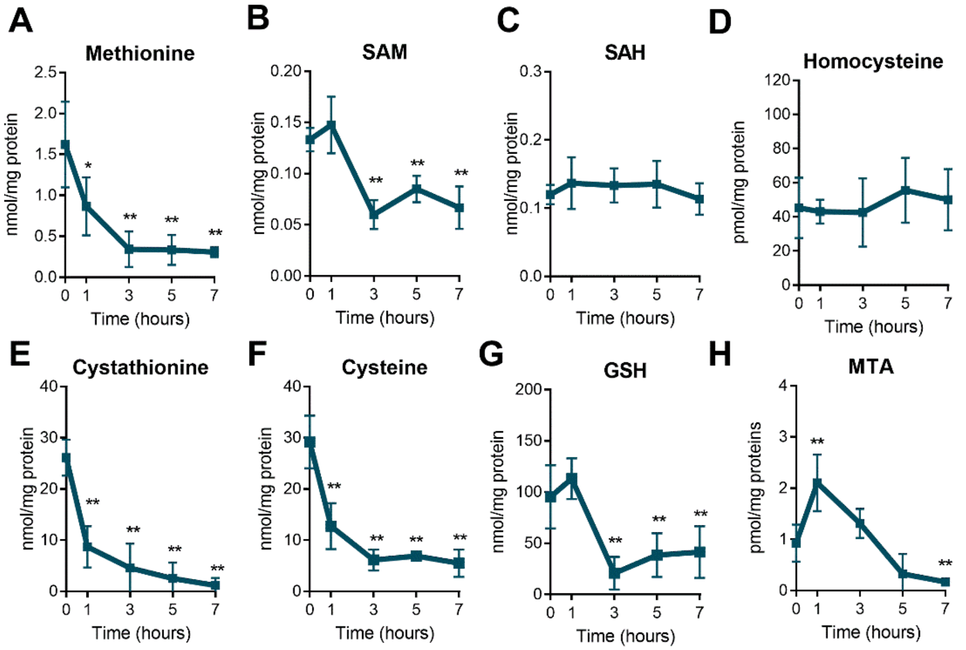

Figure 16. Levels of trans-sulfuration metabolites, GSH and MTA in pancreas during cerulein-induced acute pancreatitis. Levels of methionine (A), S-adenosylmethionine (SAM) (B), S-adenosylhomocysteine (SAH) (C), homocysteine (D), cystathionine (E), cysteine (F), reduced glutathione (GSH) (G), and methylthioadenosine (MTA) (H), in pancreas from control mice at time 0, and 1, 3, 5, and 7 h after the first cerulein injection which corresponds to 1 h after the first, third, fifth and seventh injections of cerulein. The number of mice per group was 4–6. Statistical significance is indicated as *p < 0,05 and **p < 0,01 *vs.* control mice at time 0.

1.2 Levels of proteins involved in the trans-sulfuration pathway during acute pancreatitis

In pancreatic tissue, we analyzed by proteomics the steady-state protein levels of 8 enzymes involved in the trans-sulfuration pathway (Figure 17A). Protein levels of methionine adenosyltransferase 1A (MAT1A), MAT2A and MAT2B, glycine N-methyltransferase (GNMT), cystathionine-β-synthase (CBS) and methionine synthase (MS), remained unchanged in pancreas with acute pancreatitis (Figure 17B, C, E, G).

Pancreatic levels of S-adenosylhomocysteine-hydrolase (SAHH) and cystathionase (CSE), were reduced upon cerulein-induced acute pancreatitis (Figure 17D, F).

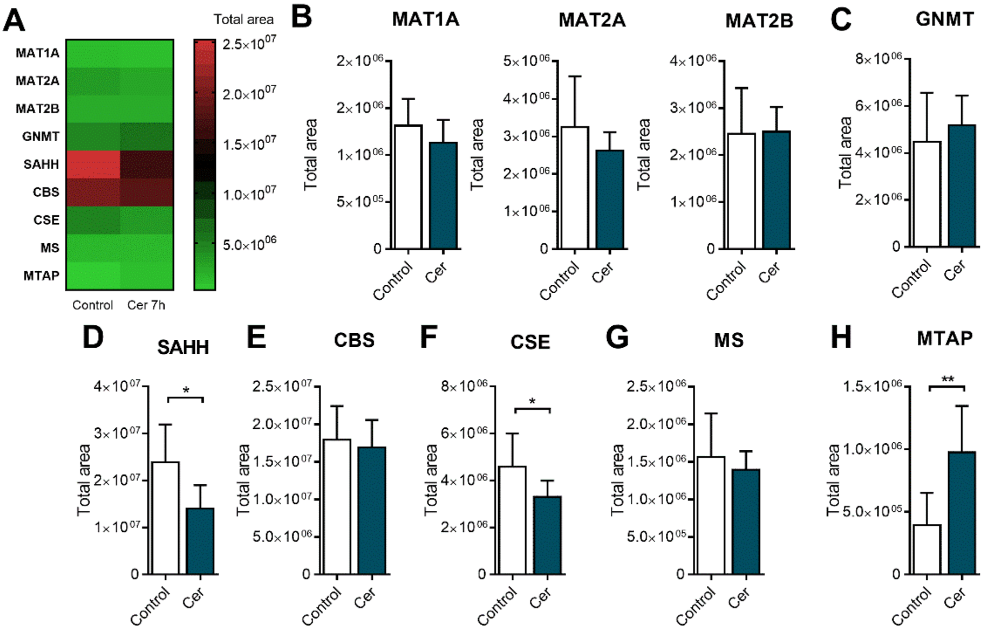

Figure 17. Protein levels of enzymes involved in trans-sulfuration pathway in pancreas with acute pancreatitis. Heatmap showing the levels of MAT1A, MAT2A, MAT2B, GNMT, SAHH, CBS, CSE, MS and MTAP, in pancreas from control mice (Control) and from mice with acute pancreatitis (1 h after the seventh injection of cerulein) (Cer) (A). Histograms showing the levels of MAT1A, MAT2A and MAT2B (B), GNMT (C), SAHH (D), CBS (E), CSE (F), MS (G), and MTAP (H), in pancreas from control mice (Control) and from mice with acute pancreatitis (1 h after the seventh injection of cerulein) (Cer). The number of mice per group was 6–8. Statistical significance is indicated as *p < 0,05 and **p < 0,01.

In contrast, the pancreatic protein levels of methylthioadenosine phosphorylase (MTAP), which is involved in MTA degradation, were increased in mice with cerulein-induced acute pancreatitis (Figure 17H).

1.3 Acute pancreatitis triggered tyrosine nitration of cystathionine-β-synthase in pancreas

Previously, it has been reported that thiol oxidation as well as tyrosine nitration of CBS may compromise its enzymatic activity impairing homocysteine metabolism through the trans-sulfuration pathway [328, 329]. Therefore, we evaluated both thiol oxidation and nitration status of CBS in pancreas from mice with acute pancreatitis. Protein tyrosine nitration was increased in pancreas in acute pancreatitis (Figure 18A) and in particular in the CBS immunoprecipitate, showing that CBS nitration was remarkably increased in pancreas with acute pancreatitis (Figure 18B).

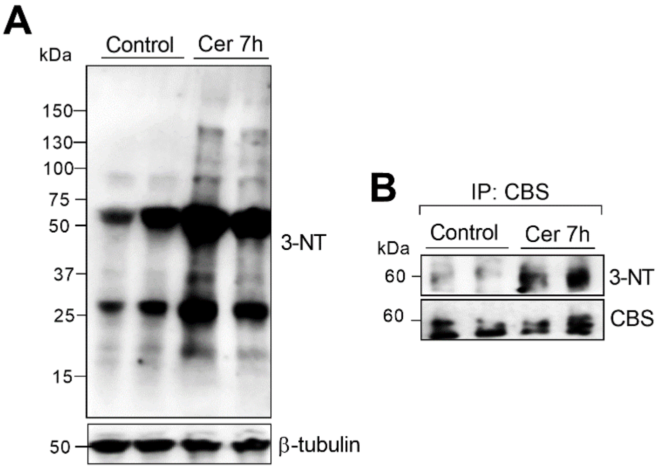

Figure 18. Levels of protein nitration and CBS nitration in pancreas with acute pancreatitis. Representative western blot of 3-nitrotyrosine in total extract (A) and in CBS immunoprecipitate (B) of pancreas from control mice (Control) and from mice with acute pancreatitis (1 h after the seventh injection of cerulein) (Cer). β-tubulin was used as loading control. The number of mice per group was 4.

However, thiol oxidation of CBS was not found in pancreas with acute pancreatitis (Figure 19).

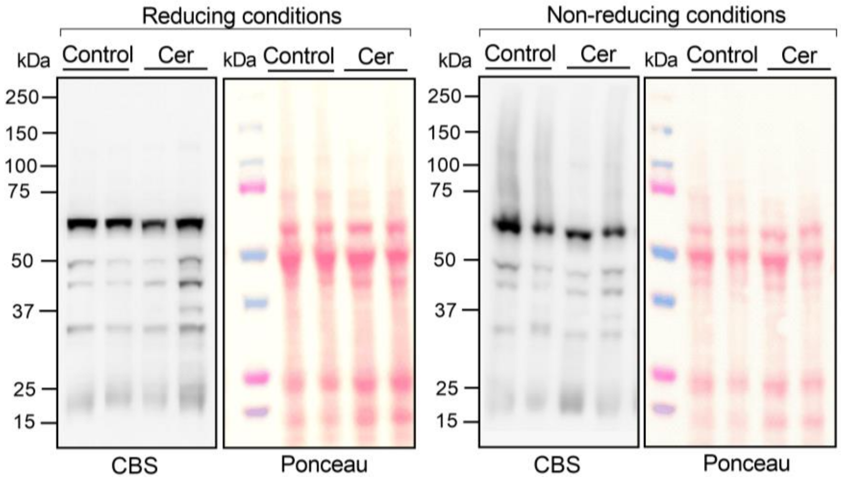
Reducing conditions
Non-reducing conditions
kDa
Control
Cer
kDa
Control
Cer
kDa
Control
Cer
kDa
Control
Cer
250
150
100
75
50
37
25
15
250
150
100
75
50
37
25
15
CBS
Ponceau
CBS
Ponceau

Figure 19. Thiol oxidation of CBS in pancreas with acute pancreatitis. Representative western blot of CBS under reducing and non-reducing conditions in pancreas from control mice (Control) and in pancreas from mice with acute pancreatitis (1h after the seventh injection of cerulein) (Cer). Ponceau staining was used as a loading control.

In parallel with the increased CBS nitration, *Nos2* gene expression and its protein levels were markedly upregulated in pancreas with acute pancreatitis (Figure 20A, B). However, mRNA levels of *Nos1* and *Nos3* did not change significantly in acute pancreatitis (Figure 20A).

1.4 Administration of S-adenosylhomocysteine triggered homocysteine accumulation in acute pancreatitis

In order to confirm the blockade of homocysteine metabolism at the level of CBS during cerulein-induced acute pancreatitis, SAM was administered and pancreatic levels of metabolites of the trans-sulfuration pathway were determined 1 h after the last cerulein injection.

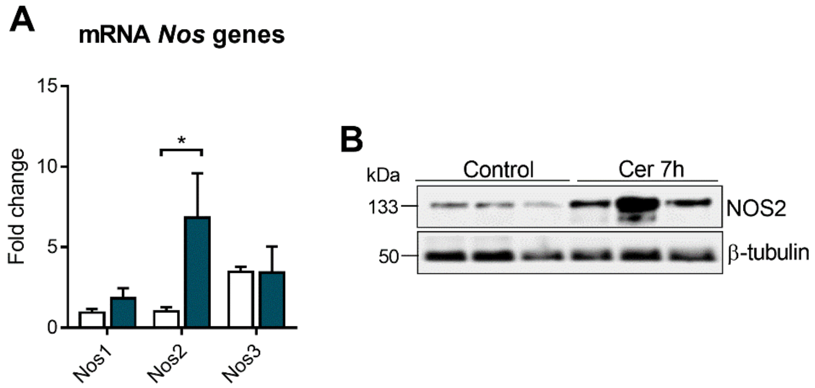

Figure 20. Gene expression of *Nos* genes and protein levels of NOS2 in pancreas with acute pancreatitis. mRNA relative expression of *Nos1, Nos2* and *Nos3* vs *Tbp* in pancreas from control mice (Control) and in pancreas from mice with acute pancreatitis (1 h after the seventh injection of cerulein) (Cer) (A). Western blot of NOS2 in pancreas from control mice (Control) and in pancreas from mice with acute pancreatitis (1 h after the seventh injection of cerulein) (Cer) (B). β-tubulin was used as loading control.

Under basal conditions, the group of control mice that received SAM injections (SAM-treated mice) exhibited higher levels of SAM and MTA in pancreas in comparison with control mice (Figure 21B, H). However, pancreatic levels of SAM and MTA diminished not only in mice with pancreatitis (Cer mice), but also in SAM-treated mice with pancreatitis (Cer + SAM mice) (Figure 21B, H). Additionally, SAH levels were low in pancreas of SAM-treated mice with pancreatitis (Cer + SAM mice) compared with control mice and also with mice with pancreatitis (Figure 21C).

In contrast with other metabolites of the trans-sulfuration pathway, pancreatic homocysteine levels were markedly increased in SAM-treated mice with pancreatitis (Cer + SAM mice) in comparison with all the other experimental groups ((Figure 21D).

Homocysteine re-methylation to methionine seems to be impaired during acute pancreatitis, as both mice with pancreatitis (Cer mice) and SAM-treated mice with pancreatitis (Cer + SAM mice) exhibited markedly diminished methionine levels in pancreas in comparison with control mice (Figure 21A).

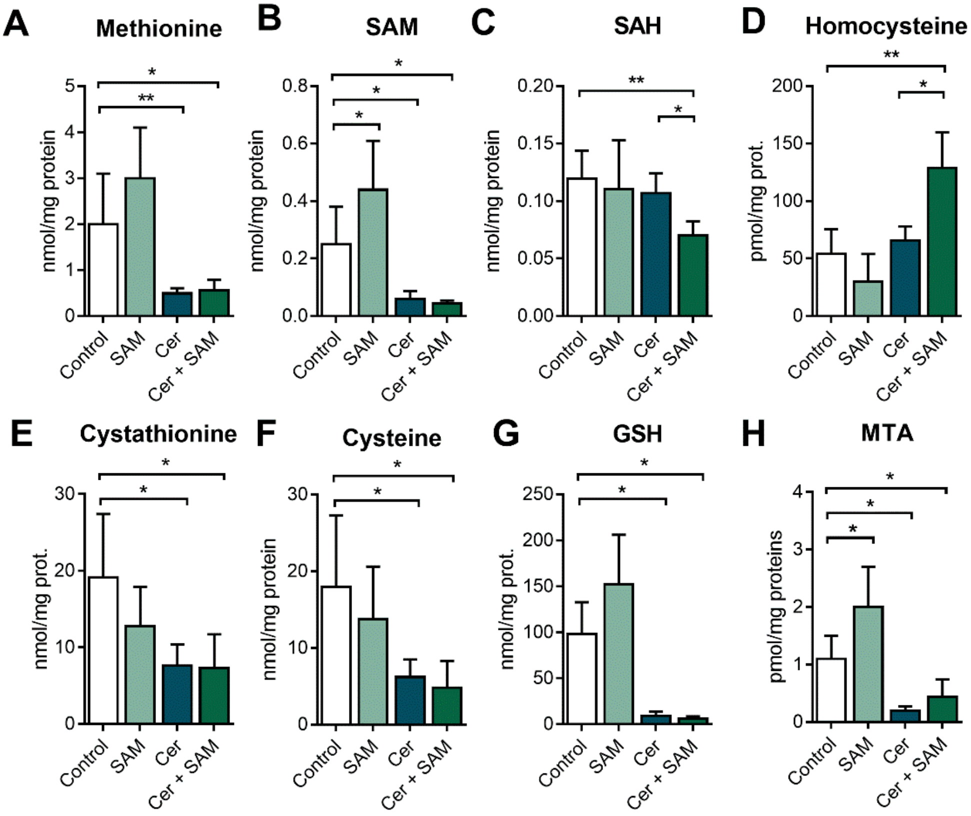

Figure 21. Levels of trans-sulfuration metabolites, GSH and MTA in pancreas from mice with acute pancreatitis treated with SAM. Levels of methionine (A), S-adenosylmethionine (SAM) (B), S-adenosylhomocysteine (SAH) (C), homocysteine (D), cystathionine (E), cysteine (F), reduced glutathione (GSH) (G), and methylthioadenosine (MTA) (H) in pancreas from control mice (Control), SAM-treated control mice (SAM), mice with acute pancreatitis (1 h after the seventh injection of cerulein) (Cer), and SAM-treated mice with acute pancreatitis (1 h after the seventh injection of cerulein) (Cer + SAM). The number of mice per group was 4–6. Statistical significance is indicated as *p < 0,05 and **p < 0,01.

In addition, treatment with SAM did not modify the pancreatic levels of cystathionine, cysteine, and GSH in mice with pancreatitis compared with those mice without SAM treatment. Thus, the levels of these metabolites remained low in these two experimental groups with pancreatitis compared with control mice (Figure 21E, F, G).

1.5 S-adenosylhomocysteine administration aggravated the inflammatory response in acute pancreatitis

To evaluate the impact of SAM treatment on the inflammatory response during acute pancreatitis, *Tnf-α* and *Il-6* gene expression were measured in pancreas and histological analysis was performed. As expected, *Tnf-α* and *Il*-6 mRNA levels were dramatically increased in pancreas in acute pancreatitis, but these levels were even higher in pancreas from SAM-treated mice with pancreatitis (Figure 22A).

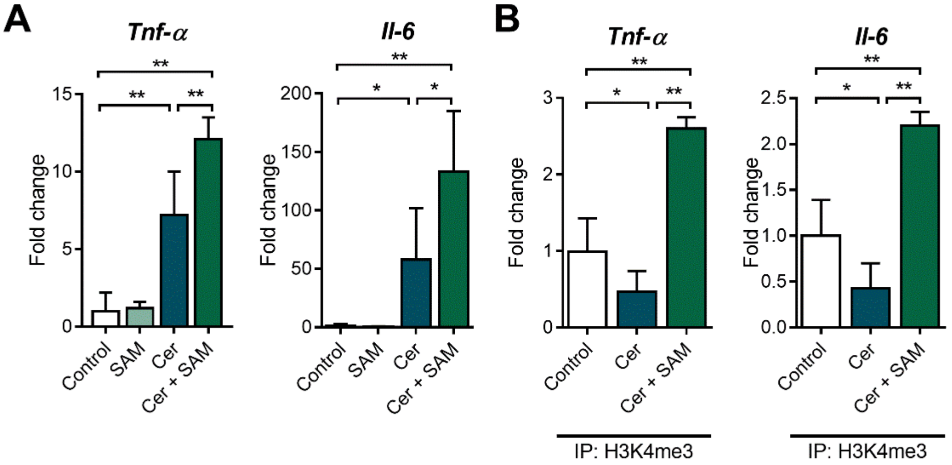

Figure 22. Gene expression of *Tnf-α* and *Il-6,* and levels of H3K4me3 in the promoter of these genes in pancreas from mice with acute pancreatitis treated with SAM. mRNA relative expression of *Tnf-α* and *Il-6* vs *Tbp* (A) and H3K4me3 levels in the promoter of *Tnf-α* and *Il-6* (B) in pancreas from control mice (Control), SAM-treated control mice (SAM), mice with acute pancreatitis (1 h after the seventh injection of cerulein) (Cer) and SAM-treated mice with acute pancreatitis (1 h after the seventh injection of cerulein) (Cer + SAM). The number of mice per group was 4–6. Statistical significance is indicated as * p < 0,05 and **p < 0,01.

We performed CHIP assay to determine the presence of the euchromatin marker H3K4me3, generally associated with active transcription [521], at the promoter regions of *Tnf-α* and *Il-6* genes. We found that the promoter regions of these two genes were enriched in H3K4me3 in pancreas from SAM-treated mice with pancreatitis in comparison with SAM-untreated mice with pancreatitis (Figure 22B).

Furthermore, histological analysis of pancreas revealed that both the inflammatory infiltrate and edema were more intense in SAM-treated mice with pancreatitis compared with SAM-untreated mice with pancreatitis (Figure 23A, B)

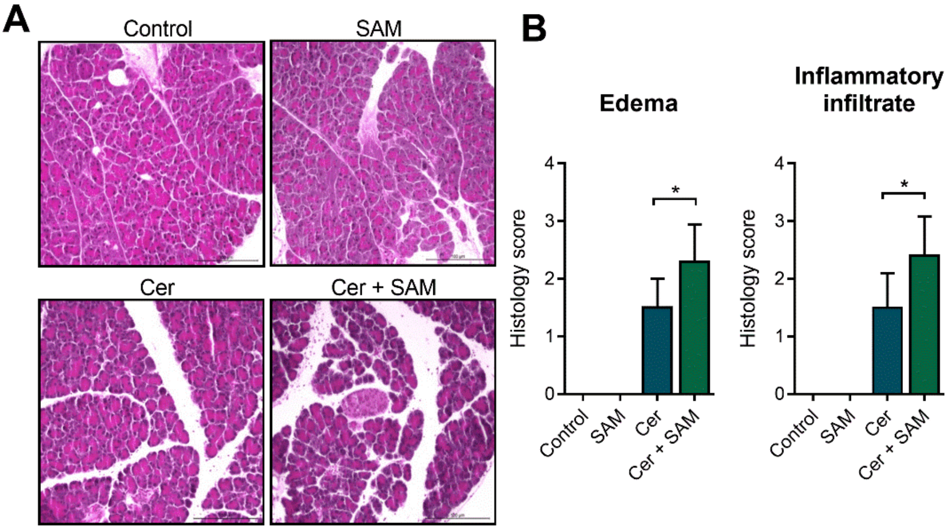

Figure 23. Histological analysis of pancreas from mice with acute pancreatitis treated with SAM. Representative histology (A) and histological scores for edema and inflammatory infiltrate (B) in pancreas from control mice (Control), SAM-treated control mice (SAM), mice with acute pancreatitis (1 h after the seventh injection of cerulein) (Cer) and SAM-treated mice with acute pancreatitis (1 h after the seventh injection of cerulein) (Cer + SAM). The number of mice per group was 4–6. Statistical significance is indicated as * p < 0,05 and **p < 0,01.

1.6 S-adenosylhomocysteine administration enhanced *Nos2* gene expression and cystathionine-β-synthase nitration in acute pancreatitis

Nos2 gene expression was higher in pancreas from SAM-treated mice with pancreatitis in comparison with untreated mice with pancreatitis (Figure 24A). H3K4me3 levels were also increased in the promoter region of *Nos2* in pancreas from SAM-treated mice with pancreatitis in comparison with untreated mice with pancreatitis (Figure 24B).

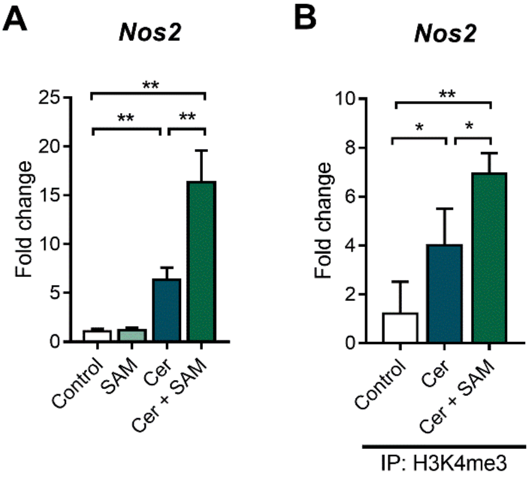

Figure 24. Gene expression of *Nos2* and levels of H3K4me3 in the promoter of *Nos2* in pancreas from mice with acute pancreatitis treated with SAM. mRNA relative expression of *Nos2* vs *Tbp* (A) and H3K4me3 levels in the promoter of *Nos2* (B) in pancreas from control mice (Control), SAM-treated control mice (SAM), mice with acute pancreatitis (1 h after the seventh injection of cerulein) (Cer), and SAM-treated mice with acute pancreatitis (1 h after the seventh injection of cerulein) (Cer + SAM). The number of mice per group was 4–6. Statistical significance is indicated as *p < 0,05 and **p < 0,01.

To assess the impact of the *Nos2* up-regulation induced by SAM on CBS nitration, we measured tyrosine nitration levels of CBS in pancreas from SAM-treated mice with pancreatitis (Cer + SAM). Indeed, SAM treatment increased nitrated levels of CBS nitration in pancreas from mice with acute pancreatitis (Figure 25).

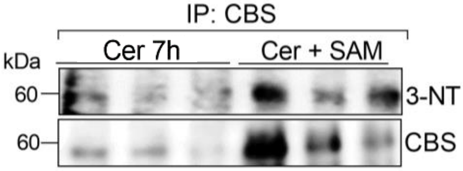

Figure 25. Levels of CBS nitration in pancreas with acute pancreatitis treated with SAM. Western blot of 3-nitrotyrosine in CBS immunoprecipitate from pancreas of mice with acute pancreatitis (1 h after the seventh injection of cerulein) (Cer), and from SAM-treated mice with acute pancreatitis (1 h after the seventh injection of cerulein) (Cer + SAM).

2 Modulation of nitrosative stress and cell death by sulfiredoxin in acute pancreatitis

Considering the peroxynitrite reductase activity of PRXs [415] and taking into account the impact of nitrosative stress in the regulation of the trans-sulfuration pathway in pancreas, we addressed the contribution of the SRX/PRX system to the regulation of redox signaling in acute pancreatitis.

2.1 Acute pancreatitis upregulated mRNA and protein levels of sulfiredoxin

Firstly, we measured the mRNA levels of SRX during the course of acute pancreatitis. Upon induction of acute pancreatitis, mRNA levels of *Srxn1* dramatically increased at 3 h and 5 h of the first cerulein injection. Indeed, *Srxn1* mRNA expression was increased ~170 folds at 5 h (Figure 26A). We performed ChIP assay to detect epigenetic markers of active transcription in the promoter of *Srxn1* after the induction of acute pancreatitis. We found a slight but significant increase in the levels of the euchromatin marker H3K4me3 in the promoter of *Srxn1* at 1 h after the first cerulein injection (Figure 26B).

In addition, protein levels of SRX increased at 3 h and thereafter with a maximum around ~3 fold at 7 h of the first cerulein injection (Figure 26C).

2.2 Acute pancreatitis triggered transient hyperoxidation of peroxiredoxins

Taking into account the marked increase in SRX levels during the course of acute pancreatitis, we decided to measure protein levels and the hyperoxidized thiol states -sulfinic and sulfonic forms- of PRX1, PRX2 and PRX3 during the course of acute pancreatitis.

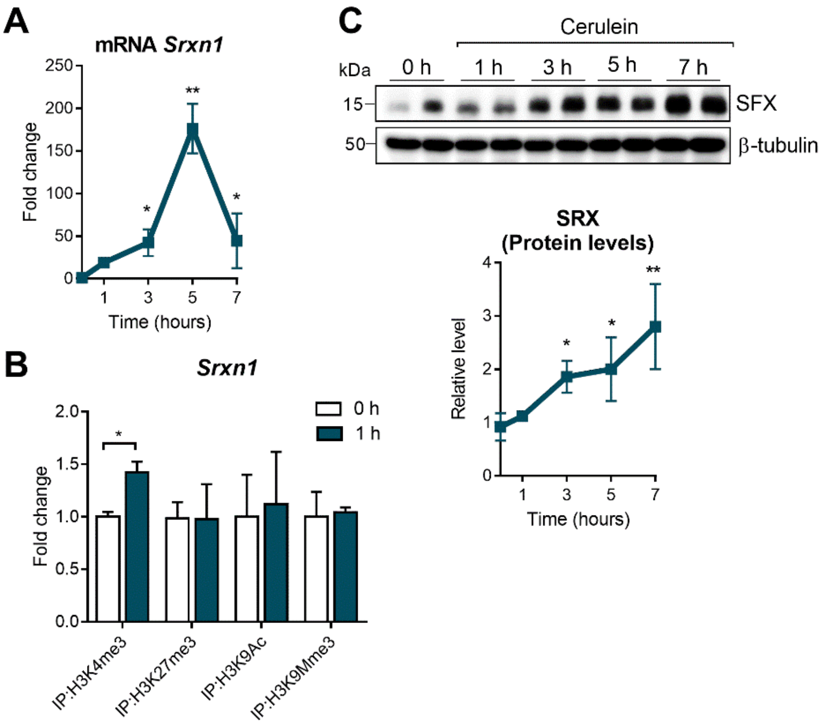

Figure 26. Gene expression and epigenetic markers in the promoter of Srxn1, and protein levels of SRX in pancreas during acute pancreatitis. mRNA relative expression of *Srxn1* vs *Tbp* in pancreas from control mice at time 0, and 1, 3, 5, and 7 h after the first cerulein injection which corresponds to 1 h after the first, third, fifth and seventh injections of cerulein (A). Levels of H3K4me3, H3K27me3, H3K9Ac and H3K9me3 in the promoter of *Srxn1* in pancreas from control mice and at 1 h after the first injection of cerulein (B). Representative western blot and densitometry quantification of SRX in pancreas from control mice at time 0, and 1, 3, 5, and 7 h after the first cerulein injection which corresponds to 1 h after the first, third, fifth and seventh injections of cerulein. β-tubulin was used as loading control (C). The number of mice per group was 4–6. Statistical significance is indicated as $*p < 0,05$ and $**p < 0,01$.

Early after the first cerulein injection (1 h), protein levels of PRX1 tended to decrease but not significantly. At 3, 5 and 7 h after the first cerulein injection, protein levels of PRX1 were significantly diminished (Figure 27A, B). Protein levels of PRX2 remained unchanged at 1 and 3 h after the first cerulein injection but decreased at 5 and 7 h (Figure 27A, B). Protein levels of PRX3 decreased only at 7 h after the first cerulein injection (Figure 27A, B).

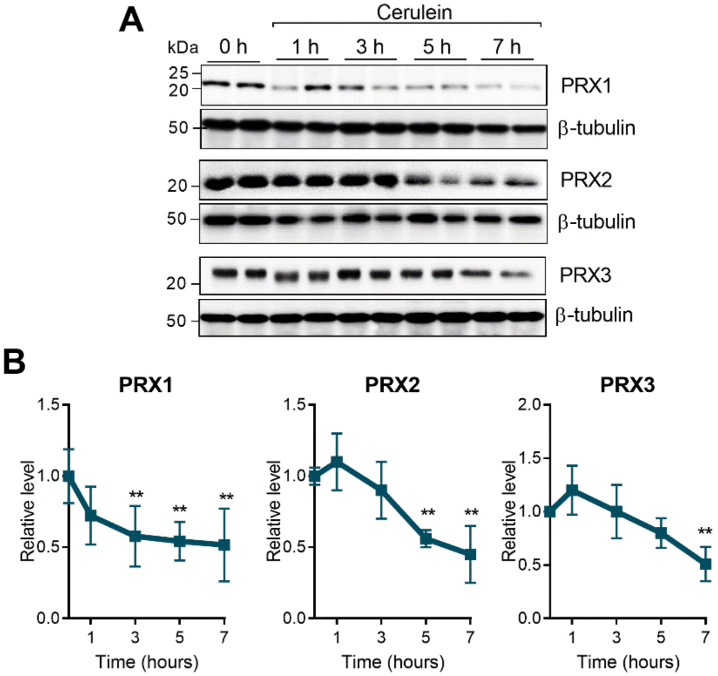

Figure 27. Protein levels of PRX1, PRX2 and PRX3 in pancreas during acute pancreatitis. Representative western blots of PRX1, PRX2 and PRX3 (A) and densitometry quantification (B) in pancreas from control mice at time 0, and 1, 3, 5, and 7 h after the first cerulein injection which corresponds to 1 h after the first, third, fifth and seventh injections of cerulein. β-tubulin was used as loading control. The number of mice per group was 4–6. Statistical significance is indicated as *p < 0,05 and **p < 0,01.

Regarding the hyperoxidized thiol states -sulfinic and sulfonic forms- of PRX1, PRX2 and PRX3, we found a transient significant increase of these forms early, at 1 h after the first injection of cerulein, coinciding with the first peak of H_2O_2 in the pancreas (Figure 28A, B, C). At 3 h, sulfinic and sulfonic forms of PRX1, PRX2 and PRX3 tended to remain increased but without significant differences vs. 0 h, and later on returned to basal levels at 5 h (Figure 28A, B).

Interestingly, sulfenic and sulfonic forms of PRX1 and PRX2 increased again at 7 h (i.e. 1 h after the seventh injection of cerulein), coinciding with the second peak of H_2O_2 (Figure 28A, B, C). In contrast, sulfonic and sulfenic forms of PRX3 did not augment 1 h after the seventh injection of cerulein (Figure 28A, B).

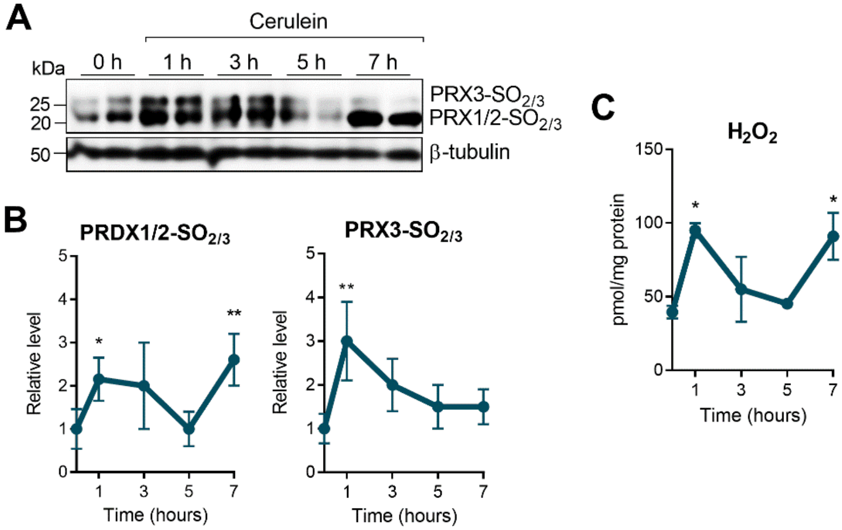

Figure 28. Protein levels of sulfinic and sulfonic forms of PRX1, PRX2 and PRX3 and levels of H_2O_2 in pancreas during acute pancreatitis. Representative western blots (A) and densitometry quantification (B) of hyperoxidized forms of PRX1, PRX2 and PRX3 in pancreas from control mice at time 0, and 1, 3, 5, and 7 h after the first cerulein injection which corresponds to 1 h after the first, third, fifth and seventh injections of cerulein. β-tubulin was used as loading control. Levels of H_2O_2 in pancreas from control mice at time 0, and 1, 3, 5, and 7 h after the first cerulein injection which corresponds to 1 h after the first, third, fifth and seventh injections of cerulein (C). The number of mice per group was 4–6. Statistical significance is indicated as $^*p < 0{,}05$ and $^{**}p < 0{,}01$.

2.3 Acute pancreatitis induced translocation of sulfiredoxin into mitochondria

As we found that mitochondrial PRX3 seems to be susceptible to SRX activity in acute pancreatitis, we measured the levels of SRX in the mitochondrial fraction of the pancreatic tissue. We found that SRX translocated into mitochondria at 1 h after the first injection of cerulein (Figure 29A), and this translocation was even more intense at 7 h (Figure 29B).

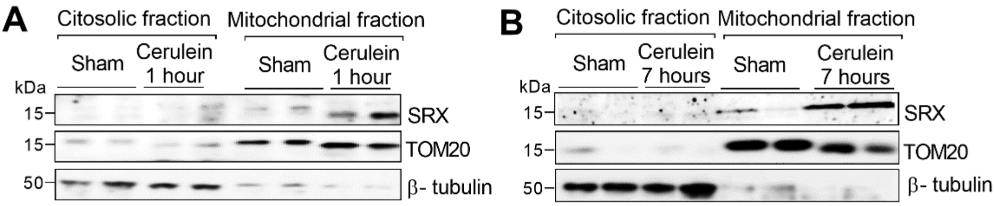
A
Citosolic fraction
Mitochondrial fraction
Sham
Cerulein 1 hour
Sham
Cerulein 1 hour
kDa
15
15
50
SRX
TOM20
β- tubulin
B
Citosolic fraction
Mitochondrial fraction
Sham
Cerulein 7 hours
Sham
Cerulein 7 hours
kDa
15
15
50
SRX
TOM20
β- tubulin

Figure 29. Mitochondrial translocation of SRX in pancreas during acute pancreatitis. Representative western blot of SRX in cytosolic and mitochondrial fraction of pancreas from sham mice and at 1 h after the first injection of cerulein (A), and after the seventh injection of cerulein (B). TOM20 was used as loading control for mitochondrial fraction. β-tubulin was used as loading control for cytosolic fraction. The number of mice per group was 4–6.

2.4 Sulfiredoxin deficiency enhanced pancreatic inflammation and necrosis in acute pancreatitis

In order to evaluate the role of SRX during acute pancreatitis, we induced acute pancreatitis in SRX KO mice.

The histological analysis of pancreas in these mice revealed that edema, inflammatory infiltrate, and necrosis were all more intense in pancreas from SRX KO mice than in pancreas from wild-type littermates with acute pancreatitis (Figure 30A, B). These results indicate that SRX deficiency increased the severity of acute pancreatitis. Accordingly, plasma amylase activities were higher in SRX KO mice than in wild-type mice during acute pancreatitis (Figure 30C).

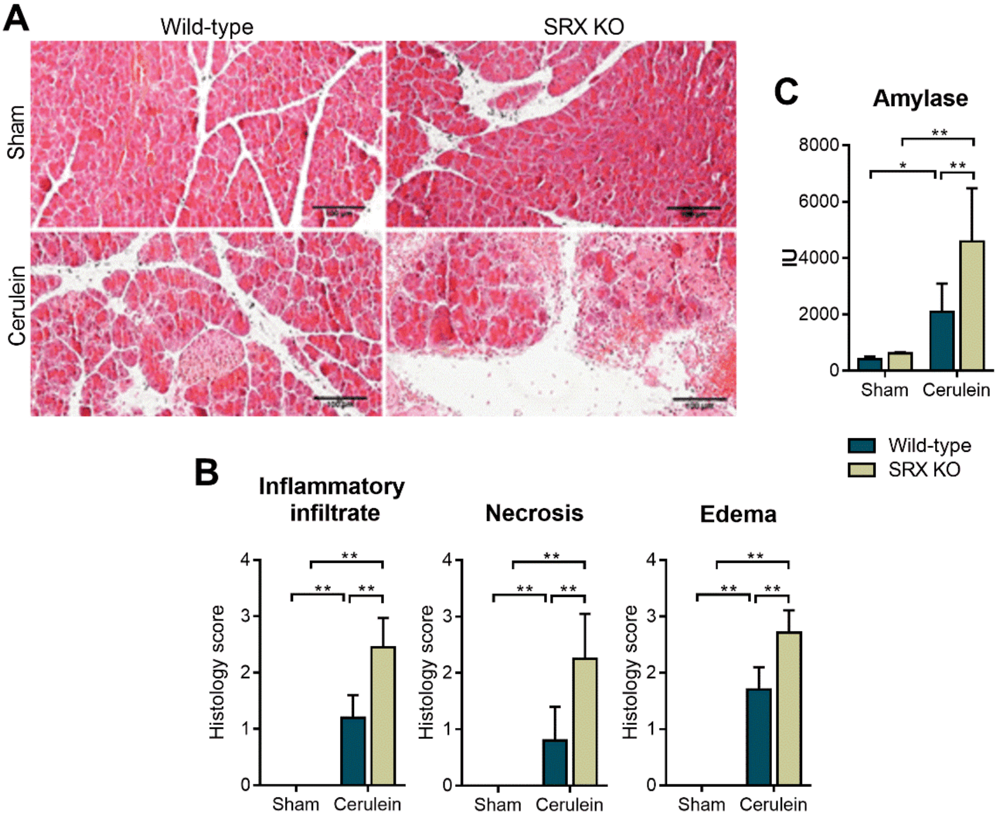

Figure 30. Histological analysis of pancreas and serum amylase activity in SRX KO mice with acute pancreatitis. Representative images of histology (A), histological scores for inflammatory infiltrate, edema and necrosis in pancreas (B) and plasma activity of amylase (C) in wild-type and SRX KO mice under basal conditions (sham) and with acute pancreatitis (at 1 h after the seventh injection of cerulein). The number of mice per group was 4-6. Statistical significance is indicated as *p < 0,05 and **p < 0,01.

Taking into account that SRX KO mice exhibited more intense inflammatory infiltrate in pancreas with pancreatitis than wild-type mice, we evaluated the inflammatory cascade in pancreas of these mice by measuring the mRNA expression of pro-inflammatory cytokines *Il-6, Tnf-α* and *Il-1β* as well as the activation of MAPKs signalling pathways.

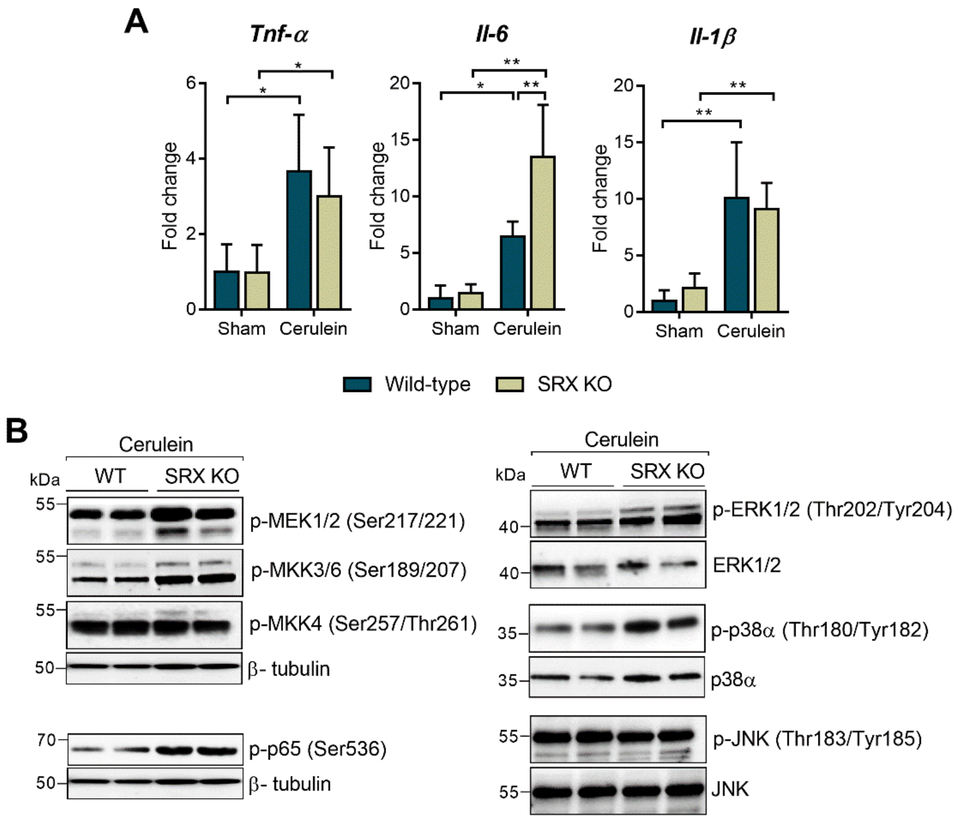

Figure 31. Gene expression of *Tnf-α*, *Il-6* and *Il-1β* together with MAPKs and NF-κB activation in pancreas from SRX KO mice with acute pancreatitis. mRNA relative expression of *Tnf-α*, *Il-6* and *Il-1β* vs *Tbp* (A). Representative western blot of p-MEK1/2 (Ser217/221), p-MKK3/6 (Ser189/207), p-MKK4 (Ser257/Thr261), p-ERK1/2 (Thr202/Tyr204), ERK, p-p38α (Thr180/Tyr182), p38α, p-JNK (Thr183/Tyr185), JNK and p-p65 (Ser536) (B) in pancreas of wild-type (WT) and SRX KO mice with acute pancreatitis (at 1 h after the seventh injection of cerulein). β-tubulin was used as loading control. The number of mice per group was 4–6. Statistical significance is indicated as *p < 0,05 and **p < 0,01.

We found that *Il-6* mRNA expression was dramatically increased in pancreas from SRX KO mice after cerulein-induced pancreatitis in comparison with pancreas from wild-type mice with pancreatitis (Figure 31A). However, although *Tnf-α* and *Il-1β* mRNAs were also upregulated in pancreas upon induction of pancreatitis, there were no differences between SRX KO mice and wild-type mice (Figure 31A).

The activation MAPKKs MEK1/2 and MKK3/6, as well as their corresponding downstream substrates ERK1/2 and p38α, were higher in the pancreas of SRX KO mice with pancreatitis compared with wild-type littermates (Figure 31B). In addition, the levels of p-p65 NF-κB subunit were increased in pancreas from SRX KO mice with pancreatitis than in wild-type with pancreatitis (Figure 31B).

On the other hand, necrotic and necroptotic cell death is characterized by the release of intracellular components including histones and DNA which it is associated with systemic complications in acute pancreatitis [522]. Thus, according to the intense necrosis-like cell death detected in SRX KO mice with pancreatitis, we found that plasma levels of cell free DNA (cfDNA) and nucleosomes were higher in these mice compared with wild-type mice (Figure 32A, B).

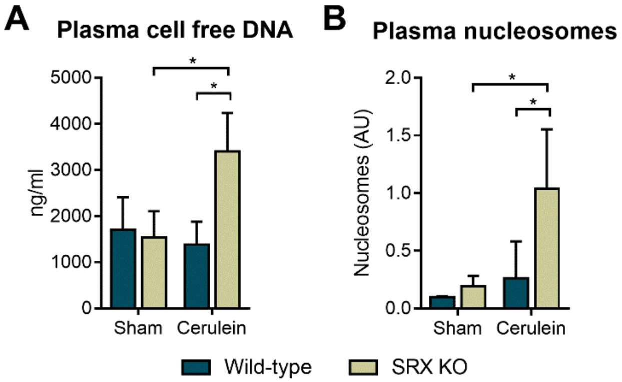

Figure 32. Plasma levels of cell free DNA and nucleosomes in SRX KO mice with acute pancreatitis. Plasma levels of cell free DNA (A) and nucleosomes (B) in wild-type and SRX KO mice both under basal conditions (sham) or after acute pancreatitis (at 1 h after the seventh injection of cerulein). The number of mice per group was 4–6. Statistical significance is indicated as *p < 0,05 and **p < 0,01.

2.5 SRX deficiency increased hyperoxidation of peroxiredoxins in acute pancreatitis

We studied the hyperoxidized thiol states -sulfinic and sulfonic forms- of PRX1, PRX2, and PRX3 in the pancreas of SRX KO mice with pancreatitis. As expected, acute pancreatitis in wild-type mice only induced a significant hyperoxidation of PRX1 and PRX2 at 7 h i.e. at 1 h after the last injection of cerulein. However, in the pancreas of SRX KO mice with pancreatitis, we found marked hyperoxidation of PRX1 and PRX2 compared with their wild type littermates, and remarkably PRX3 was intensely hyperoxidized only in SRX KO mice with acute pancreatitis (Figure 33A, B).

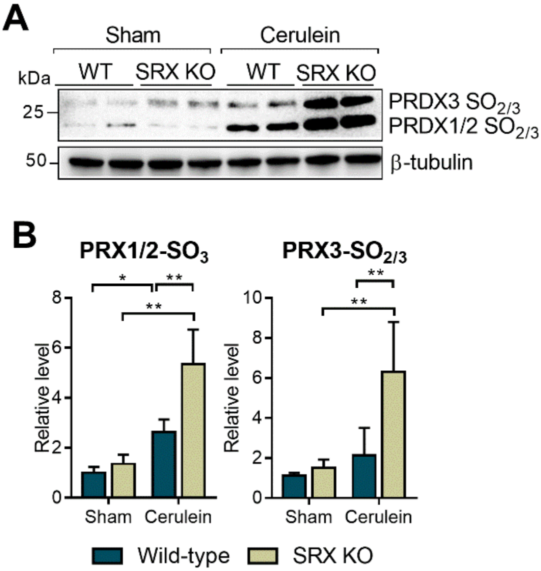

Figure 33. Protein levels of sulfinic and sulfonic forms of PRX1, PRX2 and PRX3 in the pancreas from SRX KO mice with acute pancreatitis. Representative western blot (A) and densitometry quantification (B) of hyperoxidized forms of PRX1, PRX2 and PRX3 in pancreas from wild-type (WT) mice and SRX KO mice under basal conditions (sham) and with acute pancreatitis at 7 h (i.e. at 1 h after the seventh injection of cerulein). β-tubulin was used as loading control. The number of mice per group was 4–6. Statistical significance is indicated as *p < 0,05 and **p < 0,01.

2.6 SRX deficiency enhanced mitochondrial protein nitration in acute pancreatitis

In order to assess the contribution of SRX to the regulation of nitrosative stress in pancreas during acute pancreatitis, we measured the levels of nitrated proteins in the mitochondrial fraction derived from pancreas of SRX KO mice. We found that levels of mitochondrial protein nitration were higher in SRX KO, even under basal conditions (Figure 34A). Upon pancreatitis induction, levels of nitrated proteins dramatically increased in the mitochondria from pancreas of SRX KO compared with pancreatic mitochondria from their wild-type littermates (Figure 34A).

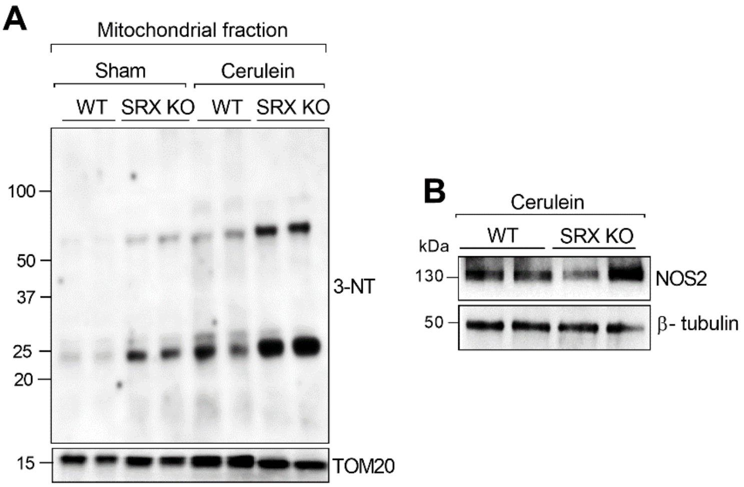

Figure 34. Mitochondrial protein nitration and NOS2 protein levels in the pancreas from SRX KO mice with acute pancreatitis. Representative western blot of 3-nitrotyrosine in mitochondrial fraction from pancreas of wild-type (WT) and SRX KO mice under basal conditions (sham) and with acute pancreatitis at 7 h (i.e. at 1 h after the seventh injection of cerulein). TOM20 was used as loading control (A). Representative western blot of NOS2 in total extract from pancreas of wild-type (WT) and SRX KO mice with acute pancreatitis at 7 h (i.e. at 1 h after the seventh injection of cerulein). β-tubulin was used as loading control (B). The number of mice per group was 4–6. Statistical significance is indicated as $^{*}p < 0,05$ and $^{**}p < 0,01$.

Importantly, protein levels of NOS2 were not significantly elevated in pancreas of SRX KO mice with pancreatitis compared with wild-type mice with pancreatitis, suggesting that NOS2 does not seem responsible for the increased levels of nitrated proteins in mitochondria from pancreas of SRX-deficient mice (Figure 34B).

2.7 SRX deficiency induced necroptosis and p53 mitochondrial translocation in acute pancreatitis

The increased levels of mitochondrial protein nitration is associated with the intense necrosis found by the histological analysis in the pancreas from SRX KO mice with pancreatitis. Therefore, we explored the activation of regulated necrosis program, necroptosis, in these mice.

As both necrosis and necroptosis provide the same features in the histological analysis [246], we measured the levels of p-MLKL, a marker of necroptosis. We found that the levels of p-MLKL were higher in the pancreas from SRX KO mice with pancreatitis compared with wild-type mice (Figure 35A). In contrast, the levels of cleaved caspase-3, a marker of apoptosis, were lower in the pancreas of SRX-deficient mice with pancreatitis than in wild-type mice (Figure 35B).

Furthermore, we found that the mRNA and protein levels of p53 were increased in the pancreas from SRX KO mice with pancreatitis compared with wild-type mice (Figure 35C). Remarkably, mitochondrial levels of p53 were dramatically augmented in the pancreas from SRX-deficient mice with pancreatitis when compared with wild-type mice (Figure 35D).

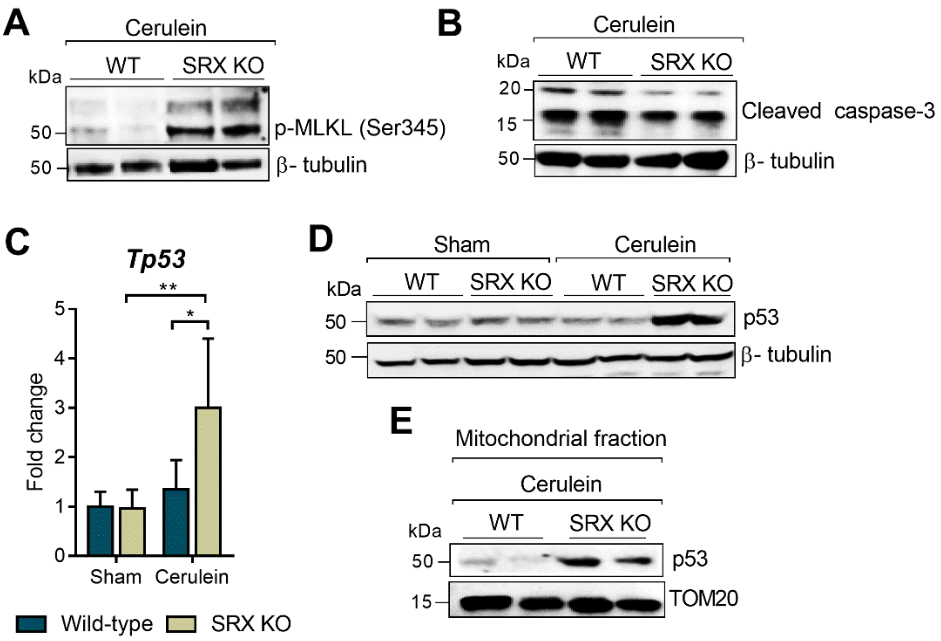

Figure 35. p-MLKL, cleaved caspase-3, and p53 levels in the pancreas from SRX KO mice with acute pancreatitis. Representative western blots of p-MLKL (A) and cleaved caspase-3 (B) in the pancreas of wild-type (WT) mice and SRX KO mice with acute pancreatitis at 7 h (1 h after the seventh injection of cerulein). β-tubulin was used as loading control. mRNA relative expression of *Tp53* vs *Tbp* (C), representative western blot of p53 (D) in pancreas of wild-type (WT) and SRX KO mice under basal conditions (sham) and with acute pancreatitis at 7 h (1 h after the seventh injection of cerulein) and in mitochondrial fraction (E) of pancreas from wild-type (WT) and SRX KO mice with acute pancreatitis at 7 h (1 h after the seventh injection of cerulein). β-tubulin was used as loading control for total extracts, and TOM20 for the mitochondrial fraction. The number of mice per group was 4–6. Statistical significance is indicated as *p < 0,05 and **p < 0,01.

2.8 Mito-TEMPO reduced inflammation and necroptosis in SRX-deficient mice with acute pancreatitis

In order to demonstrate the role of SRX regulating mitochondrial nitrosative stress and necroptosis in acute pancreatitis, we used the mitochondrial antioxidant mito-TEMPO to prevent the formation of $ONOO^-$ derived from superoxide in the mitochondria.

Firstly, we performed a histological analysis to evaluate the effect of mito-TEMPO in the pancreas from SRX-deficient mice with acute pancreatitis. The histological analysis revealed that SRX KO mice with pancreatitis treated with mito-TEMPO exhibited less necrosis, inflammatory infiltrate, and edema than untreated mice (Figure 36A, B).

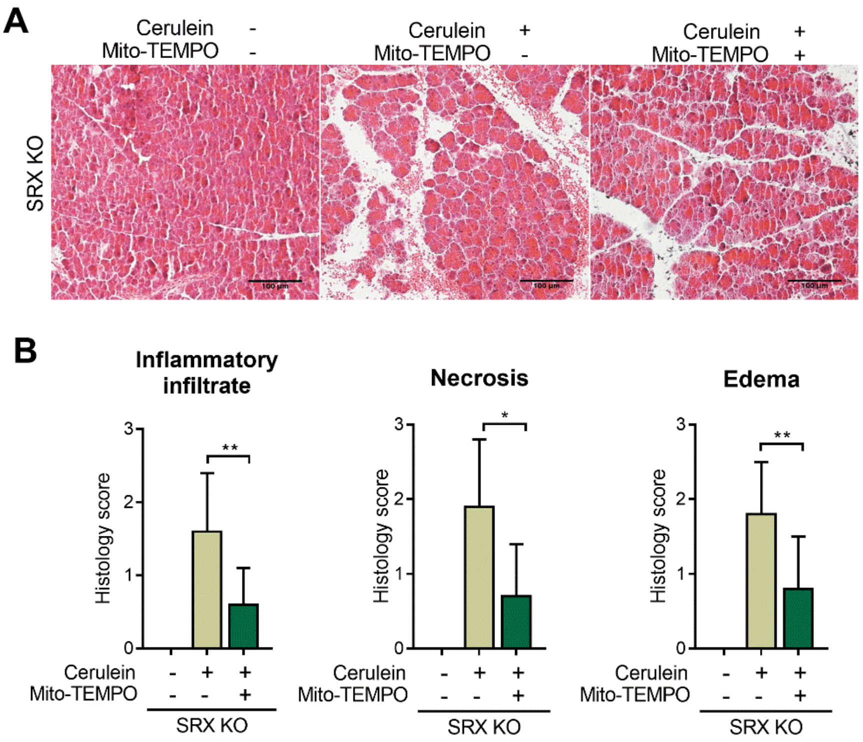
A
Cerulein -
Mito-TEMPO -
Cerulein +
Mito-TEMPO -
Cerulein +
Mito-TEMPO +
SRX KO
100 µm
B
Inflammatory infiltrate
Necrosis
Edema
Histology score
0
1
2
3
**
*
Cerulein - + +
Mito-TEMPO - - +
SRX KO

Figure 36. Histological analysis of pancreas from SRX KO mice with acute pancreatitis treated with mito-TEMPO. Representative images of histology (A) and histological scores for inflammatory infiltrate, necrosis, and edema (B) in pancreas from SRX KO mice under basal conditions (sham), with acute pancreatitis at 7 h (1 h after the seventh injection of cerulein), and with acute pancreatitis and mito-TEMPO treatment. The number of mice per group was 4–6. Statistical significance is indicated as *p < 0,05 and **p < 0,01.

In accordance with the histological analysis, plasma cDNA and plasma nucleosomes were diminished in SRX KO mice with pancreatitis treated with mito-TEMPO when compared with untreated mice (Figure 37A, B).

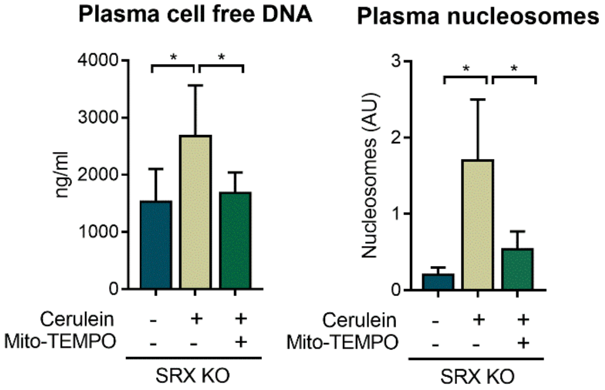

Figure 37. Plasma levels of cell free DNA and nucleosomes in the pancreas from SRX KO mice with acute pancreatitis treated with mito-TEMPO. Plasma levels of cell free DNA (A) and nucleosomes (B) in SRX KO mice under basal conditions (sham) and with acute pancreatitis at 7 h (1 h after the seventh injection of cerulein), and with acute pancreatitis and mito-TEMPO treatment. The number of mice per group was 4–6. Statistical significance is indicated as *p < 0,05 and **p < 0,01.

Hence, we decided to study necroptosis in SRX KO mice treated with mito-TEMPO. Remarkably, we found that p-MLK levels were diminished in the pancreas from SRX KO mice with acute pancreatitis treated with mito-TEMPO when compared with those untreated SRX KO mice with acute pancreatitis, indicating that necroptosis activation upon SRX deficiency was prevented with mito-TEMPO (Figure 38A).

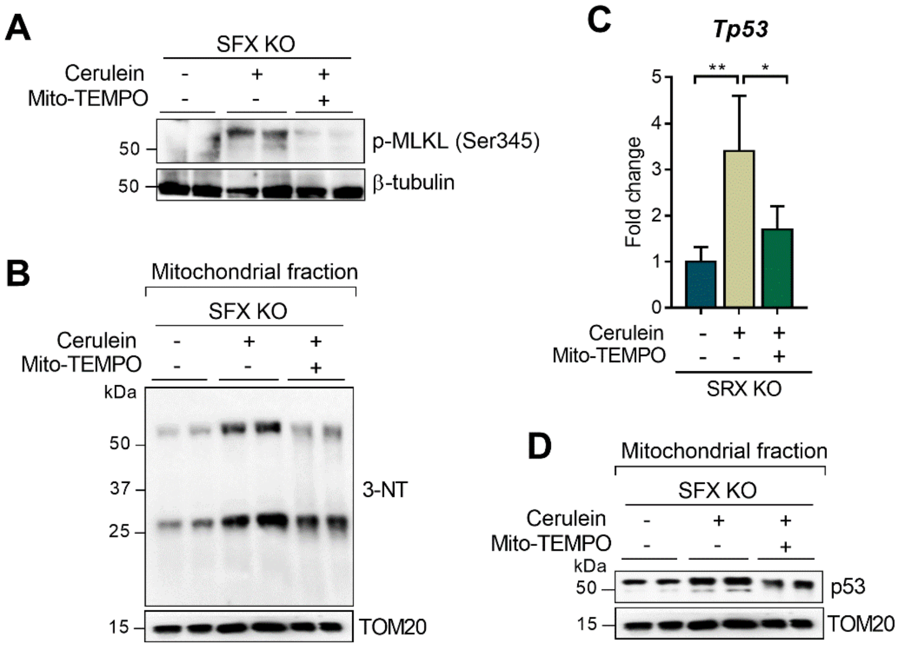

Figure 38. p-MLKL levels, mitochondrial protein nitration, gene expression of *Tp53* and mitochondrial levels of p53 in the pancreas from SRX KO mice with acute pancreatitis treated with mito-TEMPO. Representative western blot of p-MLKL in total extracts (A) and 3-nitrotyrosine in mitochondrial fraction (B) of pancreas from SRX KO mice under basal conditions (sham), with acute pancreatitis at 7 h (1 h after seventh injections of cerulein) and with acute pancreatitis and mito-TEMPO treatment. mRNA relative expression of *Tp53* vs *Tbp* (C) and representative western blot of mitochondrial p53 levels (D) in pancreas from SRX KO mice under basal conditions (sham), with acute pancreatitis at 7 h (1 h after the seventh injection of cerulein) and with acute pancreatitis and mito-TEMPO treatment. TOM20 was used as loading control (A). TOM20 was used as loading control. The number of mice per group was 4–6. Statistical significance is indicated as *p < 0,05 and **p < 0,01.

Subsequently, we studied protein nitration in the mitochondrial fraction of the pancreas from mice treated with mito-TEMPO. We found that the levels of mitochondrial protein nitration were lower in pancreas of SRX KO mice with pancreatitis treated with mito-TEMPO than in untreated mice (Figure 38B). Additionally, mito-TEMPO abrogated the up-regulation of p53 mRNA induced by acute pancreatitis in SRX KO mice. Mito-TEMPO also diminished the mitochondrial translocation of p53 into the mitochondria in SRX-deficient mice with acute pancreatitis (Figure 38C, D).

2.9 Mito-TEMPO did not recover PGC-1α downregulation in SRX-deficient mice with acute pancreatitis

We found that the mRNA expression of the gene *Ppargc1a*, encoding PGC-1α, decreased in pancreas from SRX KO mice with pancreatitis in comparison with wild-type mice with acute pancreatitis (Figure 39A). Strikingly, the mRNA levels of its target gene *Prx3* did not change between wild-type mice and SRX KO mice with acute pancreatitis (Figure 39A).

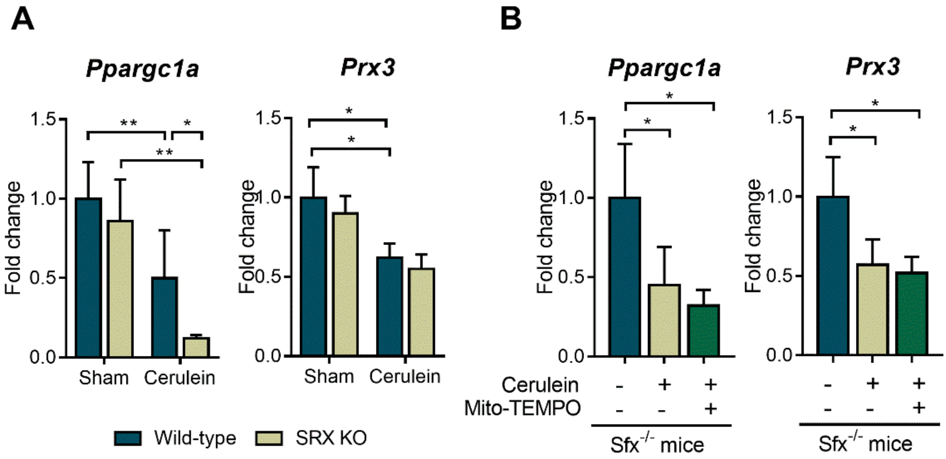

Figure 39. Gene expression of *Ppargc1a* and *Prx3* in the pancreas from SRX KO mice with acute pancreatitis and with mito-TEMPO treatment. mRNA relative expression of *PGC-1α* and *Prx3* (A) in pancreas from wild-type (WT) mice and SRX KO mice under basal conditions (sham) and with acute pancreatitis at 7 h (i.e. at 1 h after the seventh injection of cerulein). mRNA relative expression of *PGC-1α* and *Prx3* (B) in pancreas from SRX KO mice under basal conditions (sham), with acute pancreatitis at 7 h (1 h after seventh injections of cerulein) and with acute pancreatitis and mito-TEMPO treatment. The number of mice per group was 4–6. Statistical significance is indicated as $*p < 0,05$ and $**p < 0,01$.

Taking into account these results, we decided to evaluate if mito-TEMPO treatment recovered the down-regulated levels of PGC-1α found in SRX-deficient mice with acute pancreatitis. However, mito-TEMPO treatment did not recover the loss of pancreatic mRNA expression of *Ppargc1a* in SFX KO mice with pancreatitis, nor the mRNA expression of its target gene *Prx3* (Figure 39B).

3 Regulation of the inflammatory response by PGC-1α in acute pancreatitis

In this work, we studied the contribution of PGC-1α, a master regulator of the mitochondrial antioxidant defense, and oxidative metabolism in the regulation of the inflammatory cascade in acute pancreatitis.

3.1 PGC-1α levels are markedly reduced in pancreas from obese mice at basal conditions and in acute pancreatitis

PGC-1α is a master transcriptional regulator of mitochondrial biogenesis and oxidative metabolism, which suffers dysregulation in obese animals and patients [523, 524]. Taking into account that obesity increases the risk of local and systemic complications in acute pancreatitis [43, 44], our first approach was to measure PGC-1α levels in pancreas from lean or obese mice under basal conditions and in acute pancreatitis. *Ppargc1a* mRNA and PGC-1α protein levels were markedly downregulated in pancreas from obese mice under basal conditions in comparison with lean animals (Figure 40A, B). PGC-1α protein levels increased in pancreas from lean mice with cerulein-induced pancreatitis when compared with sham mice, but PGC-1α levels did not increase in pancreas from obese mice with pancreatitis and they were even lower than those from obese sham mice (Figure 40C).

3.2 PGC-1α deficiency enhanced pancreatic inflammation in acute pancreatitis

The fall in PGC-1α levels in pancreas from obese mice and from mice with SRX deficiency prompted us to assess the severity of acute pancreatitis in PGC-1α KO mice.

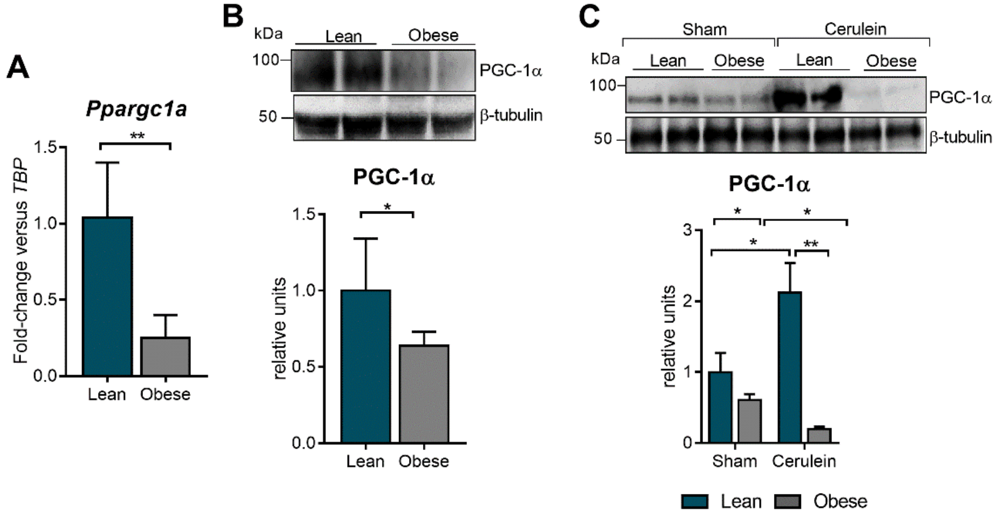

Figure 40. Gene expression and protein levels of PGC-1α in lean and obese mice at basal conditions and in acute pancreatitis. mRNA relative expression of *Ppargc1a* vs *Tbp* (A) and representative western blot of PGC-1α (B) in pancreas from lean and obese mice. Representative western blot of PGC-1α (C) in pancreas from lean and obese mice under basal conditions (sham) and with acute pancreatitis at 7 h (1 h after the seventh injection of cerulein). β-tubulin was used as loading control. The number of mice per group was 4–6. Statistical significance is indicated as *p < 0,05 and **p < 0,01.

The histological analysis revealed that both edema and inflammatory infiltrate in pancreas were more intense in PGC-1α KO mice with acute pancreatitis than in wild-type mice with pancreatitis (Figure 41A). Interestingly, even under basal conditions PGC-1α KO mice exhibited edema and inflammatory infiltrate in the pancreas, which were absent in wild-type mice at basal conditions (Figure 41A). In accordance with histological analysis, plasma amylase activity was higher in PGC-1α KO mice than in wild-type mice during acute pancreatitis (Figure 41B). All these findings indicated that PGC-1α deficiency increased the severity of acute pancreatitis.

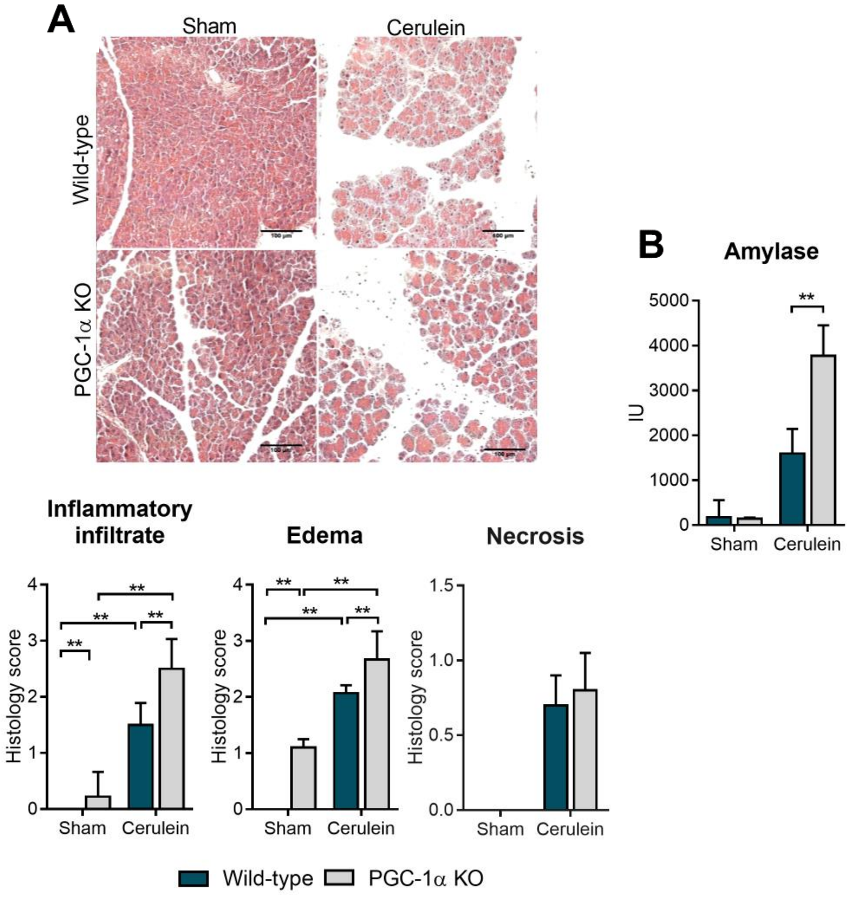

Figure 41. Histological analysis of pancreas, and plasma amylase activity of PGC-1α KO with acute pancreatitis. Representative images of histology and histological scores for inflammatory infiltrate, edema, and necrosis in pancreas (A) and amylase activity in plasma (B) from wild-type and PGC-1α KO mice under basal conditions (sham) and with acute pancreatitis at 7 h (1 h after seventh injections of cerulein). The number of mice per group was six. The statistical difference is indicated as $**p < 0.01$.

3.3 PGC1α deficiency induced apoptosis but not necroptosis in acute pancreatitis

Taking into account our previous results, we studied the up-regulation of *Srxn1* mRNA as well as the activation of necroptosis and apoptosis in the pancreas from PGC-1α KO with acute pancreatitis. As we previously observed, the mRNA levels of *Srxn1* were markedly increased in pancreas in response to acute pancreatitis. However, the *Srxn1* mRNA expression was induced up to a similar level in PGC-1α KO mice with pancreatitis compared with their wild-type counterparts (Figure 42A).

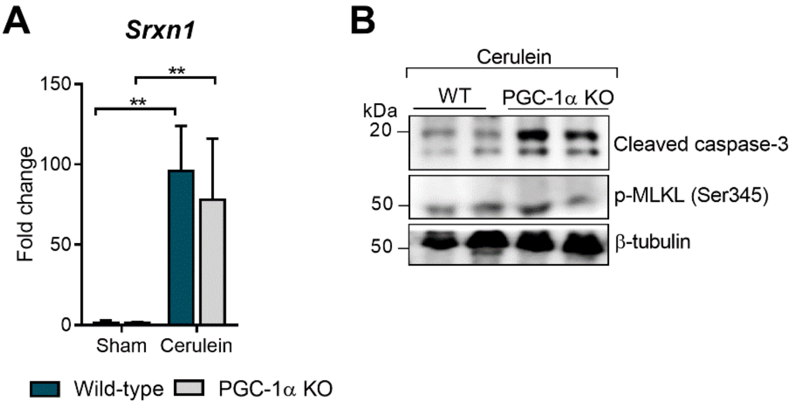

Figure 42. Gene expression of Srxn1 and western blots of cleaved caspase-3 and p-MLKL in pancreas from PGC-1α KO mice with acute pancreatitis. mRNA relative expression of *Srxn1 vs Tbp* in pancreas from wild-type and PGC-1α KO mice under basal conditions (sham) and with acute pancreatitis at 7 h (1 h after seventh injections of cerulein) (A). Representative western blots of cleaved caspase-3 and p-MLKL levels in pancreas from wild-type and PGC-1α KO mice with acute pancreatitis at 7 h (1 h after seventh injections of cerulein) (B). The number of mice per group was six. The statistical difference is indicated as **p < 0,01.

Furthermore, we found that the levels of the necroptosis marker p-MLKL did not change significantly in the pancreas from PGC-1α KO mice with pancreatitis compared with their wild-type littermates with pancreatitis (Figure 42B). In contrast, the levels of cleaved caspase-3 increased in the PGC-1α KO mice indicating that PGC-1α deficiency enhanced apoptosis in pancreas with acute pancreatitis.

3.4 PGC-1α acetylation and downregulation of its target genes in acute pancreatitis

To assess the role PGC-1 α in the regulation of the antioxidant defense, we investigated the mRNA expression levels of its target genes *Prx3, Sod2* and and *Cat*.

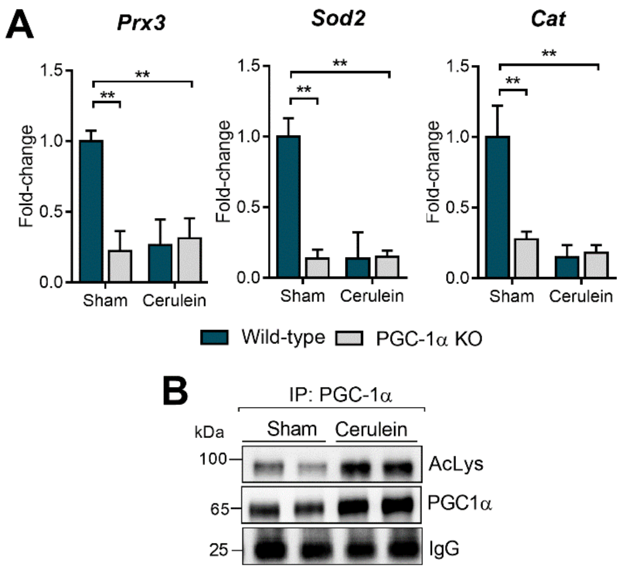

Figure 43. Gene expression of peroxiredoxin 3, superoxide dismutase 2 and catalase in the pancreas from PGC-1α KO mice with acute pancreatitis and acetylated protein levels of PGC-1α in mice with acute pancreatitis. mRNA relative expression of peroxiredoxin 3 (*Prx3),* superoxide dismutase 2 (*Sod2*) and catalase (*Cat) vs Tbp* in pancreas from wild-type mice and PGC-1α KO mice under basal conditions (sham) and with acute pancreatitis at 7 h (1 h after seventh injections of cerulein) (A). Representative western blots of acetyl-lysine PGC1-α levels in PGC1-α immunoprecipitate of pancreas from wild-type (WT) mice under basal conditions (sham) and with cerulein-induced acute pancreatitis at 7 h (1 h after seventh injections of cerulein) (B). Immunoblot of IgG in PGC1-α immunoprecipitated was used as loading control. The number of mice per group was six. The statistical difference is indicated as $^{*}p < 0{,}05$ and $^{**}p < 0{,}01$.

As expected, the lack of PGC-1α in the PGC-1α KO mice triggered a marked downregulation of *Prx3, Sod2*, and *Cat* mRNAs under basal conditions

(Figure 43A). However, in cerulein-induced pancreatitis there was a dramatic decrease in the levels of these three mRNAs only in wild-type mice, but not in PGC-1α KO mice, where these mRNA levels were kept low upon pancreatitis (Figure 43A). These results suggest that cerulein-dependent downregulation of that antioxidant defenses associated with peroxiredoxin 3, superoxide dismutase 2 and catalase could be mediated by PGC-1α inactivation.

Therefore, we decided to determine the levels of PGC-1α acetylation. Acetylated protein levels of PGC-1α increased in pancreas with acute pancreatitis (Figure 43B), which support that inactivation of PGC-1α by acetylation drives the downregulation of target antioxidant genes in response to cerulein-induced pancreatitis.

3.5 PGC-1α deficiency enhanced NF-κB activation and *Il-6* upregulation in acute pancreatitis

Considering that PGC-1α KO mice exhibited intense inflammation in pancreas with pancreatitis compared with wild-type mice, we measured the mRNA levels of pro-inflammatory cytokines *Tnf-α*, *Il-6,* and *Il-1β* in the pancreas from these mice. *Il-6* mRNA levels were dramatically increased in pancreas from PGC-1α KO mice after cerulein-induced pancreatitis compared with wild-type mice with pancreatitis (Figure 44A). However, although *Tnf-α* and *Il-1β* mRNAs were also upregulated in pancreas upon induction of pancreatitis, there were no significant differences between PGC-1α KO mice and wild-type mice (Figure 44A).

We studied if NF-κB activation is involved in the induction of *Il-6* upon PGC-1α deficiency by measuring nuclear translocation of p-p65 and recruitment of p65 to the *Il-6* promoter in pancreas from PGC-1α KO mice and wild-type mice with acute pancreatitis. We found that PGC-1α deficiency markedly enhanced nuclear translocation of p-p65 during acute pancreatitis (Figure 44B) and increased the recruitment of p65 to the *Il-6* promoter (Figure 44C). However, the recruitment of p65 to the promoters of *Tnf-α* or *Il-1β* did not change between KO and wild-type mice (Figure 44C).

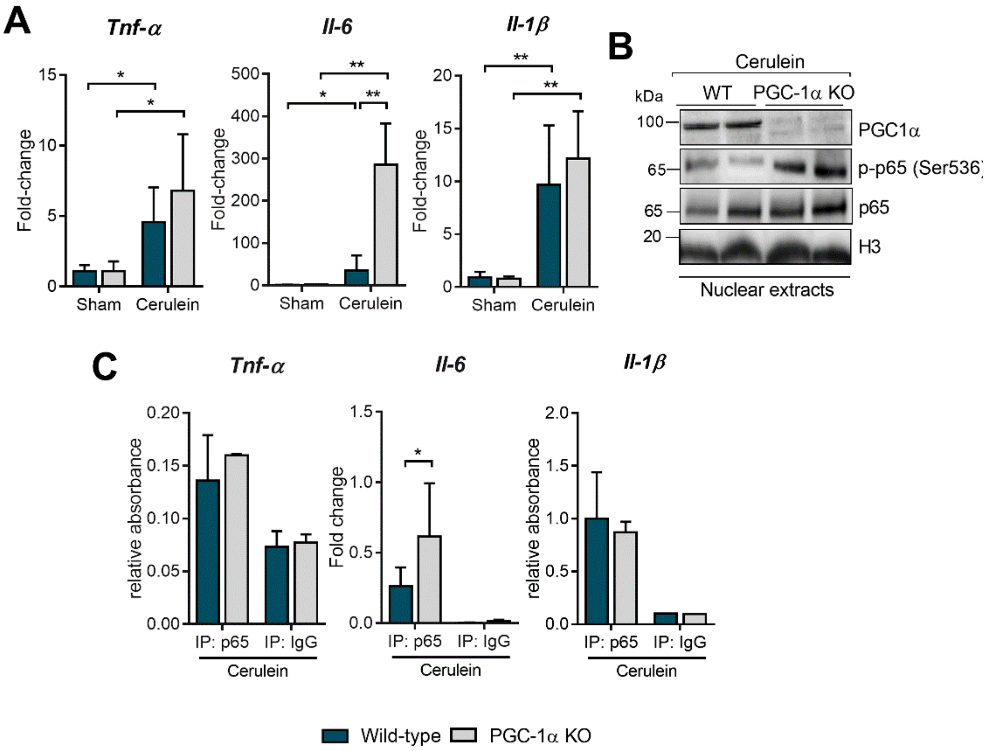

Figure 44. Gene expression of *Tnf-α*, *Il-6* and *Il-1β* and p65 recruitment to their promoters in the pancreas from PGC-1α KO mice with acute pancreatitis. mRNA relative expression of *Il-6, Tnf-α* and *Il-1β vs Tbp* in pancreas from wild-type and PGC-1α KO mice under basal conditions (sham) and with acute pancreatitis 1 h after seventh injections of cerulein (A); representative western blots of nuclear levels of PGC-1α, p-p65 (Ser536) and p65 (B); and histograms showing the recruitment of p65 in the promoter regions of *Il-6*, *Tnf-α,* and *Il-1β* (C) in pancreas from wild-type and PGC-1α KO mice with acute pancreatitis at 7 h (1 h after seventh injections of cerulein) (B). The number of mice per group was six. The statistical difference is indicated as *p < 0,05 and **p < 0,01.

3.6 PGC1α formed a complex with p-p-65 subunit of NF-κB in pancreas

Previously, it has been reported that the p65 subunit of NF-κB constitutively binds PGC-1α in cardiac cells repressing PGC-1α activity towards its target genes [525]. Hence, we performed immunoprecipitation of PGC-1α to assess whether PGC-1α formed a complex with p65 and p-p65 in pancreas in acute pancreatitis. We found that PGC-1α was constitutively bound to p65 and p-p65 in pancreas under basal conditions and the levels of the complex formed by PGC-1α and p-p65 markedly increased upon acute pancreatitis (Figure 45).

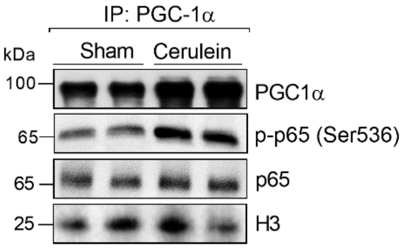

Figure 45. Complex formation between PGC-1α and p-65 in pancreas with acute pancreatitis. Representative western blots of PGC-1α, phospho-p65 (Ser536), and p65 in the PGC-1α immunoprecipitate from pancreas of wild-type (WT) mice under basal conditions (sham) and with cerulein-induced acute pancreatitis at 7 h (i.e. at 1 h after the seventh injection of cerulein); the immunoblot of IgG in PGC1-α immunoprecipitate was used as loading control. The number of mice per group was six.

3.7 PGC-1α deficiency enhanced IL-6 plasma levels inducing pulmonary infiltrate and damage in acute pancreatitis

We evaluated if the rise in *Il-6* expression in PGC-1α KO mice with acute pancreatitis led to increased levels of circulating IL-6 in these mice. We found that the plasma IL-6 levels increased around four-fold in PGC-1α KO mice with pancreatitis compared with wild-type mice with pancreatitis (Figure 46A).

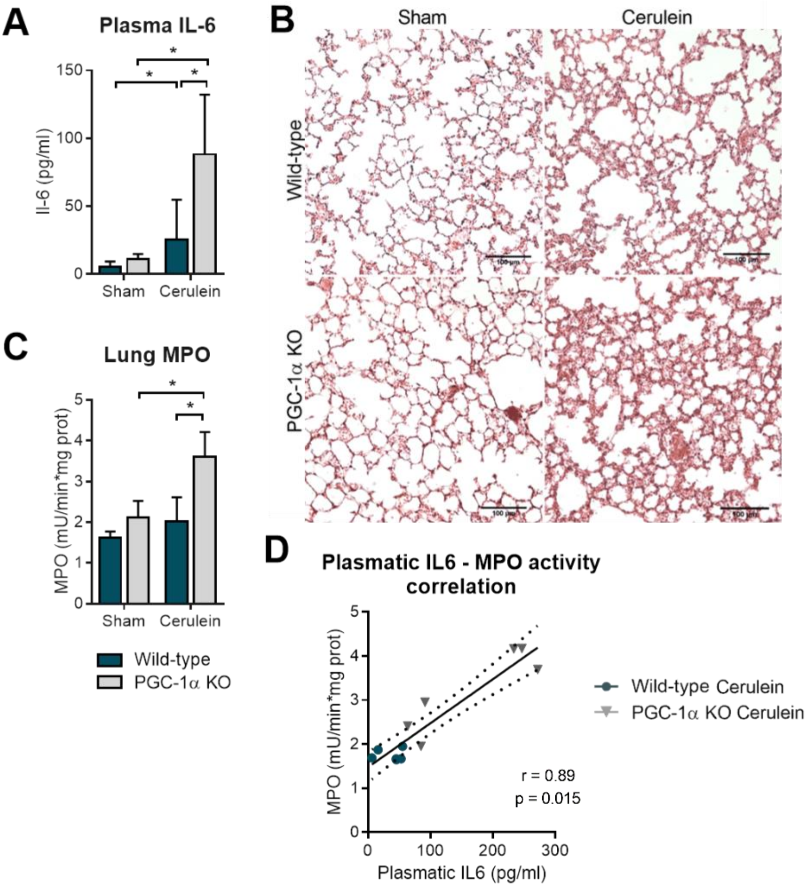

Figure 46. Plasma IL-6 levels and pulmonary myeloperoxidase activity and damage in PGC-1α KO mice with acute pancreatitis. Plasma IL-6 levels (A), representative images of histology of lungs (B), lung myeloperoxidase (MPO) activity (C) in wild-type and PGC1-α KO mice under basal conditions (sham) and after cerulein-induced acute pancreatitis at 7 h (i.e. at 1 h after the seventh cerulein injections of cerulein). Correlation between plasma IL-6 and pulmonary MPO levels in wild-type and PGC1-α KO mice after cerulein-induced acute pancreatitis (D). The number of mice per group was six. The statistical difference is indicated as *p < 0,05 and **p < 0,01.

Subsequently, we studied the impact of increased plasma IL-6 levels found in these mice by assessing pulmonary inflammation and damage. Histological analysis revealed generalized alveolar wall thickening and collapse in lungs from PGC-1α KO mice with pancreatitis, but rather low alveolar wall thickening and collapse in lungs from wild-type mice with pancreatitis (Figure 46B). In addition, myeloperoxidase (MPO) activity in lung tissue was measured as a marker of inflammatory infiltrate. We found that MPO activity increased only in PGC-1α KO mice with pancreatitis, but not in wild-type mice with pancreatitis (Figure 46C). Furthermore, we found a significant correlation ($p=0.015$; $r=0.89$) between plasma IL-6 levels and pulmonary MPO activity (Figure 46D).

3.8 gp-130 antagonist LMT-28 abrogated pulmonary damage induced by PGC-1 deficiency in acute pancreatitis

In order to demonstrate that the increased levels of IL-6 upon PGC-1α deficiency were responsible for the associated pancreatic and pulmonary damage, we blocked the IL-6 receptor gp130 using LMT-28 in PGC-1α KO mice. According to previous results [516], we confirmed the beneficial effects of LMT-28 in wild-type mice with acute pancreatitis based on the histological analysis of pancreatic tissue (Figure 47A, B). In addition, we found that LMT-28 diminished the exacerbated edema and inflammatory injury in pancreas from PGC-1α KO mice with acute pancreatitis (Fig. 47A, B).

Remarkably, blockade of the IL-6 receptor gp130 with LMT-28 abrogated the increases in both plasma IL-6 levels and pulmonary MPO activity in PGC-1α KO mice with acute pancreatitis (Fig. 48A, B). Furthermore, according to the histological analysis, LMT-28 greatly ameliorated the exacerbated pulmonary damage found in PGC-1α KO mice with acute pancreatitis (Figure 48C).

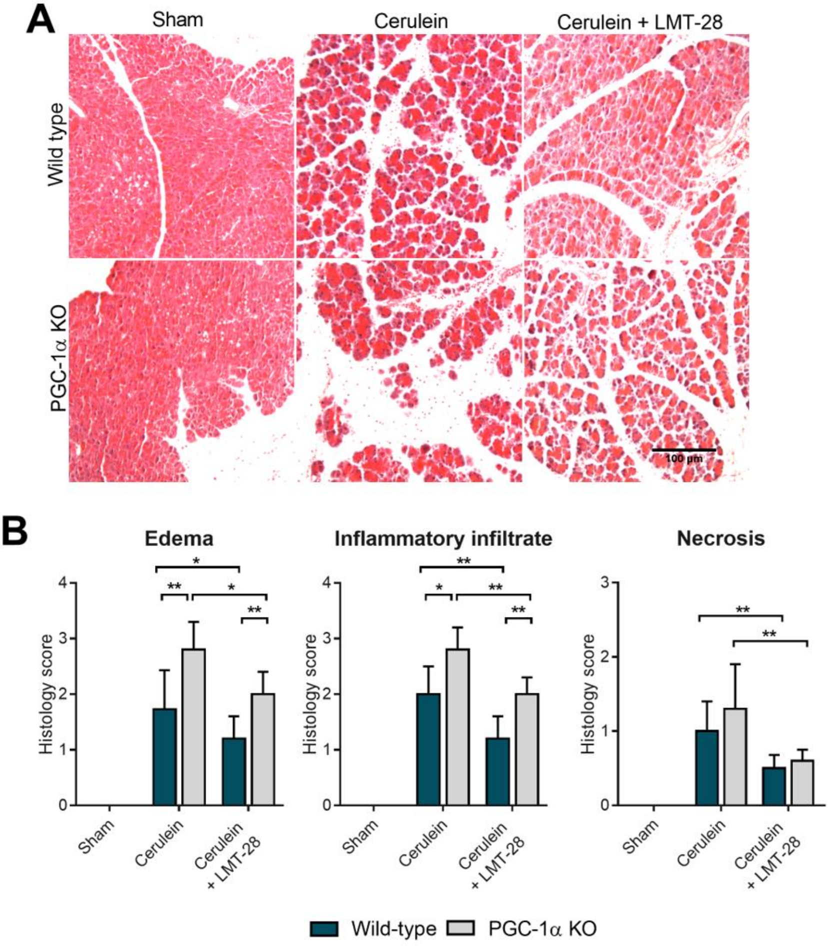
A
Sham
Cerulein
Cerulein + LMT-28
Wild type
PGC-1α KO
100 µm
B
Edema
Inflammatory infiltrate
Necrosis
Histology score
0
1
2
3
4
*
**
Sham
Cerulein
Cerulein + LMT-28
Wild-type
PGC-1α KO

Figure 47. Histological analysis of pancreas from PGC-1α KO mice with acute pancreatitis treated with LMT-28. Representative images of histology (A) and histological scores for edema, inflammatory infiltrate and necrosis (B) in pancreas from wild-type and PGC1-α KO mice under basal conditions (sham), after cerulein-induced acute pancreatitis at 7 h (i.e. at 1 h after the seventh injection with cerulein) and after acute pancreatitis and LMT-28 treatment. The number of mice per group was 4-6. The statistical difference is indicated as *p < 0,05 and **p < 0,01.

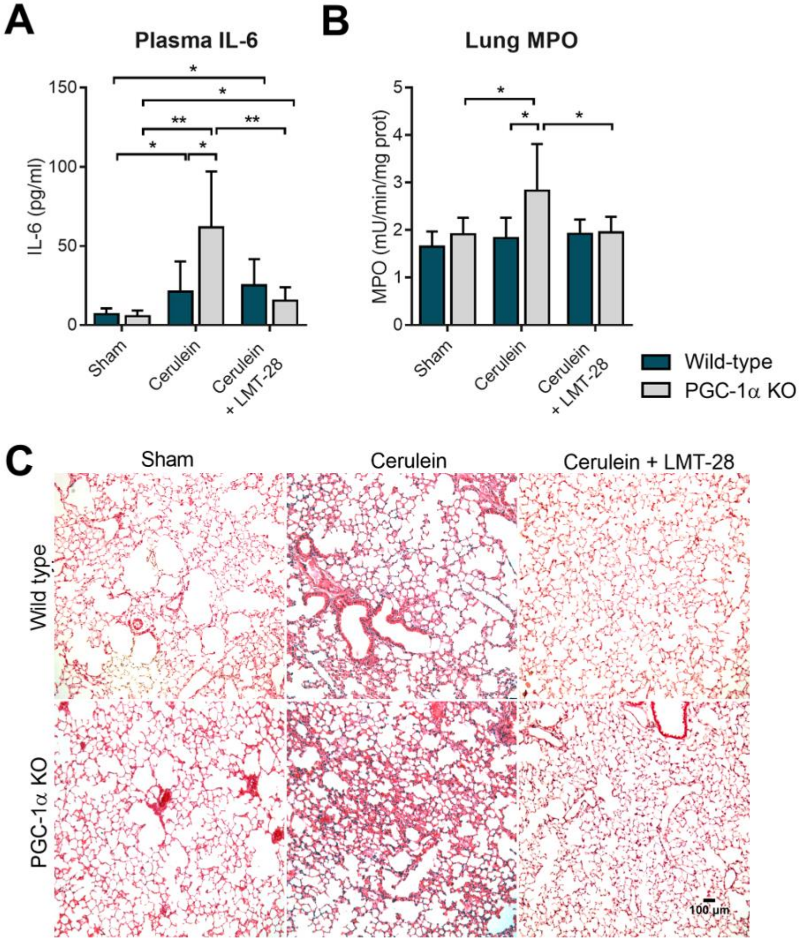

Figure 48. Plasma IL-6 levels and pulmonary damage of PGC-1α KO mice with acute pancreatitis treated with LMT-28. Plasma IL-6 levels (A) lung myeloperoxidase (MPO) activity (B) and representative histology of lungs (C) from wild-type and PGC1-α KO mice under basal conditions (sham), after cerulein-induced acute pancreatitis and after acute pancreatitis at 7 h (i.e. at 1 h after the seventh injection with cerulein), and LMT-28 treatment. The number of mice per group was 4-6. The statistical difference is indicated as *p < 0,05 and **p < 0,01.

V. DISCUSSION

1 Nitrosative stress blockades the trans-sulfuration pathway in acute pancreatitis due to nitration of cystathionine β-synthase

Nitrosative stress is a well-known feature of acute pancreatitis [453-455], but its impact on the pathophysiology of this disease is not fully elucidated. In the present work, we show that nitrosative stress induced by NOS2 upregulation in pancreas with acute pancreatitis dysregulates the trans-sulfuration pathway. We have identified the cause of this dysregulation reporting that tyrosine-nitration of cystathionine β-synthase (CBS) impairs homocysteine metabolism and blockades the metabolic flux through the trans-sulfuration pathway.

Our results show a progressive and marked depletion in pancreatic levels of methionine with parallel decrease in cystathionine and cysteine levels. S-adenosylmethionine (SAM) and reduced glutathione (GSH) levels were also rapidly depleted in pancreas during experimental acute pancreatitis in accordance with previous reports [445, 526]. In contrast, we found that pancreatic S-adenosylhomocysteine (SAH) and homocysteine levels remained unchanged upon cerulein-induced acute pancreatitis. Although the lower levels of S-adenosylhomocysteine hydrolase (SAHH) in pancreas in acute pancreatitis revealed by the proteomic analysis could restrain the metabolic flux in this point, our results clearly show that the subsequent metabolism of homocysteine is dramatically blocked in acute pancreatitis. We propose that tyrosine nitration of CBS and its resultant inactivation impairs homocysteine metabolism through the trans-sulfuration pathway in pancreas in acute pancreatitis.

CBS is a redox-sensitive and rate-limiting enzyme in the trans-sulfuration pathway responsible for homocysteine conversion to cystathionine [316]. CBS activity is allosterically activated by SAM [321] and S-glutathionylation [527], but inhibited by CO [323, 324] and NO [325, 326]. In the N-terminal domain, CBS contains a haeme cofactor that might act as a redox modulator of its enzymatic activity [317, 318]. The ferrous form of CBS exhibits lower activity than the ferric form [327]. Nevertheless, due to the low haeme redox potential (-350 mV), existence of the ferrous CBS state under physiological conditions is controversial [328, 528]. In addition, it has been reported that a redox-active disulfide bond modulates CBS activity [328]. However, we did not find thiol oxidation of CBS in acute pancreatitis. In contrast, the levels of tyrosine-nitrated CBS were markedly increased in this model of acute inflammation.

Nitration-mediated loss of CBS activity associated with elevated levels of homocysteine has been previously reported in aging rats [329]. In addition, *in vitro* experiments showed that $ONOO^{-}$ may inactivate CBS activity [529]. Accordingly, pre-treatment with the $ONOO^{-}$ scavenger FeTMPyP prevented CBS nitration and reduced homocysteine accumulation in aging rats [329]. In our model of acute inflammation, CBS nitration impairs homocysteine metabolism through the trans-sulfuration pathway restraining the availability of cysteine for GSH biosynthesis.

As occurs generally in acute inflammation, the up-regulation of *Nos2* expression induces nitrosative stress too in pancreas during acute pancreatitis [451, 452]. Accordingly, pancreatic levels of 3-nitrotyrosine, a marker of nitrosative stress, increased in mice with cerulein-induced acute pancreatitis [453-455]. Our results confirm the increased *Nos2* expression and the existence of nitrosative stress in this experimental model of acute pancreatitis. Remarkably, we show for the first time the detrimental effect of nitrosative stress on the trans-sulfuration pathway in acute pancreatitis, and specifically on CBS regulation. Furthermore, in accordance with other studies our results suggest that NOS2, but not NOS1 or NOS3, is the main source of $^{\bullet}$NO and the major contributor to nitrosative stress in pancreas during acute pancreatitis [452, 453]. In fact, pancreatic inflammation and tissue injury in pancreas of Nos2-deficient mice with acute pancreatitis was markedly reduced [453]. In contrast and strikingly, genetic deletion of Nos3 aggravated the severity of acute pancreatitis in mice [530]. Here, we are proposing that *Nos2* up-regulation causes CBS nitration and blockades homocysteine metabolism in pancreas during acute pancreatitis (Figure 49). In fact, CBS nitration might be widely associated with inflammation and with the increased levels of homocysteine found in a variety of inflammatory disorders, including inflammatory bowel disease [312], Chron's disease [313], and vascular inflammation [531].

On the other hand, it is worth noting that CBS is also involved in the synthesis of hydrogen sulfide (H_2S) together with CSE and mercaptopyruvate sulfurtransferase [347]. However, it has been demonstrated that CSE is the principal enzyme responsible for H_2S synthesis in pancreas and during acute pancreatitis [532], so the contribution of CBS in this regard seems to be minor.

In accordance with our results, CBS nitration may directly limit the ability of exogenous SAM to modulate the trans-sulfuration pathway and to rescue GSH levels in experimental acute pancreatitis. In acute pancreatitis, homocysteine levels seem in equilibrium with SAH levels, but exogenous administration of SAM breaks this equilibrium and promotes homocysteine accumulation. In fact, we found that SAM treatment increased *Nos2* expression and CBS nitration in acute pancreatitis causing the accumulation of homocysteine in the pancreatic tissue. Previously and in agreement with our results, it has been reported that an elevated homocysteine levels can increase by itself nitrosative stress through

Nos2 upregulation, inducing more CBS nitration within a vicious cycle that might promote more homocysteine accumulation [329, 352, 353].

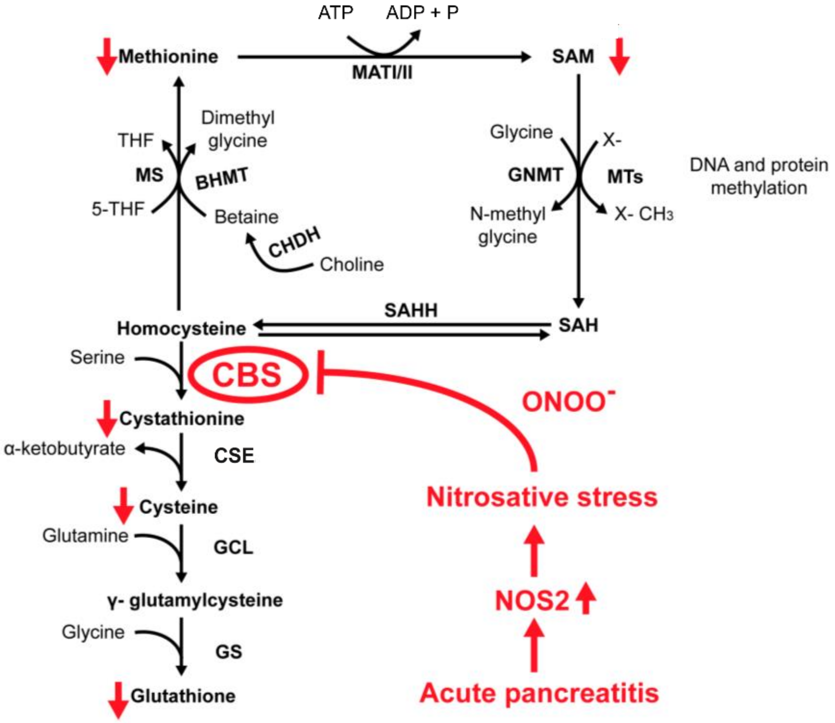
ATP
ADP + P
Methionine
MATI/II
SAM
Dimethyl glycine
THF
MS
BHMT
5-THF
Betaine
CHDH
Choline
Glycine
X-
GNMT
MTs
DNA and protein methylation
N-methyl glycine
X- CH3
SAHH
Homocysteine
SAH
Serine
CBS
ONOO-
Cystathionine
α-ketobutyrate
CSE
Cysteine
Nitrosative stress
Glutamine
GCL
γ- glutamylcysteine
NOS2
Glycine
GS
Glutathione
Acute pancreatitis

Figure 49. Acute pancreatitis induces nitration of cystathionine β-synthase (CBS) and blockade of the trans-sulfuration pathway. Nitric oxide synthase 2 (NOS2) induces nitrosative stress causing CBS tyrosine-nitration and blockade of the trans-sulfuration pathway in acute pancreatitis. MAT, methionine adenosyltransferase; SAM, S-adenosylmethionine; GNMT, glycine N-methyltransferase; MTs, methyl transferases; SAH, S-adenosylhomocysteine; SAHH, S-adenosylhomocysteine-hydrolase; CGL, cystathionine gamma-lyase; GCL, glutamate cysteine ligase; GS, glutathione synthase; CHDH, choline dehydrogenase; BHMT, betaine--homocysteine S-methyltransferase; MS, methionine synthase; THF, tetrahydrofolate; SAMDC, S-adenosylmethionine decarboxylase; dcSAM, decarboxylated SAM; MTA, methylthioadenosine; MTAP, methylthioadenosine phosphorylase; MTR-1-P, methylthioribose-1-phosphate.

Although it is known that SAM administration exhibits hepatoprotective effects against liver injury and may provide beneficial effects ameliorating inflammation-induced colon cancer in mice [310, 533], we show here that SAM treatment clearly exhibits pro-inflammatory effects in acute pancreatitis in mice suggesting that SAM supplementation in acute inflammatory disorders may not be beneficial. Our results demonstrate that exogenous SAM increased the levels of euchromatin marker tri-methylated K4 of histone 3 (H3K4me3), a signature for active transcription, in the promoter regions of *Tnf-α*, *Il-6* and *Nos2* genes enhancing their expression in mice with acute pancreatitis. Furthermore, we found more intense edema and inflammatory infiltrate in the pancreas of SAM-treated mice with pancreatitis. Consequently, acute pancreatitis was aggravated upon SAM administration.

In summary, nitrosative stress associated with acute pancreatitis causes blockade of the trans-sulfuration pathway via CBS nitration, which is enhanced by administration of S-adenosyl methionine.

2 Sulfiredoxin protects from mitochondrial nitrosative stress and necroptosis in acute pancreatitis

Mitochondria are the principal source of $ONOO^-$ and are the primary target for the cytotoxic effects of nitrosative stress [393, 394]. Extra and intra-mitochondrially formed $ONOO^-$ can diffuse into the mitochondria leading to nitration of critical mitochondrial components. $ONOO^-$-dependent protein modifications may have a dramatic impact on mitochondrial physiology and are widely associated with cell death signalling pathways [393-395]. In the present work, we show that sulfiredoxin (SRX) plays a protective role in acute pancreatitis preventing mitochondrial nitrosative stress and cell death. Pancreatic induction of SRX attenuates inflammatory response and ameliorates tissue injury by counteracting the excessive production of $ONOO^-$ in the mitochondria.

Under physiological conditions, the concerted action of SRX and 2-Cys PRXs plays a critical role orchestrating redox signalling in cells [360]. SRX is activated in cells and tissues exposed to damaging levels of ROS in order to prevent oxidative damage [534, 535]. Highly oxidizing conditions associated with inflammatory processes decisively contribute to SRX upregulation in different cell types [355, 536-538]. In particular, H_2O_2 exposure in PC12 cells increased mRNA and protein levels of SRX [355]. We show here that in pancreatic tissue, cerulein-induced acute pancreatitis triggers two transient waves of H_2O_2. The first peak coincides with elevated levels of hyperoxidized PRX1/2 and PRX3 and with the presence of active transcription epigenetic markers in the promoter of SRX. Thus, we hypothesize that H_2O_2 plays a crucial role in SRX upregulation during acute pancreatitis. Interestingly, LPS-mediated SRX induction was suppressed in NOX2-deficient bone marrow-derived macrophages [536]. Although the precise sources of ROS have not been fully elucidated in acute pancreatitis, it was suggested that ROS production mainly derives from NOX activation in acinar and immune infiltrated cells [436, 438, 539, 540]. In addition, it was previously reported that in LPS-stimulated macrophages JNK1/2-dependent phosphorylation of c-Jun –a subunit of AP1 transcription factor- was required for SRX upregulation [357, 536]. Activation of JNK1/2 and AP1 triggered the expression of cytokines in acinar cells during acute pancreatitis [158, 541] and hence, AP-1 might be also contributing to SRX upregulation in this disease.

During inflammatory processes, SRX upregulation acts as a protective mechanism to avoid excessive ROS accumulation [534-536] and it is considered crucial to prevent an excessively harmful inflammatory response [514]. Indeed, SRX KO mice exhibited high mortality after LPS-induced endotoxic shock [514]. Here, we show that SRX up-regulation protects pancreatic tissue from inflammation during acute pancreatitis. The lack of SRX in mice aggravated acute pancreatitis by increasing pancreatic inflammatory infiltrate and edema. Importantly, SRX KO mice with pancreatitis exhibited high levels of IL-6, a reliable marker of severity in acute pancreatitis [161]. These elevated levels of IL-6 could be attributed to activation of MAPKs -particularly p-p38α and p-ERK1/2- as well as NF-kB induction.

Our results highlight the role of SRX induction not only attenuating the inflammatory response during pancreatitis but also protecting pancreatic cells from necroptosis. *In vitro* studies showed that SRX ablation reduced cell viability and promoted cell damage in different cell types [355, 538]. SRX overexpression increased cell survival by protecting cells from oxidative stress [542] and it is noteworthy that enhanced levels of this protein were found in cancer cells [357, 543, 544]. Here, we show that SRX KO mice with acute pancreatitis exhibited extensive necrotic areas in pancreas evidencing the key role of SRX in the protection against this type of cell death. As a consequence of the necrosis found in pancreas during pancreatitis in mice lacking SRX, chromatin components were released into the systemic circulation. Nucleosome-associated histones and DNA released by necrotic acinar cells and neutrophils are well known DAMPs, which correlated with the severity of acute pancreatitis [522, 545-547].

In acute pancreatitis, mitochondrial dysfunction plays a critical role triggering necrotic cell death [235, 548]. Oxidative stress impairs mitochondrial bioenergetics leading to an apoptotic-to-necrosis shift in pancreatic cells [237]. In fact, stimulation of apoptosis protects from necrotizing pancreatitis, whereas inhibition of apoptosis enhanced necrosis and aggravated acute pancreatitis [176]. In the present work, we highlight the contribution of SRX in necroptosis activation during acute pancreatitis, thus providing new insights to understand the complex mechanisms behind the regulation of pancreatic cell death. Several studies have already confirmed the existence of necroptosis during acute pancreatitis and it is indeed considered a promising therapeutic target [245, 253, 270]. In fact, the activation of apoptosis and the simultaneous inhibition of necroptosis improved the outcome of pancreatitis in mice [272]. In the present work, SRX KO mice exhibited high levels of p-MLKL -a marker of necroptosis- as well as increased levels of nitrated mitochondrial proteins in pancreas during pancreatitis. However, the levels of cleaved caspase-3 were reduced in these mice. Under inflammatory conditions, NO activated SRX expression in macrophages and it was proposed that this mechanism acts as a feedback loop to prevent $ONOO^-$-associated cell damage [358]. Hence, we propose here that SRX plays a key role regulating the cell death fate of acinar cells between necroptosis and apoptosis in response to nitrosative stress.

SRX KO mice did not exhibit higher levels of NOS2 in pancreatitis than their wild-types littermates, so the increased nitrosative stress found in these mice could be ascribed to the absence of $ONOO^-$ detoxification. Recently, Radi *et al.* demonstrated that PRX3 reduces $ONOO^-$ with a rate constant of 1×10^7 M^{-1} s^{-1} at pH 7.8 and 25 °C [421]. PRX3 is a peroxiredoxin isoform located exclusively in mitochondria, the mainly sites of $ONOO^-$ formation [393, 394, 549]. Thus, according to our results, the SRX induction found in pancreatitis would be essential to maintain the redox state of PRX3 in order to prevent mitochondrial nitrosative stress during pancreatitis. Previously, it was reported that SRX translocates into the mitochondria in response to H_2O_2 to reduce and reactivate sulfinic PRX3 [359, 361] and also to prevent oxidative damage in liver [537]. In addition, downregulated levels of PRX3 were associated with increased levels of nitrated proteins in injured rat hippocampus [550]. Here, we show for the first time that SRX translocates early into pancreatic mitochondria during acute pancreatitis coinciding with high levels of H_2O_2 in pancreatic tissue. Furthermore, SRX upregulation in acute pancreatitis prevented hyperoxidation and subsequent inactivation of PRX3. However, time-course experiments during acute pancreatitis showed that although upon SRX upregulation sulfinic and sulfonic levels of PRX3 returned to the basal levels, hyperoxidized forms of PRX1 and PRX2 remained increased in pancreas with pancreatitis. Accordingly, SRX deficiency in mice augmented hyperoxidized levels of all PRXs in acute pancreatitis, and particularly, the levels of hyperoxidized PRX3 were dramatically increased in these mice. Taken together, our results reveal the key role of SRX regulating mitochondrial nitrosative stress in pancreas through the control of PRX3 redox status in mitochondria. Consequently, the lack of this mechanism in SRX KO mice inactivated PRX3 and increased the levels of mitochondrial nitrated proteins in acute pancreatitis.

In the present work, we highlight that SRX/PRX3 axis protects mitochondria from nitrosative stress in pancreas and prevents p53-mediated necroptosis. Previously, it has been reported that SRX inhibition promotes cancer cell death through ROS-mediated mitochondrial damage [551]. In addition, as a response to oxidative stress, p53 is accumulated in mitochondrial matrix leading to mPTP opening, ATP depletion and necrosis [203]. Here, we show that the lack of SRX induced p53 translocation into the mitochondria in pancreas during acute pancreatitis. The administration of MitoTEMPO, which possesses $O_2^{\bullet-}$ scavenging properties [552], demonstrated that restoration of the mitochondrial antioxidant capacity in SRX-deficient mice with pancreatitis prevented p53 translocation into mitochondria and protected from necroptosis. Accordingly, the release of chromatin components into the systemic circulation was abrogated and tissue injury was ameliorated in SRX KO mice treated with MitoTEMPO. Interestingly, it was previously reported that H_2O_2-dependent p53 upregulation augmented the levels of necrosis-related factor (NRF), a long noncoding RNA that represses miR-873, increasing RIPK1 and RIPK3 expression and promoting necroptosis in cardiomyocytes [553]. Nevertheless, the specific regulation of necroptosis by p53 is still poorly understood and further experiments are required to elucidate how increased levels of p53 in mitochondria promote necroptosis activation in acute pancreatitis.

On the other hand, previous findings have also linked mitochondrial nitrosative stress with cell death by necroptosis [554]. Nitration of the mitochondrial complex I subunit NDUFB8 induced RIP1K and RIPk3-mediated necroptosis activation in endothelial cells [554]. In our work, administration of MitoTEMPO abrogated mitochondrial protein nitration in SRX-deficient mice with acute pancreatitis. Hence, this protective effect exerted by MitoTEMPO could explain the reduced necroptosis found in these mice.

In summary, we propose here that SRX translocates into mitochondria during acute pancreatitis to maintain the activity of PRX3 against peroxynitrite, preventing mitochondrial nitrosative damage and necroptosis induction through a p53-dependent mechanism. Hence, SRX up-regulation act as a protective mechanism in pancreas to prevent inflammation, mitochondrial nitrosative stress and necroptosis during acute pancreatitis (Figure 50).

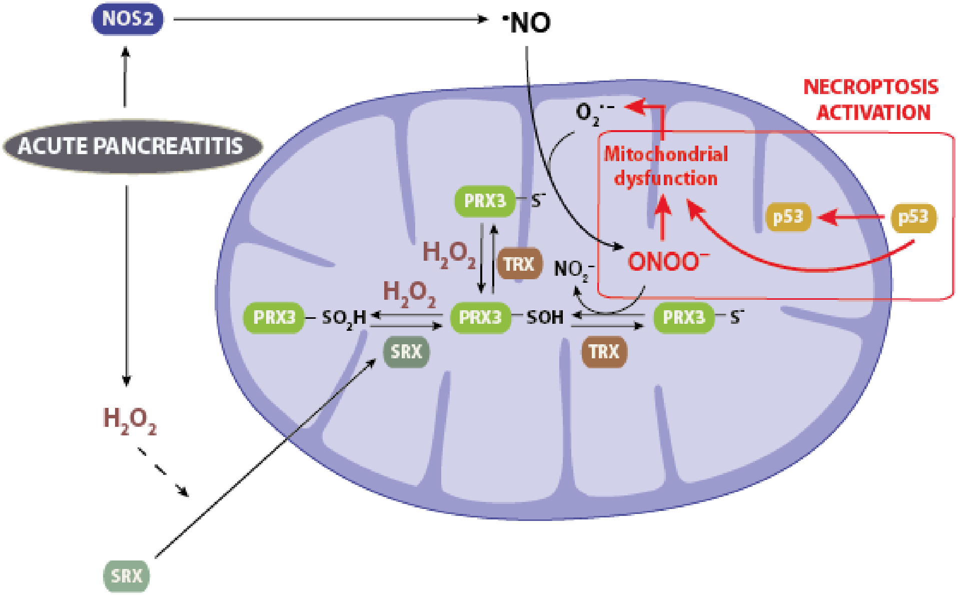
NOS2
•NO
ACUTE PANCREATITIS
NECROPTOSIS ACTIVATION
$O_2^{\cdot -}$
Mitochondrial dysfunction
PRX3 – S^-
H_2O_2
TRX
NO_2^-
$ONOO^-$
p53
p53
H_2O_2
PRX3 – SO_2H
PRX3 – SOH
PRX3 – S^-
SRX
TRX
H_2O_2
SRX

Figure 50. Proposed mechanism for the protective role of sulfiredoxin in acute pancreatitis. Sulfiredoxin (SRX) translocates into mitochondria during acute pancreatitis to maintain activated the activity of PRX3 against peroxynitrite ($ONOO^-$), preventing mitochondrial nitrosative damage, p53 mitochondrial translocation, and necroptosis. NOS2, nitric oxide synthase 2; PRX, peroxiredoxin; TRX, thioredoxin.

3 PGC1α restrains IL-6 expression via inhibition of NF-kB in acute pancreatitis

In this work we highlight the key role of PGC-1α in the inflammatory response and tissue injury in acute pancreatitis, particularly in obesity.

Our results show that obesity in mice leads to marked PGC-1α downregulation in pancreas. Previous results showed that increased saturated fatty acids as well as fatty-acid-induced hypermethylation of the *Ppargc1a* promoter decreased PGC-1α expression in muscle cells [478, 555]. We hypothesize that either of these mechanisms might be involved in the decrease in pancreatic PGC-1α levels in obese animals.

On the other hand, according to the mitochondrial dysfunction exhibited by SRX KO mice with pancreatitis, we found that the expression levels of PGC-1α, a master regulator of the mitochondrial antioxidant defense [556-558], were downregulated in these mice. SRX-deficiency exacerbated the inflammatory response in pancreas from mice with acute pancreatitis, which could explain the changes observed in PGC-1α expression. Indeed, PGC-1α mRNA levels were down-regulated by inflammation because TNF-α decreased the expression of PGC-1α *in vitro* in cardiac AC16 cells and *in vivo* in the heart of mice overexpressing TNF-α [525, 559]. In addition, LPS dramatically decreased PGC-1α levels in different tissues such as heart, kidney, muscle, and liver [560]. Accordingly, the severity of sepsis-associated acute kidney injury was correlated with PGC-1α levels in kidney [561]. The activation of NF-κB seems to exert a critical role promoting PGC-1α downregulation in inflammatory disorders as the repression of PGC-1α expression was rescued by NF-κB inhibition [562-564]. Interestingly, TNF-α repressed PGC-1α gene expression through activation of both NF-κB and p38 MAPK [562], two signaling pathways activated in SRX KO mice with acute pancreatitis.

Previously, it has been described that p53 acts as a corepressor of PGC-1α promoting cardiomyocyte necrosis in response to oxidative stress [565]. However, the elevated levels of p53 found in SRX KO mice were not associated with the low levels of PGC-1α because the administration of MitoTEMPO recovered normal levels of p53, but the expression of PGC-1α remained low in these mice. Nevertheless, the regulation of PGC-1α by p53 is an intricated question not yet fully resolved. The mouse promoter region of *Ppargc1a* exhibits two p53-binding repressive regions together with an activating region also controlled by p53 [504, 566]. Therefore, p53 can regulate the expression of PGC-1α at two different levels acting either as activator or transcriptional repressor. According to our results, downregulation of PGC-1α is independent of p53 levels in pancreas in SRK KO mice and thus, further experiments are required to elucidate the specific mechanism that underlies the abrogated expression of PGC-1α in SRX-KO mice with acute pancreatitis.

In order to clarify the role of PGC-1α in the regulation of the inflammatory cascade in acute pancreatitis, we induced acute pancreatitis in wild-type mice and PGC-1α KO mice. We found that the activity of PGC-1α on its target genes was abolished in pancreas from wild-type mice with acute pancreatitis. Thus, acute pancreatitis triggered marked downregulation of PGC-1α-dependent antioxidant genes *Prx3, Sod2 and Cat*. Interestingly, the levels of these three mRNAs were low under basal conditions and were kept low upon pancreatitis in PGC-1α KO mice. Strikingly, protein levels of PGC-1α increased in pancreas upon pancreatitis induction in wild-type mice. Nevertheless, our results show that PGC-1α acetylation increased in pancreatitis, thus explaining the transcriptional down-regulation of its antioxidant target genes. It has been previously reported that sirtuins and their deacetylase activities are reduced in acute pancreatitis [567], which potentially could lead to PGC-1α acetylation and inhibition [494]. The dramatic decrease in antioxidant defense triggered by PGC-1α inactivation might decisively contribute to the oxidative stress and inflammatory response, in particular NF-κB activation, found in pancreas from wild-type mice with acute pancreatitis.

Here, we show that PGC-1α KO mice exhibit marked upregulation of *Il-6* in pancreas increased circulating levels of IL-6 after induction of pancreatitis. NF-κB nuclear translocation and recruitment of p65 to the *Il-6* promoter drive IL-6 upregulation, which strikingly seems to be specific to this cytokine as no further upregulation was found for *Tnf-α* or *Il-1β*. Here we show that PGC-1α binds to phospho-p65 in the pancreas specially during pancreatitis, which restrains its transcriptional activity towards *Il-6*. According to our results, PGC-1α selectively modulates NF-κB and seems to function as a specific NF-κB repressor towards IL-6 in acute pancreatitis. Previously, it has been described that p65 constitutively binds to PGC-1α in human cardiac cells and mouse heart blocking its activity on target genes and remarkably, this binding was enhanced upon NF-κB activation induced by TNF-α [525].

Although it is well known that NF-κB activation in pancreas is a major event during the early course of acute pancreatitis, its global impact is context-dependent as NF-κB seems to be a double-edge sword in this disease, depending on its basal activity, its short- or long-term transcriptional effects, the intensity of its activation or the presence of specific coactivators or co-repressors. This is the case of PGC-1α that selectively modulates its transcriptional activity towards IL-6. Pharmacological inhibition of NF-κB as well as genetic deletion of p50/p105 ameliorated the inflammatory response in acute pancreatitis [108, 112, 113]. In agreement with these data, adenoviral transfer or inducible overexpression of p65 to elevate NF-κB levels in pancreas as well as acinar-cell–specific overexpression of IKKβ increased the severity of acute pancreatitis [114-116]. Nevertheless, genetic ablation of p65 in pancreatic exocrine cells markedly aggravated acinar cell injury and death in acute pancreatitis also enhancing the systemic inflammatory response, particularly in the lung [118]. Taken together, these results emphasized the pleiotropic role of NF-κB in acute inflammation probably depending on the selective genetic program activated through NF-κB in response to a specific stimulus. In acute inflammation, NF-κB forms specific signalling complexes to regulate selectively the expression of target genes in order to orchestrate a precise cell response [568]. Hence, our findings provide new insights into the regulation of NF-κB transcriptional activity by specific co-repressors, such as PGC-1α, and help to integrate and clarify the complex role of NF-κB within the context of the inflammatory process during acute pancreatitis.

The increase in circulating IL-6 levels, which is considered a reliable marker for severity in acute pancreatitis [161, 162], leads to a systemic inflammatory response in PGC-1α KO mice with acute pancreatitis. This is evidenced by the increase in pulmonary infiltrate and injury exhibited by these mice. In fact, we found a positive correlation between plasma IL-6 levels and pulmonary MPO activity in wild-type and PGC-1α KO mice. Accordingly, IL-6 KO mice exhibited reduced circulating levels of CXCL1, pulmonary inflammatory infiltrate, and acute lung injury during severe acute pancreatitis [165]. Previously, it has been reported that IL-6 secretion during the early course of acute pancreatitis is controlled by NF-κB in recruited myeloid cells [165]. In fact, administration of recombinant IL-6 enhanced acute lung injury and death rate [165]. Our findings blocking the gp130 receptor confirm the fundamental role of IL-6 induction in PGC-1α-deficient mice to trigger the pulmonary inflammatory response in acute pancreatitis. In acute pancreatitis, the systemic effects of secreted IL-6 seem to be mediated by trans-signaling through the formation of IL-6/soluble IL-6 receptor (sIL-6R) complex [165]. Accordingly, IL-6/sIL-6R complex triggered persistent and strong STAT3 phosphorylation in pancreas with acute pancreatitis enhancing the production of neutrophil attractant CXCL1 [165]. Furthermore, high circulating levels of CXCL1 mediated leukocyte infiltrate into the lung and promoted acute lung injury in acute pancreatitis [165].

According to our results in obese animals, we propose here that the increase in IL-6 levels combined with pancreatic PGC-1α deficiency would explain the enhanced systemic inflammatory response and tissue injury in the disease when high serum IL-6 levels are found in patients, and particularly in obese subjects [569, 570].

It is noteworthy that the marked downregulation of PGC-1α levels exhibited by SRX KO mice is accompanied with *Il-6* upregulation in pancreas with pancreatitis. Interestingly, as occurred in PGC-1α KO mice, the upregulation of *Il-6* in SRX KO mice was also specific for this cytokine. Thus, it is tempting to hypothesize that a common PGC-1α-dependent mechanism underlies the specific control of *Il-6* upregulation during pancreatitis in these mice. Further experiments are required to clarify this point. On the other hand, PGC-1α KO mice did not exhibit necroptosis activation in pancreas, as we found in SRX KO mice. In contrast, we found intense apoptosis in pancreas of PGC-1α KO mice, which was abrogated in SRX KO mice. Consistently with previous findings about the mutually excluded regulation between necrosis and apoptosis in acute pancreatitis [176], these results suggest that the p65-dependent mechanism which drives the selective upregulation of *Il-6* in pancreas of PGC-1α KO mice might favour apoptosis rather than necroptosis during acute pancreatitis. The intriguing question about how PGC-1α could regulate the balance between these two types of cell death requires additional experiments.

In summary, although the activity of PGC-1α seems abrogated and its antioxidant target genes are downregulated in acute pancreatitis, PGC-1α binds to p-p65 acting as a selective repressor of NF-κB towards *Il-6* in the pancreas. Thus, PGC-1α deficiency triggers NF-κB-mediated upregulation of *Il-6* in pancreas during acute pancreatitis increasing IL-6 circulating levels and enhancing the local and systemic inflammatory responses (Figure 51). Hence, taken together, these results highlight the essential role of PGC1α regulating the inflammatory cascade in acute pancreatitis and might contribute to explain the enhanced systemic inflammatory response and tissue injury associated with high serum IL-6 found in patients, particularly in obese subjects.

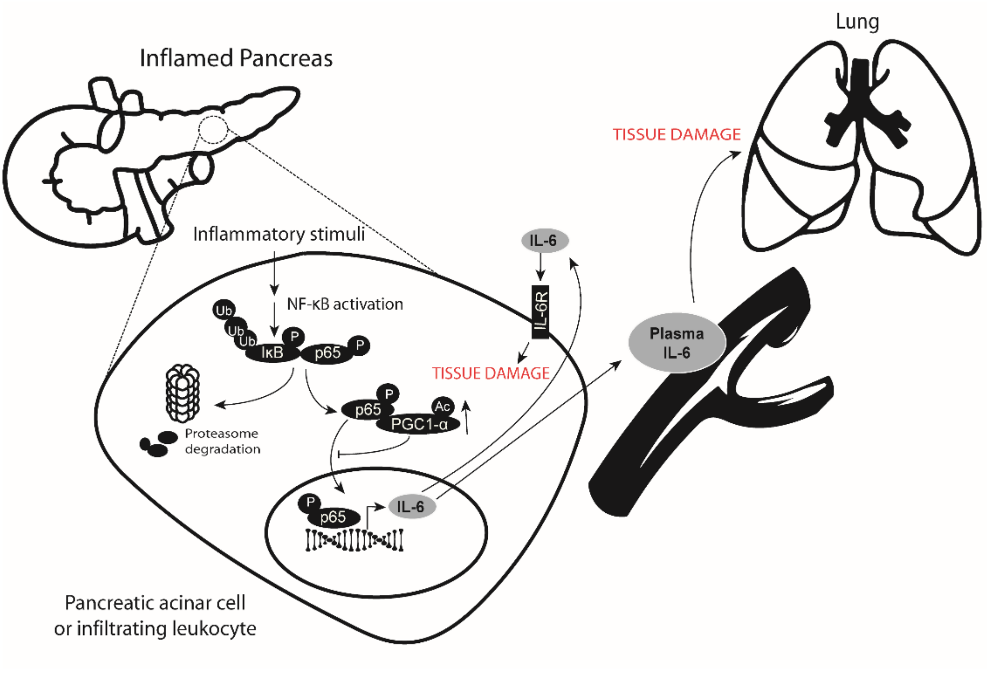
Lung
Inflamed Pancreas
TISSUE DAMAGE
Inflammatory stimuli
IL-6
NF-κB activation
Ub
Ub
Ub
P
IκB
p65
P
IL-6R
Plasma
IL-6
TISSUE DAMAGE
P
p65
Ac
PGC1-α
Proteasome
degradation
P
p65
IL-6
Pancreatic acinar cell
or infiltrating leukocyte

Figure 51. PGC-1α acts as a selective repressor of NF-κB towards *Il-6* in pancreas with acute pancreatitis. Transcriptional activity of PGC-1α is abrogated and its antioxidant targets genes are downregulated in acute pancreatitis PGC-1α binds NF-κB subunit p-p65, acting as a selective repressor of NF-κB towards interleuquin-6 (*Il-6*) in the pancreas.

VI. CONCLUSIONS

According to our results, the conclusions reached in this PhD thesis are:

1. Acute pancreatitis blockades the trans-sulfuration pathway through nitration of cystathionine β-synthase
2. Administration of S-adenosylmethionine in acute pancreatitis enhances the inflammatory response and also nitration of cystathionine β-synthase leading to homocysteine accumulation
3. Sulfiredoxin up-regulation and its translocation into the mitochondria act as a protective mechanism to prevent mitochondrial nitrosative stress and necroptosis during acute pancreatitis
4. PGC-1α protein levels markedly decreased in pancreas from obese mice with acute pancreatitis
5. PGC-1α is inactivated at least in part by acetylation in acute pancreatitis and hence, its antioxidant targets genes are downregulated in this disease
6. PGC-1α acts as a selective repressor of NF-κB towards *Il-6* in pancreas during acute pancreatitis

Bibliography

[1] Pandol, S. The exocrine pancreas. Elsevier; 2010.

[2] Standring, S.; Gray, H. Gray's anatomy: The anatomical basis of clinical practice. Elsevier; 2016.

[3] Dolensek, J.; Rupnik, M. S.; Stozer, A. Structural similarities and differences between the human and the mouse pancreas. Islets7:e1024405; 2015.

[4] Quest, L.; Lombard, M. Pancreas divisum: Opinio divisa. Gut47:317-319; 2000.

[5] Prasanna, L. C.; Rajagopal, K. V.; Thomas, H. R.; Bhat, K. M. Accessory pancreatic duct patterns and their clinical implications. J. Clin. Diagn. Res.9:AC05-7; 2015.

[6] Bastidas-Ponce, A.; Scheibner, K.; Lickert, H.; Bakhti, M. Cellular and molecular mechanisms coordinating pancreas development. Development144:2873-2888; 2017.

[7] Steer M. Chapter 3 - pancreatic physiology and functional assessment. 2012 2012:65-73.e2.

[8] Gaisano, H. Y.; Gorelick, F. S. New insights into the mechanisms of pancreatitis. Gastroenterology136:2040-2044; 2009.

[9] Weiss, F. U.; Halangk, W.; Lerch, M. M. New advances in pancreatic cell physiology and pathophysiology. Best Pract. Res. Clin. Gastroenterol.22:3-15; 2008.

[10] WÃ¤sle, B.; Edwardson, J. M. The regulation of exocytosis in the pancreatic acinar cell. Cell. Signal.14:191-197; 2002.

[11] Dale, W. E.; Turkelson, C. M.; Solomon, T. E. Role of cholecystokinin in intestinal phase and meal-induced pancreatic secretion. Am. J. Physiol.257:G782-90; 1989.

[12] Chey, W. Y.; Chang, T. Neural hormonal regulation of exocrine pancreatic secretion. Pancreatology1:320-335; 2001.

[13] Rhodes, R. A.; Skerven, G.; Chey, W. Y.; Chang, T. M. Acid-independent release of secretin and cholecystokinin by intraduodenal infusion of fat in humans. Pancreas3:391-398; 1988.

[14] Riepl, R. L.; Fiedler, F.; Teufel, J.; Lehnert, P. Effect of intraduodenal bile and taurodeoxycholate on exocrine pancreatic secretion and on plasma levels of vasoactive intestinal polypeptide and somatostatin in man. Pancreas9:109-116; 1994.

[15] Bloom, S. R.; Mitchell, S. J.; Greenberg, G. R.; Christofides, N.; Domschke, W.; Domschke, S.; Mitznegg, P.; Demling, L. Release of VIP, secretin and motilin after duodenal acidification in man. Acta Hepatogastroenterol. (Stuttg)25:365-368; 1978.

[16] Frossard, J. L.; Steer, M. L.; Pastor, C. M. Acute pancreatitis. Lancet371:143-152; 2008.

[17] Pannala, R.; Kidd, M.; Modlin, I. M. Acute pancreatitis: A historical perspective. Pancreas38:355-366; 2009.

[18] Leach, S. D.; Gorelick, F. S.; Modlin, I. M. Acute pancreatitis at its centenary. the contribution of reginald fitz. Ann. Surg.212:109-113; 1990.

[19] Frey, C. F. Classification of pancreatitis: State-of-the-art, 1986. Pancreas1:62-68; 1986.

[20] Bradley, E. L.,3rd. A clinically based classification system for acute pancreatitis. summary of the international symposium on acute pancreatitis, atlanta, ga, september 11 through 13, 1992. Arch. Surg.128:586-590; 1993.

[21] Bollen, T. L.; van Santvoort, H. C.; Besselink, M. G.; van Leeuwen, M. S.; Horvath, K. D.; Freeny, P. C.; Gooszen, H. G.; Dutch Acute Pancreatitis Study Group. The atlanta classification of acute pancreatitis revisited. Br. J. Surg.95:6-21; 2008.

[22] Banks, P. A.; Bollen, T. L.; Dervenis, C.; Gooszen, H. G.; Johnson, C. D.; Sarr, M. G.; Tsiotos, G. G.; Vege, S. S.; Acute Pancreatitis Classification Working Group. Classification of acute pancreatitis--2012: Revision of the atlanta classification and definitions by international consensus. Gut62:102-111; 2013.

[23] Bollen, T. L.; Besselink, M. G.; van Santvoort, H. C.; Gooszen, H. G.; van Leeuwen, M. S. Toward an update of the atlanta classification on acute pancreatitis: Review of new and abandoned terms. Pancreas35:107-113; 2007.

[24] Singh, V. K.; Bollen, T. L.; Wu, B. U.; Repas, K.; Maurer, R.; Yu, S.; Mortele, K. J.; Conwell, D. L.; Banks, P. A. An assessment of the severity of interstitial pancreatitis. Clin. Gastroenterol. Hepatol.9:1098-1103; 2011.

[25] Petrov, M. S.; Shanbhag, S.; Chakraborty, M.; Phillips, A. R.; Windsor, J. A. Organ failure and infection of pancreatic necrosis as determinants of mortality in patients with acute pancreatitis. Gastroenterology139:813-820; 2010.

[26] Ranson, J. H.; Rifkind, K. M.; Roses, D. F.; Fink, S. D.; Eng, K.; Spencer, F. C. Prognostic signs and the role of operative management in acute pancreatitis. Surg. Gynecol. Obstet.139:69-81; 1974.

[27] Ranson, J. H. The timing of biliary surgery in acute pancreatitis. Ann. Surg.189:654-663; 1979.

[28] Blamey, S. L.; Imrie, C. W.; O'Neill, J.; Gilmour, W. H.; Carter, D. C. Prognostic factors in acute pancreatitis. Gut25:1340-1346; 1984.

[29] Knaus, W. A.; Draper, E. A.; Wagner, D. P.; Zimmerman, J. E. APACHE II: A severity of disease classification system. Crit. Care Med.13:818-829; 1985.

[30] Larvin, M.; McMahon, M. J. APACHE-II score for assessment and monitoring of acute pancreatitis. Lancet2:201-205; 1989.

[31] Marshall, J. C.; Cook, D. J.; Christou, N. V.; Bernard, G. R.; Sprung, C. L.; Sibbald, W. J. Multiple organ dysfunction score: A reliable descriptor of a complex clinical outcome. Crit. Care Med.23:1638-1652; 1995.

[32] Vincent, J. L.; Moreno, R.; Takala, J.; Willatts, S.; De Mendonca, A.; Bruining, H.; Reinhart, C. K.; Suter, P. M.; Thijs, L. G. The SOFA (sepsis-related organ failure assessment) score to describe organ dysfunction/failure. on behalf of the working group on sepsis-related problems of the european society of intensive care medicine. Intensive Care Med.22:707-710; 1996.

[33] Lankisch, P. G.; Apte, M.; Banks, P. A. Acute pancreatitis. Lancet386:85-96; 2015.

[34] Bernard, C. Leçons de physiologie expérimentale. Bailliere2:278; 1856.

[35] Opie, E. The relation of cholelithiasis to disease of the pancreas and to fat necrosis. Johns Hopkins Hosp Bull12:19; 1901.

[36] Whitcomb, D. C. Clinical practice. acute pancreatitis. N. Engl. J. Med.354:2142-2150; 2006.

[37] Spanier, B. W.; Dijkgraaf, M. G.; Bruno, M. J. Epidemiology, aetiology and outcome of acute and chronic pancreatitis: An update. Best Pract. Res. Clin. Gastroenterol.22:45-63; 2008.

[38] Yadav, D.; Lowenfels, A. B. Trends in the epidemiology of the first attack of acute pancreatitis: A systematic review. Pancreas33:323-330; 2006.

[39] Kristiansen, L.; Gronbaek, M.; Becker, U.; Tolstrup, J. S. Risk of pancreatitis according to alcohol drinking habits: A population-based cohort study. Am. J. Epidemiol.168:932-937; 2008.

[40] Lankisch, P. G.; Lowenfels, A. B.; Maisonneuve, P. What is the risk of alcoholic pancreatitis in heavy drinkers? Pancreas25:411-412; 2002.

[41] Yadav, D.; Lowenfels, A. B. The epidemiology of pancreatitis and pancreatic cancer. Gastroenterology144:1252-1261; 2013.

[42] Lindkvist, B.; Appelros, S.; Regner, S.; Manjer, J. A prospective cohort study on risk of acute pancreatitis related to serum triglycerides, cholesterol and fasting glucose. Pancreatology12:317-324; 2012.

[43] Khatua, B.; El-Kurdi, B.; Singh, V. P. Obesity and pancreatitis. Curr. Opin. Gastroenterol.33:374-382; 2017.

[44] Pereda, J.; Perez, S.; Escobar, J.; Arduini, A.; Asensi, M.; Serviddio, G.; Sabater, L.; Aparisi, L.; Sastre, J. Obese rats exhibit high levels of fat necrosis and isoprostanes in taurocholate-induced acute pancreatitis. PLoS One7:e44383; 2012.

[45] Sempere, L.; Martinez, J.; de Madaria, E.; Lozano, B.; Sanchez-Paya, J.; Jover, R.; Perez-Mateo, M. Obesity and fat distribution imply a greater systemic inflammatory response and a worse prognosis in acute pancreatitis. Pancreatology8:257-264; 2008.

[46] Segersvard, R.; Sylvan, M.; Herrington, M.; Larsson, J.; Permert, J. Obesity increases the severity of acute experimental pancreatitis in the rat. Scand. J. Gastroenterol.36:658-663; 2001.

[47] Segersvard, R.; Tsai, J. A.; Herrington, M. K.; Wang, F. Obesity alters cytokine gene expression and promotes liver injury in rats with acute pancreatitis. Obesity (Silver Spring)16:23-28; 2008.

[48] Badalov, N.; Baradarian, R.; Iswara, K.; Li, J.; Steinberg, W.; Tenner, S. Drug-induced acute pancreatitis: An evidence-based review. Clin. Gastroenterol. Hepatol.5:648-61; quiz 644; 2007.

[49] Peery, A. F.; Crockett, S. D.; Murphy, C. C.; Lund, J. L.; Dellon, E. S.; Williams, J. L.; Jensen, E. T.; Shaheen, N. J.; Barritt, A. S.; Lieber, S. R.; Kochar, B.; Barnes, E. L.; Fan, Y. C.; Pate, V.; Galanko, J.; Baron, T. H.; Sandler, R. S. Burden and cost of gastrointestinal, liver, and pancreatic diseases in the united states: Update 2018. Gastroenterology156:254-272.e11; 2019.

[50] Roberts, S. E.; Morrison-Rees, S.; John, A.; Williams, J. G.; Brown, T. H.; Samuel, D. G. The incidence and aetiology of acute pancreatitis across europe. Pancreatology17:155-165; 2017.

[51] Valverde-Lopez, F.; Wilcox, C. M.; Redondo-Cerezo, E. Evaluation and management of acute pancreatitis in spain. Gastroenterol. Hepatol.41:618-628; 2018.

[52] Yang, A. L.; Vadhavkar, S.; Singh, G.; Omary, M. B. Epidemiology of alcohol-related liver and pancreatic disease in the united states. Arch. Intern. Med.168:649-656; 2008.

[53] Fagenholz, P. J.; Castillo, C. F.; Harris, N. S.; Pelletier, A. J.; Camargo, C. A.,Jr. Increasing united states hospital admissions for acute pancreatitis, 1988-2003. Ann. Epidemiol.17:491-497; 2007.

[54] McNabb-Baltar, J.; Ravi, P.; Isabwe, G. A.; Suleiman, S. L.; Yaghoobi, M.; Trinh, Q. D.; Banks, P. A. A population-based assessment of the burden of acute pancreatitis in the united states. Pancreas43:687-691; 2014.

[55] Krishna, S. G.; Kamboj, A. K.; Hart, P. A.; Hinton, A.; Conwell, D. L. The changing epidemiology of acute pancreatitis hospitalizations: A decade of trends and the impact of chronic pancreatitis. Pancreas46:482-488; 2017.

[56] Chiari, H. Über die selbstverdauung des menschlichen pankreas. zeitschrift für heilkunde. Zeitschrift Für Heilkunde17:69-96; 1896.

[57] Geokas, M. C.; Rinderknecht, H. Free proteolytic enzymes in pancreatic juice of patients with acute pancreatitis. Am. J. Dig. Dis.19:591-598; 1974.

[58] Ji,Baoan; Logsdon, C.,D. Digesting new information about the role of trypsin in pancreatitis. Gastroenterology141:1972-1975; 2011.

[59] Whitcomb, D. C.; Gorry, M. C.; Preston, R. A.; Furey, W.; Sossenheimer, M. J.; Ulrich, C. D.; Martin, S. P.; Gates, L. K.,Jr; Amann, S. T.; Toskes, P. P.; Liddle, R.; McGrath, K.; Uomo, G.; Post, J. C.; Ehrlich, G. D. Hereditary pancreatitis is caused by a mutation in the cationic trypsinogen gene. Nat. Genet.14:141-145; 1996.

[60] Nathan, J. D.; Romac, J.; Peng, R. Y.; Peyton, M.; Macdonald, R. J.; Liddle, R. A. Transgenic expression of pancreatic secretory trypsin inhibitor-I ameliorates secretagogue-induced pancreatitis in mice. Gastroenterology128:717-727; 2005.

[61] Koike, H.; Steer, M. L.; Meldolesi, J. Pancreatic effects of ethionine: Blockade of exocytosis and appearance of crinophagy and autophagy precede cellular necrosis. Am. J. Physiol.242:G297-307; 1982.

[62] Watanabe, O.; Baccino, F. M.; Steer, M. L.; Meldolesi, J. Supramaximal caerulein stimulation and ultrastructure of rat pancreatic acinar cell: Early morphological changes during development of experimental pancreatitis. Am. J. Physiol.246:G457-67; 1984.

[63] Otani, T.; Chepilko, S. M.; Grendell, J. H.; Gorelick, F. S. Codistribution of TAP and the granule membrane protein GRAMP-92 in rat caerulein-induced pancreatitis. Am. J. Physiol.275:G999-G1009; 1998.

[64] Van Acker, G. J.; Saluja, A. K.; Bhagat, L.; Singh, V. P.; Song, A. M.; Steer, M. L. Cathepsin B inhibition prevents trypsinogen activation and reduces pancreatitis severity. Am. J. Physiol. Gastrointest. Liver Physiol.283:G794-800; 2002.

[65] Halangk, W.; Lerch, M. M.; Brandt-Nedelev, B.; Roth, W.; Ruthenbuerger, M.; Reinheckel, T.; Domschke, W.; Lippert, H.; Peters, C.; Deussing, J. Role of cathepsin B in intracellular trypsinogen activation and the onset of acute pancreatitis. J. Clin. Invest.106:773-781; 2000.

[66] Halangk, W.; Kruger, B.; Ruthenburger, M.; Sturzebecher, J.; Albrecht, E.; Lippert, H.; Lerch, M. M. Trypsin activity is not involved in premature, intrapancreatic trypsinogen activation. Am. J. Physiol. Gastrointest. Liver Physiol.282:G367-74; 2002.

[67] Meister, T.; Niehues, R.; Hahn, D.; Domschke, W.; Sendler, M.; Lerch, M. M.; Schnekenburger, J. Missorting of cathepsin B into the secretory compartment of CI-MPR/IGFII-deficient mice does not induce spontaneous trypsinogen activation but leads to enhanced trypsin activity during experimental

pancreatitis--without affecting disease severity. J. Physiol. Pharmacol.61:565-575; 2010.

[68] Gerasimenko, J. V.; Lur, G.; Sherwood, M. W.; Ebisui, E.; Tepikin, A. V.; Mikoshiba, K.; Gerasimenko, O. V.; Petersen, O. H. Pancreatic protease activation by alcohol metabolite depends on Ca2+ release via acid store IP3 receptors. Proc. Natl. Acad. Sci. U. S. A.106:10758-10763; 2009.

[69] Kruger, B.; Albrecht, E.; Lerch, M. M. The role of intracellular calcium signaling in premature protease activation and the onset of pancreatitis. Am. J. Pathol.157:43-50; 2000.

[70] Raraty, M.; Ward, J.; Erdemli, G.; Vaillant, C.; Neoptolemos, J. P.; Sutton, R.; Petersen, O. H. Calcium-dependent enzyme activation and vacuole formation in the apical granular region of pancreatic acinar cells. Proc. Natl. Acad. Sci. U. S. A.97:13126-13131; 2000.

[71] Kim, M. S.; Lee, K. P.; Yang, D.; Shin, D. M.; Abramowitz, J.; Kiyonaka, S.; Birnbaumer, L.; Mori, Y.; Muallem, S. Genetic and pharmacologic inhibition of the Ca2+ influx channel TRPC3 protects secretory epithelia from Ca2+-dependent toxicity. Gastroenterology140:2107-15, 2115.e1-4; 2011.

[72] Orabi, A. I.; Shah, A. U.; Ahmad, M. U.; Choo-Wing, R.; Parness, J.; Jain, D.; Bhandari, V.; Husain, S. Z. Dantrolene mitigates caerulein-induced pancreatitis in vivo in mice. Am. J. Physiol. Gastrointest. Liver Physiol.299:G196-204; 2010.

[73] Gorelick, F. S.; Thrower, E. The acinar cell and early pancreatitis responses. Clin. Gastroenterol. Hepatol.7:S10-4; 2009.

[74] Niederau, C.; Grendell, J. H. Intracellular vacuoles in experimental acute pancreatitis in rats and mice are an acidified compartment. J. Clin. Invest.81:229-236; 1988.

[75] Guillaumes, S.; Blanco, I.; Villanueva, A.; Sans, M. D.; Clave, P.; Chabas, A.; Farre, A.; Lluis, F. Chloroquine stabilizes pancreatic lysosomes and improves survival of mice with diet-induced acute pancreatitis. Pancreas14:262-266; 1997.

[76] Waterford, S. D.; Kolodecik, T. R.; Thrower, E. C.; Gorelick, F. S. Vacuolar ATPase regulates zymogen activation in pancreatic acini. J. Biol. Chem.280:5430-5434; 2005.

[77] Gukovskaya, A. S.; Gukovsky, I. Autophagy and pancreatitis. Am. J. Physiol. Gastrointest. Liver Physiol.303:G993-G1003; 2012.

[78] Mareninova, O. A.; Hermann, K.; French, S. W.; O'Konski, M. S.; Pandol, S. J.; Webster, P.; Erickson, A. H.; Katunuma, N.; Gorelick, F. S.; Gukovsky, I.; Gukovskaya, A. S. Impaired autophagic flux mediates acinar cell vacuole formation and trypsinogen activation in rodent models of acute pancreatitis. J. Clin. Invest.119:3340-3355; 2009.

[79] Gukovsky, I.; Pandol, S. J.; Mareninova, O. A.; Shalbueva, N.; Jia, W.; Gukovskaya, A. S. Impaired autophagy and organellar dysfunction in pancreatitis. J. Gastroenterol. Hepatol.27 Suppl 2:27-32; 2012.

[80] Willemer, S.; Bialek, R.; Adler, G. Localization of lysosomal and digestive enzymes in cytoplasmic vacuoles in caerulein-pancreatitis. Histochemistry94:161-170; 1990.

[81] Wartmann, T.; Mayerle, J.; Kahne, T.; Sahin-Toth, M.; Ruthenburger, M.; Matthias, R.; Kruse, A.; Reinheckel, T.; Peters, C.; Weiss, F. U.; Sendler, M.; Lippert, H.; Schulz, H. U.; Aghdassi, A.; Dummer, A.; Teller, S.; Halangk, W.; Lerch, M. M. Cathepsin L inactivates human trypsinogen, whereas cathepsin L-deletion reduces the severity of pancreatitis in mice. Gastroenterology138:726-737; 2010.

[82] Halangk, W.; Kruger, B.; Ruthenburger, M.; Sturzebecher, J.; Albrecht, E.; Lippert, H.; Lerch, M. M. Trypsin activity is not involved in premature, intrapancreatic trypsinogen activation. Am. J. Physiol. Gastrointest. Liver Physiol.282:G367-74; 2002.

[83] Kereszturi, E.; Szmola, R.; Kukor, Z.; Simon, P.; Weiss, F. U.; Lerch, M. M.; Sahin-Toth, M. Hereditary pancreatitis caused by mutation-induced misfolding of human cationic trypsinogen: A novel disease mechanism. Hum. Mutat.30:575-582; 2009.

[84] Dawra, R.; Sah, R. P.; Dudeja, V.; Rishi, L.; Talukdar, R.; Garg, P.; Saluja, A. K. Intra-acinar trypsinogen activation mediates early stages of pancreatic injury but not inflammation in mice with acute pancreatitis. Gastroenterology141:2210-2217.e2; 2011.

[85] Ji, B.; Gaiser, S.; Chen, X.; Ernst, S. A.; Logsdon, C. D. Intracellular trypsin induces pancreatic acinar cell death but not NF-kappaB activation. J. Biol. Chem.284:17488-17498; 2009.

[86] Gaiser, S.; Daniluk, J.; Liu, Y.; Tsou, L.; Chu, J.; Lee, W.; Longnecker, D. S.; Logsdon, C. D.; Ji, B. Intracellular activation of trypsinogen in transgenic mice induces acute but not chronic pancreatitis. Gut60:1379-1388; 2011.

[87] Kereszturi, E.; Sahin-Toth, M. Intracellular autoactivation of human cationic trypsinogen mutants causes reduced trypsinogen secretion and acinar cell death. J. Biol. Chem.284:33392-33399; 2009.

[88] Habtezion, A.; Gukovskaya, A. S.; Pandol, S. J. Acute pancreatitis: A multifaceted set of organelle and cellular interactions. Gastroenterology156:1941-1950; 2019.

[89] Chen, L.; Deng, H.; Cui, H.; Fang, J.; Zuo, Z.; Deng, J.; Li, Y.; Wang, X.; Zhao, L. Inflammatory responses and inflammation-associated diseases in organs. Oncotarget9:7204-7218; 2017.

[90] Gukovskaya, A. S.; Gukovsky, I.; Algul, H.; Habtezion, A. Autophagy, inflammation, and immune dysfunction in the pathogenesis of pancreatitis. Gastroenterology153:1212-1226; 2017.

[91] Sen, R.; Baltimore, D. Multiple nuclear factors interact with the immunoglobulin enhancer sequences. Cell46:705-716; 1986.

[92] Ghosh, G.; Wang, V. Y.; Huang, D. B.; Fusco, A. NF-kappaB regulation: Lessons from structures. Immunol. Rev.246:36-58; 2012.

[93] Zhang, Q.; Lenardo, M. J.; Baltimore, D. 30 years of NF-kappaB: A blossoming of relevance to human pathobiology. Cell168:37-57; 2017.

[94] Hayden, M. S.; Ghosh, S. NF-kappaB, the first quarter-century: Remarkable progress and outstanding questions. Genes Dev.26:203-234; 2012.

[95] Moynagh, P. N. The NF-kappaB pathway. J. Cell. Sci.118:4589-4592; 2005.

[96] Karin, M.; Cao, Y.; Greten, F. R.; Li, Z. W. NF-kappaB in cancer: From innocent bystander to major culprit. Nat. Rev. Cancer.2:301-310; 2002.

[97] Oeckinghaus, A.; Ghosh, S. The NF-kappaB family of transcription factors and its regulation. Cold Spring Harb Perspect. Biol.1:a000034; 2009.

[98] Schuster, M.; Annemann, M.; Plaza-Sirvent, C.; Schmitz, I. Atypical IkappaB proteins - nuclear modulators of NF-kappaB signaling. Cell. Commun. Signal.11:23-811X-11-23; 2013.

[99] Hayden, M. S.; Ghosh, S. Shared principles in NF-kappaB signaling. Cell132:344-362; 2008.

[100] Sun, S. C. Non-canonical NF-kappaB signaling pathway. Cell Res.21:71-85; 2011.

[101] Hinz, M.; Scheidereit, C. The IkappaB kinase complex in NF-kappaB regulation and beyond. EMBO Rep.15:46-61; 2014.

[102] Viatour, P.; Merville, M. P.; Bours, V.; Chariot, A. Phosphorylation of NF-kappaB and IkappaB proteins: Implications in cancer and inflammation. Trends Biochem. Sci.30:43-52; 2005.

[103] Kato, T.,Jr; Delhase, M.; Hoffmann, A.; Karin, M. CK2 is a C-terminal IkappaB kinase responsible for NF-kappaB activation during the UV response. Mol. Cell12:829-839; 2003.

[104] Bohuslav, J.; Chen, L. F.; Kwon, H.; Mu, Y.; Greene, W. C. p53 induces NF-kappaB activation by an IkappaB kinase-independent mechanism involving phosphorylation of p65 by ribosomal S6 kinase 1. J. Biol. Chem.279:26115-26125; 2004.

[105] Wan, F.; Lenardo, M. J. Specification of DNA binding activity of NF-kappaB proteins. Cold Spring Harb Perspect. Biol.1:a000067; 2009.

[106] Smale, S. T. Dimer-specific regulatory mechanisms within the NF-kappaB family of transcription factors. Immunol. Rev.246:193-204; 2012.

[107] Gukovsky, I.; Gukovskaya, A. S.; Blinman, T. A.; Zaninovic, V.; Pandol, S. J. Early NF-kappaB activation is associated with hormone-induced pancreatitis. Am. J. Physiol.275:G1402-14; 1998.

[108] Rakonczay, Z.,Jr; Hegyi, P.; Takacs, T.; McCarroll, J.; Saluja, A. K. The role of NF-kappaB activation in the pathogenesis of acute pancreatitis. Gut57:259-267; 2008.

[109] Kang, R.; Lotze, M. T.; Zeh, H. J.; Billiar, T. R.; Tang, D. Cell death and DAMPs in acute pancreatitis. Mol. Med.20:466-477; 2014.

[110] Hoque, R.; Sohail, M.; Malik, A.; Sarwar, S.; Luo, Y.; Shah, A.; Barrat, F.; Flavell, R.; Gorelick, F.; Husain, S.; Mehal, W. TLR9 and the NLRP3 inflammasome link acinar cell death with inflammation in acute pancreatitis. Gastroenterology141:358-369; 2011.

[111] Li, G.; Wu, X.; Yang, L.; He, Y.; Liu, Y.; Jin, X.; Yuan, H. TLR4-mediated NF-kappaB signaling pathway mediates HMGB1-induced pancreatic injury in mice with severe acute pancreatitis. Int. J. Mol. Med.37:99-107; 2016.

[112] Altavilla, D.; Famulari, C.; Passaniti, M.; Galeano, M.; Macri, A.; Seminara, P.; Minutoli, L.; Marini, H.; Calo, M.; Venuti, F. S.; Esposito, M.; Squadrito, F. Attenuated cerulein-induced pancreatitis in nuclear factor-kappaB-deficient mice. Lab. Invest.83:1723-1732; 2003.

[113] Gukovsky, I.; Gukovskaya, A. Nuclear factor-kappaB in pancreatitis: Jack-of-all-trades, but which one is more important? Gastroenterology144:26-29; 2013.

[114] Chen, X.; Ji, B.; Han, B.; Ernst, S. A.; Simeone, D.; Logsdon, C. D. NF-kappaB activation in pancreas induces pancreatic and systemic inflammatory response. Gastroenterology122:448-457; 2002.

[115] Huang, H.; Liu, Y.; Daniluk, J.; Gaiser, S.; Chu, J.; Wang, H.; Li, Z. S.; Logsdon, C. D.; Ji, B. Activation of nuclear factor-kappaB in acinar cells increases the severity of pancreatitis in mice. Gastroenterology144:202-210; 2013.

[116] Baumann, B.; Wagner, M.; Aleksic, T.; von Wichert, G.; Weber, C. K.; Adler, G.; Wirth, T. Constitutive IKK2 activation in acinar cells is sufficient to induce pancreatitis in vivo. J. Clin. Invest.117:1502-1513; 2007.

[117] Li, N.; Wu, X.; Holzer, R. G.; Lee, J. H.; Todoric, J.; Park, E. J.; Ogata, H.; Gukovskaya, A. S.; Gukovsky, I.; Pizzo, D. P.; VandenBerg, S.; Tarin, D.; Atay, C.; Arkan, M. C.; Deerinck, T. J.; Moscat, J.; Diaz-Meco, M.; Dawson, D.; Erkan, M.; Kleeff, J.; Karin, M. Loss of acinar cell IKKalpha triggers spontaneous pancreatitis in mice. J. Clin. Invest.123:2231-2243; 2013.

[118] Algul, H.; Treiber, M.; Lesina, M.; Nakhai, H.; Saur, D.; Geisler, F.; Pfeifer, A.; Paxian, S.; Schmid, R. M. Pancreas-specific RelA/p65 truncation increases susceptibility of acini to inflammation-associated cell death following cerulein pancreatitis. J. Clin. Invest.117:1490-1501; 2007.

[119] Neuhofer, P.; Liang, S.; Einwachter, H.; Schwerdtfeger, C.; Wartmann, T.; Treiber, M.; Zhang, H.; Schulz, H. U.; Dlubatz, K.; Lesina, M.; Diakopoulos, K. N.; Wormann, S.; Halangk, W.; Witt, H.; Schmid, R. M.; Algul, H. Deletion of IkappaBalpha activates RelA to reduce acute pancreatitis in mice through up-regulation of Spi2A. Gastroenterology144:192-201; 2013.

[120] Cargnello, M.; Roux, P. P. Activation and function of the MAPKs and their substrates, the MAPK-activated protein kinases. Microbiol. Mol. Biol. Rev.75:50-83; 2011.

[121] Roux, P. P.; Blenis, J. ERK and p38 MAPK-activated protein kinases: A family of protein kinases with diverse biological functions. Microbiol. Mol. Biol. Rev.68:320-344; 2004.

[122] Goedert, M.; Cuenda, A.; Craxton, M.; Jakes, R.; Cohen, P. Activation of the novel stress-activated protein kinase SAPK4 by cytokines and cellular stresses is mediated by SKK3 (MKK6); comparison of its substrate specificity with that of other SAP kinases. Embo J.16:3563-3571; 1997.

[123] Samuel, I.; Zaheer, A.; Fisher, R. A. In vitro evidence for role of ERK, p38, and JNK in exocrine pancreatic cytokine production. J. Gastrointest. Surg.10:1376-1383; 2006.

[124] Twait, E.; Williard, D. E.; Samuel, I. Dominant negative p38 mitogen-activated protein kinase expression inhibits NF-kappaB activation in AR42J cells. Pancreatology10:119-128; 2010.

[125] Minutoli, L.; Altavilla, D.; Marini, H.; Passaniti, M.; Bitto, A.; Seminara, P.; Venuti, F. S.; Famulari, C.; Macri, A.; Versaci, A.; Squadrito, F. Protective effects of SP600125 a new inhibitor of c-jun N-terminal kinase (JNK) and extracellular-regulated kinase (ERK1/2) in an experimental model of cerulein-induced pancreatitis. Life Sci.75:2853-2866; 2004.

[126] Mazzon, E.; Impellizzeri, D.; Di Paola, R.; Paterniti, I.; Esposito, E.; Cappellani, A.; Bramanti, P.; Cuzzocrea, S. Effects of mitogen-activated protein kinase signaling pathway inhibition on the development of cerulein-induced acute pancreatitis in mice. Pancreas41:560-570; 2012.

[127] Tietz, A. B.; Malo, A.; Diebold, J.; Kotlyarov, A.; Herbst, A.; Kolligs, F. T.; Brandt-Nedelev, B.; Halangk, W.; Gaestel, M.; Goke, B.; Schafer, C. Gene deletion of MK2 inhibits TNF-alpha and IL-6 and protects against cerulein-induced pancreatitis. Am. J. Physiol. Gastrointest. Liver Physiol.290:G1298-306; 2006.

[128] Vonlaufen, A.; Apte, M. V.; Imhof, B. A.; Frossard, J. L. The role of inflammatory and parenchymal cells in acute pancreatitis. J. Pathol.213:239-248; 2007.

[129] Kany, S.; Vollrath, J. T.; Relja, B. Cytokines in inflammatory disease. Int. J. Mol. Sci.20:10.3390/ijms20236008; 2019.

[130] Kusske, A. M.; Rongione, A. J.; Reber, H. A. Cytokines and acute pancreatitis. Gastroenterology110:639-642; 1996.

[131] Makhija, R.; Kingsnorth, A. N. Cytokine storm in acute pancreatitis. J. Hepatobiliary. Pancreat. Surg.9:401-410; 2002.

[132] Carswell, E. A.; Old, L. J.; Kassel, R. L.; Green, S.; Fiore, N.; Williamson, B. An endotoxin-induced serum factor that causes necrosis of tumors. Proc. Natl. Acad. Sci. U. S. A.72:3666-3670; 1975.

[133] Sedger, L. M.; McDermott, M. F. TNF and TNF-receptors: From mediators of cell death and inflammation to therapeutic giants - past, present and future. Cytokine Growth Factor Rev.25:453-472; 2014.

[134] Moss, M. L.; Jin, S. L.; Milla, M. E.; Bickett, D. M.; Burkhart, W.; Carter, H. L.; Chen, W. J.; Clay, W. C.; Didsbury, J. R.; Hassler, D.; Hoffman, C. R.; Kost, T. A.; Lambert, M. H.; Leesnitzer, M. A.; McCauley, P.; McGeehan, G.; Mitchell, J.; Moyer, M.; Pahel, G.; Rocque, W.; Overton, L. K.; Schoenen, F.; Seaton, T.; Su, J. L.; Becherer, J. D. Cloning of a disintegrin metalloproteinase that processes precursor tumour-necrosis factor-alpha. Nature385:733-736; 1997.

[135] Malleo, G.; Mazzon, E.; Siriwardena, A. K.; Cuzzocrea, S. Role of tumor necrosis factor-alpha in acute pancreatitis: From biological basis to clinical evidence. Shock28:130-140; 2007.

[136] Gukovskaya, A. S.; Gukovsky, I.; Zaninovic, V.; Song, M.; Sandoval, D.; Gukovsky, S.; Pandol, S. J. Pancreatic acinar cells produce, release, and respond to tumor necrosis factor-alpha. role in regulating cell death and pancreatitis. J. Clin. Invest.100:1853-1862; 1997.

[137] Vaccaro, M. I.; Ropolo, A.; Grasso, D.; Calvo, E. L.; Ferreria, M.; Iovanna, J. L.; Lanosa, G. Pancreatic acinar cells submitted to stress activate TNF-alpha gene expression. Biochem. Biophys. Res. Commun.268:485-490; 2000.

[138] Ramudo, L.; Manso, M. A.; Sevillano, S.; de Dios, I. Kinetic study of TNF-alpha production and its regulatory mechanisms in acinar cells during acute pancreatitis induced by bile-pancreatic duct obstruction. J. Pathol.206:9-16; 2005.

[139] Ethridge, R. T.; Hashimoto, K.; Chung, D. H.; Ehlers, R. A.; Rajaraman, S.; Evers, B. M. Selective inhibition of NF-kappaB attenuates the severity of cerulein-induced acute pancreatitis. J. Am. Coll. Surg.195:497-505; 2002.

[140] Chu, W. M. Tumor necrosis factor. Cancer Lett.328:222-225; 2013.

[141] Norman, J. G.; Fink, G. W.; Messina, J.; Carter, G.; Franz, M. G. Timing of tumor necrosis factor antagonism is critical in determining outcome in murine lethal acute pancreatitis. Surgery120:515-521; 1996.

[142] Hughes, C. B.; Grewal, H. P.; Gaber, L. W.; Kotb, M.; El-din, A. B.; Mann, L.; Gaber, A. O. Anti-TNFalpha therapy improves survival and ameliorates the pathophysiologic sequelae in acute pancreatitis in the rat. Am. J. Surg.171:274-280; 1996.

[143] Malleo, G.; Mazzon, E.; Genovese, T.; Di Paola, R.; Muia, C.; Centorrino, T.; Siriwardena, A. K.; Cuzzocrea, S. Etanercept attenuates the development of cerulein-induced acute pancreatitis in mice: A comparison with TNF-alpha genetic deletion. Shock27:542-551; 2007.

[144] Gomez-Cambronero, L.; Camps, B.; de La Asuncion, J. G.; Cerda, M.; Pellin, A.; Pallardo, F. V.; Calvete, J.; Sweiry, J. H.; Mann, G. E.; Vina, J.; Sastre, J. Pentoxifylline ameliorates cerulein-induced pancreatitis in rats: Role of glutathione and nitric oxide. J. Pharmacol. Exp. Ther.293:670-676; 2000.

[145] Escobar, J.; Pereda, J.; Arduini, A.; Sandoval, J.; Moreno, M. L.; Perez, S.; Sabater, L.; Aparisi, L.; Cassinello, N.; Hidalgo, J.; Joosten, L. A.; Vento, M.; Lopez-Rodas, G.; Sastre, J. Oxidative and nitrosative stress in acute pancreatitis. modulation by pentoxifylline and oxypurinol. Biochem. Pharmacol.83:122-130; 2012.

[146] Hirano, T.; Yasukawa, K.; Harada, H.; Taga, T.; Watanabe, Y.; Matsuda, T.; Kashiwamura, S.; Nakajima, K.; Koyama, K.; Iwamatsu, A. Complementary DNA for a novel human interleukin (BSF-2) that induces B lymphocytes to produce immunoglobulin. Nature324:73-76; 1986.

[147] Rose-John, S. Interleukin-6 family cytokines. Cold Spring Harb Perspect. Biol.10:10.1101/cshperspect.a028415; 2018.

[148] Nakashima, K.; Taga, T. gp130 and the IL-6 family of cytokines: Signaling mechanisms and thrombopoietic activities. Semin. Hematol.35:210-221; 1998.

[149] Stark, G. R.; Cheon, H.; Wang, Y. Responses to cytokines and interferons that depend upon JAKs and STATs. Cold Spring Harb Perspect. Biol.10:10.1101/cshperspect.a028555; 2018.

[150] Yu, H.; Lee, H.; Herrmann, A.; Buettner, R.; Jove, R. Revisiting STAT3 signalling in cancer: New and unexpected biological functions. Nat. Rev. Cancer.14:736-746; 2014.

[151] Huynh, J.; Chand, A.; Gough, D.; Ernst, M. Therapeutically exploiting STAT3 activity in cancer - using tissue repair as a road map. Nat. Rev. Cancer.19:82-96; 2019.

[152] Hillmer, E. J.; Zhang, H.; Li, H. S.; Watowich, S. S. STAT3 signaling in immunity. Cytokine Growth Factor Rev.31:1-15; 2016.

[153] Mullberg, J.; Schooltink, H.; Stoyan, T.; Heinrich, P. C.; Rose-John, S. Protein kinase C activity is rate limiting for shedding of the interleukin-6 receptor. Biochem. Biophys. Res. Commun.189:794-800; 1992.

[154] Mullberg, J.; Schooltink, H.; Stoyan, T.; Gunther, M.; Graeve, L.; Buse, G.; Mackiewicz, A.; Heinrich, P. C.; Rose-John, S. The soluble interleukin-6 receptor is generated by shedding. Eur. J. Immunol.23:473-480; 1993.

[155] Mackiewicz, A.; Schooltink, H.; Heinrich, P. C.; Rose-John, S. Complex of soluble human IL-6-receptor/IL-6 up-regulates expression of acute-phase proteins. J. Immunol.149:2021-2027; 1992.

[156] Jones, S. A.; Richards, P. J.; Scheller, J.; Rose-John, S. IL-6 transsignaling: The in vivo consequences. J. Interferon Cytokine Res.25:241-253; 2005.

[157] Kang, M.; Park, K. S.; Seo, J. Y.; Kim, H. Lycopene inhibits IL-6 expression in cerulein-stimulated pancreatic acinar cells. Genes Nutr.6:117-123; 2011.

[158] Vaquero, E.; Gukovsky, I.; Zaninovic, V.; Gukovskaya, A. S.; Pandol, S. J. Localized pancreatic NF-kappaB activation and inflammatory response in taurocholate-induced pancreatitis. Am. J. Physiol. Gastrointest. Liver Physiol.280:G1197-208; 2001.

[159] Gukovsky, I.; Gukovskaya, A. S.; Blinman, T. A.; Zaninovic, V.; Pandol, S. J. Early NF-kappaB activation is associated with hormone-induced pancreatitis. Am. J. Physiol.275:G1402-14; 1998.

[160] Yu, J. H.; Kim, K. H.; Kim, H. SOCS 3 and PPAR-gamma ligands inhibit the expression of IL-6 and TGF-beta1 by regulating JAK2/STAT3 signaling in pancreas. Int. J. Biochem. Cell Biol.40:677-688; 2008.

[161] Leser, H. G.; Gross, V.; Scheibenbogen, C.; Heinisch, A.; Salm, R.; Lausen, M.; Ruckauer, K.; Andreesen, R.; Farthmann, E. H.; Scholmerich, J. Elevation of serum interleukin-6 concentration precedes acute-phase response and reflects severity in acute pancreatitis. Gastroenterology101:782-785; 1991.

[162] Viedma, J. A.; Perez-Mateo, M.; Dominguez, J. E.; Carballo, F. Role of interleukin-6 in acute pancreatitis. comparison with C-reactive protein and phospholipase A. Gut33:1264-1267; 1992.

[163] Chao, K. C.; Chao, K. F.; Chuang, C. C.; Liu, S. H. Blockade of interleukin 6 accelerates acinar cell apoptosis and attenuates experimental acute pancreatitis in vivo. Br. J. Surg.93:332-338; 2006.

[164] Chen, K. L.; Lv, Z. Y.; Yang, H. W.; Liu, Y.; Long, F. W.; Zhou, B.; Sun, X. F.; Peng, Z. H.; Zhou, Z. G.; Li, Y. Effects of tocilizumab on experimental severe acute pancreatitis and associated acute lung injury. Crit. Care Med.44:e664-77; 2016.

[165] Zhang, H.; Neuhofer, P.; Song, L.; Rabe, B.; Lesina, M.; Kurkowski, M. U.; Treiber, M.; Wartmann, T.; Regner, S.; Thorlacius, H.; Saur, D.; Weirich, G.; Yoshimura, A.; Halangk, W.; Mizgerd, J. P.; Schmid, R. M.; Rose-John, S.; Algul, H. IL-6 trans-signaling promotes pancreatitis-associated lung injury and lethality. J. Clin. Invest.123:1019-1031; 2013.

[166] Sims, J. E.; Smith, D. E. The IL-1 family: Regulators of immunity. Nat. Rev. Immunol.10:89-102; 2010.

[167] Dinarello, C. A. Overview of the IL-1 family in innate inflammation and acquired immunity. Immunol. Rev.281:8-27; 2018.

[168] Dinarello, C. A.; Renfer, L.; Wolff, S. M. Human leukocytic pyrogen: Purification and development of a radioimmunoassay. Proc. Natl. Acad. Sci. U. S. A.74:4624-4627; 1977.

[169] Martin-Sanchez, F.; Diamond, C.; Zeitler, M.; Gomez, A. I.; Baroja-Mazo, A.; Bagnall, J.; Spiller, D.; White, M.; Daniels, M. J.; Mortellaro, A.; Penalver, M.; Paszek, P.; Steringer, J. P.; Nickel, W.; Brough, D.; Pelegrin, P. Inflammasome-dependent IL-1beta release depends upon membrane permeabilisation. Cell Death Differ.23:1219-1231; 2016.

[170] Latz, E.; Xiao, T. S.; Stutz, A. Activation and regulation of the inflammasomes. Nat. Rev. Immunol.13:397-411; 2013.

[171] Fink, G. W.; Norman, J. G. Specific changes in the pancreatic expression of the interleukin 1 family of genes during experimental acute pancreatitis. Cytokine9:1023-1027; 1997.

[172] Hoque, R.; Sohail, M.; Malik, A.; Sarwar, S.; Luo, Y.; Shah, A.; Barrat, F.; Flavell, R.; Gorelick, F.; Husain, S.; Mehal, W. TLR9 and the NLRP3 inflammasome link acinar cell death with inflammation in acute pancreatitis. Gastroenterology141:358-369; 2011.

[173] Paszkowski, A. S.; Rau, B.; Mayer, J. M.; Moller, P.; Beger, H. G. Therapeutic application of caspase 1/interleukin-1beta-converting enzyme inhibitor decreases the death rate in severe acute experimental pancreatitis. Ann. Surg.235:68-76; 2002.

[174] Criddle, D. N.; Gerasimenko, J. V.; Baumgartner, H. K.; Jaffar, M.; Voronina, S.; Sutton, R.; Petersen, O. H.; Gerasimenko, O. V. Calcium signalling and pancreatic cell death: Apoptosis or necrosis? Cell Death Differ.14:1285-1294; 2007.

[175] Bhatia, M.; Wallig, M. A.; Hofbauer, B.; Lee, H. S.; Frossard, J. L.; Steer, M. L.; Saluja, A. K. Induction of apoptosis in pancreatic acinar cells reduces the severity of acute pancreatitis. Biochem. Biophys. Res. Commun.246:476-483; 1998.

[176] Mareninova, O. A.; Sung, K. F.; Hong, P.; Lugea, A.; Pandol, S. J.; Gukovsky, I.; Gukovskaya, A. S. Cell death in pancreatitis: Caspases protect from necrotizing pancreatitis. J. Biol. Chem.281:3370-3381; 2006.

[177] Kaiser, A. M.; Saluja, A. K.; Sengupta, A.; Saluja, M.; Steer, M. L. Relationship between severity, necrosis, and apoptosis in five models of experimental acute pancreatitis. Am. J. Physiol.269:C1295-304; 1995.

[178] Bhatia, M. Apoptosis versus necrosis in acute pancreatitis. Am. J. Physiol. Gastrointest. Liver Physiol.286:G189-96; 2004.

[179] Ziegler, U.; Groscurth, P. Morphological features of cell death. News Physiol. Sci.19:124-128; 2004.

[180] Reed, J. C. Mechanisms of apoptosis. Am. J. Pathol.157:1415-1430; 2000.

[181] Nhan, T. Q.; Liles, W. C.; Schwartz, S. M. Physiological functions of caspases beyond cell death. Am. J. Pathol.169:729-737; 2006.

[182] Li, J.; Yuan, J. Caspases in apoptosis and beyond. Oncogene27:6194-6206; 2008.

[183] Irmler, M.; Thome, M.; Hahne, M.; Schneider, P.; Hofmann, K.; Steiner, V.; Bodmer, J. L.; Schroter, M.; Burns, K.; Mattmann, C.; Rimoldi, D.; French, L. E.; Tschopp, J. Inhibition of death receptor signals by cellular FLIP. Nature388:190-195; 1997.

[184] Salvesen, G. S.; Duckett, C. S. IAP proteins: Blocking the road to death's door. Nat. Rev. Mol. Cell Biol.3:401-410; 2002.

[185] Bratton, S. B.; Lewis, J.; Butterworth, M.; Duckett, C. S.; Cohen, G. M. XIAP inhibition of caspase-3 preserves its association with the apaf-1 apoptosome and prevents CD95- and bax-induced apoptosis. Cell Death Differ.9:881-892; 2002.

[186] Chai, J.; Shiozaki, E.; Srinivasula, S. M.; Wu, Q.; Datta, P.; Alnemri, E. S.; Shi, Y. Structural basis of caspase-7 inhibition by XIAP. Cell104:769-780; 2001.

[187] Singh, R.; Letai, A.; Sarosiek, K. Regulation of apoptosis in health and disease: The balancing act of BCL-2 family proteins. Nat. Rev. Mol. Cell Biol.20:175-193; 2019.

[188] Reubold, T. F.; Eschenburg, S. A molecular view on signal transduction by the apoptosome. Cell. Signal.24:1420-1425; 2012.

[189] Dorstyn, L.; Akey, C. W.; Kumar, S. New insights into apoptosome structure and function. Cell Death Differ.25:1194-1208; 2018.

[190] Du, C.; Fang, M.; Li, Y.; Li, L.; Wang, X. Smac, a mitochondrial protein that promotes cytochrome c-dependent caspase activation by eliminating IAP inhibition. Cell102:33-42; 2000.

[191] Verhagen, A. M.; Ekert, P. G.; Pakusch, M.; Silke, J.; Connolly, L. M.; Reid, G. E.; Moritz, R. L.; Simpson, R. J.; Vaux, D. L. Identification of DIABLO, a mammalian protein that promotes apoptosis by binding to and antagonizing IAP proteins. Cell102:43-53; 2000.

[192] Suzuki, Y.; Imai, Y.; Nakayama, H.; Takahashi, K.; Takio, K.; Takahashi, R. A serine protease, HtrA2, is released from the mitochondria and interacts with XIAP, inducing cell death. Mol. Cell8:613-621; 2001.

[193] Danial, N. N. BCL-2 family proteins: Critical checkpoints of apoptotic cell death. Clin. Cancer Res.13:7254-7263; 2007.

[194] Huang, D. C.; Strasser, A. BH3-only proteins-essential initiators of apoptotic cell death. Cell103:839-842; 2000.

[195] Wang, C.; Youle, R. J. The role of mitochondria in apoptosis*. Annu. Rev. Genet.43:95-118; 2009.

[196] Hatano, E.; Bradham, C. A.; Stark, A.; Iimuro, Y.; Lemasters, J. J.; Brenner, D. A. The mitochondrial permeability transition augments fas-induced apoptosis in mouse hepatocytes. J. Biol. Chem.275:11814-11823; 2000.

[197] Szalai, G.; Krishnamurthy, R.; Hajnoczky, G. Apoptosis driven by IP(3)-linked mitochondrial calcium signals. Embo J.18:6349-6361; 1999.

[198] Circu, M. L.; Aw, T. Y. Reactive oxygen species, cellular redox systems, and apoptosis. Free Radic. Biol. Med.48:749-762; 2010.

[199] Redza-Dutordoir, M.; Averill-Bates, D. A. Activation of apoptosis signalling pathways by reactive oxygen species. Biochim. Biophys. Acta1863:2977-2992; 2016.

[200] Aubrey, B. J.; Kelly, G. L.; Janic, A.; Herold, M. J.; Strasser, A. How does p53 induce apoptosis and how does this relate to p53-mediated tumour suppression? Cell Death Differ.25:104-113; 2018.

[201] Pietsch, E. C.; Sykes, S. M.; McMahon, S. B.; Murphy, M. E. The p53 family and programmed cell death. Oncogene27:6507-6521; 2008.

[202] Kastenhuber, E. R.; Lowe, S. W. Putting p53 in context. Cell170:1062-1078; 2017.

[203] Vaseva, A. V.; Marchenko, N. D.; Ji, K.; Tsirka, S. E.; Holzmann, S.; Moll, U. M. P53 opens the mitochondrial permeability transition pore to trigger necrosis. Cell149:1536-1548; 2012.

[204] Marchenko, N. D.; Moll, U. M. Mitochondrial death functions of p53. Mol. Cell. Oncol.1:e955995; 2014.

[205] Leu, J. I.; Dumont, P.; Hafey, M.; Murphy, M. E.; George, D. L. Mitochondrial p53 activates bak and causes disruption of a bak-Mcl1 complex. Nat. Cell Biol.6:443-450; 2004.

[206] Pietsch, E. C.; Perchiniak, E.; Canutescu, A. A.; Wang, G.; Dunbrack, R. L.; Murphy, M. E. Oligomerization of BAK by p53 utilizes conserved residues of the p53 DNA binding domain. J. Biol. Chem.283:21294-21304; 2008.

[207] Brooks, C. L.; Gu, W. p53 ubiquitination: Mdm2 and beyond. Mol. Cell21:307-315; 2006.

[208] D'Orazi, G.; Cecchinelli, B.; Bruno, T.; Manni, I.; Higashimoto, Y.; Saito, S.; Gostissa, M.; Coen, S.; Marchetti, A.; Del Sal, G.; Piaggio, G.; Fanciulli, M.; Appella, E.; Soddu, S. Homeodomain-interacting protein kinase-2

phosphorylates p53 at ser 46 and mediates apoptosis. Nat. Cell Biol.4:11-19; 2002.

[209] Hofmann, T. G.; Moller, A.; Sirma, H.; Zentgraf, H.; Taya, Y.; Droge, W.; Will, H.; Schmitz, M. L. Regulation of p53 activity by its interaction with homeodomain-interacting protein kinase-2. Nat. Cell Biol.4:1-10; 2002.

[210] Zacchi, P.; Gostissa, M.; Uchida, T.; Salvagno, C.; Avolio, F.; Volinia, S.; Ronai, Z.; Blandino, G.; Schneider, C.; Del Sal, G. The prolyl isomerase Pin1 reveals a mechanism to control p53 functions after genotoxic insults. Nature419:853-857; 2002.

[211] Marchenko, N. D.; Wolff, S.; Erster, S.; Becker, K.; Moll, U. M. Monoubiquitylation promotes mitochondrial p53 translocation. Embo J.26:923-934; 2007.

[212] Mancini, F.; Di Conza, G.; Pellegrino, M.; Rinaldo, C.; Prodosmo, A.; Giglio, S.; D'Agnano, I.; Florenzano, F.; Felicioni, L.; Buttitta, F.; Marchetti, A.; Sacchi, A.; Pontecorvi, A.; Soddu, S.; Moretti, F. MDM4 (MDMX) localizes at the mitochondria and facilitates the p53-mediated intrinsic-apoptotic pathway. Embo J.28:1926-1939; 2009.

[213] Gukovskaya, A. S.; Gukovsky, I.; Zaninovic, V.; Song, M.; Sandoval, D.; Gukovsky, S.; Pandol, S. J. Pancreatic acinar cells produce, release, and respond to tumor necrosis factor-alpha. role in regulating cell death and pancreatitis. J. Clin. Invest.100:1853-1862; 1997.

[214] Malka, D.; Vasseur, S.; Bodeker, H.; Ortiz, E. M.; Dusetti, N. J.; Verrando, P.; Dagorn, J. C.; Iovanna, J. L. Tumor necrosis factor alpha triggers antiapoptotic mechanisms in rat pancreatic cells through pancreatitis-associated protein I activation. Gastroenterology119:816-828; 2000.

[215] Karin, M.; Lin, A. NF-kappaB at the crossroads of life and death. Nat. Immunol.3:221-227; 2002.

[216] Shigekawa, M.; Hikita, H.; Kodama, T.; Shimizu, S.; Li, W.; Uemura, A.; Miyagi, T.; Hosui, A.; Kanto, T.; Hiramatsu, N.; Tatsumi, T.; Takeda, K.; Akira, S.;

Takehara, T. Pancreatic STAT3 protects mice against caerulein-induced pancreatitis via PAP1 induction. Am. J. Pathol.181:2105-2113; 2012.

[217] Yuan, J.; Liu, Y.; Tan, T.; Guha, S.; Gukovsky, I.; Gukovskaya, A.; Pandol, S. J. Protein kinase d regulates cell death pathways in experimental pancreatitis. Front. Physiol.3:60; 2012.

[218] Liu, Y.; Chen, X. D.; Yu, J.; Chi, J. L.; Long, F. W.; Yang, H. W.; Chen, K. L.; Lv, Z. Y.; Zhou, B.; Peng, Z. H.; Sun, X. F.; Li, Y.; Zhou, Z. G. Deletion of XIAP reduces the severity of acute pancreatitis via regulation of cell death and nuclear factor-kappaB activity. Cell. Death Dis.8:e2685; 2017.

[219] Kim, J. S.; He, L.; Lemasters, J. J. Mitochondrial permeability transition: A common pathway to necrosis and apoptosis. Biochem. Biophys. Res. Commun.304:463-470; 2003.

[220] Zong, W. X.; Thompson, C. B. Necrotic death as a cell fate. Genes Dev.20:1-15; 2006.

[221] Karch, J.; Molkentin, J. D. Regulated necrotic cell death: The passive aggressive side of bax and bak. Circ. Res.116:1800-1809; 2015.

[222] Kroemer, G.; Galluzzi, L.; Brenner, C. Mitochondrial membrane permeabilization in cell death. Physiol. Rev.87:99-163; 2007.

[223] Chalmers, S.; Nicholls, D. G. The relationship between free and total calcium concentrations in the matrix of liver and brain mitochondria. J. Biol. Chem.278:19062-19070; 2003.

[224] Batandier, C.; Leverve, X.; Fontaine, E. Opening of the mitochondrial permeability transition pore induces reactive oxygen species production at the level of the respiratory chain complex I. J. Biol. Chem.279:17197-17204; 2004.

[225] Daiber, A. Redox signaling (cross-talk) from and to mitochondria involves mitochondrial pores and reactive oxygen species. Biochim. Biophys. Acta1797:897-906; 2010.

[226] Sung, K. F.; Odinokova, I. V.; Mareninova, O. A.; Rakonczay, Z.,Jr; Hegyi, P.; Pandol, S. J.; Gukovsky, I.; Gukovskaya, A. S. Prosurvival bcl-2 proteins stabilize pancreatic mitochondria and protect against necrosis in experimental pancreatitis. Exp. Cell Res.315:1975-1989; 2009.

[227] Voronina, S. G.; Barrow, S. L.; Simpson, A. W.; Gerasimenko, O. V.; da Silva Xavier, G.; Rutter, G. A.; Petersen, O. H.; Tepikin, A. V. Dynamic changes in cytosolic and mitochondrial ATP levels in pancreatic acinar cells. Gastroenterology138:1976-1987; 2010.

[228] Voronina, S. G.; Barrow, S. L.; Gerasimenko, O. V.; Petersen, O. H.; Tepikin, A. V. Effects of secretagogues and bile acids on mitochondrial membrane potential of pancreatic acinar cells: Comparison of different modes of evaluating DeltaPsim. J. Biol. Chem.279:27327-27338; 2004.

[229] Mukherjee, R.; Mareninova, O. A.; Odinokova, I. V.; Huang, W.; Murphy, J.; Chvanov, M.; Javed, M. A.; Wen, L.; Booth, D. M.; Cane, M. C.; Awais, M.; Gavillet, B.; Pruss, R. M.; Schaller, S.; Molkentin, J. D.; Tepikin, A. V.; Petersen, O. H.; Pandol, S. J.; Gukovsky, I.; Criddle, D. N.; Gukovskaya, A. S.; Sutton, R.; NIHR Pancreas Biomedical Research Unit. Mechanism of mitochondrial permeability transition pore induction and damage in the pancreas: Inhibition prevents acute pancreatitis by protecting production of ATP. Gut65:1333-1346; 2016.

[230] Toth, E.; Maleth, J.; Zavogyan, N.; Fanczal, J.; Grassalkovich, A.; Erdos, R.; Pallagi, P.; Horvath, G.; Tretter, L.; Balint, E. R.; Rakonczay, Z.,Jr; Venglovecz, V.; Hegyi, P. Novel mitochondrial transition pore inhibitor N-methyl-4-isoleucine cyclosporin is a new therapeutic option in acute pancreatitis. J. Physiol.597:5879-5898; 2019.

[231] Gukovskaya, A. S.; Gukovsky, I.; Jung, Y.; Mouria, M.; Pandol, S. J. Cholecystokinin induces caspase activation and mitochondrial dysfunction in pancreatic acinar cells. roles in cell injury processes of pancreatitis. J. Biol. Chem.277:22595-22604; 2002.

[232] Odinokova, I. V.; Sung, K. F.; Mareninova, O. A.; Hermann, K.; Evtodienko, Y.; Andreyev, A.; Gukovsky, I.; Gukovskaya, A. S. Mechanisms regulating cytochrome c release in pancreatic mitochondria. Gut58:431-442; 2009.

[233] Baumgartner, H. K.; Gerasimenko, J. V.; Thorne, C.; Ferdek, P.; Pozzan, T.; Tepikin, A. V.; Petersen, O. H.; Sutton, R.; Watson, A. J.; Gerasimenko, O. V. Calcium elevation in mitochondria is the main Ca2+ requirement for mitochondrial permeability transition pore (mPTP) opening. J. Biol. Chem.284:20796-20803; 2009.

[234] Gerasimenko, J. V.; Gerasimenko, O. V.; Petersen, O. H. The role of Ca2+ in the pathophysiology of pancreatitis. J. Physiol.592:269-280; 2014.

[235] Mukherjee, R.; Mareninova, O. A.; Odinokova, I. V.; Huang, W.; Murphy, J.; Chvanov, M.; Javed, M. A.; Wen, L.; Booth, D. M.; Cane, M. C.; Awais, M.; Gavillet, B.; Pruss, R. M.; Schaller, S.; Molkentin, J. D.; Tepikin, A. V.; Petersen, O. H.; Pandol, S. J.; Gukovsky, I.; Criddle, D. N.; Gukovskaya, A. S.; Sutton, R.; NIHR Pancreas Biomedical Research Unit. Mechanism of mitochondrial permeability transition pore induction and damage in the pancreas: Inhibition prevents acute pancreatitis by protecting production of ATP. Gut65:1333-1346; 2016.

[236] Booth, D. M.; Murphy, J. A.; Mukherjee, R.; Awais, M.; Neoptolemos, J. P.; Gerasimenko, O. V.; Tepikin, A. V.; Petersen, O. H.; Sutton, R.; Criddle, D. N. Reactive oxygen species induced by bile acid induce apoptosis and protect against necrosis in pancreatic acinar cells. Gastroenterology140:2116-2125; 2011.

[237] Armstrong, J. A.; Cash, N. J.; Ouyang, Y.; Morton, J. C.; Chvanov, M.; Latawiec, D.; Awais, M.; Tepikin, A. V.; Sutton, R.; Criddle, D. N. Oxidative stress alters mitochondrial bioenergetics and modifies pancreatic cell death independently of cyclophilin D, resulting in an apoptosis-to-necrosis shift. J. Biol. Chem.293:8032-8047; 2018.

[238] Hitomi, J.; Christofferson, D. E.; Ng, A.; Yao, J.; Degterev, A.; Xavier, R. J.; Yuan, J. Identification of a molecular signaling network that regulates a cellular necrotic cell death pathway. Cell135:1311-1323; 2008.

[239] Vanden Berghe, T.; Vanlangenakker, N.; Parthoens, E.; Deckers, W.; Devos, M.; Festjens, N.; Guerin, C. J.; Brunk, U. T.; Declercq, W.; Vandenabeele, P. Necroptosis, necrosis and secondary necrosis converge on similar cellular disintegration features. Cell Death Differ.17:922-930; 2010.

[240] Feoktistova, M.; Leverkus, M. Programmed necrosis and necroptosis signalling. Febs J.282:19-31; 2015.

[241] Vanden Berghe, T.; Linkermann, A.; Jouan-Lanhouet, S.; Walczak, H.; Vandenabeele, P. Regulated necrosis: The expanding network of non-apoptotic cell death pathways. Nat. Rev. Mol. Cell Biol.15:135-147; 2014.

[242] Choi, M. E.; Price, D. R.; Ryter, S. W.; Choi, A. M. K. Necroptosis: A crucial pathogenic mediator of human disease. JCI Insight4:10.1172/jci.insight.128834. eCollection 2019 Aug 8; 2019.

[243] Newton, K.; Manning, G. Necroptosis and inflammation. Annu. Rev. Biochem.85:743-763; 2016.

[244] Weinlich, R.; Oberst, A.; Beere, H. M.; Green, D. R. Necroptosis in development, inflammation and disease. Nat. Rev. Mol. Cell Biol.18:127-136; 2017.

[245] Wang, G.; Qu, F. Z.; Li, L.; Lv, J. C.; Sun, B. Necroptosis: A potential, promising target and switch in acute pancreatitis. Apoptosis21:121-129; 2016.

[246] Khoury, M. K.; Gupta, K.; Franco, S. R.; Liu, B. Necroptosis in the pathophysiology of disease. Am. J. Pathol.190:272-285; 2020.

[247] Vercammen, D.; Beyaert, R.; Denecker, G.; Goossens, V.; Van Loo, G.; Declercq, W.; Grooten, J.; Fiers, W.; Vandenabeele, P. Inhibition of caspases increases the sensitivity of L929 cells to necrosis mediated by tumor necrosis factor. J. Exp. Med.187:1477-1485; 1998.

[248] Holler, N.; Zaru, R.; Micheau, O.; Thome, M.; Attinger, A.; Valitutti, S.; Bodmer, J. L.; Schneider, P.; Seed, B.; Tschopp, J. Fas triggers an alternative, caspase-8-independent cell death pathway using the kinase RIP as effector molecule. Nat. Immunol.1:489-495; 2000.

[249] Linkermann, A.; Green, D. R. Necroptosis. N. Engl. J. Med.370:455-465; 2014.

[250] Wegner, K. W.; Saleh, D.; Degterev, A. Complex pathologic roles of RIPK1 and RIPK3: Moving beyond necroptosis. Trends Pharmacol. Sci.38:202-225; 2017.

[251] Oberst, A.; Dillon, C. P.; Weinlich, R.; McCormick, L. L.; Fitzgerald, P.; Pop, C.; Hakem, R.; Salvesen, G. S.; Green, D. R. Catalytic activity of the caspase-8-FLIP(L) complex inhibits RIPK3-dependent necrosis. Nature471:363-367; 2011.

[252] Newton, K.; Wickliffe, K. E.; Dugger, D. L.; Maltzman, A.; Roose-Girma, M.; Dohse, M.; Komuves, L.; Webster, J. D.; Dixit, V. M. Cleavage of RIPK1 by caspase-8 is crucial for limiting apoptosis and necroptosis. Nature574:428-431; 2019.

[253] He, S.; Wang, L.; Miao, L.; Wang, T.; Du, F.; Zhao, L.; Wang, X. Receptor interacting protein kinase-3 determines cellular necrotic response to TNF-alpha. Cell137:1100-1111; 2009.

[254] Wang, H.; Sun, L.; Su, L.; Rizo, J.; Liu, L.; Wang, L. F.; Wang, F. S.; Wang, X. Mixed lineage kinase domain-like protein MLKL causes necrotic membrane disruption upon phosphorylation by RIP3. Mol. Cell54:133-146; 2014.

[255] Cai, Z.; Jitkaew, S.; Zhao, J.; Chiang, H. C.; Choksi, S.; Liu, J.; Ward, Y.; Wu, L. G.; Liu, Z. G. Plasma membrane translocation of trimerized MLKL protein is required for TNF-induced necroptosis. Nat. Cell Biol.16:55-65; 2014.

[256] Dondelinger, Y.; Declercq, W.; Montessuit, S.; Roelandt, R.; Goncalves, A.; Bruggeman, I.; Hulpiau, P.; Weber, K.; Sehon, C. A.; Marquis, R. W.; Bertin, J.; Gough, P. J.; Savvides, S.; Martinou, J. C.; Bertrand, M. J.; Vandenabeele, P. MLKL compromises plasma membrane integrity by binding to phosphatidylinositol phosphates. Cell. Rep.7:971-981; 2014.

[257] Marshall, K. D.; Baines, C. P. Necroptosis: Is there a role for mitochondria? Front. Physiol.5:323; 2014.

[258] Vanlangenakker, N.; Vanden Berghe, T.; Bogaert, P.; Laukens, B.; Zobel, K.; Deshayes, K.; Vucic, D.; Fulda, S.; Vandenabeele, P.; Bertrand, M. J. cIAP1 and TAK1 protect cells from TNF-induced necrosis by preventing RIP1/RIP3-dependent reactive oxygen species production. Cell Death Differ.18:656-665; 2011.

[259] Davis, C. W.; Hawkins, B. J.; Ramasamy, S.; Irrinki, K. M.; Cameron, B. A.; Islam, K.; Daswani, V. P.; Doonan, P. J.; Manevich, Y.; Madesh, M. Nitration of the mitochondrial complex I subunit NDUFB8 elicits RIP1- and RIP3-mediated necrosis. Free Radic. Biol. Med.48:306-317; 2010.

[260] Zhang, Y.; Su, S. S.; Zhao, S.; Yang, Z.; Zhong, C. Q.; Chen, X.; Cai, Q.; Yang, Z. H.; Huang, D.; Wu, R.; Han, J. RIP1 autophosphorylation is promoted by mitochondrial ROS and is essential for RIP3 recruitment into necrosome. Nat. Commun.8:14329; 2017.

[261] Zhu, P.; Hu, S.; Jin, Q.; Li, D.; Tian, F.; Toan, S.; Li, Y.; Zhou, H.; Chen, Y. Ripk3 promotes ER stress-induced necroptosis in cardiac IR injury: A mechanism involving calcium overload/XO/ROS/mPTP pathway. Redox Biol.16:157-168; 2018.

[262] Wang, Z.; Jiang, H.; Chen, S.; Du, F.; Wang, X. The mitochondrial phosphatase PGAM5 functions at the convergence point of multiple necrotic death pathways. Cell148:228-243; 2012.

[263] Zhang, L.; Jiang, F.; Chen, Y.; Luo, J.; Liu, S.; Zhang, B.; Ye, Z.; Wang, W.; Liang, X.; Shi, W. Necrostatin-1 attenuates ischemia injury induced cell death in rat tubular cell line NRK-52E through decreased Drp1 expression. Int. J. Mol. Sci.14:24742-24754; 2013.

[264] Zhang, S.; Che, L.; He, C.; Huang, J.; Guo, N.; Shi, J.; Lin, Y.; Lin, Z. Drp1 and RB interaction to mediate mitochondria-dependent necroptosis induced by cadmium in hepatocytes. Cell. Death Dis.10:523-019-1730-y; 2019.

[265] Tait, S. W.; Oberst, A.; Quarato, G.; Milasta, S.; Haller, M.; Wang, R.; Karvela, M.; Ichim, G.; Yatim, N.; Albert, M. L.; Kidd, G.; Wakefield, R.; Frase, S.; Krautwald, S.; Linkermann, A.; Green, D. R. Widespread mitochondrial

depletion via mitophagy does not compromise necroptosis. Cell. Rep.5:878-885; 2013.

[266] Murphy, J. M.; Czabotar, P. E.; Hildebrand, J. M.; Lucet, I. S.; Zhang, J. G.; Alvarez-Diaz, S.; Lewis, R.; Lalaoui, N.; Metcalf, D.; Webb, A. I.; Young, S. N.; Varghese, L. N.; Tannahill, G. M.; Hatchell, E. C.; Majewski, I. J.; Okamoto, T.; Dobson, R. C.; Hilton, D. J.; Babon, J. J.; Nicola, N. A.; Strasser, A.; Silke, J.; Alexander, W. S. The pseudokinase MLKL mediates necroptosis via a molecular switch mechanism. Immunity39:443-453; 2013.

[267] Remijsen, Q.; Goossens, V.; Grootjans, S.; Van den Haute, C.; Vanlangenakker, N.; Dondelinger, Y.; Roelandt, R.; Bruggeman, I.; Goncalves, A.; Bertrand, M. J.; Baekelandt, V.; Takahashi, N.; Berghe, T. V.; Vandenabeele, P. Depletion of RIPK3 or MLKL blocks TNF-driven necroptosis and switches towards a delayed RIPK1 kinase-dependent apoptosis. Cell. Death Dis.5:e1004; 2014.

[268] Moujalled, D. M.; Cook, W. D.; Murphy, J. M.; Vaux, D. L. Necroptosis induced by RIPK3 requires MLKL but not Drp1. Cell. Death Dis.5:e1086; 2014.

[269] Linkermann, A.; Brasen, J. H.; Darding, M.; Jin, M. K.; Sanz, A. B.; Heller, J. O.; De Zen, F.; Weinlich, R.; Ortiz, A.; Walczak, H.; Weinberg, J. M.; Green, D. R.; Kunzendorf, U.; Krautwald, S. Two independent pathways of regulated necrosis mediate ischemia-reperfusion injury. Proc. Natl. Acad. Sci. U. S. A.110:12024-12029; 2013.

[270] Wu, J.; Huang, Z.; Ren, J.; Zhang, Z.; He, P.; Li, Y.; Ma, J.; Chen, W.; Zhang, Y.; Zhou, X.; Yang, Z.; Wu, S. Q.; Chen, L.; Han, J. Mlkl knockout mice demonstrate the indispensable role of mlkl in necroptosis. Cell Res.23:994-1006; 2013.

[271] Linkermann, A.; Brasen, J. H.; De Zen, F.; Weinlich, R.; Schwendener, R. A.; Green, D. R.; Kunzendorf, U.; Krautwald, S. Dichotomy between RIP1- and RIP3-mediated necroptosis in tumor necrosis factor-alpha-induced shock. Mol. Med.18:577-586; 2012.

[272] Ma, X.; Conklin, D. J.; Li, F.; Dai, Z.; Hua, X.; Li, Y.; Xu-Monette, Z. Y.; Young, K. H.; Xiong, W.; Wysoczynski, M.; Sithu, S. D.; Srivastava, S.; Bhatnagar, A.;

Li, Y. The oncogenic microRNA miR-21 promotes regulated necrosis in mice. Nat. Commun.6:7151; 2015.

[273] Sies H. On the history of oxidative stress: Concept and some aspects of current development. Current Opinion in Toxicology 2018 February 2018;7:122-126.

[274] Schieber, M.; Chandel, N. ROS function in redox signaling and oxidative stress. Current Biology24:R45-R462; 2014.

[275] Jones, D. P. Redefining oxidative stress. Antioxidants & Redox Signaling8:1865-1879; 2006.

[276] Sies, H. Oxidative stress: A concept in redox biology and medicine. Redox Biol.4:180-183; 2015.

[277] Niki, E. Oxidative stress and antioxidants: Distress or eustress? Arch. Biochem. Biophys.595:19-24; 2016.

[278] Sies, H. Hydrogen peroxide as a central redox signaling molecule in physiological oxidative stress: Oxidative eustress. Redox Biol.11:613-619; 2017.

[279] Valko, M.; Leibfritz, D.; Moncol, J.; Cronin, M. T.; Mazur, M.; Telser, J. Free radicals and antioxidants in normal physiological functions and human disease. Int. J. Biochem. Cell Biol.39:44-84; 2007.

[280] Droge, W. Free radicals in the physiological control of cell function. Physiol. Rev.82:47-95; 2002.

[281] Jones, D. P. Radical-free biology of oxidative stress. Am. J. Physiol. Cell. Physiol.295:C849-68; 2008.

[282] Leung, P. S.; Chan, Y. C. Role of oxidative stress in pancreatic inflammation. Antioxid. Redox Signal.11:135-165; 2009.

[283] Valko, M.; Leibfritz, D.; Moncol, J.; Cronin, M. T.; Mazur, M.; Telser, J. Free radicals and antioxidants in normal physiological functions and human disease. Int. J. Biochem. Cell Biol.39:44-84; 2007.

[284] Brand, M. D. Mitochondrial generation of superoxide and hydrogen peroxide as the source of mitochondrial redox signaling. Free Radic. Biol. Med.100:14-31; 2016.

[285] Brand, M. D.; Affourtit, C.; Esteves, T. C.; Green, K.; Lambert, A. J.; Miwa, S.; Pakay, J. L.; Parker, N. Mitochondrial superoxide: Production, biological effects, and activation of uncoupling proteins. Free Radic. Biol. Med.37:755-767; 2004.

[286] Di Meo, S.; Reed, T. T.; Venditti, P.; Victor, V. M. Role of ROS and RNS sources in physiological and pathological conditions. Oxid Med. Cell. Longev2016:1245049; 2016.

[287] Paravicini, T. M.; Touyz, R. M. NADPH oxidases, reactive oxygen species, and hypertension: Clinical implications and therapeutic possibilities. Diabetes Care31 Suppl 2:S170-80; 2008.

[288] Bedard, K.; Krause, K. H. The NOX family of ROS-generating NADPH oxidases: Physiology and pathophysiology. Physiol. Rev.87:245-313; 2007.

[289] Brandes, R. P.; Weissmann, N.; Schroder, K. Nox family NADPH oxidases: Molecular mechanisms of activation. Free Radic. Biol. Med.76:208-226; 2014.

[290] Valko, M.; Leibfritz, D.; Moncol, J.; Cronin, M. T.; Mazur, M.; Telser, J. Free radicals and antioxidants in normal physiological functions and human disease. Int. J. Biochem. Cell Biol.39:44-84; 2007.

[291] Kalyanaraman, B. Teaching the basics of redox biology to medical and graduate students: Oxidants, antioxidants and disease mechanisms. Redox Biol.1:244-257; 2013.

[292] Fukai, T.; Ushio-Fukai, M. Superoxide dismutases: Role in redox signaling, vascular function, and diseases. Antioxid. Redox Signal.15:1583-1606; 2011.

[293] De Deken, X.; Corvilain, B.; Dumont, J. E.; Miot, F. Roles of DUOX-mediated hydrogen peroxide in metabolism, host defense, and signaling. Antioxid. Redox Signal.20:2776-2793; 2014.

[294] Hauptmann, N.; Grimsby, J.; Shih, J. C.; Cadenas, E. The metabolism of tyramine by monoamine oxidase A/B causes oxidative damage to mitochondrial DNA. Arch. Biochem. Biophys.335:295-304; 1996.

[295] Hey-Mogensen, M.; Goncalves, R. L.; Orr, A. L.; Brand, M. D. Production of superoxide/H2O2 by dihydroorotate dehydrogenase in rat skeletal muscle mitochondria. Free Radic. Biol. Med.72:149-155; 2014.

[296] Quinlan, C. L.; Perevoshchikova, I. V.; Hey-Mogensen, M.; Orr, A. L.; Brand, M. D. Sites of reactive oxygen species generation by mitochondria oxidizing different substrates. Redox Biol.1:304-312; 2013.

[297] Starkov, A. A.; Fiskum, G.; Chinopoulos, C.; Lorenzo, B. J.; Browne, S. E.; Patel, M. S.; Beal, M. F. Mitochondrial alpha-ketoglutarate dehydrogenase complex generates reactive oxygen species. J. Neurosci.24:7779-7788; 2004.

[298] Lipinski, B. Hydroxyl radical and its scavengers in health and disease. Oxid Med. Cell. Longev2011:809696; 2011.

[299] Aquilano, K.; Baldelli, S.; Ciriolo, M. R. Glutathione: New roles in redox signaling for an old antioxidant. Front. Pharmacol.5:196; 2014.

[300] Lu, S. C. Regulation of glutathione synthesis. Mol. Aspects Med.30:42-59; 2009.

[301] Lushchak, V. I. Glutathione homeostasis and functions: Potential targets for medical interventions. J. Amino Acids2012:736837; 2012.

[302] Lievers, K. J.; Kluijtmans, L. A.; Blom, H. J. Genetics of hyperhomocysteinaemia in cardiovascular disease. Ann. Clin. Biochem.40:46-59; 2003.

[303] Zhang, H.; Forman, H. J. Glutathione synthesis and its role in redox signaling. Semin. Cell Dev. Biol.23:722-728; 2012.

[304] Perez, S.; Pereda, J.; Sabater, L.; Sastre, J. Redox signaling in acute pancreatitis. Redox Biol.5:1-14; 2015.

[305] Ren, X.; Zou, L.; Zhang, X.; Branco, V.; Wang, J.; Carvalho, C.; Holmgren, A.; Lu, J. Redox signaling mediated by thioredoxin and glutathione systems in the central nervous system. Antioxid. Redox Signal.27:989-1010; 2017.

[306] Martinov, M. V.; Vitvitsky, V. M.; Banerjee, R.; Ataullakhanov, F. I. The logic of the hepatic methionine metabolic cycle. Biochim. Biophys. Acta1804:89-96; 2010.

[307] Tavares, C. D.; Sharabi, K.; Dominy, J. E.; Lee, Y.; Isasa, M.; Orozco, J. M.; Jedrychowski, M. P.; Kamenecka, T. M.; Griffin, P. R.; Gygi, S. P.; Puigserver, P. The methionine transamination pathway controls hepatic glucose metabolism through regulation of the GCN5 acetyltransferase and the PGC-1alpha transcriptional coactivator. J. Biol. Chem.291:10635-10645; 2016.

[308] Pajares, M. A.; Perez-Sala, D. Mammalian sulfur amino acid metabolism: A nexus between redox regulation, nutrition, epigenetics, and detoxification. Antioxid. Redox Signal.29:408-452; 2018.

[309] Thomas, D.; Becker, A.; Surdin-Kerjan, Y. Reverse methionine biosynthesis from S-adenosylmethionine in eukaryotic cells. J. Biol. Chem.275:40718-40724; 2000.

[310] Lu, S. C.; Mato, J. M. S-adenosylmethionine in liver health, injury, and cancer. Physiol. Rev.92:1515-1542; 2012.

[311] Soda, K. Polyamine metabolism and gene methylation in conjunction with one-carbon metabolism. Int. J. Mol. Sci.19:3106. doi: 10.3390/ijms19103106. eCollection 2018 Oct; 2018.

[312] Danese, S.; Sgambato, A.; Papa, A.; Scaldaferri, F.; Pola, R.; Sans, M.; Lovecchio, M.; Gasbarrini, G.; Cittadini, A.; Gasbarrini, A. Homocysteine triggers mucosal microvascular activation in inflammatory bowel disease. Am. J. Gastroenterol.100:886-895; 2005.

[313] Chowers, Y.; Sela, B. A.; Holland, R.; Fidder, H.; Simoni, F. B.; Bar-Meir, S. Increased levels of homocysteine in patients with crohn's disease are related to folate levels. Am. J. Gastroenterol.95:3498-3502; 2000.

[314] Shiao, S. P. K.; Lie, A.; Yu, C. H. Meta-analysis of homocysteine-related factors on the risk of colorectal cancer. Oncotarget9:25681-25697; 2018.

[315] Rahman, S. H.; Srinivasan, A. R.; Nicolaou, A. Transsulfuration pathway defects and increased glutathione degradation in severe acute pancreatitis. Dig. Dis. Sci.54:675-682; 2009.

[316] Sbodio, J. I.; Snyder, S. H.; Paul, B. D. Regulators of the transsulfuration pathway. Br. J. Pharmacol.176:583-593; 2019.

[317] Majtan, T.; Freeman, K. M.; Smith, A. T.; Burstyn, J. N.; Kraus, J. P. Purification and characterization of cystathionine beta-synthase bearing a cobalt protoporphyrin. Arch. Biochem. Biophys.508:25-30; 2011.

[318] Meier, M.; Janosik, M.; Kery, V.; Kraus, J. P.; Burkhard, P. Structure of human cystathionine beta-synthase: A unique pyridoxal 5'-phosphate-dependent heme protein. Embo J.20:3910-3916; 2001.

[319] Kery, V.; Poneleit, L.; Meyer, J. D.; Manning, M. C.; Kraus, J. P. Binding of pyridoxal 5'-phosphate to the heme protein human cystathionine beta-synthase. Biochemistry38:2716-2724; 1999.

[320] Banerjee, R.; Evande, R.; Kabil, O.; Ojha, S.; Taoka, S. Reaction mechanism and regulation of cystathionine beta-synthase. Biochim. Biophys. Acta1647:30-35; 2003.

[321] Ereno-Orbea, J.; Majtan, T.; Oyenarte, I.; Kraus, J. P.; Martinez-Cruz, L. A. Structural insight into the molecular mechanism of allosteric activation of

human cystathionine beta-synthase by S-adenosylmethionine. Proc. Natl. Acad. Sci. U. S. A.111:E3845-52; 2014.

[322] Prudova, A.; Bauman, Z.; Braun, A.; Vitvitsky, V.; Lu, S. C.; Banerjee, R. S-adenosylmethionine stabilizes cystathionine beta-synthase and modulates redox capacity. Proc. Natl. Acad. Sci. U. S. A.103:6489-6494; 2006.

[323] Taoka, S.; West, M.; Banerjee, R. Characterization of the heme and pyridoxal phosphate cofactors of human cystathionine beta-synthase reveals nonequivalent active sites. Biochemistry38:2738-2744; 1999.

[324] Puranik, M.; Weeks, C. L.; Lahaye, D.; Kabil, O.; Taoka, S.; Nielsen, S. B.; Groves, J. T.; Banerjee, R.; Spiro, T. G. Dynamics of carbon monoxide binding to cystathionine beta-synthase. J. Biol. Chem.281:13433-13438; 2006.

[325] Taoka, S.; Banerjee, R. Characterization of NO binding to human cystathionine beta-synthase: Possible implications of the effects of CO and NO binding to the human enzyme. J. Inorg. Biochem.87:245-251; 2001.

[326] Vicente, J. B.; Colaco, H. G.; Mendes, M. I.; Sarti, P.; Leandro, P.; Giuffre, A. NO* binds human cystathionine beta-synthase quickly and tightly. J. Biol. Chem.289:8579-8587; 2014.

[327] Taoka, S.; Ohja, S.; Shan, X.; Kruger, W. D.; Banerjee, R. Evidence for heme-mediated redox regulation of human cystathionine beta-synthase activity. J. Biol. Chem.273:25179-25184; 1998.

[328] Niu, W.; Wang, J.; Qian, J.; Wang, M.; Wu, P.; Chen, F.; Yan, S. Allosteric control of human cystathionine beta-synthase activity by a redox active disulfide bond. J. Biol. Chem.293:2523-2533; 2018.

[329] Wang, H.; Sun, Q.; Zhou, Y.; Zhang, H.; Luo, C.; Xu, J.; Dong, Y.; Wu, Y.; Liu, H.; Wang, W. Nitration-mediated deficiency of cystathionine beta-synthase activity accelerates the progression of hyperhomocysteinemia. Free Radic. Biol. Med.113:519-529; 2017.

[330] Sun, Q.; Collins, R.; Huang, S.; Holmberg-Schiavone, L.; Anand, G. S.; Tan, C. H.; van-den-Berg, S.; Deng, L. W.; Moore, P. K.; Karlberg, T.; Sivaraman, J.

Structural basis for the inhibition mechanism of human cystathionine gamma-lyase, an enzyme responsible for the production of H(2)S. J. Biol. Chem.284:3076-3085; 2009.

[331] Garcia-Garcia, A.; Zavala-Flores, L.; Rodriguez-Rocha, H.; Franco, R. Thiol-redox signaling, dopaminergic cell death, and parkinson's disease. Antioxid. Redox Signal.17:1764-1784; 2012.

[332] Bolduc, J. A.; Nelson, K. J.; Haynes, A. C.; Lee, J.; Reisz, J. A.; Graff, A. H.; Clodfelter, J. E.; Parsonage, D.; Poole, L. B.; Furdui, C. M.; Lowther, W. T. Novel hyperoxidation resistance motifs in 2-cys peroxiredoxins. J. Biol. Chem.293:11901-11912; 2018.

[333] Rhee, S. G.; Kil, I. S. Multiple functions and regulation of mammalian peroxiredoxins. Annu. Rev. Biochem.86:749-775; 2017.

[334] Cox, A. G.; Pearson, A. G.; Pullar, J. M.; Jonsson, T. J.; Lowther, W. T.; Winterbourn, C. C.; Hampton, M. B. Mitochondrial peroxiredoxin 3 is more resilient to hyperoxidation than cytoplasmic peroxiredoxins. Biochem. J.421:51-58; 2009.

[335] Sun, Y.; Hegamyer, G.; Colburn, N. H. Molecular cloning of five messenger RNAs differentially expressed in preneoplastic or neoplastic JB6 mouse epidermal cells: One is homologous to human tissue inhibitor of metalloproteinases-3. Cancer Res.54:1139-1144; 1994.

[336] Lim, J. C.; Choi, H. I.; Park, Y. S.; Nam, H. W.; Woo, H. A.; Kwon, K. S.; Kim, Y. S.; Rhee, S. G.; Kim, K.; Chae, H. Z. Irreversible oxidation of the active-site cysteine of peroxiredoxin to cysteine sulfonic acid for enhanced molecular chaperone activity. J. Biol. Chem.283:28873-28880; 2008.

[337] Biteau, B.; Labarre, J.; Toledano, M. B. ATP-dependent reduction of cysteine-sulphinic acid by S. cerevisiae sulphiredoxin. Nature425:980-984; 2003.

[338] Rhee, S. G.; Jeong, W.; Chang, T. S.; Woo, H. A. Sulfiredoxin, the cysteine sulfinic acid reductase specific to 2-cys peroxiredoxin: Its discovery, mechanism of action, and biological significance. Kidney Int. Suppl.(106):S3-8. doi:S3-8; 2007.

[339] Peskin, A. V.; Dickerhof, N.; Poynton, R. A.; Paton, L. N.; Pace, P. E.; Hampton, M. B.; Winterbourn, C. C. Hyperoxidation of peroxiredoxins 2 and 3: Rate constants for the reactions of the sulfenic acid of the peroxidatic cysteine. J. Biol. Chem.288:14170-14177; 2013.

[340] Rhee, S. G. Overview on peroxiredoxin. Mol. Cells39:1-5; 2016.

[341] Biteau, B.; Labarre, J.; Toledano, M. B. ATP-dependent reduction of cysteine-sulphinic acid by S. cerevisiae sulphiredoxin. Nature425:980-984; 2003.

[342] Ramesh, A.; Varghese, S. S.; Doraiswamy, J.; Malaiappan, S. Role of sulfiredoxin in systemic diseases influenced by oxidative stress. Redox Biol.2:1023-1028; 2014.

[343] Perkins, A.; Nelson, K. J.; Parsonage, D.; Poole, L. B.; Karplus, P. A. Peroxiredoxins: Guardians against oxidative stress and modulators of peroxide signaling. Trends Biochem. Sci.40:435-445; 2015.

[344] Lowther, W. T.; Haynes, A. C. Reduction of cysteine sulfinic acid in eukaryotic, typical 2-cys peroxiredoxins by sulfiredoxin. Antioxid. Redox Signal.15:99-109; 2011.

[345] Lei, K.; Townsend, D. M.; Tew, K. D. Protein cysteine sulfinic acid reductase (sulfiredoxin) as a regulator of cell proliferation and drug response. Oncogene27:4877-4887; 2008.

[346] Rhee, S. G.; Kil, I. S. Mitochondrial H2O2 signaling is controlled by the concerted action of peroxiredoxin III and sulfiredoxin: Linking mitochondrial function to circadian rhythm. Free Radic. Biol. Med.100:73-80; 2016.

[347] Cao, X.; Ding, L.; Xie, Z. Z.; Yang, Y.; Whiteman, M.; Moore, P. K.; Bian, J. S. A review of hydrogen sulfide synthesis, metabolism, and measurement: Is modulation of hydrogen sulfide a novel therapeutic for cancer? Antioxid. Redox Signal.31:1-38; 2019.

[348] Jang, H. H.; Lee, K. O.; Chi, Y. H.; Jung, B. G.; Park, S. K.; Park, J. H.; Lee, J. R.; Lee, S. S.; Moon, J. C.; Yun, J. W.; Choi, Y. O.; Kim, W. Y.; Kang, J. S.; Cheong, G. W.; Yun, D. J.; Rhee, S. G.; Cho, M. J.; Lee, S. Y. Two enzymes in one; two

yeast peroxiredoxins display oxidative stress-dependent switching from a peroxidase to a molecular chaperone function. Cell117:625-635; 2004.

[349] Imlay, J. A. Cellular defenses against superoxide and hydrogen peroxide. Annu. Rev. Biochem.77:755-776; 2008.

[350] Barranco-Medina, S.; Lazaro, J. J.; Dietz, K. J. The oligomeric conformation of peroxiredoxins links redox state to function. FEBS Lett.583:1809-1816; 2009.

[351] MacDiarmid, C. W.; Taggart, J.; Kerdsomboon, K.; Kubisiak, M.; Panascharoen, S.; Schelble, K.; Eide, D. J. Peroxiredoxin chaperone activity is critical for protein homeostasis in zinc-deficient yeast. J. Biol. Chem.288:31313-31327; 2013.

[352] Mayo, J. N.; Beard, R. S.,Jr; Price, T. O.; Chen, C. H.; Erickson, M. A.; Ercal, N.; Banks, W. A.; Bearden, S. E. Nitrative stress in cerebral endothelium is mediated by mGluR5 in hyperhomocysteinemia. J. Cereb. Blood Flow Metab.32:825-834; 2012.

[353] Welch, G. N.; Upchurch, G. R.,Jr; Farivar, R. S.; Pigazzi, A.; Vu, K.; Brecher, P.; Keaney, J. F.,Jr; Loscalzo, J. Homocysteine-induced nitric oxide production in vascular smooth-muscle cells by NF-kappa B-dependent transcriptional activation of Nos2. Proc. Assoc. Am. Physicians110:22-31; 1998.

[354] Garcia-Garcia, A.; Zavala-Flores, L.; Rodriguez-Rocha, H.; Franco, R. Thiol-redox signaling, dopaminergic cell death, and parkinson's disease. Antioxid. Redox Signal.17:1764-1784; 2012.

[355] Li, Q.; Yu, S.; Wu, J.; Zou, Y.; Zhao, Y. Sulfiredoxin-1 protects PC12 cells against oxidative stress induced by hydrogen peroxide. J. Neurosci. Res.91:861-870; 2013.

[356] Soriano, F. X.; Baxter, P.; Murray, L. M.; Sporn, M. B.; Gillingwater, T. H.; Hardingham, G. E. Transcriptional regulation of the AP-1 and Nrf2 target gene sulfiredoxin. Mol. Cells27:279-282; 2009.

[357] Wei, Q.; Jiang, H.; Matthews, C. P.; Colburn, N. H. Sulfiredoxin is an AP-1 target gene that is required for transformation and shows elevated expression in human skin malignancies. Proc. Natl. Acad. Sci. U. S. A.105:19738-19743; 2008.

[358] Abbas, K.; Breton, J.; Planson, A. G.; Bouton, C.; Bignon, J.; Seguin, C.; Riquier, S.; Toledano, M. B.; Drapier, J. C. Nitric oxide activates an Nrf2/sulfiredoxin antioxidant pathway in macrophages. Free Radic. Biol. Med.51:107-114; 2011.

[359] Noh, Y. H.; Baek, J. Y.; Jeong, W.; Rhee, S. G.; Chang, T. S. Sulfiredoxin translocation into mitochondria plays a crucial role in reducing hyperoxidized peroxiredoxin III. J. Biol. Chem.284:8470-8477; 2009.

[360] Kil, I. S.; Lee, S. K.; Ryu, K. W.; Woo, H. A.; Hu, M. C.; Bae, S. H.; Rhee, S. G. Feedback control of adrenal steroidogenesis via H2O2-dependent, reversible inactivation of peroxiredoxin III in mitochondria. Mol. Cell46:584-594; 2012.

[361] Kil, I. S.; Ryu, K. W.; Lee, S. K.; Kim, J. Y.; Chu, S. Y.; Kim, J. H.; Park, S.; Rhee, S. G. Circadian oscillation of sulfiredoxin in the mitochondria. Mol. Cell59:651-663; 2015.

[362] Netto, L. E. S.; Antunes, F. The roles of peroxiredoxin and thioredoxin in hydrogen peroxide sensing and in signal transduction. Mol. Cells39:65-71; 2016.

[363] Wood, Z. A.; Poole, L. B.; Karplus, P. A. Peroxiredoxin evolution and the regulation of hydrogen peroxide signaling. Science300:650-653; 2003.

[364] Rhee, S. G.; Woo, H. A. Multiple functions of peroxiredoxins: Peroxidases, sensors and regulators of the intracellular messenger H(2)O(2), and protein chaperones. Antioxid. Redox Signal.15:781-794; 2011.

[365] Travasso, R. D. M.; Sampaio Dos Aidos, F.; Bayani, A.; Abranches, P.; Salvador, A. Localized redox relays as a privileged mode of cytoplasmic hydrogen peroxide signaling. Redox Biol.12:233-245; 2017.

[366] Cao, J.; Schulte, J.; Knight, A.; Leslie, N. R.; Zagozdzon, A.; Bronson, R.; Manevich, Y.; Beeson, C.; Neumann, C. A. Prdx1 inhibits tumorigenesis via regulating PTEN/AKT activity. Embo J.28:1505-1517; 2009.

[367] Sobotta, M. C.; Liou, W.; Stocker, S.; Talwar, D.; Oehler, M.; Ruppert, T.; Scharf, A. N.; Dick, T. P. Peroxiredoxin-2 and STAT3 form a redox relay for H2O2 signaling. Nat. Chem. Biol.11:64-70; 2015.

[368] Jarvis, R. M.; Hughes, S. M.; Ledgerwood, E. C. Peroxiredoxin 1 functions as a signal peroxidase to receive, transduce, and transmit peroxide signals in mammalian cells. Free Radic. Biol. Med.53:1522-1530; 2012.

[369] Furchgott, R. F.; Zawadzki, J. V. The obligatory role of endothelial cells in the relaxation of arterial smooth muscle by acetylcholine. Nature288:373-376; 1980.

[370] Palmer, R. M.; Ferrige, A. G.; Moncada, S. Nitric oxide release accounts for the biological activity of endothelium-derived relaxing factor. Nature327:524-526; 1987.

[371] Ignarro, L. J.; Buga, G. M.; Wood, K. S.; Byrns, R. E.; Chaudhuri, G. Endothelium-derived relaxing factor produced and released from artery and vein is nitric oxide. Proc. Natl. Acad. Sci. U. S. A.84:9265-9269; 1987.

[372] Liu, V. W.; Huang, P. L. Cardiovascular roles of nitric oxide: A review of insights from nitric oxide synthase gene disrupted mice. Cardiovasc. Res.77:19-29; 2008.

[373] Pacher, P.; Beckman, J. S.; Liaudet, L. Nitric oxide and peroxynitrite in health and disease. Physiol. Rev.87:315-424; 2007.

[374] Matsumoto, A.; Gow, A. J. Membrane transfer of S-nitrosothiols. Nitric Oxide25:102-107; 2011.

[375] Radi, R. Oxygen radicals, nitric oxide, and peroxynitrite: Redox pathways in molecular medicine. Proc. Natl. Acad. Sci. U. S. A.115:5839-5848; 2018.

[376] Bartesaghi, S.; Radi, R. Fundamentals on the biochemistry of peroxynitrite and protein tyrosine nitration. Redox Biol.14:618-625; 2018.

[377] Zaffagnini, M.; De Mia, M.; Morisse, S.; Di Giacinto, N.; Marchand, C. H.; Maes, A.; Lemaire, S. D.; Trost, P. Protein S-nitrosylation in photosynthetic organisms: A comprehensive overview with future perspectives. Biochim. Biophys. Acta1864:952-966; 2016.

[378] Klatt, P.; Lamas, S. Regulation of protein function by S-glutathiolation in response to oxidative and nitrosative stress. Eur. J. Biochem.267:4928-4944; 2000.

[379] Sengupta, R.; Holmgren, A. Thioredoxin and thioredoxin reductase in relation to reversible S-nitrosylation. Antioxid. Redox Signal.18:259-269; 2013.

[380] Shahani, N.; Sawa, A. Nitric oxide signaling and nitrosative stress in neurons: Role for S-nitrosylation. Antioxid. Redox Signal.14:1493-1504; 2011.

[381] Gusarov, I.; Nudler, E. Protein S-nitrosylation: Enzymatically controlled, but intrinsically unstable, post-translational modification. Mol. Cell69:351-353; 2018.

[382] Fernando, V.; Zheng, X.; Walia, Y.; Sharma, V.; Letson, J.; Furuta, S. S-nitrosylation: An emerging paradigm of redox signaling. Antioxidants (Basel)8:10.3390/antiox8090404; 2019.

[383] Beckman, J. S.; Beckman, T. W.; Chen, J.; Marshall, P. A.; Freeman, B. A. Apparent hydroxyl radical production by peroxynitrite: Implications for endothelial injury from nitric oxide and superoxide. Proc. Natl. Acad. Sci. U. S. A.87:1620-1624; 1990.

[384] Radi, R.; Beckman, J. S.; Bush, K. M.; Freeman, B. A. Peroxynitrite oxidation of sulfhydryls. the cytotoxic potential of superoxide and nitric oxide. J. Biol. Chem.266:4244-4250; 1991.

[385] Radi, R.; Beckman, J. S.; Bush, K. M.; Freeman, B. A. Peroxynitrite-induced membrane lipid peroxidation: The cytotoxic potential of superoxide and nitric oxide. Arch. Biochem. Biophys.288:481-487; 1991.

[386] Ferrer-Sueta, G.; Campolo, N.; Trujillo, M.; Bartesaghi, S.; Carballal, S.; Romero, N.; Alvarez, B.; Radi, R. Biochemistry of peroxynitrite and protein tyrosine nitration. Chem. Rev.118:1338-1408; 2018.

[387] Beckman, J. S.; Ischiropoulos, H.; Zhu, L.; van der Woerd, M.; Smith, C.; Chen, J.; Harrison, J.; Martin, J. C.; Tsai, M. Kinetics of superoxide dismutase- and iron-catalyzed nitration of phenolics by peroxynitrite. Arch. Biochem. Biophys.298:438-445; 1992.

[388] Ischiropoulos, H.; Zhu, L.; Beckman, J. S. Peroxynitrite formation from macrophage-derived nitric oxide. Arch. Biochem. Biophys.298:446-451; 1992.

[389] Ischiropoulos, H.; Zhu, L.; Chen, J.; Tsai, M.; Martin, J. C.; Smith, C. D.; Beckman, J. S. Peroxynitrite-mediated tyrosine nitration catalyzed by superoxide dismutase. Arch. Biochem. Biophys.298:431-437; 1992.

[390] Radi, R. Nitric oxide, oxidants, and protein tyrosine nitration. Proc. Natl. Acad. Sci. U. S. A.101:4003-4008; 2004.

[391] Schopfer, F. J.; Baker, P. R.; Freeman, B. A. NO-dependent protein nitration: A cell signaling event or an oxidative inflammatory response? Trends Biochem. Sci.28:646-654; 2003.

[392] Lee, J. R.; Kim, J. K.; Lee, S. J.; Kim, K. P. Role of protein tyrosine nitration in neurodegenerative diseases and atherosclerosis. Arch. Pharm. Res.32:1109-1118; 2009.

[393] Radi, R.; Cassina, A.; Hodara, R. Nitric oxide and peroxynitrite interactions with mitochondria. Biol. Chem.383:401-409; 2002.

[394] Radi, R.; Cassina, A.; Hodara, R.; Quijano, C.; Castro, L. Peroxynitrite reactions and formation in mitochondria. Free Radic. Biol. Med.33:1451-1464; 2002.

[395] Poderoso, J. J. The formation of peroxynitrite in the applied physiology of mitochondrial nitric oxide. Arch. Biochem. Biophys.484:214-220; 2009.

[396] Yamakura, F.; Taka, H.; Fujimura, T.; Murayama, K. Inactivation of human manganese-superoxide dismutase by peroxynitrite is caused by exclusive nitration of tyrosine 34 to 3-nitrotyrosine. J. Biol. Chem.273:14085-14089; 1998.

[397] MacMillan-Crow, L. A.; Crow, J. P.; Thompson, J. A. Peroxynitrite-mediated inactivation of manganese superoxide dismutase involves nitration and oxidation of critical tyrosine residues. Biochemistry37:1613-1622; 1998.

[398] Poderoso, J. J.; Carreras, M. C.; Lisdero, C.; Riobo, N.; Schopfer, F.; Boveris, A. Nitric oxide inhibits electron transfer and increases superoxide radical production in rat heart mitochondria and submitochondrial particles. Arch. Biochem. Biophys.328:85-92; 1996.

[399] Cassina, A.; Radi, R. Differential inhibitory action of nitric oxide and peroxynitrite on mitochondrial electron transport. Arch. Biochem. Biophys.328:309-316; 1996.

[400] Cleeter, M. W.; Cooper, J. M.; Darley-Usmar, V. M.; Moncada, S.; Schapira, A. H. Reversible inhibition of cytochrome c oxidase, the terminal enzyme of the mitochondrial respiratory chain, by nitric oxide. implications for neurodegenerative diseases. FEBS Lett.345:50-54; 1994.

[401] Borutaite, V.; Budriunaite, A.; Brown, G. C. Reversal of nitric oxide-, peroxynitrite- and S-nitrosothiol-induced inhibition of mitochondrial respiration or complex I activity by light and thiols. Biochim. Biophys. Acta1459:405-412; 2000.

[402] Pearce, L. L.; Epperly, M. W.; Greenberger, J. S.; Pitt, B. R.; Peterson, J. Identification of respiratory complexes I and III as mitochondrial sites of damage following exposure to ionizing radiation and nitric oxide. Nitric Oxide5:128-136; 2001.

[403] Radi, R.; Rodriguez, M.; Castro, L.; Telleri, R. Inhibition of mitochondrial electron transport by peroxynitrite. Arch. Biochem. Biophys.308:89-95; 1994.

[404] Han, D.; Canali, R.; Garcia, J.; Aguilera, R.; Gallaher, T. K.; Cadenas, E. Sites and mechanisms of aconitase inactivation by peroxynitrite: Modulation by citrate and glutathione. Biochemistry44:11986-11996; 2005.

[405] Aulak, K. S.; Miyagi, M.; Yan, L.; West, K. A.; Massillon, D.; Crabb, J. W.; Stuehr, D. J. Proteomic method identifies proteins nitrated in vivo during inflammatory challenge. Proc. Natl. Acad. Sci. U. S. A.98:12056-12061; 2001.

[406] Vieira, H. L.; Belzacq, A. S.; Haouzi, D.; Bernassola, F.; Cohen, I.; Jacotot, E.; Ferri, K. F.; El Hamel, C.; Bartle, L. M.; Melino, G.; Brenner, C.; Goldmacher, V.; Kroemer, G. The adenine nucleotide translocator: A target of nitric oxide, peroxynitrite, and 4-hydroxynonenal. Oncogene20:4305-4316; 2001.

[407] Konorev, E. A.; Hogg, N.; Kalyanaraman, B. Rapid and irreversible inhibition of creatine kinase by peroxynitrite. FEBS Lett.427:171-174; 1998.

[408] Szabo, C.; Ischiropoulos, H.; Radi, R. Peroxynitrite: Biochemistry, pathophysiology and development of therapeutics. Nat. Rev. Drug Discov.6:662-680; 2007.

[409] Virag, L.; Scott, G. S.; Cuzzocrea, S.; Marmer, D.; Salzman, A. L.; Szabo, C. Peroxynitrite-induced thymocyte apoptosis: The role of caspases and poly (ADP-ribose) synthetase (PARS) activation. Immunology94:345-355; 1998.

[410] Virag, L.; Marmer, D. J.; Szabo, C. Crucial role of apopain in the peroxynitrite-induced apoptotic DNA fragmentation. Free Radic. Biol. Med.25:1075-1082; 1998.

[411] Virag, L.; Szabo, E.; Gergely, P.; Szabo, C. Peroxynitrite-induced cytotoxicity: Mechanism and opportunities for intervention. Toxicol. Lett.140-141:113-124; 2003.

[412] Lin, K. T.; Xue, J. Y.; Lin, M. C.; Spokas, E. G.; Sun, F. F.; Wong, P. Y. Peroxynitrite induces apoptosis of HL-60 cells by activation of a caspase-3 family protease. Am. J. Physiol.274:C855-60; 1998.

[413] Virag, L.; Szabo, C. Inhibition of poly(ADP-ribose) synthetase (PARS) and protection against peroxynitrite-induced cytotoxicity by zinc chelation. Br. J. Pharmacol.126:769-777; 1999.

[414] Virag, L.; Scott, G. S.; Antal-Szalmas, P.; O'Connor, M.; Ohshima, H.; Szabo, C. Requirement of intracellular calcium mobilization for peroxynitrite-induced poly(ADP-ribose) synthetase activation and cytotoxicity. Mol. Pharmacol.56:824-833; 1999.

[415] Trujillo, M.; Ferrer-Sueta, G.; Radi, R. Peroxynitrite detoxification and its biologic implications. Antioxid. Redox Signal.10:1607-1620; 2008.

[416] Bryk, R.; Griffin, P.; Nathan, C. Peroxynitrite reductase activity of bacterial peroxiredoxins. Nature407:211-215; 2000.

[417] Manta, B.; Hugo, M.; Ortiz, C.; Ferrer-Sueta, G.; Trujillo, M.; Denicola, A. The peroxidase and peroxynitrite reductase activity of human erythrocyte peroxiredoxin 2. Arch. Biochem. Biophys.484:146-154; 2009.

[418] Dubuisson, M.; Vander Stricht, D.; Clippe, A.; Etienne, F.; Nauser, T.; Kissner, R.; Koppenol, W. H.; Rees, J. F.; Knoops, B. Human peroxiredoxin 5 is a peroxynitrite reductase. FEBS Lett.571:161-165; 2004.

[419] Trujillo, M.; Clippe, A.; Manta, B.; Ferrer-Sueta, G.; Smeets, A.; Declercq, J. P.; Knoops, B.; Radi, R. Pre-steady state kinetic characterization of human peroxiredoxin 5: Taking advantage of Trp84 fluorescence increase upon oxidation. Arch. Biochem. Biophys.467:95-106; 2007.

[420] Toledo, J. C.,Jr; Audi, R.; Ogusucu, R.; Monteiro, G.; Netto, L. E.; Augusto, O. Horseradish peroxidase compound I as a tool to investigate reactive protein-cysteine residues: From quantification to kinetics. Free Radic. Biol. Med.50:1032-1038; 2011.

[421] De Armas, M. I.; Esteves, R.; Viera, N.; Reyes, A. M.; Mastrogiovanni, M.; Alegria, T. G. P.; Netto, L. E. S.; Tortora, V.; Radi, R.; Trujillo, M. Rapid peroxynitrite reduction by human peroxiredoxin 3: Implications for the fate of oxidants in mitochondria. Free Radic. Biol. Med.130:369-378; 2019.

[422] Benfeitas, R.; Selvaggio, G.; Antunes, F.; Coelho, P. M.; Salvador, A. Hydrogen peroxide metabolism and sensing in human erythrocytes: A validated kinetic model and reappraisal of the role of peroxiredoxin II. Free Radic. Biol. Med.74:35-49; 2014.

[423] Peskin, A. V.; Low, F. M.; Paton, L. N.; Maghzal, G. J.; Hampton, M. B.; Winterbourn, C. C. The high reactivity of peroxiredoxin 2 with H(2)O(2) is not reflected in its reaction with other oxidants and thiol reagents. J. Biol. Chem.282:11885-11892; 2007.

[424] Cox, A. G.; Peskin, A. V.; Paton, L. N.; Winterbourn, C. C.; Hampton, M. B. Redox potential and peroxide reactivity of human peroxiredoxin 3. Biochemistry48:6495-6501; 2009.

[425] Trujillo, M.; Alvarez, B.; Radi, R. One- and two-electron oxidation of thiols: Mechanisms, kinetics and biological fates. Free Radic. Res.50:150-171; 2016.

[426] Schulz, H. U.; Niederau, C.; Klonowski-Stumpe, H.; Halangk, W.; Luthen, R.; Lippert, H. Oxidative stress in acute pancreatitis. Hepatogastroenterology46:2736-2750; 1999.

[427] Tsai, K.; Wang, S. S.; Chen, T. S.; Kong, C. W.; Chang, F. Y.; Lee, S. D.; Lu, F. J. Oxidative stress: An important phenomenon with pathogenetic significance in the progression of acute pancreatitis. Gut42:850-855; 1998.

[428] Que, R.; Cao, L.; Ding, G.; Hu, J.; Mao, K.; Wang, G. Correlation of nitric oxide and other free radicals with the severity of acute pancreatitis and complicated systemic inflammatory response syndrome. Pancreas39:536-540; 2010.

[429] Winterbourn, C. C.; Bonham, M. J.; Buss, H.; Abu-Zidan, F. M.; Windsor, J. A. Elevated protein carbonyls as plasma markers of oxidative stress in acute pancreatitis. Pancreatology3:375-382; 2003.

[430] Abu-Zidan, F. M.; Bonham, M. J.; Windsor, J. A. Severity of acute pancreatitis: A multivariate analysis of oxidative stress markers and modified glasgow criteria. Br. J. Surg.87:1019-1023; 2000.

[431] Tsang, S. W.; Guan, Y. F.; Wang, J.; Bian, Z. X.; Zhang, H. J. Inhibition of pancreatic oxidative damage by stilbene derivative dihydro-resveratrol: Implication for treatment of acute pancreatitis. Sci. Rep.6:22859; 2016.

[432] Closa, D.; Bulbena, O.; Rosello-Catafau, J.; Fernandez-Cruz, L.; Gelpi, E. Effect of prostaglandins and superoxide dismutase administration on oxygen free radical production in experimental acute pancreatitis. Inflammation17:563-571; 1993.

[433] Closa, D.; Bulbena, O.; Hotter, G.; Rosello-Catafau, J.; Fernandez-Cruz, L.; Gelpi, E. Xanthine oxidase activation in cerulein- and taurocholate-induced acute pancreatitis in rats. Arch. Int. Physiol. Biochim. Biophys.102:167-170; 1994.

[434] Devenyi, Z. J.; Orchard, J. L.; Powers, R. E. Xanthine oxidase activity in mouse pancreas: Effects of caerulein-induced acute pancreatitis. Biochem. Biophys. Res. Commun.149:841-845; 1987.

[435] Yu, J. H.; Lim, J. W.; Kim, H.; Kim, K. H. NADPH oxidase mediates interleukin-6 expression in cerulein-stimulated pancreatic acinar cells. Int. J. Biochem. Cell Biol.37:1458-1469; 2005.

[436] Yu, J. H.; Lim, J. W.; Kim, K. H.; Morio, T.; Kim, H. NADPH oxidase and apoptosis in cerulein-stimulated pancreatic acinar AR42J cells. Free Radic. Biol. Med.39:590-602; 2005.

[437] Shen, A.; Kim, H. J.; Oh, G. S.; Lee, S. B.; Lee, S.; Pandit, A.; Khadka, D.; Sharma, S.; Kim, S. Y.; Choe, S. K.; Yang, S. H.; Cho, E. Y.; Shim, H.; Park, R.; Kwak, T. H.; So, H. S. Pharmacological stimulation of NQO1 decreases NADPH levels and ameliorates acute pancreatitis in mice. Cell. Death Dis.10:5-018-1252-z; 2018.

[438] Gukovskaya, A. S.; Vaquero, E.; Zaninovic, V.; Gorelick, F. S.; Lusis, A. J.; Brennan, M. L.; Holland, S.; Pandol, S. J. Neutrophils and NADPH oxidase mediate intrapancreatic trypsin activation in murine experimental acute pancreatitis. Gastroenterology122:974-984; 2002.

[439] Neuschwander-Tetri, B. A.; Ferrell, L. D.; Sukhabote, R. J.; Grendell, J. H. Glutathione monoethyl ester ameliorates caerulein-induced pancreatitis in the mouse. J. Clin. Invest.89:109-116; 1992.

[440] Pereda, J.; Escobar, J.; Sandoval, J.; Rodriguez, J. L.; Sabater, L.; Pallardo, F. V.; Torres, L.; Franco, L.; Vina, J.; Lopez-Rodas, G.; Sastre, J. Glutamate cysteine ligase up-regulation fails in necrotizing pancreatitis. Free Radic. Biol. Med.44:1599-1609; 2008.

[441] Rahman, S. H.; Ibrahim, K.; Larvin, M.; Kingsnorth, A.; McMahon, M. J. Association of antioxidant enzyme gene polymorphisms and glutathione status with severe acute pancreatitis. Gastroenterology126:1312-1322; 2004.

[442] Neuschwander-Tetri, B. A.; Ferrell, L. D.; Sukhabote, R. J.; Grendell, J. H. Glutathione monoethyl ester ameliorates caerulein-induced pancreatitis in the mouse. J. Clin. Invest.89:109-116; 1992.

[443] Alsfasser, G.; Gock, M.; Herzog, L.; Gebhard, M. M.; Herfarth, C.; Klar, E.; Schmidt, J. Glutathione depletion with L-buthionine-(S,R)-sulfoximine demonstrates deleterious effects in acute pancreatitis of the rat. Dig. Dis. Sci.47:1793-1799; 2002.

[444] Moreno, M. L.; Escobar, J.; Izquierdo-Alvarez, A.; Gil, A.; Perez, S.; Pereda, J.; Zapico, I.; Vento, M.; Sabater, L.; Marina, A.; Martinez-Ruiz, A.; Sastre, J. Disulfide stress: A novel type of oxidative stress in acute pancreatitis. Free Radic. Biol. Med.70:265-277; 2014.

[445] Lu, S. C.; Gukovsky, I.; Lugea, A.; Reyes, C. N.; Huang, Z. Z.; Chen, L.; Mato, J. M.; Bottiglieri, T.; Pandol, S. J. Role of S-adenosylmethionine in two experimental models of pancreatitis. Faseb J.17:56-58; 2003.

[446] Esrefoglu, M.; Gul, M.; Ates, B.; Batcioglu, K.; Selimoglu, M. A. Antioxidative effect of melatonin, ascorbic acid and N-acetylcysteine on caerulein-induced pancreatitis and associated liver injury in rats. World J. Gastroenterol.12:259-264; 2006.

[447] Czako, L.; Takacs, T.; Varga, I. S.; Tiszlavicz, L.; Hai, D. Q.; Hegyi, P.; Matkovics, B.; Lonovics, J. Oxidative stress in distant organs and the effects of allopurinol during experimental acute pancreatitis. Int. J. Pancreatol.27:209-216; 2000.

[448] Dabrowski, A.; Gabryelewicz, A.; Wereszczynska-Siemiatkowska, U.; Chyczewski, L. Oxygen-derived free radicals in cerulein-induced acute pancreatitis. Scand. J. Gastroenterol.23:1245-1249; 1988.

[449] Kikuchi, Y.; Shimosegawa, T.; Moriizumi, S.; Kimura, K.; Satoh, A.; Koizumi, M.; Kato, I.; Epstein, C. J.; Toyota, T. Transgenic copper/zinc-superoxide dismutase ameliorates caerulein-induced pancreatitis in mice. Biochem. Biophys. Res. Commun.233:177-181; 1997.

[450] Ohashi, S.; Nishio, A.; Nakamura, H.; Kido, M.; Ueno, S.; Uza, N.; Inoue, S.; Kitamura, H.; Kiriya, K.; Asada, M.; Tamaki, H.; Matsuura, M.; Kawasaki, K.; Fukui, T.; Watanabe, N.; Nakase, H.; Yodoi, J.; Okazaki, K.; Chiba, T. Protective roles of redox-active protein thioredoxin-1 for severe acute pancreatitis. Am. J. Physiol. Gastrointest. Liver Physiol.290:G772-81; 2006.

[451] Ueno, N.; Kashiwamura, S.; Ueda, H.; Okamura, H.; Tsuji, N. M.; Hosohara, K.; Kotani, J.; Marukawa, S. Role of interleukin 18 in nitric oxide production and pancreatic damage during acute pancreatitis. Shock24:564-570; 2005.

[452] Ang, A. D.; Adhikari, S.; Ng, S. W.; Bhatia, M. Expression of nitric oxide synthase isoforms and nitric oxide production in acute pancreatitis and associated lung injury. Pancreatology9:150-159; 2009.

[453] Cuzzocrea, S.; Mazzon, E.; Dugo, L.; Serraino, I.; Centorrino, T.; Ciccolo, A.; Van de Loo, F. A.; Britti, D.; Caputi, A. P.; Thiemermann, C. Inducible nitric oxide synthase-deficient mice exhibit resistance to the acute pancreatitis induced by cerulein. Shock17:416-422; 2002.

[454] Cuzzocrea, S.; Pisano, B.; Dugo, L.; Ianaro, A.; Britti, D.; Patel, N. S.; Di Paola, R.; Genovese, T.; Di Rosa, M.; Caputi, A. P.; Thiemermann, C. Rosiglitazone, a ligand of the peroxisome proliferator-activated receptor-gamma, reduces acute pancreatitis induced by cerulein. Intensive Care Med.30:951-956; 2004.

[455] Balachandra, S.; Genovese, T.; Mazzon, E.; Di Paola, R.; Thiemerman, C.; Siriwardena, A. K.; Cuzzocrea, S. Inhibition of tyrosine-kinase-mediated cellular signaling by tyrphostins AG 126 and AG556 modulates murine experimental acute pancreatitis. Surgery138:913-923; 2005.

[456] DiMagno, M. J.; Williams, J. A.; Hao, Y.; Ernst, S. A.; Owyang, C. Endothelial nitric oxide synthase is protective in the initiation of caerulein-induced acute pancreatitis in mice. Am. J. Physiol. Gastrointest. Liver Physiol.287:G80-7; 2004.

[457] DiMagno, M. J. Nitric oxide pathways and evidence-based perturbations in acute pancreatitis. Pancreatology7:403-408; 2007.

[458] Puigserver, P.; Wu, Z.; Park, C. W.; Graves, R.; Wright, M.; Spiegelman, B. M. A cold-inducible coactivator of nuclear receptors linked to adaptive thermogenesis. Cell92:829-839; 1998.

[459] Mastropasqua, F.; Girolimetti, G.; Shoshan, M. PGC1alpha: Friend or foe in cancer? Genes (Basel)9:10.3390/genes9010048; 2018.

[460] Eisele, P. S.; Salatino, S.; Sobek, J.; Hottiger, M. O.; Handschin, C. The peroxisome proliferator-activated receptor gamma coactivator 1alpha/beta (PGC-1) coactivators repress the transcriptional activity of NF-kappaB in skeletal muscle cells. J. Biol. Chem.288:2246-2260; 2013.

[461] Kadlec, A. O.; Chabowski, D. S.; Ait-Aissa, K.; Gutterman, D. D. Role of PGC-1alpha in vascular regulation: Implications for atherosclerosis. Arterioscler. Thromb. Vasc. Biol.36:1467-1474; 2016.

[462] Perez, S.; Rius-Perez, S.; Finamor, I.; Marti-Andres, P.; Prieto, I.; Garcia, R.; Monsalve, M.; Sastre, J. Obesity causes PGC-1alpha deficiency in the pancreas leading to marked IL-6 upregulation via NF-kappaB in acute pancreatitis. J. Pathol.247:48-59; 2019.

[463] Chen, S. D.; Yang, D. I.; Lin, T. K.; Shaw, F. Z.; Liou, C. W.; Chuang, Y. C. Roles of oxidative stress, apoptosis, PGC-1alpha and mitochondrial biogenesis in cerebral ischemia. Int. J. Mol. Sci.12:7199-7215; 2011.

[464] Liang, H.; Ward, W. F. PGC-1alpha: A key regulator of energy metabolism. Adv. Physiol. Educ.30:145-151; 2006.

[465] Villena, J. A. New insights into PGC-1 coactivators: Redefining their role in the regulation of mitochondrial function and beyond. Febs J.282:647-672; 2015.

[466] Puigserver, P.; Adelmant, G.; Wu, Z.; Fan, M.; Xu, J.; O'Malley, B.; Spiegelman, B. M. Activation of PPARgamma coactivator-1 through transcription factor docking. Science286:1368-1371; 1999.

[467] Knutti, D.; Kaul, A.; Kralli, A. A tissue-specific coactivator of steroid receptors, identified in a functional genetic screen. Mol. Cell. Biol.20:2411-2422; 2000.

[468] Lin, J.; Handschin, C.; Spiegelman, B. M. Metabolic control through the PGC-1 family of transcription coactivators. Cell. Metab.1:361-370; 2005.

[469] Kressler, D.; Schreiber, S. N.; Knutti, D.; Kralli, A. The PGC-1-related protein PERC is a selective coactivator of estrogen receptor alpha. J. Biol. Chem.277:13918-13925; 2002.

[470] Lin, J.; Puigserver, P.; Donovan, J.; Tarr, P.; Spiegelman, B. M. Peroxisome proliferator-activated receptor gamma coactivator 1beta (PGC-1beta), a novel PGC-1-related transcription coactivator associated with host cell factor. J. Biol. Chem.277:1645-1648; 2002.

[471] Martinez-Redondo, V.; Jannig, P. R.; Correia, J. C.; Ferreira, D. M.; Cervenka, I.; Lindvall, J. M.; Sinha, I.; Izadi, M.; Pettersson-Klein, A. T.; Agudelo, L. Z.; Gimenez-Cassina, A.; Brum, P. C.; Dahlman-Wright, K.; Ruas, J. L. Peroxisome proliferator-activated receptor gamma coactivator-1 alpha isoforms selectively regulate multiple splicing events on target genes. J. Biol. Chem.291:15169-15184; 2016.

[472] Fernandez-Marcos, P. J.; Auwerx, J. Regulation of PGC-1alpha, a nodal regulator of mitochondrial biogenesis. Am. J. Clin. Nutr.93:884S-90; 2011.

[473] Herzig, S.; Long, F.; Jhala, U. S.; Hedrick, S.; Quinn, R.; Bauer, A.; Rudolph, D.; Schutz, G.; Yoon, C.; Puigserver, P.; Spiegelman, B.; Montminy, M. CREB

regulates hepatic gluconeogenesis through the coactivator PGC-1. Nature413:179-183; 2001.

[474] Daitoku, H.; Yamagata, K.; Matsuzaki, H.; Hatta, M.; Fukamizu, A. Regulation of PGC-1 promoter activity by protein kinase B and the forkhead transcription factor FKHR. Diabetes52:642-649; 2003.

[475] Borniquel, S.; Garcia-Quintans, N.; Valle, I.; Olmos, Y.; Wild, B.; Martinez-Granero, F.; Soria, E.; Lamas, S.; Monsalve, M. Inactivation of Foxo3a and subsequent downregulation of PGC-1 alpha mediate nitric oxide-induced endothelial cell migration. Mol. Cell. Biol.30:4035-4044; 2010.

[476] Hino, S.; Sakamoto, A.; Nagaoka, K.; Anan, K.; Wang, Y.; Mimasu, S.; Umehara, T.; Yokoyama, S.; Kosai, K.; Nakao, M. FAD-dependent lysine-specific demethylase-1 regulates cellular energy expenditure. Nat. Commun.3:758; 2012.

[477] Shi, Y.; Lan, F.; Matson, C.; Mulligan, P.; Whetstine, J. R.; Cole, P. A.; Casero, R. A.; Shi, Y. Histone demethylation mediated by the nuclear amine oxidase homolog LSD1. Cell119:941-953; 2004.

[478] Barres, R.; Osler, M. E.; Yan, J.; Rune, A.; Fritz, T.; Caidahl, K.; Krook, A.; Zierath, J. R. Non-CpG methylation of the PGC-1alpha promoter through DNMT3B controls mitochondrial density. Cell. Metab.10:189-198; 2009.

[479] Knutti, D.; Kressler, D.; Kralli, A. Regulation of the transcriptional coactivator PGC-1 via MAPK-sensitive interaction with a repressor. Proc. Natl. Acad. Sci. U. S. A.98:9713-9718; 2001.

[480] Puigserver, P.; Rhee, J.; Lin, J.; Wu, Z.; Yoon, J. C.; Zhang, C. Y.; Krauss, S.; Mootha, V. K.; Lowell, B. B.; Spiegelman, B. M. Cytokine stimulation of energy expenditure through p38 MAP kinase activation of PPARgamma coactivator-1. Mol. Cell8:971-982; 2001.

[481] Fan, M.; Rhee, J.; St-Pierre, J.; Handschin, C.; Puigserver, P.; Lin, J.; Jaeger, S.; Erdjument-Bromage, H.; Tempst, P.; Spiegelman, B. M. Suppression of mitochondrial respiration through recruitment of p160 myb binding protein to PGC-1alpha: Modulation by p38 MAPK. Genes Dev.18:278-289; 2004.

[482] Li, X.; Monks, B.; Ge, Q.; Birnbaum, M. J. Akt/PKB regulates hepatic metabolism by directly inhibiting PGC-1alpha transcription coactivator. Nature447:1012-1016; 2007.

[483] Stahel, P.; Kim, J. J.; Cieslar, S. R.; Warrington, J. M.; Xiao, C.; Cant, J. P. Supranutritional selenium intake from enriched milk casein impairs hepatic insulin sensitivity via attenuated IRS/PI3K/AKT signaling and decreased PGC-1alpha expression in male sprague-dawley rats. J. Nutr. Biochem.41:142-150; 2017.

[484] Anderson, R. M.; Barger, J. L.; Edwards, M. G.; Braun, K. H.; O'Connor, C. E.; Prolla, T. A.; Weindruch, R. Dynamic regulation of PGC-1alpha localization and turnover implicates mitochondrial adaptation in calorie restriction and the stress response. Aging Cell.7:101-111; 2008.

[485] Theeuwes, W. F.; Gosker, H. R.; Langen, R. C. J.; Pansters, N. A. M.; Schols, A. M. W. J.; Remels, A. H. V. Inactivation of glycogen synthase kinase 3beta (GSK-3beta) enhances mitochondrial biogenesis during myogenesis. Biochim. Biophys. Acta Mol. Basis Dis.1864:2913-2926; 2018.

[486] Rodgers, J. T.; Haas, W.; Gygi, S. P.; Puigserver, P. Cdc2-like kinase 2 is an insulin-regulated suppressor of hepatic gluconeogenesis. Cell. Metab.11:23-34; 2010.

[487] Olson, B. L.; Hock, M. B.; Ekholm-Reed, S.; Wohlschlegel, J. A.; Dev, K. K.; Kralli, A.; Reed, S. I. SCFCdc4 acts antagonistically to the PGC-1alpha transcriptional coactivator by targeting it for ubiquitin-mediated proteolysis. Genes Dev.22:252-264; 2008.

[488] Lerin, C.; Rodgers, J. T.; Kalume, D. E.; Kim, S. H.; Pandey, A.; Puigserver, P. GCN5 acetyltransferase complex controls glucose metabolism through transcriptional repression of PGC-1alpha. Cell. Metab.3:429-438; 2006.

[489] Coste, A.; Louet, J. F.; Lagouge, M.; Lerin, C.; Antal, M. C.; Meziane, H.; Schoonjans, K.; Puigserver, P.; O'Malley, B. W.; Auwerx, J. The genetic ablation of SRC-3 protects against obesity and improves insulin sensitivity by reducing the acetylation of PGC-1{alpha}. Proc. Natl. Acad. Sci. U. S. A.105:17187-17192; 2008.

[490] Rodgers, J. T.; Lerin, C.; Haas, W.; Gygi, S. P.; Spiegelman, B. M.; Puigserver, P. Nutrient control of glucose homeostasis through a complex of PGC-1alpha and SIRT1. Nature434:113-118; 2005.

[491] Canto, C.; Gerhart-Hines, Z.; Feige, J. N.; Lagouge, M.; Noriega, L.; Milne, J. C.; Elliott, P. J.; Puigserver, P.; Auwerx, J. AMPK regulates energy expenditure by modulating NAD+ metabolism and SIRT1 activity. Nature458:1056-1060; 2009.

[492] Li, S. Y.; Susztak, K. The role of peroxisome proliferator-activated receptor gamma coactivator 1alpha (PGC-1alpha) in kidney disease. Semin. Nephrol.38:121-126; 2018.

[493] Ventura-Clapier, R.; Garnier, A.; Veksler, V. Transcriptional control of mitochondrial biogenesis: The central role of PGC-1alpha. Cardiovasc. Res.79:208-217; 2008.

[494] Fernandez-Marcos, P. J.; Auwerx, J. Regulation of PGC-1alpha, a nodal regulator of mitochondrial biogenesis. Am. J. Clin. Nutr.93:884S-90; 2011.

[495] Virbasius, J. V.; Scarpulla, R. C. Activation of the human mitochondrial transcription factor A gene by nuclear respiratory factors: A potential regulatory link between nuclear and mitochondrial gene expression in organelle biogenesis. Proc. Natl. Acad. Sci. U. S. A.91:1309-1313; 1994.

[496] Martinez-Redondo, V.; Pettersson, A. T.; Ruas, J. L. The hitchhiker's guide to PGC-1alpha isoform structure and biological functions. Diabetologia58:1969-1977; 2015.

[497] Rodgers, J. T.; Puigserver, P. Fasting-dependent glucose and lipid metabolic response through hepatic sirtuin 1. Proc. Natl. Acad. Sci. U. S. A.104:12861-12866; 2007.

[498] Valle, I.; Alvarez-Barrientos, A.; Arza, E.; Lamas, S.; Monsalve, M. PGC-1alpha regulates the mitochondrial antioxidant defense system in vascular endothelial cells. Cardiovasc. Res.66:562-573; 2005.

[499] Olmos, Y.; Valle, I.; Borniquel, S.; Tierrez, A.; Soria, E.; Lamas, S.; Monsalve, M. Mutual dependence of Foxo3a and PGC-1alpha in the induction of oxidative stress genes. J. Biol. Chem.284:14476-14484; 2009.

[500] St-Pierre, J.; Drori, S.; Uldry, M.; Silvaggi, J. M.; Rhee, J.; Jager, S.; Handschin, C.; Zheng, K.; Lin, J.; Yang, W.; Simon, D. K.; Bachoo, R.; Spiegelman, B. M. Suppression of reactive oxygen species and neurodegeneration by the PGC-1 transcriptional coactivators. Cell127:397-408; 2006.

[501] Cherry, A. D.; Suliman, H. B.; Bartz, R. R.; Piantadosi, C. A. Peroxisome proliferator-activated receptor gamma co-activator 1-alpha as a critical co-activator of the murine hepatic oxidative stress response and mitochondrial biogenesis in staphylococcus aureus sepsis. J. Biol. Chem.289:41-52; 2014.

[502] Sanchez-Ramos, C.; Prieto, I.; Tierrez, A.; Laso, J.; Valdecantos, M. P.; Bartrons, R.; Rosello-Catafau, J.; Monsalve, M. PGC-1alpha downregulation in steatotic liver enhances ischemia-reperfusion injury and impairs ischemic preconditioning. Antioxid. Redox Signal.27:1332-1346; 2017.

[503] Lu, Z.; Xu, X.; Hu, X.; Fassett, J.; Zhu, G.; Tao, Y.; Li, J.; Huang, Y.; Zhang, P.; Zhao, B.; Chen, Y. PGC-1 alpha regulates expression of myocardial mitochondrial antioxidants and myocardial oxidative stress after chronic systolic overload. Antioxid. Redox Signal.13:1011-1022; 2010.

[504] Aquilano, K.; Baldelli, S.; Pagliei, B.; Cannata, S. M.; Rotilio, G.; Ciriolo, M. R. p53 orchestrates the PGC-1alpha-mediated antioxidant response upon mild redox and metabolic imbalance. Antioxid. Redox Signal.18:386-399; 2013.

[505] Sun, L.; Zang, W. J.; Wang, H.; Zhao, M.; Yu, X. J.; He, X.; Miao, Y.; Zhou, J. Acetylcholine promotes ROS detoxification against hypoxia/reoxygenation-induced oxidative stress through FoxO3a/PGC-1alpha dependent superoxide dismutase. Cell. Physiol. Biochem.34:1614-1625; 2014.

[506] Anastasi, A.; Erspamer, V.; Endean, R. Isolation and structure of caerulein, an active decapeptide from the skin of hyla caerulea. Experientia23:699-700; 1967.

[507] Lampel, M.; Kern, H. F. Acute interstitial pancreatitis in the rat induced by excessive doses of a pancreatic secretagogue. Virchows Arch. A Pathol. Anat. Histol.373:97-117; 1977.

[508] Lerch, M. M.; Gorelick, F. S. Models of acute and chronic pancreatitis. Gastroenterology144:1180-1193; 2013.

[509] Foster, J. R. A review of animal models of nonneoplastic pancreatic diseases. Toxicol. Pathol.42:243-259; 2014.

[510] Niederau, C.; Ferrell, L. D.; Grendell, J. H. Caerulein-induced acute necrotizing pancreatitis in mice: Protective effects of proglumide, benzotript, and secretin. Gastroenterology88:1192-1204; 1985.

[511] Su, K. H.; Cuthbertson, C.; Christophi, C. Review of experimental animal models of acute pancreatitis. HPB (Oxford)8:264-286; 2006.

[512] Silva-Vaz, P.; Abrantes, A. M.; Castelo-Branco, M.; Gouveia, A.; Botelho, M. F.; Tralhao, J. G. Murine models of acute pancreatitis: A critical appraisal of clinical relevance. Int. J. Mol. Sci.20:10.3390/ijms20112794; 2019.

[513] Gorelick, F. S.; Lerch, M. M. Do animal models of acute pancreatitis reproduce human disease? Cell. Mol. Gastroenterol. Hepatol.4:251-262; 2017.

[514] Planson, A. G.; Palais, G.; Abbas, K.; Gerard, M.; Couvelard, L.; Delaunay, A.; Baulande, S.; Drapier, J. C.; Toledano, M. B. Sulfiredoxin protects mice from lipopolysaccharide-induced endotoxic shock. Antioxid. Redox Signal.14:2071-2080; 2011.

[515] Lin, J.; Wu, P. H.; Tarr, P. T.; Lindenberg, K. S.; St-Pierre, J.; Zhang, C. Y.; Mootha, V. K.; Jager, S.; Vianna, C. R.; Reznick, R. M.; Cui, L.; Manieri, M.; Donovan, M. X.; Wu, Z.; Cooper, M. P.; Fan, M. C.; Rohas, L. M.; Zavacki, A. M.; Cinti, S.; Shulman, G. I.; Lowell, B. B.; Krainc, D.; Spiegelman, B. M. Defects in adaptive energy metabolism with CNS-linked hyperactivity in PGC-1alpha null mice. Cell119:121-135; 2004.

[516] Hong, S. S.; Choi, J. H.; Lee, S. Y.; Park, Y. H.; Park, K. Y.; Lee, J. Y.; Kim, J.; Gajulapati, V.; Goo, J. I.; Singh, S.; Lee, K.; Kim, Y. K.; Im, S. H.; Ahn, S. H.; Rose-John, S.; Heo, T. H.; Choi, Y. A novel small-molecule inhibitor targeting the IL-6 receptor beta subunit, glycoprotein 130. J. Immunol.195:237-245; 2015.

[517] Lopez-Ferrer, D.; Martinez-Bartolome, S.; Villar, M.; Campillos, M.; Martin-Maroto, F.; Vazquez, J. Statistical model for large-scale peptide identification in databases from tandem mass spectra using SEQUEST. Anal. Chem.76:6853-6860; 2004.

[518] Mora, M. I.; Molina, M.; Odriozola, L.; Elortza, F.; Mato, J. M.; Sitek, B.; Zhang, P.; He, F.; Latasa, M. U.; Avila, M. A.; Corrales, F. J. Prioritizing popular proteins in liver cancer: Remodelling one-carbon metabolism. J. Proteome Res.16:4506-4514; 2017.

[519] MacLean, B.; Tomazela, D. M.; Shulman, N.; Chambers, M.; Finney, G. L.; Frewen, B.; Kern, R.; Tabb, D. L.; Liebler, D. C.; MacCoss, M. J. Skyline: An open source document editor for creating and analyzing targeted proteomics experiments. Bioinformatics26:966-968; 2010.

[520] Van Laethem, J. L.; Eskinazi, R.; Louis, H.; Rickaert, F.; Robberecht, P.; Deviere, J. Multisystemic production of interleukin 10 limits the severity of acute pancreatitis in mice. Gut43:408-413; 1998.

[521] Gates, L. A.; Foulds, C. E.; O'Malley, B. W. Histone marks in the 'driver's seat': Functional roles in steering the transcription cycle. Trends Biochem. Sci.42:977-989; 2017.

[522] Perez, S.; Finamor, I.; Marti-Andres, P.; Pereda, J.; Campos, A.; Domingues, R.; Haj, F.; Sabater, L.; de-Madaria, E.; Sastre, J. Role of obesity in the release of extracellular nucleosomes in acute pancreatitis: A clinical and experimental study. Int. J. Obes. (Lond)43:158-168; 2019.

[523] Eisele, P. S.; Handschin, C. Functional crosstalk of PGC-1 coactivators and inflammation in skeletal muscle pathophysiology. Semin. Immunopathol.36:27-53; 2014.

[524] Handschin, C.; Choi, C. S.; Chin, S.; Kim, S.; Kawamori, D.; Kurpad, A. J.; Neubauer, N.; Hu, J.; Mootha, V. K.; Kim, Y. B.; Kulkarni, R. N.; Shulman, G. I.; Spiegelman, B. M. Abnormal glucose homeostasis in skeletal muscle-specific PGC-1alpha knockout mice reveals skeletal muscle-pancreatic beta cell crosstalk. J. Clin. Invest.117:3463-3474; 2007.

[525] Alvarez-Guardia, D.; Palomer, X.; Coll, T.; Davidson, M. M.; Chan, T. O.; Feldman, A. M.; Laguna, J. C.; Vazquez-Carrera, M. The p65 subunit of NF-kappaB binds to PGC-1alpha, linking inflammation and metabolic disturbances in cardiac cells. Cardiovasc. Res.87:449-458; 2010.

[526] Perez, S.; Rius-Perez, S.; Finamor, I.; Marti-Andres, P.; Prieto, I.; Garcia, R.; Monsalve, M.; Sastre, J. Obesity causes PGC-1alpha deficiency in the pancreas leading to marked IL-6 upregulation via NF-kappaB in acute pancreatitis. J. Pathol.247:48-59; 2019.

[527] Niu, W. N.; Yadav, P. K.; Adamec, J.; Banerjee, R. S-glutathionylation enhances human cystathionine beta-synthase activity under oxidative stress conditions. Antioxid. Redox Signal.22:350-361; 2015.

[528] Singh, S.; Madzelan, P.; Stasser, J.; Weeks, C. L.; Becker, D.; Spiro, T. G.; Penner-Hahn, J.; Banerjee, R. Modulation of the heme electronic structure and cystathionine beta-synthase activity by second coordination sphere ligands: The role of heme ligand switching in redox regulation. J. Inorg. Biochem.103:689-697; 2009.

[529] Celano, L.; Gil, M.; Carballal, S.; Duran, R.; Denicola, A.; Banerjee, R.; Alvarez, B. Inactivation of cystathionine beta-synthase with peroxynitrite. Arch. Biochem. Biophys.491:96-105; 2009.

[530] DiMagno, M. J.; Williams, J. A.; Hao, Y.; Ernst, S. A.; Owyang, C. Endothelial nitric oxide synthase is protective in the initiation of caerulein-induced acute pancreatitis in mice. Am. J. Physiol. Gastrointest. Liver Physiol.287:G80-7; 2004.

[531] Papatheodorou, L.; Weiss, N. Vascular oxidant stress and inflammation in hyperhomocysteinemia. Antioxid. Redox Signal.9:1941-1958; 2007.

[532] Ang, A. D.; Adhikari, S.; Ng, S. W.; Bhatia, M. Expression of nitric oxide synthase isoforms and nitric oxide production in acute pancreatitis and associated lung injury. Pancreatology9:150-159; 2009.

[533] Li, T. W.; Yang, H.; Peng, H.; Xia, M.; Mato, J. M.; Lu, S. C. Effects of S-adenosylmethionine and methylthioadenosine on inflammation-induced colon cancer in mice. Carcinogenesis33:427-435; 2012.

[534] Bae, S. H.; Sung, S. H.; Cho, E. J.; Lee, S. K.; Lee, H. E.; Woo, H. A.; Yu, D. Y.; Kil, I. S.; Rhee, S. G. Concerted action of sulfiredoxin and peroxiredoxin I protects against alcohol-induced oxidative injury in mouse liver. Hepatology53:945-953; 2011.

[535] Yu, S.; Wang, X.; Lei, S.; Chen, X.; Liu, Y.; Zhou, Y.; Zhou, Y.; Wu, J.; Zhao, Y. Sulfiredoxin-1 protects primary cultured astrocytes from ischemia-induced damage. Neurochem. Int.82:19-27; 2015.

[536] Kim, H.; Jung, Y.; Shin, B. S.; Kim, H.; Song, H.; Bae, S. H.; Rhee, S. G.; Jeong, W. Redox regulation of lipopolysaccharide-mediated sulfiredoxin induction, which depends on both AP-1 and Nrf2. J. Biol. Chem.285:34419-34428; 2010.

[537] Bae, S. H.; Sung, S. H.; Lee, H. E.; Kang, H. T.; Lee, S. K.; Oh, S. Y.; Woo, H. A.; Kil, I. S.; Rhee, S. G. Peroxiredoxin III and sulfiredoxin together protect mice from pyrazole-induced oxidative liver injury. Antioxid. Redox Signal.17:1351-1361; 2012.

[538] Baek, J. Y.; Han, S. H.; Sung, S. H.; Lee, H. E.; Kim, Y. M.; Noh, Y. H.; Bae, S. H.; Rhee, S. G.; Chang, T. S. Sulfiredoxin protein is critical for redox balance and survival of cells exposed to low steady-state levels of H2O2. J. Biol. Chem.287:81-89; 2012.

[539] Shen, A.; Kim, H. J.; Oh, G. S.; Lee, S. B.; Lee, S.; Pandit, A.; Khadka, D.; Sharma, S.; Kim, S. Y.; Choe, S. K.; Yang, S. H.; Cho, E. Y.; Shim, H.; Park, R.; Kwak, T. H.; So, H. S. Pharmacological stimulation of NQO1 decreases NADPH levels and ameliorates acute pancreatitis in mice. Cell. Death Dis.10:5-018-1252-z; 2018.

[540] Hirano, K.; Chen, W. S.; Chueng, A. L.; Dunne, A. A.; Seredenina, T.; Filippova, A.; Ramachandran, S.; Bridges, A.; Chaudry, L.; Pettman, G.; Allan, C.; Duncan, S.; Lee, K. C.; Lim, J.; Ma, M. T.; Ong, A. B.; Ye, N. Y.; Nasir, S.; Mulyanidewi, S.; Aw, C. C.; Oon, P. P.; Liao, S.; Li, D.; Johns, D. G.; Miller, N. D.; Davies, C. H.; Browne, E. R.; Matsuoka, Y.; Chen, D. W.; Jaquet, V.; Rutter, A. R. Discovery of GSK2795039, a novel small molecule NADPH oxidase 2 inhibitor. Antioxid. Redox Signal.23:358-374; 2015.

[541] Gukovsky, I.; Reyes, C. N.; Vaquero, E. C.; Gukovskaya, A. S.; Pandol, S. J. Curcumin ameliorates ethanol and nonethanol experimental pancreatitis. Am. J. Physiol. Gastrointest. Liver Physiol.284:G85-95; 2003.

[542] Li, X.; He, P.; Wang, X. L.; Zhang, S.; Devejian, N.; Bennett, E.; Cai, C. Sulfiredoxin-1 enhances cardiac progenitor cell survival against oxidative stress via the upregulation of the ERK/NRF2 signal pathway. Free Radic. Biol. Med.123:8-19; 2018.

[543] Jiang, H.; Wu, L.; Chen, J.; Mishra, M.; Chawsheen, H. A.; Zhu, H.; Wei, Q. Sulfiredoxin promotes colorectal cancer cell invasion and metastasis through a novel mechanism of enhancing EGFR signaling. Mol. Cancer. Res.13:1554-1566; 2015.

[544] Mishra, M.; Jiang, H.; Chawsheen, H. A.; Gerard, M.; Toledano, M. B.; Wei, Q. Nrf2-activated expression of sulfiredoxin contributes to urethane-induced lung tumorigenesis. Cancer Lett.432:216-226; 2018.

[545] Merza, M.; Hartman, H.; Rahman, M.; Hwaiz, R.; Zhang, E.; Renstrom, E.; Luo, L.; Morgelin, M.; Regner, S.; Thorlacius, H. Neutrophil extracellular traps induce trypsin activation, inflammation, and tissue damage in mice with severe acute pancreatitis. Gastroenterology149:1920-1931.e8; 2015.

[546] Murthy, P.; Singhi, A. D.; Ross, M. A.; Loughran, P.; Paragomi, P.; Papachristou, G. I.; Whitcomb, D. C.; Zureikat, A. H.; Lotze, M. T.; Zeh Iii, H. J.; Boone, B. A. Enhanced neutrophil extracellular trap formation in acute pancreatitis contributes to disease severity and is reduced by chloroquine. Front. Immunol.10:28; 2019.

[547] Ou, X.; Cheng, Z.; Liu, T.; Tang, Z.; Huang, W.; Szatmary, P.; Zheng, S.; Sutton, R.; Toh, C. H.; Zhang, N.; Wang, G. Circulating histone levels reflect disease severity in animal models of acute pancreatitis. Pancreas44:1089-1095; 2015.

[548] Gukovskaya, A. S.; Gukovsky, I. Which way to die: The regulation of acinar cell death in pancreatitis by mitochondria, calcium, and reactive oxygen species. Gastroenterology140:1876-1880; 2011.

[549] Watabe, S.; Hiroi, T.; Yamamoto, Y.; Fujioka, Y.; Hasegawa, H.; Yago, N.; Takahashi, S. Y. SP-22 is a thioredoxin-dependent peroxide reductase in mitochondria. Eur. J. Biochem.249:52-60; 1997.

[550] Hattori, F.; Murayama, N.; Noshita, T.; Oikawa, S. Mitochondrial peroxiredoxin-3 protects hippocampal neurons from excitotoxic injury in vivo. J. Neurochem.86:860-868; 2003.

[551] Kim, H.; Lee, G. R.; Kim, J.; Baek, J. Y.; Jo, Y. J.; Hong, S. E.; Kim, S. H.; Lee, J.; Lee, H. I.; Park, S. K.; Kim, H. M.; Lee, H. J.; Chang, T. S.; Rhee, S. G.; Lee, J. S.; Jeong, W. Sulfiredoxin inhibitor induces preferential death of cancer cells through reactive oxygen species-mediated mitochondrial damage. Free Radic. Biol. Med.91:264-274; 2016.

[552] Apostolova, N.; Victor, V. M. Molecular strategies for targeting antioxidants to mitochondria: Therapeutic implications. Antioxid. Redox Signal.22:686-729; 2015.

[553] Wang, K.; Liu, F.; Liu, C. Y.; An, T.; Zhang, J.; Zhou, L. Y.; Wang, M.; Dong, Y. H.; Li, N.; Gao, J. N.; Zhao, Y. F.; Li, P. F. The long noncoding RNA NRF regulates programmed necrosis and myocardial injury during ischemia and reperfusion by targeting miR-873. Cell Death Differ.23:1394-1405; 2016.

[554] Davis, C. W.; Hawkins, B. J.; Ramasamy, S.; Irrinki, K. M.; Cameron, B. A.; Islam, K.; Daswani, V. P.; Doonan, P. J.; Manevich, Y.; Madesh, M. Nitration of the mitochondrial complex I subunit NDUFB8 elicits RIP1- and RIP3-mediated necrosis. Free Radic. Biol. Med.48:306-317; 2010.

[555] Crunkhorn, S.; Dearie, F.; Mantzoros, C.; Gami, H.; da Silva, W. S.; Espinoza, D.; Faucette, R.; Barry, K.; Bianco, A. C.; Patti, M. E. Peroxisome proliferator activator receptor gamma coactivator-1 expression is reduced in obesity: Potential pathogenic role of saturated fatty acids and p38 mitogen-activated protein kinase activation. J. Biol. Chem.282:15439-15450; 2007.

[556] Scarpulla, R. C. Metabolic control of mitochondrial biogenesis through the PGC-1 family regulatory network. Biochim. Biophys. Acta1813:1269-1278; 2011.

[557] LeBleu, V. S.; O'Connell, J. T.; Gonzalez Herrera, K. N.; Wikman, H.; Pantel, K.; Haigis, M. C.; de Carvalho, F. M.; Damascena, A.; Domingos Chinen, L. T.; Rocha, R. M.; Asara, J. M.; Kalluri, R. PGC-1alpha mediates mitochondrial biogenesis and oxidative phosphorylation in cancer cells to promote metastasis. Nat. Cell Biol.16:992-1003, 1-15; 2014.

[558] St-Pierre, J.; Drori, S.; Uldry, M.; Silvaggi, J. M.; Rhee, J.; Jager, S.; Handschin, C.; Zheng, K.; Lin, J.; Yang, W.; Simon, D. K.; Bachoo, R.; Spiegelman, B. M. Suppression of reactive oxygen species and neurodegeneration by the PGC-1 transcriptional coactivators. Cell127:397-408; 2006.

[559] Adams, R. H.; Porras, A.; Alonso, G.; Jones, M.; Vintersten, K.; Panelli, S.; Valladares, A.; Perez, L.; Klein, R.; Nebreda, A. R. Essential role of p38alpha MAP kinase in placental but not embryonic cardiovascular development. Mol. Cell6:109-116; 2000.

[560] Kim, M. S.; Shigenaga, J. K.; Moser, A. H.; Feingold, K. R.; Grunfeld, C. Suppression of estrogen-related receptor alpha and medium-chain acyl-coenzyme A dehydrogenase in the acute-phase response. J. Lipid Res.46:2282-2288; 2005.

[561] Tran, M.; Tam, D.; Bardia, A.; Bhasin, M.; Rowe, G. C.; Kher, A.; Zsengeller, Z. K.; Akhavan-Sharif, M. R.; Khankin, E. V.; Saintgeniez, M.; David, S.; Burstein, D.; Karumanchi, S. A.; Stillman, I. E.; Arany, Z.; Parikh, S. M. PGC-1alpha promotes recovery after acute kidney injury during systemic inflammation in mice. J. Clin. Invest.121:4003-4014; 2011.

[562] Palomer, X.; Alvarez-Guardia, D.; Rodriguez-Calvo, R.; Coll, T.; Laguna, J. C.; Davidson, M. M.; Chan, T. O.; Feldman, A. M.; Vazquez-Carrera, M. TNF-alpha reduces PGC-1alpha expression through NF-kappaB and p38 MAPK leading to increased glucose oxidation in a human cardiac cell model. Cardiovasc. Res.81:703-712; 2009.

[563] Feingold, K.; Kim, M. S.; Shigenaga, J.; Moser, A.; Grunfeld, C. Altered expression of nuclear hormone receptors and coactivators in mouse heart during the acute-phase response. Am. J. Physiol. Endocrinol. Metab.286:E201-7; 2004.

[564] Planavila, A.; Sanchez, R. M.; Merlos, M.; Laguna, J. C.; Vazquez-Carrera, M. Atorvastatin prevents peroxisome proliferator-activated receptor gamma coactivator-1 (PGC-1) downregulation in lipopolysaccharide-stimulated H9c2 cells. Biochim. Biophys. Acta1736:120-127; 2005.

[565] Villeneuve, C.; Guilbeau-Frugier, C.; Sicard, P.; Lairez, O.; Ordener, C.; Duparc, T.; De Paulis, D.; Couderc, B.; Spreux-Varoquaux, O.; Tortosa, F.; Garnier, A.; Knauf, C.; Valet, P.; Borchi, E.; Nediani, C.; Gharib, A.; Ovize, M.; Delisle, M. B.; Parini, A.; Mialet-Perez, J. p53-PGC-1alpha pathway mediates oxidative mitochondrial damage and cardiomyocyte necrosis induced by monoamine oxidase-A upregulation: Role in chronic left ventricular dysfunction in mice. Antioxid. Redox Signal.18:5-18; 2013.

[566] Sahin, E.; Colla, S.; Liesa, M.; Moslehi, J.; Muller, F. L.; Guo, M.; Cooper, M.; Kotton, D.; Fabian, A. J.; Walkey, C.; Maser, R. S.; Tonon, G.; Foerster, F.; Xiong, R.; Wang, Y. A.; Shukla, S. A.; Jaskelioff, M.; Martin, E. S.; Heffernan, T. P.; Protopopov, A.; Ivanova, E.; Mahoney, J. E.; Kost-Alimova, M.; Perry, S. R.; Bronson, R.; Liao, R.; Mulligan, R.; Shirihai, O. S.; Chin, L.; DePinho, R. A. Telomere dysfunction induces metabolic and mitochondrial compromise. Nature470:359-365; 2011.

[567] Shen, A.; Kim, H. J.; Oh, G. S.; Lee, S. B.; Lee, S. H.; Pandit, A.; Khadka, D.; Choe, S. K.; Kwak, S. C.; Yang, S. H.; Cho, E. Y.; Kim, H. S.; Kim, H.; Park, R.; Kwak, T. H.; So, H. S. NAD(+) augmentation ameliorates acute pancreatitis through regulation of inflammasome signalling. Sci. Rep.7:3006-017-03418-0; 2017.

[568] Rius-Perez, S.; Perez, S.; Marti-Andres, P.; Monsalve, M.; Sastre, J. Nuclear factor kappa B signaling complexes in acute inflammation. Antioxid. Redox Signal. 2020.

[569] Park, J.; Chang, J. H.; Park, S. H.; Lee, H. J.; Lim, Y. S.; Kim, T. H.; Kim, C. W.; Han, S. W. Interleukin-6 is associated with obesity, central fat distribution, and disease severity in patients with acute pancreatitis. Pancreatology15:59-63; 2015.

[570] Pini, M.; Rhodes, D. H.; Castellanos, K. J.; Hall, A. R.; Cabay, R. J.; Chennuri, R.; Grady, E. F.; Fantuzzi, G. Role of IL-6 in the resolution of pancreatitis in obese mice. J. Leukoc. Biol.91:957-966; 2012.

Resumen

1. INTRODUCCIÓN

La pancreatitis aguda es un proceso inflamatorio agudo de la glándula pancreática que conduce frecuentemente a complicaciones locales y sistémicas. En la actualidad, es la principal causa de admisión hospitalaria por enfermedad gastrointestinal y su incidencia ha aumentado considerablemente durante la última década.

Las causas de la pancreatitis aguda son variadas, destacando entre las más frecuentes la presencia de cálculos biliares y el consumo excesivo de alcohol. Sin embargo, en los últimos años han surgido nuevos factores de riesgo como la obesidad, la diabetes tipo 2, el tabaquismo y el abuso de medicamentos, factores relacionados todos ellos con un aumento significativo de la incidencia de esta patología. En lo que se refiere a la obesidad, se considera un factor pronóstico de gravedad en la pancreatitis aguda debido a que las complicaciones locales y sistémicas son más frecuentes en los pacientes obesos. Además, los pacientes con pancreatitis aguda grave presentan un mayor porcentaje de grasa corporal que las personas con pancreatitis aguda leve.

Entre los mecanismos fisiopatológicos más relevantes en las primeras fases de la pancreatitis aguda se encuentran: la activación intracelular de proteasas, la alteración en la secreción de las células acinares, la activación de la respuesta inflamatoria y la muerte celular. Con frecuencia, estos mecanismos actúan sinérgicamente durante el inicio y la progresión de la pancreatitis aguda. De hecho, la activación de la respuesta inflamatoria en el páncreas puede conducir a una lesión más severa de las células acinares que, en los casos más graves, produce necrosis induciendo a su vez más inflamación. La necrosis se considera el principal tipo de muerte celular en las células acinares durante la pancreatitis aguda y su aparición, a diferencia de la apoptosis, se correlaciona con la gravedad de esta patología.

Tradicionalmente se ha considerado la necrosis como una forma de muerte celular no regulada. Por el contrario, en los últimos años se ha definido una nueva forma de muerte celular programada, llamada necroptosis, diferente de la necrosis. La necroptosis es un tipo de muerte inflamatoria que se caracteriza por la liberación de materiales intracelulares que pueden actuar como patrones moleculares asociados a daño (DAMPs), y por lo tanto, inducir una respuesta inflamatoria a nivel sistémico. En consecuencia, la necroptosis parece desempeñar un papel decisivo en las enfermedades inflamatorias, incluyendo entre ellas a la pancreatitis aguda.

La activación de la respuesta inflamatoria en el páncreas implica una activación coordinada de diferentes vías de señalización celular, entre las que destacan aquellas reguladas por el factor nuclear kappa-B (NF-κB). Aunque la activación de NF-κB en la pancreatitis aguda ha sido ampliamente estudiada, diferentes trabajos muestran que este factor de transcripción ejerce un papel pleiotrópico en la regulación de la respuesta inflamatoria durante la pancreatitis aguda. NF-κB puede inducir o reprimir la expresión de cientos de genes, muchos de ellos esenciales en la regulación de los procesos inflamatorios del páncreas como son las citoquinas proinflamatorias. Entre estas últimas se encuentra la interleuquina-6, cuyos niveles séricos elevados se consideran marcador de gravedad en la pancreatitis aguda.

Cabe destacar que una característica fundamental de NF-κB es su capacidad para regular, de forma selectiva, la transcripción de determinados genes diana, lo que permite modular adecuadamente la respuesta celular a estímulos inflamatorios particulares. En los últimos años, se ha observado que las interacciones de NF-κB con otros factores de transcripción, así como con determinadas proteínas reguladoras, contribuyen de forma decisiva a la especificidad de la actividad transcripcional de NF-κB.

El estrés oxidativo es un factor clave implicado en la respuesta inflamatoria y en el daño de las células acinares durante la pancreatitis aguda. El aumento en los niveles de especies reactivas de oxígeno, así como una alteración en la regulación de los sistemas antioxidantes contribuyen decisivamente a desestabilizar el equilibrio redox en las células acinares del páncreas. En este sentido, la pancreatitis aguda se caracteriza por una marcada depleción en los niveles de glutatión reducido debido probablemente a una alteración en los mecanismos reguladores de la vía de la transulfuración. La vía de la transulfuración es una ruta metabólica que conduce a la formación de cisteína, el principal factor limitante para la síntesis del glutatión. Utilizando S-adenosilmetionina (SAM), S-adenosilhomocisteína (SAH), homocisteína y cistationina como intermediarios, la vía de transulfuración metaboliza la metionina en cisteína. Por lo tanto, dada su implicación en la síntesis del glutatión, el metabolismo de la metionina a través de la vía de transulfuración contribuye decisivamente al mantenimiento de la homeostasis redox en las células.

Junto con el estrés oxidativo, el estrés nitrosativo está también asociado a la fisiopatología de la pancreatitis aguda. El estrés nitrosativo se produce como consecuencia del aumento de la producción de especies reactivas del nitrógeno, entre las que se encuentra el peroxinitrito. El peroxinitrito es un potente agente oxidante que se produce como resultado de la reacción del óxido nítrico con el superóxido. Debido a su alta reactividad, el peroxinitrito puede reaccionar y alterar un gran número de biomoléculas pudiendo producir un daño irreversible en las células. Entre las principales alteraciones que produce el peroxinitrito se encuentra la nitración de proteínas, una modificación química que implica el reemplazo de hidrógeno por un grupo nitro (-NO_2) en la posición 3 del anillo fenólico de la tirosina libre o unida a proteínas, produciendo 3-nitrotirosina.

En la pancreatitis aguda, el estrés nitrosativo se produce como consecuencia del aumento en la expresión de la enzima óxido nítrico sintasa 2 (NOS2), una de las isoformas responsables de la síntesis de óxido nítrico. Como resultado del aumento del estrés nitrosativo en la pancreatitis aguda, se produce un incremento de proteínas nitradas en el páncreas que contribuye a exacerbar el daño celular.

El mantenimiento del estado redox mitocondrial es fundamental para la supervivencia celular. Las mitocondrias se consideran la fuente principal de peroxinitrito y como consecuencia, estos orgánulos son una importante diana del daño oxidativo mediado por estrés nitrosativo. En este sentido, la nitración de proteínas tiene un impacto significativo en la fisiología mitocondrial y en concreto, en la regulación de las vías de señalización de muerte celular.

Teniendo en cuenta estos antecedentes, el mantenimiento de la defensa antioxidante mitocondrial resulta clave para prevenir el daño oxidativo durante los procesos inflamatorios. En este contexto, el cofactor transcripcional PGC-1α regula la expresión de los genes *Sod2, catalasa, Prx3, Prx5, Ucp-2, Trxr2*, and *Trx2* y, en consecuencia, protege a las células del daño oxidativo mitocondrial. Cabe destacar que la actividad de PGC-1α está íntimamente relacionada con el metabolismo, ya que entre sus funciones fisiológicas se encuentra la regulación del metabolismo oxidativo y de la biogénesis mitocondrial. De hecho, la deficiencia en PGC-1α conduce a un metabolismo glucolítico, disminución de la expresión de enzimas antioxidantes y un incremento del estrés oxidativo en diferentes tejidos.

Por otra parte, las especies reactivas del oxígeno y del nitrógeno no solo causan daño tisular, sino que pueden actuar también como señales intracelulares, jugando un papel fundamental en la regulación de la respuesta inflamatoria. Las peroxirredoxinas son unas proteínas clave en la señalización intracelular debido a que actúan modulando los niveles celulares de peróxido de hidrógeno y de peroxinitrito. Las peroxirredoxinas se clasifican en tres subfamilias (peroxirredoxinas 2-Cys típicas, peroxirredoxinas 2-Cys atípicas y peroxirredoxinas 1-Cys) en función del mecanismo catalítico utilizado por cada una de ellas. En los tres tipos de peroxirredoxinas, el primer paso del mecanismo catalítico consiste en el ataque del grupo sulfhidrilo de una cisteína clave en la estructura de estas proteínas (cisteína peroxidática) al peróxido, produciendo cisteína en estado sulfénico (-SOH). En el segundo paso del mecanismo catalítico, esta cisteína en estado sulfénico (-SOH) forma un puente disulfuro con el grupo sulfhidrilo de una cisteína situada en el extremo carboxilo terminal de otra peroxirredoxina, formando un dímero de peroxirredoxina y liberando agua en esta reacción. Este enlace disulfuro es reducido posteriormente por la tiorredoxina en el tercer paso del mecanismo catalítico.

Eventualmente, bajo condiciones altamente oxidantes, la cisteína en estado sulfénico (-SOH) puede oxidarse a estado sulfínico ($-SO_2H$) o sulfónico ($-SO_3H$), modificaciones que conducen a su inactivación. Si bien el estado sulfónico es irreversible, las perroxirredoxinas en estado sulfínico pueden retornar al estado sulfénico por acción de la sulfirredoxina. De hecho, como respuesta al estrés oxidativo, la expresión de sulfirredoxina aumenta para prevenir la inactivación de las peroxirredoxinas. Además, la sulfirredoxina puede translocar a la mitocondria evitando así la hiperoxidación e inactivación de la peroxirredoxina 3, una isoforma de las peroxirredoxinas de mamífero localizada exclusivamente en las mitocondrias.

2. OBJETIVOS

El objetivo general de esta Tesis es hallar nuevos mecanismos involucrados en la regulación redox de la defensa antioxidante y la cascada inflamatoria en la pancreatitis aguda, así como evaluar su impacto en la fisiopatología de esta enfermedad.

Los objetivos específicos son:

1. Estudiar la regulación redox de la vía de transulfuración en el páncreas con pancreatitis aguda y su contribución a la depleción del glutatión.

2. Evaluar el papel de la sulfirredoxina en la regulación de la cascada inflamatoria y la muerte celular en la pancreatitis aguda.

3. Evaluar la contribución de PGC-1α en la regulación de la defensa antioxidante y la respuesta inflamatoria en la pancreatitis aguda.

3. METODOLOGÍA

En este trabajo, se ha utilizado el modelo experimental de pancreatitis aguda inducida por ceruleína en ratones. Este modelo está basado en las propiedades secretagogas de la ceruleína, un análogo de la colecistoquinina. Este modelo experimental se ha utilizado ampliamente para estudiar los eventos intracelulares asociados con las fases tempranas de la pancreatitis aguda, incluida la activación de proteasas, las cascadas de señalización celular y las vías de muerte celular.

El modelo de pancreatitis aguda inducido por ceruleína en ratón se establece mediante la administración de siete inyecciones (50 µg/kg de peso corporal cada inyección) intra-peritoneales en intervalos de una hora. A los ratones control se les administró suero fisiológico (NaCl al 0,9%) en las mimas condiciones. Los animales se sacrificaron 1 h después de la primera, tercera, quinta y séptima inyección de ceruleína, dependiendo del estudio experimental. La eutanasia de los ratones se llevó a cabo bajo condiciones de anestesia con isoflurano al 3–5%. Posteriormente, se extrajo la sangre, el páncreas y los pulmones para su posterior estudio. El sacrificio fue confirmado por dislocación cervical.

La inducción de la pancreatitis aguda se llevó a cabo mediante la administración de ceruleína tanto en ratones *lean* como obesos. La obesidad en ratones macho se indujo con una dieta rica en grasas (42% de lípidos). Los ratones se alimentaron con esta dieta durante 4-6 semanas. Esta dieta induce obesidad y resistencia a la insulina en 4 semanas. La dieta control y la dieta rica en grasas se obtuvo de Envigo® (TD88137).

Para estudiar la regulación redox de la vía de transulfuración en el páncreas con pancreatitis aguda y su papel en la depleción del glutatión, un grupo de animales fue tratado con S-adenosilmetionina. La S-adenosilmetionina se administró por vía intraperitoneal (15 mg/kg de peso corporal) 10 minutos antes de la primera y la cuarta inyección de ceruleína. Se administró solución salina fisiológica (NaCl al 0.9%) al grupo control de animales. Además, un grupo de estos animales controles también recibió inyecciones de SAM.

Para investigar el posible papel que la sulfirredoxina cumple en la regulación de la cascada inflamatoria y la muerte celular durante la pancreatitis aguda se han utilizado ratones macho C57BL/6 knock-out deficientes en sulfirredoxina (KO) proporcionados por el Dr. Michel Toledano (Commissariat à l'Energie Atomique, Bâtiment Le Ponant D - 25, rue Leblanc – 75015 Paris, France).

Un grupo de estos animales fue tratado con el antioxidante mitocondrial MitoTEMPO (Sigma-Aldrich, St. Louis, MO, EE. UU.). Este tratamiento se administró por vía intraperitoneal (25 mg/kg de peso corporal) 10 minutos antes de la primera y cuarta inyección de ceruleína.

Para evaluar la contribución de PGC-1α en la regulación de la defensa antioxidante y la respuesta inflamatoria en la pancreatitis aguda, se han utilizado ratones macho C57BL/6 wild-type y ratones knock-out deficientes en PGC-1α (C57BL/6 PGC-1α$^{-/-}$). Los ratones C57BL/6 y knock-out de PGC-1α fueron proporcionados por la Dra. María Monsalve, investigadora del Instituto de Investigaciones Biomédicas "Alberto Sols" (IIBM) (Madrid, España).

Un grupo de estos animales fue tratado con el antagonista del receptor gp130 de la IL-6, LMT-28 (Sigma-Aldrich, St. Louis, MO, EE. UU.) Estos animales recibieron una dosis de 1 mg/kg de peso corporal por sonda oral 1 h antes de la primera y cuarta inyección de ceruleína. Para ello, el LMT-28 fue disuelto en 0,5% de carboximetilcelulosa (Sigma-Aldrich, St. Louis, MO, EE. UU.). La carboximetilcelulosa (0,5%) se administró como vehículo.

Los animales de experimentación recibieron cuidado y fueron manejados de acuerdo con la Declaración de Helsinki de 1964, revisada en 2000 en Edimburgo, y con las regulaciones europeas (Council Directive 2010/63/EU) así como con los estudios aprobados por la Comisión de Ética de Experimentación Animal de la Universidad de Valencia.

Las técnicas experimentales utilizadas en este trabajo se enumeran a continuación:

- Espectrometría de masas UHPLC MS/MS
- Cuantificación de proteínas mediante MRM
- Western blott
- Inmunoprecipitación de proteínas
- Análisis de la expresión génica mediante RT-PCR
- Análisis epigenético mediante inmunoprecipitación de la cromatina (ChIP)
- Análisis de los niveles de peróxido de hidrógeno mediante fluorimetría
- Análisis de los niveles de DNA libre en plasma mediante fluorimetría
- Análisis de los niveles de interlequina-6 en plasma mediante Enzyme-Linked ImmunoSorbent Assay (ELISA)
- Análisis de los niveles de nucleosomas extracelulares en plasma mediante Enzyme-Linked ImmunoSorbent Assay (ELISA)
- Medida de la actividad mieloperoxidasa en tejido mediante colorimetría
- Medida de la actividad amilasa en plasma mediante colorimetría
- Técnica histológica

Todos los resultados se expresaron como media ± desviación estándar. El análisis estadístico se realizó en dos fases. En primer lugar, se llevó a cabo la comparación general de los grupos experimentales utilizando el análisis de varianza unidireccional (ANOVA). Si la comparación resultó significativa, se analizaron las diferencias entre los grupos experimentales mediante la prueba de Bonferroni.

4. RESULTADOS Y DISCUSIÓN

4.1. Regulación de la vía de la transulfuración en la pancreatitis aguda

En este trabajo se midieron los niveles de los metabolitos de la vía de la transulfuración durante la inducción de la pancreatitis aguda. Si bien los niveles pancreáticos de metionina, S-adenosilmetionina, cistationina, cisteína y GSH disminuyeron significativamente durante el curso de la pancreatitis aguda, los niveles de S-adenosilhomocisteína y de homocisteína permanecieron sin cambios.

Resultados previos muestran que la nitración de la cistationina beta-sintasa (CBS), una enzima clave en la regulación de la vía de la transulfuración, compromete el catabolismo de la homocisteína. En base a estos estudios y teniendo en cuenta que el estrés nitrosativo juega un papel relevante en la fisiopatología de la pancreatitis aguda, nos planteamos valorar los niveles de nitración de la CBS. Como resultado, hemos observado que durante la pancreatitis se produce un aumento significativo de los niveles de nitración de la CBS, probablemente asociado a la sobreexpresión de la óxido nítrico sintasa 2 (NOS2).

Para demostrar el papel esencial que la nitración de la CBS juega en el bloqueo de la vía de transulfuración, se estudiaron los niveles de sus metabolitos en ratones con pancreatitis aguda tratados con S-adenolsilmetionina. Como resultado del bloqueo existente en la vía de la transulfuración debido a la nitración de la CBS, el tratamiento con S-adenosilhomocitseína resultó ineficaz en la pancreatitis aguda experimental. De hecho, la administración de S-adenolsilmetionina originó un aumento de homocisteína en el tejido pancreático. Además, la administración de S-adenosilhomocitseína causó un incremento de los niveles de histona H3 trimetilada en la lisina 4, marcador epigenético de transcripción activa, en los promotores de *Tnf-α, Il-6* y *Nos2*. Como consecuencia de esta actividad transcripcional, observamos un aumento de la expresión génica de estas citoquinas proinflamatorias, incremento que puede contribuir a una mayor severidad de la pancreatitis aguda.

En general, estos resultados muestran por primera vez los efectos adversos del estrés nitrosativo sobre la vía de la transulfuración en la pancreatitis aguda. Asimismo, contribuyen a esclarecer los mecanismos subyacentes responsables del aumento de los niveles de homocisteína en los procesos inflamatorios.

4.2. Modulación del estrés nitrosativo y la muerte celular por sulfirredoxina en pancreatitis aguda

Teniendo en cuenta la actividad peroxinitrito reductasa de las peroxirredoxinas y el impacto del estrés nitrosativo en la regulación de la vía de transulfuración en el páncreas, en este trabajo nos planteamos estudiar la contribución del sistema sulfirredoxina/peroxirredoxina a la regulación del estrés nitrosativo y la señalización redox en la pancreatitis aguda.

En primer lugar, hemos observado un aumento significativo en los niveles de sulfirredoxina durante la inducción de la pancreatitis aguda. Además, en fases tempranas de la evolución de la pancreatitis aguda, se produjo un aumento de las formas hiperoxidadas (sufínica y sulfónica) de la peroxirredoxina-1,2 y 3, resultado que coincide con un aumento de los niveles de peróxido de hidrógeno en el páncreas durante la enfermedad. En la fase final de la inducción de la pancreatitis aguda, coincidiendo con un nuevo pico de peróxido de hidrógeno, los niveles hiperoxidados de peroxirredoxina 1 y 2 vuelven a aumentar, pero no así los de peroxirredoxina 3. Por tanto, y de acuerdo con estos resultados, el aumento en los niveles de sulfirredoxina durante la pancreatitis aguda contribuyen a prevenir específicamente la hiperoxidación de la peroxirredoxina 3, una isoforma exclusivamente localizada en las mitocondrias. De hecho, en este trabajo, hemos comprobado que durante la inducción de la pancreatitis agua, la sulfirredoxina migra a la mitocondria, situación que permitiría evitar específicamente la hiperoxidación de la peroxirredoxina 3.

Para investigar el papel que la sulfirredoxina cumple en el mantenimiento del estado redox durante la pancreatitis aguda se han utilizado ratones macho C57BL/6 knock-out deficientes en sulfirredoxina (KO). Como consecuencia de la deficiencia en sulfirredoxina, se ha observado una mayor presencia de peroxirredoxina 1,2 Y 3 en estado hiperoxidado en los ratones KO respecto a los wild-type (WT) tras la inducción de la pancreatitis aguda. Además, el estudio histológico del páncreas de ratones KO con pancreatitis aguda muestra niveles mayores de necrosis, infiltrado inflamatorio y edema respecto de los ratones control.

De acuerdo con los mayores niveles de infiltrado inflamatorio observado en el páncreas de ratones deficientes en sulfirredoxina con pancreatitis aguda, se ha detectado un mayor grado de fosforilación de las MAPKKs MEK1/2 y MKK3/6 así como de sus correspondientes sustratos MAPK, ERK 1/2 y p38α. Además, se han observado mayores niveles de p-p65 y de interlequina-6 en el páncreas de ratones KO de sulfirredoxina con pancreatitis aguda respecto de los ratones wild-type con pancreatitis.

Teniendo en cuenta el aumento de la necrosis observada en el páncreas de ratones deficientes en sulfirredoxina con pancreatitits aguda, se decidió estudiar una posible activación de la necrosis programada, necroptosis, en estos ratones. Los ratones deficientes en sulfirredoxina exhibieron mayores niveles del marcador de necroptosis p-MLKL en el tejido pancreático. Además, hemos observado mayores niveles de nitración de proteínas mitocondriales y un aumento de la expresión y traslocación a la mitocondria de p53, hecho que podría estar dirigiendo la activación de la muerte por necroptosis en estos ratones. Este aumento en la activación de la necroptosis parece estar correlacionado con el aumento de los niveles de ADN libre y de nucleosomas extracelulares hallados en el plasma de ratones deficientes en sulfirredoxina con pancreatitis aguda.

Con el fin de demostrar el papel que podría jugar la sulfirredoxina en la regulación del estrés nitrosativo mitocondrial y la necroptosis en la pancreatitis aguda, utilizamos el antioxidante mitocondrial mito-TEMPO para prevenir la formación de peroxinitrito en las mitocondrias de ratones deficientes en sulfirredoxina. El análisis histológico reveló que los ratones deficientes en sulfirredoxina con pancreatitis y tratados con mito-TEMPO exhibieron un menor índice de necrosis, una disminución en el infiltrado inflamatorio y una reducción en el edema que los ratones no tratados. De acuerdo con esto, los niveles de p-MLKL, así como los niveles plasmáticos de ADN libre y nucleosomas extracelulares disminuyeron en ratones deficientes en sulfirredoxina con pancreatitis tratados con mito-TEMPO en comparación con aquellos no tratados. Además, el tratamiento con mito-TEMPO disminuyó la nitración de proteínas mitocondriales y previno la traslocación de p53 a las mitocondrias de estos ratones.

Tomados en conjunto, estos resultados muestran que la sulfirredoxina juega un papel protector relevante durante la pancreatitis aguda al prevenir la hiperoxidación de la peroxirredoxina 3. Cabe destacar que los ratones deficientes en sulfirredoxina no mostraron aumento de NOS2, por lo que el incremento en el estrés nitrosativo mitocondrial hallado en estos ratones solo parece atribuirse a una alteración de la capacidad de detoxificación del peroxinitrito. Por tanto, y dado que recientemente se ha demostrado que la peroxirredoxina 3 reduce eficazmente el peroxinitrito, nosotros proponemos que la sulfirredoxina migra a las mitocondrias durante la pancreatitis aguda para mantener activa la actividad peroxidasa de la peroxirredoxina 3 frente al peroxinitrito (ONOO-) con el fin de evitar el daño nitrosativo mitocondrial, la translocación mitocondrial de p53 y la activación de la necroptosis.

4.3. Papel de PGC-1α en la regulación de la respuesta inflamatoria en la pancreatitis aguda

En este trabajo se ha estudiado la contribución de PGC-1α en la regulación de la defensa antioxidante y la respuesta inflamatoria en la pancreatitis aguda. Como se ha comentado anteriormente, la obesidad es un factor pronóstico de gravedad en la pancreatitis aguda debido a que las complicaciones locales y sistémicas son más frecuentes en los pacientes obesos. Por otro lado, y en relación con estos estudios, se ha observado que la actividad de PGC-1α está alterada en la obesidad. Teniendo en cuenta estos antecedentes, en este trabajo hemos comprobado que la expresión de PGC-1α está disminuida en un modelo de obesidad experimental inducido por dieta grasa en ratones. En base a esta disminución en la expresión de PGC-1α en los ratones obesos y con el fin de aclarar el papel de PGC-1α en la regulación de la cascada inflamatoria en la pancreatitis aguda, nos hemos planteado estudiar la pancreatitis aguda en ratones PGC-1α KO.

La inducción de la pancreatitis aguda disminuyó la expresión transcripcional de *Prx3*, *Sod2* y *Cat*, genes antioxidantes dependientes de PGC-1α, en los ratones *wild-type*. Como era de esperar, los ratones deficientes en PGC-1α mostraron niveles de expresión bajos de estos genes en condiciones basales y tras la inducción de la pancreatitis aguda. Sorprendentemente y teniendo en cuenta el resultado anterior, los niveles proteicos de PGC-1α aumentaron en el páncreas tras la inducción de pancreatitis en los ratones control. A continuación, nos planteamos estudiar el grado de acetilación de PGC-1α, modificación post-traduccional responsable de la inhibición de su actividad reguladora sobre la transcripción. Nuestros resultados revelaron que el aumento proteico de PGC-1α iba acompañado de un incremento en su grado de acetilación tras la inducción de la pancreatitis, y, por lo tanto, podría explicar la disminución transcripcional que habíamos observado en sus genes diana antioxidantes. En concordancia con estos hallazgos, previamente se ha demostrado que las sirtuinas y su actividad desacetilasa está inhibida en la pancreatitis aguda, hecho que podría conducir a la acetilación e inhibición de PGC-1α que hemos observado. Por otro lado, la disminución en la defensa antioxidante provocada por la inactivación de PGC-1α en la pancreatitis aguda podría contribuir decisivamente a la aparición de estrés oxidativo y a la activación y amplificación de la respuesta inflamatoria, en particular a través de un factor sensible al estado redox como es NF-κB.

Respecto al estudio de la respuesta inflamatoria, los ratones PGC-1α KO exhibieron un marcado aumento de IL-6 tanto en sus niveles de ARNm en el tejido pancreático como en el plasma. De forma destacable, también se observó en los ratones KO que la translocación nuclear de NF-κB y el reclutamiento de p65 al promotor de *Il-6* indujo la expresión génica de esta citoquina de forma específica, ya que no se detectó inducción de la expresión de otras citoquinas proinflamatorias como *Tnf-α* o *Il-1β*. Además, en este trabajo hemos comprobado que PGC-1α se une a la forma fosforilada de p65 durante la pancreatitis, lo que limita la actividad de NF-κB sobre la transcripción de *Il-6*. En este sentido cabe destacar que anteriormente se ha descrito que los niveles de expresión de la citoquina pro-inflamatoria IL-6 se asocia con la severidad de la pancreatitis aguda.

Finalmente, nos planteamos valorar las posibles repercusiones sistémicas del incremento plasmático de la IL-6. Observamos que estos niveles elevados de IL-6 conducen a un mayor daño pulmonar en los ratones PGC-1α KO, y que este daño sistémico típico de la pancreatitis aguda se pudo prevenir mediante la administración de LMT-28, un antagonista del receptor gp-130 de la IL-6.

Tomados en conjunto, nuestros resultados muestran un mecanismo novedoso de la regulación de la expresión de IL-6 a través de PGC-1α que, actuando como represor selectivo de la actividad de NF-kB, modula la expresión de esta citoquina durante la pancreatitis aguda. Estos resultados contribuyen a esclarecer el impacto de niveles elevados de IL-6 circulantes en la pancreatitis aguda y especialmente, en pacientes obesos con pancreatitis aguda. De hecho, la deficiencia de PGC-1α podría explicar el aumento de la respuesta inflamatoria sistémica y lesión tisular que acontece en pacientes con niveles elevados de IL-6 en plasma, en particular en los pacientes obesos.

5. CONCLUSIONES

De acuerdo con nuestros resultados, las conclusiones alcanzadas en esta Tesis Doctoral son:

1. La pancreatitis aguda bloquea la vía de transulfuración a través de la nitración de la cistationina β-sintasa

2. La administración de S-adenosilmetionina en la pancreatitis aguda aumenta la respuesta inflamatoria y la nitración de la cistationina β-sintasa lo que conduce a la acumulación de homocisteína

3. La sobreexpresión de sulfiredoxina y su translocación a la mitocondria actúan como mecanismos protectores para prevenir el estrés nitrosativo mitocondrial y la necroptosis durante la pancreatitis aguda.

4. Los niveles proteicos de PGC-1α disminuyen notablemente en el páncreas de ratones obesos con pancreatitis aguda

5. En la pancreatitis aguda, PGC-1α se inactiva, al menos en parte, por acetilación lo que conduce a la inhibición de la expresión de sus genes antioxidantes diana

6. Durante la pancreatitis aguda, PGC-1α actúa en el páncreas como un represor selectivo de NF-κB respecto de la expresión de *Il-6*